3-Loop Contributions to Heavy Flavor Wilson Coefficients of Neutral and Charged Current DIS

Dissertation

zur Erlangung des wissenschaftlichen Grades

Dr. rer. nat.

der Fakultät Physik der Technischen Universität Dortmund

vorgelegt von

Alexander Hasselhuhn[a,b,c]

geboren am 25.10.1984 in Essen

Betreuer: Prof. Dr. Johannes Blümlein[a,b]

[a] *Technische Universität Dortmund, Fakultät Physik*
Otto-Hahn-Str. 4, D-44221 Dortmund

[b] *Deutsches Elektronen-Synchrotron, DESY*
Platanenallee 6, D-15738 Zeuthen

[c] *Research Institute for Symbolic Computation, RISC*
Altenbergerstraße 69, A-4040 Linz, Austria

eingereicht am 3. Juni 2013

Gutachter:

Prof. Dr. Johannes Blümlein, Deutsches Elektronen-Synchrotron, Zeuthen

Prof. Dr. Gudrun Hiller, Technische Universität Dortmund

Prof. Dr. Matthias Steinhauser, Karlsruher Institut für Technologie

"The establishment by the mid-1970's of QCD as the correct theory of the strong interactions completed what is now known prosaically as the Standard Model. [...] However, the situation is a bit like the way that the Navier-Stokes equation accounts for the flow of water. The equations are at some level obviously correct, but there are only a few, limited circumstances in which their consequences can be worked out in any detail. [...] the discovery of asymptotic freedom was a genuinely crucial event. For some, it made everything clear. For others, it was only the beginning. And for yet others, it was the beginning of the final chapter."

H. David Politzer -
Nobel Lecture: The Dilemma of Attribution, 2004

Contents

List of Publications

(i) Journal Publications

1. J. Ablinger, J. Blümlein, A. Hasselhuhn, S. Klein, C. Schneider, F. Wißbrock:
Massive 3-Loop Ladder Diagrams for Quarkonic Local Operator Matrix Elements,
arxiv: 1206.2252 [hep-ph], DESY 12-056, DO-TH-12/17, TTK-12-26, SFB/CPP-12-37, LPN12-055,
Nucl. Phys. B **864** (2012) 52–84

2. J. Blümlein, A. Hasselhuhn, S. Klein, C. Schneider:
The $O(\alpha_s^3 n_f T_F^2 C_{A,F})$ Contributions to the Gluonic Massive Operator Matrix Elements,
arxiv: 1205.4184 [hep-ph], DESY 12-055, DO-TH-12/13, SFB/CPP-12-28, LPN12-052,
Nucl. Phys. B **866** (2013) 196–211

3. J. Blümlein, A. Hasselhuhn, P. Kovacikova, S. Moch:
$O(\alpha_s)$ Heavy Flavor Corrections to Charged Current Deep-Inelastic Scattering in Mellin Space,
arxiv: 1104.3449 [hep-ph], DESY 11-032, DO-TH-11/06, SFB/CPP-11-19, LPN11-19,
Phys. Lett. B **700** (2011) 294–304

(ii) Conference-Proceedings

4. J. Ablinger, J. Blümlein, A. De Freitas, A. Hasselhuhn, S. Klein, C. Raab, M. Round, C. Schneider, F. Wißbrock:
Three-Loop Contributions to the Gluonic Massive Operator Matrix Elements at General Values of N,
arxiv: 1212.6823 [hep-ph], DESY 12-232, DO-TH-12/38, SFB/CPP-12-106, LPN12-142,
Proceedings of the 11th DESY Workshop on Elementary Particle Physics "Loops and Legs in Quantum Field Theory", Wernigerode, Germany, 2012,
PoS **LL2012** (2012) 033

5. J. Ablinger, J. Blümlein, A. De Freitas, A. Hasselhuhn, S. Klein, C. Schneider, F. Wißbrock:
New Results on the 3-Loop Heavy Flavor Wilson Coefficients in Deep-Inelastic Scattering,
arxiv: 1212.5950 [hep-ph], DESY 12-247, DO-TH-12/29, SFB/CPP-12-104, LPN12-141,
To appear in the Proceedings of the 36th International Conference on High Energy Physics (ICHEP 2012), Melbourne, Australia, 2012

6. J. Blümlein, A. Hasselhuhn, C. Schneider:
Evaluation of Multi-Sums for Large Scale Problems,
arXiv: 1202.4303 [math-ph], DESY 10-247, DO-TH-12/06, SFB/CPP-12-13, LPN12-038,
Proceedings of the 10th International Symposium on Radiative Corrections (Applications of Quantum Field Theory to Phenomenology), Mamallapuram, India, 2011,
PoS **RADCOR2011** (2011) 032

7. J. Ablinger, J. Blümlein, A. Hasselhuhn, S. Klein, C. Schneider, F. Wißbrock:
New Heavy Flavor Contributions to the DIS Structure Function $F_2(x, Q^2)$ at $O(\alpha_s^3)$,
arXiv: 1202.2700 [hep-ph], DESY 10-065, DO-TH-12/05, SFB/CPP-12-09, LPN2-036,
Proceedings of the 10th International Symposium on Radiative Corrections (Applications of Quantum Field Theory to Phenomenology), Mamallapuram, India, 2011,
PoS **RADCOR2011** (2011) 031

8. J. Ablinger, I. Bierenbaum, J. Blümlein, A. Hasselhuhn, S. Klein, C. Schneider, F. Wißbrock:
   Heavy Flavor DIS Wilson coefficients in the asymptotic regime,
   arxiv: 1007.0375 [hep-ph], DESY 10-093, IFIC/10-22, TTK-10-38, SFB/CPP-10-58, Proceedings of the 10th DESY Workshop on Elementary Particle Physics "Loops and Legs in Quantum Field Theory", Wörlitz, Germany, 2010,
   Nucl. Phys. B (Proc. Suppl.) **205–206** (2010) 242–249

Three further journal publications on Chapters 7 and 9 as well as 10.4 and 10.5 are in preparation.

1 Introduction

The understanding of the substructure of matter in terms of fundamental particles and their interactions is one of the principal research objectives at the high energy frontier. In particular, the structure of the protons and neutrons, described by the interaction of quarks and gluons, is of great interest. Apart from a general interest in the understanding of the fundamental composition of atomic nuclei, protons are used in high energy collision experiments, such as H1 and ZEUS at HERA, D0 and CDF at the Tevatron, and ATLAS and CMS at the Large Hadron Collider (LHC). A precise description of the proton substructure and the interaction among its constituents is thus of particular importance for finding new effects in the Standard Model of particle physics and beyond.

The notion of quarks of three different flavors as constituents of the hadrons was developed in 1964 [1–3] to systematize the plethora of states which had been discovered at that time. Among other observations, the question for the compatibility of the observed Δ^{++} and Δ^{-} resonances with Pauli statistics indicated the existence of a new quantum number [4], which became known as color. The measurement of the branching fractions $\sigma(e^+e^- \to \text{hadrons})/\sigma(e^+e^- \to \mu^+\mu^-)$ [5] later indicated the existence of three such color states for each quark flavor, taking into account the fractional electric charges of the quarks. A direct way of measuring the color degree of freedom, consists in comparing the leptonic decay width of the τ-lepton with its purely hadronic width, which is free of electric quark charge-effects in lowest order, since it is mediated by a charged current process, cf. [6, 7].

Further experimental evidence for point like constituents was given by analyses of deep-inelastic proton electron scattering cross sections, parameterized by the structure functions F_2 and F_L. The kinematic quantities to describe the process are the total energy ν transfered to the hadron, and the virtuality Q^2 of the photon exchanged between the photon and the hadron. A series of experiments at SLAC and MIT [8–14] showed that in the studied range of kinematic parameters F_2 was independent of the virtuality of the photon. This property, known as scaling, had already been predicted by Bjorken [15]. Furthermore, the longitudinal structure function F_L was found to be small compared to F_2, which confirmed a prediction by Callan and Gross [16], and thus pointed towards spin-1/2 constituents taking a dominant part in the scattering process.

The discoveries of scaling led Feynman to introduce his parton model of the hadrons [17–19]. It describes the proton as consisting of point like constituents, which take part in the scattering process instead of the whole nucleon. Later these constituents were identified as the fermionic quarks and bosonic gluons. Deep-inelastic scattering then proceeds as scattering of the exchanged virtual electroweak gauge boson with one of the individual quarks in lowest order. Free quarks, however, had never been observed experimentally, they rather appeared bound in hadrons. This raised the question for the nature of this binding force. A prerequisite for the quantum field theory describing the interactions among the partons was the introduction of gauge theories derived from unbroken non-abelian gauge groups by Yang and Mills [20]. The renormalizability of them, i.e. the existence of a procedure to cancel infinites in the theory without loss of the predictive power, was proven by 't Hooft in 1971 [21]. Based on these developments, quantum chromodynamics (QCD) was proposed as the theory of the strong interaction [22–24], see also [25, 26]. This gauge theory describes the dynamics of color triplet quarks interacting with color octet gluons. The QCD coupling strength was found to decrease for increasing energies [27, 28], a property known as asymptotic freedom. This property proved the existence of kinematic ranges, where the coupling strength is small and hence perturbative calculations are possible. On the other hand, the growing coupling strength at lower energies, resp. larger distances, gave an explanation as to why free quarks are never observed in experiments.

As a tool for studying deep-inelastic scattering reactions within QCD, the expansion of operator products at light like distances, called light cone expansion, became important [29–31]. It gave a justification [31–34] for Feynman's intuitive model, extended by the QCD interaction [35–37]. Furthermore, the light cone expansion paved the way for the development of factorization theorems [38–46], which state that universal non-perturbative portions factorize to all orders in perturbation theory from the scattering amplitudes at leading twist [47]. In this approximation the structure functions are therefore described by non-perturbative parton distribution functions (PDFs), which carry all the universal long distance effects, and Wilson coefficients, which contain all the process dependent short distance behaviour. Hence the Wilson coefficients can be calculated in perturbation theory as a power series in the strong coupling constant α_s, ordering the contributions in terms of Feynman diagrams by their number of loops.

The introduction of an interaction among the partons, however, violates the property of scaling, and yields a quantitative prediction for the size of these scaling violations. In fact, it is a property of renormalizable quantum field theories to predict the energy scale dependence of theory parameters in terms of the renormalization group equations [48–52]. It was the experimental observation of these scaling violations [53, 54], together with the quantitative derivation from QCD, that marked the success of QCD and brought a wide acceptance for it as the theory of the strong interaction. At present the experiments covering the largest area in the space of x- and Q^2-values are the ones performed at HERA [55], with $6 \cdot 10^{-7} \leq x \leq 0.65$ and $0.045\ \text{GeV}^2 \leq Q^2 \leq 30000\ \text{GeV}^2$. With modern next-to-next-to-leading order (NNLO) QCD analyses [56–61], the structure functions are described with deviations at the percent level and below. QCD analyses are performed, extracting the PDFs as well as the theory parameters, like the strong coupling constant and quark masses, from experimental data. This requires the precise knowledge of the Wilson coefficients for the scattering processes in question. The value and precision of the strong coupling constant α_s serve as common measures for the quality of the extractions and as important discriminants for different PDF fits, cf. [62]. Currently, the uncertainty in individual determinations amounts to about $O(1\%)$, however, there are still systematic differences between the results obtained by different groups; for different sources of these deviations, see e.g. [56]. Among them are the treatment of subleading terms in the light cone expansion, the incompatibility or lower quality of certain data sets as well as the treatment of heavy quarks in deep-inelastic scattering. Heavy quark contributions to deep-inelastic scattering are of particular interest, since they are sensitive to the gluon content of the proton, which is constrained to a lesser degree in deep-inelastic scattering off only massless partons. Furthermore, in proton-proton collisions at the LHC the gluon PDF yields large contributions, e.g. through the gluon-gluon fusion channel for the production of the Higgs boson, see e.g. [7].

The results and methods presented in this thesis contribute to the description of heavy quark production in deep-inelastic scattering. As was already indicated, heavy quark production plays an essential role in constraining the gluon distribution at lower values of x and the precision measurement of the strong coupling constant α_s [63]. Therefore, a precise quantitative description of the heavy flavor contributions to deep-inelastic scattering is needed. Since at present the light flavor Wilson coefficients of neutral current deep-inelastic scattering are known at $O(\alpha_s^3)$ [64], the same precision is required concerning the heavy flavor corrections. The 1-loop corrections in the unpolarized case were calculated in Refs. [65–68] and in the polarized case in [69]. The unpolarized 2-loop corrections via the electromagnetic current were calculated in [70–72]. While the light flavor Wilson coefficients up to three loops are given analytically in terms of harmonic sums, the 2-loop heavy flavor Wilson coefficients are only available in semi-analytic form. The exact heavy quark corrections to charged current deep-inelastic scattering are presently known at $O(\alpha_s)$ [73, 74].

At scales much larger than the mass of the heavy quark, i.e. $Q^2 \gg m^2$, the heavy flavor Wilson coefficients factorize into the light flavor Wilson coefficients, and massive operator matrix elements (OMEs). For the structure function F_2, this asymptotic representation holds at the percent level if $Q^2 \geq 10m^2$ [75]. The NLO contributions to the massive OMEs were obtained in [76] and checked in a recalculation in [77–80]. In the course of these calculations also parts were obtained which are needed for the renormalization of the NNLO contributions. Using the 2-loop OMEs as well as the corresponding light flavor Wilson coefficients [81–85], heavy quark corrections to charged current deep-inelastic scattering were given in [86]. However, they represented only a part of the two loop contributions. In revisiting these corrections all terms are derived and a few errors are corrected in this thesis.

For the NNLO massive OMEs a sequence of Mellin moments was given in [87] for $N = 2, \ldots, 10$, in some cases up to $N = 14$. However, for phenomenological application the analytic results for general values of N are necessary. Their calculation requires completely different theoretical and mathematical techniques compared to the case of fixed moments. In the present thesis efforts are spent to derive a series of further contributions of this kind, extending the known 2-loop results.

In [88], a large number of integrals were calculated, which are related to 2-loop diagrams by the insertion of an additional quark bubble, assigning a mass to one of the quark lines, and keeping the other one massless. These contributions constitute a complete color factor, and thus form a renormalizable subclass of graphs. The calculation of these graphs is possible adapting and extending methods used in the recalculation of the NLO corrections to the OMEs in [77–80]. The basic idea of the corresponding method is to represent the integrals via suitable hypergeometric functions. Since the calculations are performed with dimensional regularization [89–92] in $D = 4 + \varepsilon$ space-time dimensions, the integrals are functions of two variables, N and ε. However, when expanding these functions in a Laurent series in ε, only finitely many terms are needed. In this context, the hypergeometric function representations are useful, since their convergent series representations allow for a Laurent expansion in ε on the summand level.

The subsequent simplification of sums is possible by symbolic summation algorithms which are implemented in the Mathematica package Sigma [93–101]. Although initially developed for general purposes, Feynman diagram calculations became an interesting and demanding application for these algorithms, leading to further improvements. At the same time the specific needs of this application asked for the development of more specialized methods for the evaluation of multi-sums occurring in Feynman diagram calculations. These led to the code EvaluateMultiSums [101–103], which contains strategies for efficient application of the summation algorithms in Sigma as well as methods for successive Laurent expansion in ε.

As mentioned earlier, the calculation of the massive OMEs leads to expressions containing nested harmonic sums. Their structural relations [104–107] are necessary for a compact representation of the results. To determine these relations for the nested harmonic sums and related quantities, the Mathematica package HarmonicSums was developed [108–111], which systematically constructs all known relations, and reduces a set of nested harmonic sums to a small number of basis sums. It also includes other operations on harmonic sums and their generalizations, which include asymptotic expansion and their relations to iterated integrals like harmonic polylogarithms.

In this thesis, the missing 3-loop corrections of $O(\alpha_s^3 T_F n_f)$ contributing to gluonic operator matrix elements are calculated, adapting the algorithms from above. These graphs are needed in order to define PDFs in a variable flavor number scheme. Such a scheme reorders the perturbative expansion, such as to remove collinear singularities that occur for very high scales Q^2. As a consequence it allows for the definition of an effective heavy quark PDF.

The calculation of Feynman diagrams with more complicated topologies reveals a higher complexity than the bubble-insertion graphs mentioned above. On the one hand, Appell functions and thus double series representations emerge naturally. On the other hand, the operator insertions demand the introduction of nested finite sums to higher depth. In general also convergence of the derived series representations is more difficult to ensure. Therefore, a large part of the thesis is devoted to the calculation of scalar prototypes for two classes of graphs : graphs with ladder topology and graphs with two distinct heavy quark lines with the same mass. For the former class, the method applied to the $O(\alpha_s^3 T_F n_f)$-graphs is paradigmatic. Here the emphasis is on exploring the flexibility in the paradigm and relaxing limitations from the summation side. For the latter class, the calculation paradigm is enhanced, using Mellin-Barnes integrals for the representation of the higher hypergeometric functions and interlacing summation and integration. Properties of iterated integrals as well as their relation to generalizations of harmonic sums become an essential part of the integration procedure.

In order to explain the present work from the technological point of view, some comments will be given on technologies related to the calculations performed in this thesis as well as in similar calculations. The Wilson coefficients are expressed in terms of Feynman integrals, which initially were calculated by hand at lowest order in the coupling constant. However, with the demand for increasing precision, the amount of integrals to solve grew, requiring the automation of the calculations in computer programs. At the same time also the mathematical complexity increased, making the development of general solution methods for larger classes of integrals necessary. In order to make the calculation of integrals algorithmic, several techniques were developed, such as expansions in Gegenbauer polynomials [112], sets of relations deriving from integration by parts [113], and complex contour integrals that are referred to as Mellin-Barnes integrals [114–117]. Furthermore, as was noted in [77–79], the integrals represent hypergeometric functions, which can deliver series representations. These are suitable for symbolic summation methods [93–101], allowing for a very elegant solution of large classes of integrals, see e.g. [88].

In the computations, classes of iterated integrals like polylogarithms [118–122] and their special values [123] were found. In order to yield compact representations of the results, algebraic relations were needed among the polylogarithms, and the iterated nature led to systematic methods for deriving such relations [122, 123]. Furthermore, precise numeric evaluations can also be obtained in a systematic way [124, 125]. The light cone expansion makes the integrals represent functions of a positive integer variable N. They turn out to be connected by Mellin transformations to the QCD improved parton model expressions [31]. As a result, in higher order calculations employing the light cone expansion, nested harmonic sums [64, 77–80, 104, 126, 127] occur. Similarly to the iterated integrals, nested sums imply algebraic [104, 105, 128] and structural relations [106–111], which allow to obtain compact representations for expressions involving them. At the same time the iterated nature allows for the algorithmic construction of analytic continuations and other relations.

The outline of the thesis is as follows. In Chapter 2 the kinematics of deep-inelastic scattering is presented and the structure functions are defined. In Chapter 3 the parton model is introduced, along with the methods for deriving QCD corrections. Chapter 4 presents the general structure of heavy quark corrections in the asymptotic regime. In Chapter 5 the main mathematical notions and methods for the thesis are briefly reviewed. After introducing the basic concepts and methods, new contributions are presented.

Chapter 6 is devoted to the calculation of the bubble-insertion type diagrams constituting the $O(\alpha_s^3 n_f T_F^2)$ contributions to the gluonic OMEs, which are necessary for the definition of variable flavor number schemes. In order to complete the 2-loop corrections in the polarized case, the corresponding massive OMEs are computed in Chapter 7, employing similar methods

as in the previous Chapter. Furthermore, in the following Chapters, methods for the calculation of more complicated massive topologies are developed on scalar prototype graphs. In Chapter 8, the calculation of so-called ladder and V-graph topologies is presented in detail, exploiting representations in terms of hypergeometric series. In Chapter 9, graphs with two distinct fermion lines are considered, which are carrying the same mass. A method is presented, which makes use of a Mellin-Barnes representation and utilizes the algebra of certain iterated integrals. Finally, the heavy quark corrections to charged current deep-inelastic scattering are extended to the second loop order in Chapter 10. Since asymptotic heavy quark coefficient functions are naturally expressed in N-space, the present lowest order heavy quark corrections are expressed and implemented in N-space first. The asymptotic representations of the 2-loop corrections are developed subsequently in terms of the massive OMEs and light flavor Wilson coefficients up to two loops. Chapter 11 gives the conclusions. Appendices A–F deal with a series of technical details.

Parts of the work presented in this thesis were already published in journals and conference proceedings. The $O(\alpha_s^3 n_f T_F^2)$ contributions to the massive OMEs $A_{gq,Q}$, and $A_{gg,Q}$ computed in Chapter 6 appeared in part in [101, 129, 130], and were published entirely in [131]. Intermediate results of the calculations of the 3-loop ladder diagrams in Chapter 8 appeared in [102, 129, 132]. The results were published completely in [133]. Parts of the results of the calculation of the diagrams with two distinct massive lines of equal mass in Chapter 9 were published in [130, 132]. The Mellin space expressions of the $O(\alpha_s)$ heavy flavor contributions to charged current DIS, together with a precise numerical implementation were published in [134]. Additionally, intermediate results were presented by the author on several conferences and workshops, such as the DPG Frühjahrstagungen 2010, 2011 and 2012, the DESY Theory Workshop in Hamburg 2010, the meeting of the DFG Sonderforschungsbereich Tansregio 9 in Karlsruhe 2011, and the meeting of the LHCPhenoNet initial training network in Ravello 2012.

2 Deep-Inelastic Scattering

In this Chapter, the kinematic variables used to describe deep-inelastic scattering will be introduced. Due to kinematic considerations, and symmetries of the electromagnetic and weak interaction, the hadronic part of the cross section will be parameterized in terms of the structure functions.

2.1 Kinematics

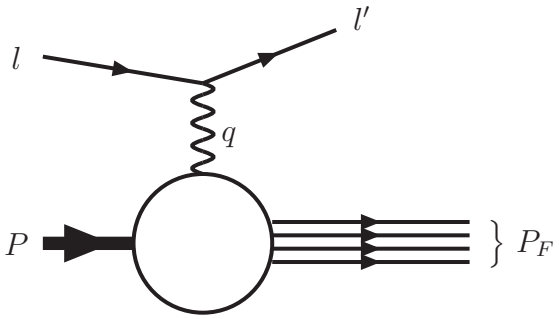

Figure 1: Deep-inelastic scattering

The kinematics of the deep-inelastic scattering process is depicted in Fig. 1. We will only consider single gauge boson exchange, while other contributions are covered by the electroweak radiative corrections, see e.g. [135]. The electroweak gauge boson of momentum q scatters off the constituents of the nucleon. In this way deep-inelastic scattering probes the substructure of protons and neutrons at large scales Q^2. The measurement of the final state is performed inclusively, i.e. all hadronic final states are summed over kinematically. As a consequence, the process depends on only two independent kinematic variables. In the following we define those, which are commonly used:

- The virtuality of the gauge boson

$$Q^2 = -q^2 = -(l - l')^2,\ Q^2 > 0 \tag{1}$$

  is the absolute value of the square of the boson momentum q.

- The square of the total center of mass energy

$$s = (l + P)^2 . \tag{2}$$

- The mass square of the hadronic final state is called

$$W^2 = P_F^2 = (q + P)^2 . \tag{3}$$

- The total energy transfer to the hadronic system has the form

$$\nu = \frac{P.q}{M} = \frac{1}{2M}(W^2 + Q^2 - M^2) , \tag{4}$$

  where M is the nucleon mass with $M^2 = P^2$.

At low values of Q^2 and large values of x also target mass corrections are important [136, 137]. The Bjorken scaling variable x and the inelasticity variable y are defined by:

$$x \equiv \frac{-q^2}{2P.q} = \frac{Q^2}{2M\nu} = \frac{Q^2}{W^2+Q^2-M^2}, \tag{5}$$

$$y \equiv \frac{P.q}{P.l} = \frac{2M\nu}{s} = \frac{W^2+Q^2-M^2}{s-M^2}, \tag{6}$$

neglecting the lepton mass. From these definitions one obtains

$$Q^2 = xys. \tag{7}$$

In this thesis Z-γ-mixing is not considered, which is sufficient if $Q^2 \leq 500$ GeV^2 [138]. The electroweak radiative corrections to DIS are available in [135, 139, 140], so we are only concerned with QCD corrections. Furthermore, we will mostly consider unpolarized DIS in the following.

The kinematic region, where the scattering is referred to as *deep-inelastic* is defined by $Q^2 > 4$ GeV^2 and $W > 2$ GeV, see e.g. [62]. The Bjorken limit [15], as commonly formulated [141, 142], is defined as the limit $Q^2, \nu \to \infty$ while $x = Q^2/2M\nu$ is kept fixed.

2.2 Matrix Element and Structure Functions

The interaction contribution to the Lagrangian density reads for the electromagnetic current, cf. [141–143]:

$$\mathcal{L}_{\text{int,em}} = eJ^\mu_{\text{em}} A_\mu \tag{8}$$

and for the weak current

$$\mathcal{L}_{\text{int,W}} = \frac{g_W}{2\sqrt{2}} J^\mu_{\text{W}} W_\mu, \tag{9}$$

with e the electric charge and g_w the weak charge, A_μ and W_μ the electromagnetic and charged weak fields, and J^μ_{em} and J^μ_W the associated fermionic currents.

Following the presentation in [144] the differential cross section for deep-inelastic scattering has the form:

$$\frac{d^3\sigma}{dxdyd\theta} = \frac{y\alpha^2}{Q^4} \sum_i \eta_i(Q^2) L^{\mu\nu}_{i,l} W^i_{\mu\nu}, \tag{10}$$

where in the present case of electromagnetic and charged current scattering i indicates the cases $i = \text{em}, W^-, W^+$ and l denotes the incoming lepton or antileptons. For unpolarized scattering the dependence on the azimuthal angle θ is trivial. The normalization constants $\eta_i(Q^2)$ have the values:

$$\eta^{\text{em}}(Q^2) = 1 \tag{11}$$

$$\eta^{W^-}(Q^2) = \eta^{W^+}(Q^2) = \frac{1}{2}\frac{G_F^2 Q^4}{(4\pi)^2\alpha^2}\left[\frac{M_W^2}{Q^2+M_W^2}\right]^2. \tag{12}$$

Note that in this thesis the electroweak part of the scattering process is only considered in Born approximation The leptonic tensors are then obtained by Dirac algebra. In the electromagnetic channel the massless leptonic tensor has the form:

$$L^{\text{em},e^-}_{\mu\nu} = L^{\text{em},e^+}_{\mu\nu} = \frac{1}{2}\sum_{\sigma,\sigma'} \bar{u}(l,\sigma)\gamma_\mu u(l',\sigma')\bar{u}(l',\sigma')\gamma_\nu u(l,\sigma) \tag{13}$$

$$= 2\left(l_\mu l'_\nu + l_\nu l'_\mu - \frac{Q^2}{2} g_{\mu\nu}\right), \tag{14}$$

while in the charged current channel one finds

$$L^{W^-,e^-}_{\mu\nu} = L^{W^+,\nu}_{\mu\nu} = \frac{1}{4}\sum_{\sigma,\sigma'} \bar{u}(l,\sigma)\gamma_\mu(1-\gamma_5)u(l',\sigma')\bar{u}(l',\sigma')\gamma_\nu(1-\gamma_5)u(l,\sigma) \tag{15}$$

$$= 2\left(l_\mu l'_\nu + l_\nu l'_\mu - \frac{Q^2}{2} g_{\mu\nu} + i\varepsilon_{\mu\nu\alpha\beta} l_\alpha l'_\beta\right), \tag{16}$$

$$L^{W^+,e^+}_{\mu\nu} = L^{W^-,\bar{\nu}}_{\mu\nu} = \frac{1}{4}\sum_{\sigma,\sigma'} \bar{v}(l,\sigma)\gamma_\nu(1-\gamma_5)v(l',\sigma')\bar{v}(l',\sigma')\gamma_\mu(1-\gamma_5)v(l,\sigma) \tag{17}$$

$$= 2\left(l_\mu l'_\nu + l_\nu l'_\mu - \frac{Q^2}{2} g_{\mu\nu} - i\varepsilon_{\mu\nu\alpha\beta} l_\alpha l'_\beta\right). \tag{18}$$

The hadronic tensor on the other hand, contains the nontrivial dynamics due to the hadron substructure, and will be subject to all further investigations. It has the form:

$$W^i_{\mu\nu}(q,P) = \frac{1}{4\pi}\sum_S \int d^4z\; e^{iq.z}\langle P,S \mid [J^{i\dagger}_\mu(z), J^i_\nu(0)] \mid P,S\rangle\,, \tag{19}$$

were the currents are indexed as follows $J^{W^+}_\mu := J^{\mathrm{W}}_\mu$, $J^{W^-}_\mu := J^{\mathrm{W}\dagger}_\mu$. Due to the optical theorem the hadronic tensor is related to the imaginary part of the forward Compton amplitude $T_{\mu\nu}$:

$$W^i_{\mu\nu}(q,P) = \frac{1}{\pi}\,\mathrm{Im}\,T^i_{\mu\nu}(q,P)\,, \tag{20}$$

where

$$T^i_{\mu\nu}(q,P) = i\int d^4z\; e^{iq.z}\sum_S \langle P,S \mid \mathsf{T} J^{i\dagger}_\mu(z) J^i_\nu(0) \mid P,S\rangle\,, \tag{21}$$

and T denotes time-ordering of the following operator product. The crossing transformation $q \to -q$, $\mu \leftrightarrow \nu$ has the effects $T^{\mathrm{em}}_{\nu\mu}(-q,P) = T^{\mathrm{em}}_{\mu\nu}(q,P)$ and $T^{W^\pm}_{\nu\mu}(-q,P) = T^{W^\mp}_{\mu\nu}(q,P)$ [145, 146]. It will, however, be useful to consider combinations which are either even or odd under crossing, so we define

$$T^{W^+\pm W^-}_{\mu\nu}(q,P) := T^{W^+}_{\mu\nu}(q,P) \pm T^{W^-}_{\nu\mu}(q,P)\,. \tag{22}$$

Due to its Lorentz structure, the hadronic tensor may in general be parameterized by 14 different structure functions (obeying Lorentz and time reversal invariance) [144–146], while current conservation, unpolarized initial states as well as neglecting target and quark mass corrections at the Born diagram level reduce them to only three structure functions:

$$W_{\mu\nu} = \frac{e_{\mu\nu}}{2x}F_L(x,Q^2) + \frac{d_{\mu\nu}}{2x}F_2(x,Q^2) + i\varepsilon_{\mu\nu\lambda\sigma}\frac{P_\lambda q_\sigma}{2P.q}F_3(x,Q^2)\,, \tag{23}$$

with the tensors

$$e_{\mu\nu} = \left(g_{\mu\nu} + \frac{q_\mu q_\nu}{Q^2}\right), \tag{24}$$

$$d_{\mu\nu} = \frac{4x^2}{Q^2}\left\{P_\mu P_\nu + \frac{q_\mu P_\nu + q_\nu P_\mu}{2x} - \frac{Q^2}{4x^2}g_{\mu\nu}\right\}. \tag{25}$$

The corresponding cross section for the electromagnetic current then takes the form

$$\frac{d\sigma}{dxdy} = \frac{2\pi\alpha^2}{Q^2xy}\left\{[1+(1-y)^2]F_2(x,Q^2) - y^2F_L(x,Q^2)\right\} . \tag{26}$$

The corresponding cross section formulae and expressions for the charged current processes will be given in Chapter 10.

3 The QCD Improved Parton Model

In the last Chapter, kinematics and symmetries of the currents were used to parameterize the hadronic tensor in terms of scalar functions F_i. In this Chapter, these structure functions shall be related to matrix elements of the underlying theory, which is QCD. This will be done in two approaches: First the more intuitive "parton model" is presented and later the field theoretic "operator product expansion on the light cone" is applied.

3.1 The Parton Model in Born Approximation

Using current algebra Bjorken predicted [15] a property of the structure functions called scaling. The structure functions of deep-inelastic scattering depend on 2 independent kinematic variables (cf. Section 2.1) e.g. Q^2, ν. Scaling means that in the limit $Q^2, \nu \to \infty$ keeping the ratio Q^2/ν finite, the structure functions effectively depend on this ratio, and hence on x, only. This prediction was soon confirmed experimentally [8–11] in the kinematic range accessible at that time.

To account for the fact of scaling, Feynman proposed the parton model [18]. The observed strict correlation $2\nu x = Q^2$ may be expressed by a δ-distribution $\delta(2\nu x - Q^2)$, which directly leads to the interpretation of the scattering off charged point-like particles, after a short calculation. These point-like particles were named partons. The model makes use of the idea, that the time scale of a scattering reaction of the electron with the proton is much shorter than the timescale of the binding force, which is called "impulse" approximation [147]. The hadronic tensor is then an incoherent sum of contributions from all partons, see e.g. [62],

$$W_{\mu\nu} = \frac{1}{4\pi} \sum_q \int_0^1 d\xi \; f_q(\xi) \frac{2P^0}{2p^0} |M_q|^2 2\pi\delta(p'^2 - m^2) \,, \tag{27}$$

with the following squared and spin-averaged matrix element for the boson-parton subsystem:

$$|M_q|^2 = 2e_q^2 \left[p_\mu p'_\nu + p_\nu p'_\mu - g_{\mu\nu} p.p' \right] . \tag{28}$$

Here p and p' are the momenta of the parton before and after the scattering, respectively. The sum runs over all types of partons q distinguished by their quantum numbers, and $f_q(\xi)$ is the parton number density function of parton q, which means it is the probability density for hitting a parton of type q with momentum fraction ξ in the proton.

The parton is assumed to carry a fraction ξ of the proton momentum P in collinear kinematics:

$$p = \xi P, \quad p^0 = \xi P^0 \,. \tag{29}$$

Applying momentum conservation $p' = \xi p + q$, the δ-distribution then fixes the momentum fraction:

$$\delta(p'^2 - m^2) = \frac{1}{q.P} \delta\left(\xi - \frac{Q^2 + m^2}{2q.P} \right) = \frac{1}{q.P} \delta\left(\xi - \frac{Q^2 + m^2}{Q^2} x \right) . \tag{30}$$

The cross section therefore takes the following form:

$$\frac{d^2\sigma}{dx\, dy} = \frac{2\pi\alpha^2}{Q^2 y} \sum_q e_q^2 f_q^2(\xi) (1 + (1-y)^2) \,. \tag{31}$$

For vanishing quark masses, a comparison with (26) yields the structure function F_2 showing the property of scaling:

$$F_2(x, Q^2) = F_2(x) = x \sum_q e_q^2 f_q(x)\,, \tag{32}$$

as well as the Callan-Gross relation [16]

$$F_L(x, Q^2) = 0\,. \tag{33}$$

For non-vanishing parton masses in the final state, the δ-distribution introduces an additional Q^2-dependence via the value of the momentum fraction:

$$\xi = \frac{Q^2 + m^2}{Q^2} x\,. \tag{34}$$

This phenomenon is called slow rescaling [137, 148–151], which vanishes as Q^2 becomes larger. It effectively bounds x from above:

$$x \leq \frac{Q^2}{Q^2 + m^2}\,. \tag{35}$$

Furthermore, it introduces a lower bound on ξ with

$$\xi = x + \frac{m^2}{2MyE_l} > \frac{m^2}{2MyE_l}\,, \tag{36}$$

where E_l denotes the incoming lepton energy in the rest frame of the hadron. This introduces a threshold for heavy quark production, due to $\xi < 1$, cf. [137],

$$E_l > \frac{m^2}{2M}\,, \tag{37}$$

which contributes to charged current deep-inelastic scattering.

3.2 QCD and the Operator Product Expansion on the Light Cone

In its original form, the parton model did not include interactions among the partons. As a binding force, quantum chromodynamics was proposed in [24]. Meanwhile it is the established theory of the strong interactions and is presented in many surveys, e.g. [141–143, 152, 153], for historical surveys see also [25, 26]. Its Lagrangian at the classical level is given by

$$\mathcal{L}_{\text{class}} = \sum_q \bar{\psi}_q (i\partial\!\!\!/ - m_q)\psi_q + g \sum_q \bar{\psi}_q \gamma_\mu B_a^\mu t^a \psi_q - \frac{1}{4} G_a^{\mu\nu} G^a_{\mu\nu}\,, \tag{38}$$

$$G_q^{\mu\nu} = \partial^\mu B_a^\nu - \partial^\nu B_a^\mu + g f_{abc} B_b^\mu B_c^\nu\,. \tag{39}$$

Here ψ_q denotes color triplet bispinors of quark flavor q, B_a are the gluon fields, where $a = 1, .., 8$. The generators t^a are expressed through the Gell-Mann matrices λ^a in color space by $t_a = \frac{1}{2}\lambda^a$. It is constructed as a gauge theory with an exact $SU(3)$ symmetry in color space. Its algebra is therefore non-abelian, i.e. the gauge theory is an example for a Yang-Mills theory [20].

For the strong coupling constant, also the following notations will be used:

$$\alpha_s \equiv \frac{g^2}{4\pi}\,, \tag{40}$$

$$a_s \equiv \frac{\alpha_s}{4\pi}\,. \tag{41}$$

For the quantization of this Lagrangian one has to add a part that fixes the gauge either covariantly introducing ghost fields [154] $\omega, \bar{\omega}$, that cancel the unphysical gluon degrees of freedom:

$$\mathcal{L}^{\xi}_{\rm GF} = -\frac{1}{2(1-\xi)}(\partial.B)^2 + (\partial_\mu\bar{\omega}_a)(\delta_{ab}\partial^\mu - g f_{abc}B^\mu_c)\omega_b\,, \tag{42}$$

or one requires the extra degrees of freedom to cancel explicitly, e.g. in an axial gauge [155], see e.g. [141],

$$\mathcal{L}^{n}_{\rm GF} = -\frac{1}{2\beta}(n.B)^2\,, \tag{43}$$

where the limit $\beta \to 0$ is to be taken such that $n.B = 0$ holds as an operator relation. The axial gauge depends on an arbitrary physical vector n with $n^2 \leq 0$.

Normally in higher order calculations the Fermi-Feynman gauge ($\xi = 0$) is used, which yields the gluon propagator

$$i\delta_{ab}\frac{-g^{\mu\nu}}{k^2 + i\varepsilon}\,, \tag{44}$$

while also the propagator in an axial gauge will be useful

$$i\frac{-g^{\mu\nu} - n^2k^\mu k^\nu/(k.n)^2 + (n^\mu k^\nu + n^\nu k^\mu)/(n.k)}{k^2 + i\varepsilon}\,. \tag{45}$$

The renormalizability of QCD as a massless Yang-Mills theory was proven by 't Hooft [21] in 1971. QCD was shown to develop a decreasing coupling constant in the limit of high energies or short distances [27, 28, 156], a feature denoted by asymptotic freedom. It delivers an argument for Feynman's assumption of effectively noninteracting partons in high energy collisions implying scaling, while at the same time it points towards the existence of confinement [157], due to the growing interaction strength for larger distances. This becomes important already at the size of the nucleon's radius. This means especially that macroscopic objects, such as the protons, neutrons, and pions are always color neutral.

Due to the asymptotic freedom, perturbation theory is applicable at sufficiently short distances, i.e. deep inside hadrons. It is therefore worthwhile to formulate this limit precisely. The tool used for this purpose is the expansion of an operator product at light like distances, which will henceforth be called light cone expansion (LCE).

In order to properly define products of currents at small space-like distances, K. Wilson and others proposed [29, 158, 159] to expand these products in a series of finite higher dimensional operators, with coefficient functions, which are subsequently called Wilson coefficients. They carry the eventual short distance singularities. To describe deep-inelastic scattering, the kinematic situation is, however, different: here the dominant contribution comes from operators at close to light like distances. Fortunately also in this region operator products may be expanded in a series of higher dimensional operators [30, 31, 160]. Apart from their canonical dimension d, the operators in this region carry another quantum number, the spin N.

A quantum number of central importance is the twist τ [47],

$$\tau = d - N\,, \tag{46}$$

since operators of the same twist may mix under renormalization.

An advantage of this representation comes from the fact, that the dominant contributions to deep-inelastic scattering come from the region of leading twist. The kinematic range for this approximation can be sketched as x being away from the boundaries 0 and 1, and Q^2 sufficiently large. The expansion has the form [29–31, 158, 160]:

$$\lim_{\xi^2\to 0} \mathsf{T} J(x)J(0) \sim \sum_{i,N,\tau} \bar{C}^N_{i,\tau}(\xi^2,\mu^2)\xi_{\mu_1}\ldots\xi_{\mu_N} O^{\mu_1\cdots\mu_N}_{i,\tau}(0,\mu^2)\,. \tag{47}$$

The leading twist contributions are shown to agree with the parton model, see e.g. [62, 142, 143], where hadronic matrix elements of the operators $O_{i,\tau}$ correspond to the parton distribution functions. The coefficient functions to the corresponding operators may be calculated in perturbation theory. The procedure for such calculations is outlined in e.g. [81, 82, 85, 143]. The collinear singularities of the Wilson coefficients can be factorized and absorbed into the renormalized parton distribution functions [38–46]. Higher twist contributions are naturally obtained, by the above expansion [161, 162], see also [62] and references therein[1].

In [172, 173] the higher twist contribution to the structure functions F_2 of the deuteron and proton were extracted from DIS non-singlet data, assuming that these contributions are negligible in the kinematic domain of $Q^2 \geq 4$ GeV^2 and $W^2 \geq 12.5$ GeV^2. Here parton distribution functions are extracted and the corresponding leading twist predictions for 4 GeV$^2 \leq W^2 \leq 12.5$ GeV^2 are subtracted from the data, see also [56]. This analysis shows, that current higher twist estimates strongly depend on the loop order used for the leading twist analysis. To reliably determine the higher twist contributions, at least the 3-loop approximation at $\tau = 2$ is required. Furthermore, neglecting higher twist effects in QCD analyses of DIS data leads to wrong determinations of the strong coupling α_s [56, 174].

Since nucleons couple to the electromagnetic and weak force via quark currents, for four active flavors u, d, s, c the currents have the form, see e.g. [141],

$$J^{\rm em}_\mu = e_u \bar{u}_u \gamma_\mu u_u + e_d \bar{u}_d \gamma_\mu u_d + e_s \bar{u}_s \gamma_\mu u_s + e_c \bar{u}_c \gamma_\mu u_c\,, \tag{48}$$

$$\begin{aligned} J^{\rm W}_\mu = {} & V_{ud}\bar{u}_u\gamma_\mu(1-\gamma_5)u_d + V_{us}\bar{u}_u\gamma_\mu(1-\gamma_5)u_s \\ & + V_{cd}\bar{u}_c\gamma_\mu(1-\gamma_5)u_d + V_{cs}\bar{u}_c\gamma_\mu(1-\gamma_5)u_s\,, \end{aligned} \tag{49}$$

where $e_u = e_c = 2/3$, $e_d = e_s = -1/3$, and V_{ij} are the CKM matrix elements [175, 176]. For the operator product expansion, these are considered in matrix notation:

$$J^{\rm em}_\mu = \bar{\psi}\Lambda^{\rm em}\gamma_\mu\psi := \begin{pmatrix} \bar{u}_u \\ \bar{u}_d \\ \bar{u}_c \\ \bar{u}_s \end{pmatrix}^T \begin{pmatrix} e_u & 0 & 0 & 0 \\ 0 & e_d & 0 & 0 \\ 0 & 0 & e_c & 0 \\ 0 & 0 & 0 & e_s \end{pmatrix} \gamma_\mu \begin{pmatrix} u_u \\ u_d \\ u_c \\ u_s \end{pmatrix}\,, \tag{50}$$

$$J^W_\mu = \bar{\psi}\Lambda^W\gamma_\mu(1-\gamma_5)\psi := \begin{pmatrix} \bar{u}_u \\ \bar{u}_d \\ \bar{u}_c \\ \bar{u}_s \end{pmatrix}^T \begin{pmatrix} 0 & V_{ud} & 0 & V_{us} \\ 0 & 0 & 0 & 0 \\ 0 & V_{cd} & 0 & V_{cs} \\ 0 & 0 & 0 & 0 \end{pmatrix} \gamma_\mu(1-\gamma_5) \begin{pmatrix} u_u \\ u_d \\ u_c \\ u_s \end{pmatrix}\,. \tag{51}$$

[1] Partonic descriptions of higher twist contributions are also possible [163–171].

For the following combinations of the weak currents the flavor matrix becomes (anti)hermitian:

$$J_\mu^W \pm J_\mu^{W\dagger} = \bar\psi \Lambda^{W\pm W} \gamma_\mu(1-\gamma_5)\psi := \begin{pmatrix} \bar u_u \\ \bar u_d \\ \bar u_c \\ \bar u_s \end{pmatrix}^T \begin{pmatrix} 0 & V_{ud} & 0 & V_{us} \\ \pm\bar V_{ud} & 0 & \pm\bar V_{cd} & 0 \\ 0 & V_{cd} & 0 & V_{cs} \\ \pm\bar V_{us} & 0 & \pm\bar V_{cs} & 0 \end{pmatrix} \gamma_\mu(1-\gamma_5) \begin{pmatrix} u_u \\ u_d \\ u_c \\ u_s \end{pmatrix} . \quad (52)$$

At leading twist the light cone expansion of the product of currents in (19) takes the form [30, 160], see also [143]:

$$\begin{aligned} \tilde T_{\mu\nu}^{\rm em} :=\ & i\int d^4z\, e^{iq.z}\, \mathsf{T} J_\mu^{\dagger i}(z) J_\nu^i(0) \\ =\ & \sum_{N,j}\Big[-(g_{\mu\mu_1}g_{\nu\mu_2}q^2 - g_{\mu\mu_1}q_\nu q_{\mu_2} - q_\mu q_{\mu_1}g_{\nu\mu_2} + g_{\mu\nu}q_{\mu_1}q_{\mu_2})C_{2,N}^j\left(\frac{Q^2}{\mu^2},g^2\right) \\ & + \left(g_{\mu\nu} - \frac{q_\mu q_\nu}{q^2}\right) q_{\mu_1}q_{\mu_2} C_{L,N}^j\left(\frac{Q^2}{\mu^2},g^2\right) - i\varepsilon_{\alpha\beta\mu\nu}g_{\alpha\mu_1}q_\beta q_{\mu_2} C_{3,N}^j\left(\frac{Q^2}{\mu^2},g^2\right)\Big] \\ & q_{\mu_3}\dots q_{\mu_N}\left(\frac{2}{Q^2}\right)^N O_j^{\mu_1\dots\mu_N} . \end{aligned} \quad (53)$$

The operators contributing at leading twist are:

$$O_{q,r;\mu_1,\dots,\mu_N}^{\rm NS} = i^{N-1}\mathbf{S}[\bar\psi\gamma_{\mu_1}D_{\mu_2}\dots D_{\mu_N}\lambda_r\psi] - \text{trace terms}, \quad (54)$$

$$O_{q;\mu_1,\dots,\mu_N}^{\rm S} = i^{N-1}\mathbf{S}[\bar\psi\gamma_{\mu_1}D_{\mu_2}\dots D_{\mu_N}\psi] - \text{trace terms}, \quad (55)$$

$$O_{g;\mu_1,\dots,\mu_N} = 2i^{N-2}\mathbf{SSp}[F_{\mu_1\alpha}^a D_{\mu_2}\dots D_{\mu_{N-1}}F_{\mu_N}^{\alpha,a}] - \text{trace terms}, \quad (56)$$

where $\mathbf{S}$ denotes symmetrization of the Lorentz indices $\mu_1,\dots,\mu_N$, $\mathbf{Sp}$ the color trace, ψ denotes the quark field, $F_{\mu\nu}^a$ the gluon field strength tensor, D_μ the covariant derivative and λ_r the generators of the group $SU(n)_{flavor}$ with n active flavors. In general, via linear combinations of non-singlet operators, a whole family of non-singlet operators is formed, which correspond to linear combinations of the generators λ_r. For the definition of parton distributions, one considers the (n dimensional) flavor diagonal matrices:

$$\lambda_k = \text{diag}(\underbrace{0,\dots,0}_{k-1},1,\underbrace{0,\dots,0}_{n-k}) - \frac{1}{n}\text{diag}(\underbrace{1,\dots,1}_{n}) . \quad (57)$$

Taking matrix elements of these operators using the proton states yields the hadronic operator matrix elements:

$$\frac{1}{2}\sum_S \langle P,S \mid O_{q,k;\mu_1,\dots,\mu_N}^{\rm NS} \mid P,S\rangle = A_{q,N}^{{\rm NS},k}(\mu^2)P_{\mu_1}\dots P_{\mu_N} + \text{trace terms}, \quad (58)$$

$$\frac{1}{2}\sum_S \langle P,S \mid O_{q;\mu_1,\dots,\mu_N}^{\rm S} \mid P,S\rangle = A_{q,N}^{\rm S}(\mu^2)P_{\mu_1}\dots P_{\mu_N} + \text{trace terms}, \quad (59)$$

$$\frac{1}{2}\sum_S \langle P,S \mid O_{g;\mu_1,\dots,\mu_N} \mid P,S\rangle = A_{g,N}(\mu^2)P_{\mu_1}\dots P_{\mu_N} + \text{trace terms}. \quad (60)$$

One obtains

$$T_{\mu\nu} = \sum_{j,N}\frac{1}{x^N}\left[e_{\mu\nu}C_{L,N}^j\left(\frac{Q^2}{\mu^2},g^2\right) + d_{\mu\nu}C_{2,N}^j\left(\frac{Q^2}{\mu^2},g^2\right) - i\varepsilon_{\mu\nu\alpha\beta}\frac{P_\alpha q_\beta}{2P.q}C_{3,N}^j\left(\frac{Q^2}{\mu^2},g^2\right)\right]A_N^j\left(\mu^2\right) . \quad (61)$$

Using dispersion relations, Mellin moments of the structure functions may be written as [31]:

$$\int_0^1 dx\, x^{N-2} F_L(x,Q^2) = \sum_j A_N^j(\mu^2)\, C_L^j\left(N, \frac{Q^2}{\mu^2}\right), \tag{62}$$

$$\int_0^1 dx\, x^{N-2} F_2(x,Q^2) = \sum_j A_N^j(\mu^2)\, C_2^j\left(N, \frac{Q^2}{\mu^2}\right), \tag{63}$$

$$\int_0^1 dx\, x^{N-1} F_3(x,Q^2) = \sum_j A_N^j(\mu^2)\, C_3^j\left(N, \frac{Q^2}{\mu^2}\right), \tag{64}$$

with j indexing the gluon, quark singlet, and quark non-singlet operators. For massless quarks, the last equation on the right hand side contains only the non-singlet contribution.

3.3 Light Flavor Wilson Coefficients and Parton Distribution Functions

A description of scattering reactions has to relate color neutral objects with the colored quark and gluon degrees of freedom, and hence non-perturbative contributions might spoil a purely perturbative picture. Fortunately, for large enough scales Q^2, a factorization of these quantities is possible [38–46], which gives the following structure, if all quarks are treated massless:

$$\begin{aligned} F_i(x,Q^2) = x\frac{1}{n_f}\sum_q e_q^2 \Bigg[&\Sigma(x,\mu^2) \otimes C_{i,q}^{\rm S}\left(x, \frac{Q^2}{\mu^2}\right) + G(x,\mu^2) \otimes C_{i,g}\left(x, \frac{Q^2}{\mu^2}\right) \\ &+ n_f \Delta_q(x,\mu^2) \otimes C_{i,q}^{\rm NS}\left(x, \frac{Q^2}{\mu^2}\right)\Bigg], \quad i = 2, L\,. \end{aligned} \tag{65}$$

Here n_f is the number of quark flavors, e_q are their electric charges, G, Σ and Δ_q denote the parton distribution functions (PDF) of the gluon, the singlet combination of quark flavors, and the non-singlet combination for each flavor q, respectively. The sum runs over all light flavors, typically u, d, s. The functions $C_{i,q}^{\rm NS}$, $C_{i,q}^{\rm S}$, $C_{i,g}$ are the (flavor) non-singlet, singlet and gluonic Wilson coefficients, cf. [64, 81–83]. Usually the singlet contribution is split into the non-singlet and a pure singlet contribution:

$$C_{i,q}^{\rm S} = C_{i,q}^{\rm NS} + C_{i,q}^{\rm PS}\,. \tag{66}$$

The symbol $\otimes$ denotes Mellin convolution:

$$f(x) \otimes g(x) = \int_0^1 dy \int_0^1 dz\, \delta(x - yz) f(y) g(z)\,. \tag{67}$$

Denoting the parton distributions of the individual flavors by their initials, e.g. $u(x,\mu^2)$, $d(x,\mu^2)$, $s(x,\mu^2)$, the pure singlet and non-singlet combinations are given by:

$$\Sigma = \sum_q \left[q\left(x,\mu^2\right) + \bar{q}\left(x,\mu^2\right)\right], \tag{68}$$

$$\Delta_q = q\left(x,\mu^2\right) + \bar{q}\left(x,\mu^2\right) - \frac{1}{n_f}\Sigma\left(x,\mu^2\right). \tag{69}$$

Using Equations (62–64) and (65), the hadronic operator matrix elements can be related to the PDFs, cf. [143]:

$$A_{q,N}^{{\rm NS},k}(\mu^2) = \int_0^1 dx\, x^{N-1} \Delta_k(x,\mu^2)\,, \tag{70}$$

$$A_{q,N}^{\rm S}(\mu^2) = \int_0^1 dx\, x^{N-1} \Sigma(x,\mu^2)\,, \tag{71}$$

$$A_{g,N}(\mu^2) = \int_0^1 dx\, x^{N-1} G(x,\mu^2)\,. \tag{72}$$

In the following, the Mellin-space and the x-space representations are written with the same function name and exchanging the letters x, and N, i.e.:

$$\Delta_k(N,\mu^2) := A_{q,N}^{{\rm NS},k}(\mu^2)\,, \tag{73}$$

$$\Sigma(N,\mu^2) := A_{q,N}^{\rm S}(\mu^2)\,, \tag{74}$$

$$G(N,\mu^2) := A_{g,N}(\mu^2)\,. \tag{75}$$

The parton distribution functions are non-perturbative and process independent quantities, which may be determined in fits to scattering data [55, 56, 59, 60, 177–180]. The Wilson coefficients describe the process dependent parts and are calculable in perturbation theory. The factorization introduces an unphysical scale, the factorization scale μ_F^2, which is chosen to be equal to the renormalization scale, denoted by μ^2 below. Its effect gradually disappears calculating higher order corrections, since the structure functions are independent of μ^2.

For the renormalization of the operators a set of renormalization constants is defined:

$$O_{q,r;\mu_1,...,\mu_N}^{\sf NS} = Z^{\sf NS}(\mu^2) \hat{O}_{q,r;\mu_1,...,\mu_N}^{\sf NS}\,, \tag{76}$$

$$O_{i;\mu_1,...,\mu_N}^{\sf S} = Z_{ij}^{\sf S}(\mu^2) \hat{O}_{j;\mu_1,...,\mu_N}^{\sf S}\,,\ i = q,g\,. \tag{77}$$

Here the hat denotes the renormalized operators, and a sum over j is understood. The Z-factors impart a scale dependence to the operators, which can be described by renormalization group equations [48–52, 181]. One therefore defines the total derivative w.r.t. the renormalization scale:

$$\mathcal{D}(\mu^2) \equiv \mu^2 \frac{\partial}{\partial \mu^2} + \beta(a_s(\mu^2)) \frac{\partial}{\partial a_s(\mu^2)} - \gamma_m(a_s(\mu^2)) m(\mu^2) \frac{\partial}{\partial m(\mu^2)}\,, \tag{78}$$

where the QCD β-function and the mass anomalous dimension are given by:

$$\beta(a_s(\mu^2)) \equiv \mu^2 \frac{\partial a_s(\mu^2)}{\partial \mu^2}\,, \tag{79}$$

$$\gamma_m(a_s(\mu^2))) \equiv -\frac{\mu^2}{m(\mu^2)} \frac{\partial m(\mu^2)}{\partial \mu^2}\,. \tag{80}$$

Then one uses the condition for the observable structure functions to be independent of the renormalization scale, i.e.

$$\mathcal{D}(\mu^2) F_i(x,Q^2) = 0\,, \tag{81}$$

to derive the renormalization group equations for the OMEs, cf. [143],

$$\frac{d}{d\ln\mu^2} \begin{pmatrix} \Sigma(n_f,N,\mu^2) \\ G(n_f,N,\mu^2) \end{pmatrix} = -\frac{1}{2} \begin{pmatrix} \gamma_{qq} & \gamma_{qg} \\ \gamma_{gq} & \gamma_{gg} \end{pmatrix} \begin{pmatrix} \Sigma(n_f,N,\mu^2) \\ G(n_f,N,\mu^2) \end{pmatrix}\,, \tag{82}$$

$$\frac{d}{d\ln\mu^2} \Delta_k(n_f,N,\mu^2) = -\frac{1}{2} \gamma_{qq}^{\sf NS} \Delta_k(n_f,N,\mu^2)\,, \tag{83}$$

and for the Wilson coefficients

$$\frac{d}{d\ln\mu^2} \begin{pmatrix} C_{q,i}^{\rm PS}(n_f,N,Q^2/\mu^2) \\ C_{g,i}(n_f,N,Q^2/\mu^2) \end{pmatrix} = \frac{1}{2} \begin{pmatrix} \gamma_{qq} & \gamma_{qg} \\ \gamma_{gq} & \gamma_{gg} \end{pmatrix} \begin{pmatrix} C_{q,i}^{\rm PS}(n_f,N,Q^2/\mu^2) \\ C_{g,i}(n_f,N,Q^2/\mu^2) \end{pmatrix}\,, \tag{84}$$

$$\frac{d}{d\ln\mu^2} C_{q,i}^{\rm NS}(n_f, N, Q^2/\mu^2) \;=\; \frac{1}{2}\gamma_{qq}^{\sf NS} C_{q,i}^{\rm NS}(n_f, N, Q^2/\mu^2)\,, \tag{85}$$

The anomalous dimensions are then obtained from the Z-factors by

$$\gamma_{qq}^{\sf NS} = \mu Z^{-1,{\sf NS}}(\mu^2)\frac{\partial}{\partial\mu} Z^{\sf NS}(\mu^2)\,, \tag{86}$$

$$\gamma_{ij}^{\sf S} = \mu Z_{il}^{-1,{\sf S}}(\mu^2)\frac{\partial}{\partial\mu} Z_{lj}^{\sf S}(\mu^2)\,. \tag{87}$$

The leading order [32, 34, 182, 183], next to leading order [184–191] and next-to-next-to leading order [126, 127, 192–195] anomalous dimensions are known. The light flavor Wilson coefficients for deep-inelastic scattering by photon exchange were calculated to $O(\alpha_s)$ [196–199], $O(\alpha_s^2)$ [81–83, 200–202] and $O(\alpha_s^3)$ [64]. The heavy flavor contributions will be discussed in further detail in the next Chapter.

With the precise knowledge of higher order corrections to the Wilson coefficients it is possible to determine the PDFs accurately from DIS data. However, as can be seen from (65), the fit to the deep-inelastic structure functions alone constrains combinations of quark PDFs. In addition it also constrains the gluon distribution, however, to a lesser extent, since the influence of the gluon initial states only enter through QCD corrections, and hence are suppressed by a factor of α_s. As a consequence, PDF analyses make use of the process independence of the PDFs and combine data from different processes, such as DIS on proton or deuteron targets, DIS via charged currents, semi inclusive DIS, the Drell-Yan process [203] and jet cross sections in hadron-hadron collisions.

Especially for the constraint of the gluon distribution, heavy quark pair production is of major interest, since its dominant contribution comes from the virtual-photon-gluon fusion process [65–68, 204]. Since the gluon distribution rises steeply towards low values of x, in this region heavy quark contributions are important and may amount up to 25–35%.

4 Heavy Flavor Contributions

The presence of a quark field with a non-negligible mass can lead to sizable corrections with respect to the purely massless case, particularly for reference scales of the order of the mass. Within perturbative QCD, the difference between "heavy" and "light" quarks is defined comparing their mass to the scale $\Lambda_{\rm QCD}$:

- If $m^2 \lesssim \Lambda^2_{\rm QCD}$, one talks about (generically) light quarks, which can be produced in the non-perturbative regime of QCD. Hence to each light quark a parton distribution function is associated. It is treated as massless in perturbative calculations.
- If $m^2 \gg \Lambda^2_{\rm QCD}$, the quark is called (generically) heavy, it can thus only be produced radiatively in final states. Hence no generic parton distribution is associated with it. However, due to a scheme change, a heavy quark parton distribution can be constructed for $Q^2 \gg m^2$, as will be seen below.

Looking at recent values for these parameters [7] one finds $\Lambda_{\rm QCD} \sim 200 - 300$ MeV so that the on-shell masses for the quarks lead to the following classifications:

$$\underbrace{m_u \approx 2 \text{ MeV},\ m_d \approx 5 \text{ MeV},\ m_s \approx 100 \text{ MeV}}_{\text{light}},\ \underbrace{m_c \approx 1.3 \text{ GeV},\ m_b \approx 4.2 \text{ GeV},\ m_t \approx 173 \text{ GeV}}_{\text{heavy}}\ . \tag{88}$$

Following the classification in [205], one can distinguish kinematic regions of a scattering process with respect to the present heavy quark mass (assuming n_f other light quarks):

- $m^2 \gg Q^2$: Decoupling region. Due to the Appelquist-Carazzone theorem [206], the heavy quark effectively decouples in QCD, i.e. diagrams containing a heavy quark line are suppressed by orders of Q^2/m^2. Parameters of the theory are renormalized in a scheme with n_f light flavors (n_f-flavor scheme).
- $m^2 \sim Q^2$: Threshold region. Graphs with massive lines give sizable corrections and the process contains full dependence on both scales. The parameters of the theory may still be renormalized in an n_f-flavor scheme, while the heavy quark mass enters through Wilson coefficients.
- $m^2 \ll Q^2$: Asymptotic region. The heavy quark can eventually be treated like the other light quarks, i.e. effectively $n_f + 1$ light flavors are present, the parameters of the theory are renormalized in an (n_f+1)-flavor scheme. A parton distribution function is assigned to the "heavy" quark. However, process independent transition coefficients emerge [75, 87].

When a calculation in the n_f-flavor scheme is considered deep in the asymptotic region, massive lines become effectively massless and thus develop infrared and collinear singularities. The Bloch-Nordsieck theorem [207] guarantees the cancellation of infrared divergencies, while the Konshita-Lee-Nauenberg (KLN) theorem [208, 209] states that if there are degenerate sets of incoming or outgoing states, then collinear divergencies cancel when all diagrams connected to these sets are taken into account.

However, for deep-inelastic scattering the leading twist approximation implies that there is only one parton in the initial state, so the KLN theorem is not applicable, and collinear (or mass) singularities remain. That these can be factorized from the hard scattering cross sections order by order in perturbation theory is assured by the factorization theorems [38–46], which make it

possible to absorb these singularities into the parton distribution functions. The dependence on the mass is thereby carried by matrix elements of the operators in (54–56). The result coincides with the $(n_f + 1)$-flavor scheme which in this context of heavy quark corrections is also referred to as zero mass variable flavor scheme (ZMVFNS). A "heavy" quark density can be calculated as described in [75, 87]. Changes between these schemes will be discussed further in Chapter 6.

It should be noted that the calculations of Feynman graphs with a massive line introduces more complicated functions and integrals, than in the purely massless case. This can be seen from the fact, that the 3-loop corrections to the light flavor Wilson coefficients of electromagnetic DIS were published completely as analytic results [64], while already the 2-loop corrections to the heavy flavor Wilson coefficients were given as semianalytic codes [70–72].

It is this complexity which makes one consider another interesting kinematic region, which will be of larger interest in the rest of the thesis. It is the region where the mass m is much smaller than the reference scale μ so that power corrections can be safely neglected, but is still large enough such that logarithms of the type $\ln(m^2/\mu^2)$ do not spoil the convergence of the perturbative expansion. In this region the Wilson coefficients factorize into mass-dependent operator matrix elements and the massless Wilson coefficient [76], and thereby reduce the complexity of the calculations.

The massive contributions to the neutral current DIS structure functions are known to LO [65–68, 204, 210] and NLO [70–72]. Furthermore, approximate NNLO results [211, 212] were obtained via threshold resummation. These are also valid somewhat above threshold, since the gluon distribution rises steeply for low momentum fractions, and photon gluon fusion is the dominant process for heavy flavor production. Approximate NLO contributions are also available in the asymptotic region [76]. In [76] the asymptotic representations were shown to hold for $Q^2/m^2 \gtrsim 10$ in case of F_2. In case of F_L the range of validity starts at far higher scales $Q^2/m^2 \gtrsim 800$; the corresponding 3-loop corrections were given in [213].

The charged current Wilson coefficients were calculated to $O(\alpha_s)$ [73, 74, 214–217]. Further details on the heavy flavor contributions in this case will be given in Chapter 10.

In several experimental [218–221] and phenomenological [65–68, 70–72, 204, 222–224] studies the scaling violations of heavy flavor contributions to the DIS structure functions were shown to have a different shape as compared to the massless case, and allow for accessing the gluon density in neutral current DIS. In charged current processes they give a handle on the strange quark content of the hadrons [74, 225, 226].

4.1 Heavy Quark Wilson Coefficients in the Region $Q^2 \gg m^2$

The following presentation of the formalism to include heavy quark corrections is restricted to DIS by photon exchange. For the charged current case the reader is referred to Chapter 10.

The heavy quark contributions to the Wilson coefficients of (65) can be split into two classes:

- $L_{i,q}^{\rm S}, L_{i,g}, L_{i,q}^{\rm NS}$: Here all diagrams contribute, where the photon couples to a light quark line, and heavy quarks contribute via pair production and loop corrections.

- $H_{i,q}^{\rm PS}, H_{i,g}$: In the diagrams for these functions the photon couples to the heavy quark line. Here no NS-contributions are present, since these would only be necessary for intrinsic charm scenarios, which are experimentally disfavored, cf. e.g. [227].

In terms of these Wilson coefficients, the heavy flavor contributions to the structure functions

for $Q^2 \gg m^2$ can be written [76]:

$$F_i(x,Q^2,m^2) = x\frac{1}{n_f}\sum_q e_q^2\Biggl\{\Sigma\left(x,\mu^2\right)\otimes L_{i,q}^{\rm S}\left(x,\frac{Q^2}{m^2},\frac{m^2}{\mu^2}\right) + G(\left(x,\mu^2\right)\otimes L_{i,g}\left(x,\frac{Q^2}{m^2},\frac{m^2}{\mu^2}\right) + n_f\Delta_q\left(x,\mu^2\right)\otimes L_{i,q}^{\rm NS}\left(x,\frac{Q^2}{m^2},\frac{m^2}{\mu^2}\right)\Biggr\} + xe_Q^2\Biggl\{\Sigma\left(x,\mu^2\right)\otimes H_{i,q}^{\rm PS}\left(x,\frac{Q^2}{m^2},\frac{m^2}{\mu^2}\right) + G\left(x,\mu^2\right)\otimes H_{i,g}\left(x,\frac{Q^2}{m^2},\frac{m^2}{\mu^2}\right)\Biggr\}, \quad i = 2, L\,. \tag{89}$$

Here n_f denotes the number of light flavors and the sum runs over these flavors. e_Q denotes the electric charge of the heavy flavor.

As was mentioned earlier, the derivation of the asymptotic representation [76] follows the mass factorization prescription in the light flavor case [83]. As a consequence, the heavy flavor Wilson coefficients are written as combinations of light flavor Wilson coefficients and massive operator matrix elements:

$$C_{q,(2,L)}^{\sf NS}\Bigl(N,n_f,\frac{Q^2}{\mu^2}\Bigr) + L_{q,(2,L)}^{\sf NS}\Bigl(N,n_f+1,\frac{Q^2}{\mu^2},\frac{m^2}{\mu^2}\Bigr) = A_{qq,Q}^{\sf NS}\Bigl(N,n_f+1,\frac{m^2}{\mu^2}\Bigr)C_{q,(2,L)}^{\sf NS}\Bigl(N,n_f+1,\frac{Q^2}{\mu^2}\Bigr), \tag{90}$$

$$\begin{aligned} C_{q,(2,L)}^{\sf PS}(n_f) + L_{q,(2,L)}^{\sf PS}(n_f+1) &= \Bigl[A_{qq,Q}^{\sf NS}(n_f+1) + A_{qq,Q}^{\sf PS}(n_f+1) + A_{Qq}^{\sf PS}(n_f+1)\Bigr] \\ &\quad\times n_f\tilde{C}_{q,(2,L)}^{\sf PS}(n_f+1) + A_{qq,Q}^{\sf PS}(n_f+1)C_{q,(2,L)}^{\sf NS}(n_f+1) \\ &\quad + A_{gq,Q}(n_f+1)n_f\tilde{C}_{g,(2,L)}(n_f+1)\,, \end{aligned} \tag{91}$$

$$\begin{aligned} C_{g,(2,L)}(n_f) + L_{g,(2,L)}(n_f+1) &= A_{gg,Q}(n_f+1)n_f\tilde{C}_{g,(2,L)}(n_f+1) \\ &\quad + A_{qg,Q}(n_f+1)C_{q,(2,L)}^{\sf NS}(n_f+1) \\ &\quad + \Bigl[A_{qg,Q}(n_f+1) + A_{Qg}(n_f+1)\Bigr]n_f\tilde{C}_{q,(2,L)}^{\sf PS}(n_f+1)\,, \end{aligned} \tag{92}$$

$$\begin{aligned} H_{q,(2,L)}^{\sf PS}(n_f+1) &= A_{Qq}^{\sf PS}(n_f+1)\Bigl[C_{q,(2,L)}^{\sf NS}(n_f+1) + \tilde{C}_{q,(2,L)}^{\sf PS}(n_f+1)\Bigr] \\ &\quad + \Bigl[A_{qq,Q}^{\sf NS}(n_f+1) + A_{qq,Q}^{\sf PS}(n_f+1)\Bigr]\tilde{C}_{q,(2,L)}^{\sf PS}(n_f+1) \\ &\quad + A_{gq,Q}(n_f+1)\tilde{C}_{g,(2,L)}(n_f+1)\,, \end{aligned} \tag{93}$$

$$\begin{aligned} H_{g,(2,L)}(n_f+1) &= A_{gg,Q}(n_f+1)\tilde{C}_{g,(2,L)}(n_f+1) + A_{qg,Q}(n_f+1)\tilde{C}_{q,(2,L)}^{\sf PS}(n_f+1) \\ &\quad + A_{Qg}(n_f+1)\Bigl[C_{q,(2,L)}^{\sf NS}(n_f+1) + \tilde{C}_{q,(2,L)}^{\sf PS}(n_f+1)\Bigr]\,. \end{aligned} \tag{94}$$

Here for the Wilson coefficients the following notation is introduced:

$$\tilde{C}_j(n_f) \equiv \frac{1}{n_f}C_j(n_f)\,, \quad \tilde{C}_j(n_f+1) \equiv \frac{1}{n_f+1}C_j(n_f+1)\,. \tag{95}$$

The arguments n_f+1 of the OMEs and heavy flavor Wilson coefficients denote the number of flavors, which are n_f light and one heavy flavors, these arguments will be dropped in the following.

The light flavor Wilson coefficients depend on the number of flavors, which are treated as light. If the dependence is not written explicitly, the argument is assumed to be set to n_f. The scale dependences of the light flavor Wilson coefficients, the massive OMEs, and the heavy flavor Wilson coefficients are always understood as indicated in (90).

The operator matrix elements $A^{\rm NS}_{qq,Q}$, $A^{\rm PS}_{qq,Q}$, $A^{\rm PS}_{Qq}$, $A_{gq,Q}$, $A_{qg,Q}$, A_{Qg} and $A_{gg,Q}$ are closely related to the Green's functions:

$$\hat{G}^{ij}_{\alpha,Q} = \quad J_N \langle q,j \mid O_\alpha \mid q,i \rangle_Q \,, \tag{96}$$

$$\hat{G}^{ab}_{\alpha,Q,\mu\nu} = \quad J_N \langle g,\nu,b \mid O_\alpha \mid g,\mu,a \rangle_Q \,, \tag{97}$$

where in the external states the color indices for the fundamental (i,j), and adjoint (a,b) representation are written explicitly. Furthermore, the subscript Q indicates that only contributions are taken into account, in which heavy quark lines occur, and α indexes the operators (54–56), i.e.

$$O_\alpha \in \{O^{\rm NS}_{q,k;\mu_1,\ldots,\mu_N}, O^{\rm S}_{q;\mu_1,\ldots,\mu_N} O^{\rm NS}_{Q,r;\mu_1,\ldots,\mu_N}, O^{\rm S}_{Q;\mu_1,\ldots,\mu_N} O_{g;\mu_1,\ldots,\mu_N}\} \,. \tag{98}$$

The operator matrix elements are then defined via projections in the following way [87, 184, 185, 228, 229]. The source factor

$$J_N = \Delta_{\mu_1} \ldots \Delta_{\mu_N} \tag{99}$$

with $\Delta^2 = 0$ has been introduced, in order to explicitly remove the trace terms in (54–56). The Green's functions still bear a Lorentz or spinor structure, as well as color indices. These structures are due to the properties of the partonic state, and are symbolically contained in the index α. The operator matrix elements are defined by projecting this structure to 1. There are two ways to construct the projector for the Green's functions with external gluon states [87]:

$$P^{(1),\mu\nu}_{g,ab} \equiv - \frac{\delta_{ab}}{N_c^2-1} \frac{g^{\mu\nu}}{D-2} (\Delta\cdot p)^{-N} \,, \tag{100}$$

$$P^{(2),\mu\nu}_{g,ab} \equiv \frac{\delta_{ab}}{N_c^2-1} \frac{1}{D-2} (\Delta\cdot p)^{-N} \left(-g^{\mu\nu} + \frac{p^\mu \Delta^\nu + p^\nu \Delta^\mu}{\Delta\cdot p} \right) . \tag{101}$$

The first one keeps contributions from nonphysical gluon states, which are removed by the inclusion of graphs with external ghost lines. The second one also removes these unphysical parts, external ghost lines are not necessary. The projector for external quark lines has the form

$$P^{ij}_q \equiv \frac{\delta^{ij}}{N_c} (\Delta\cdot p)^{-N} \frac{1}{4} \mathsf{Tr}\, \not{p} \,, \tag{102}$$

where the operand is first multiplied with $\not{p}$, and then the spinor trace is taken. Here i,j denote color indices in the fundamental representation.

The operator matrix elements are then defined as projections of the Green's functions [87]:

$$\hat{\hat{A}}_{qg,Q} \left(\frac{\hat{m}^2}{\mu^2}, \varepsilon, N \right) = P^{(1,2),\mu\nu}_{g,ab} \hat{G}^{ab}_{qg,Q,\mu\nu} \,, \tag{103}$$

$$\hat{\hat{A}}_{Qg} \left(\frac{\hat{m}^2}{\mu^2}, \varepsilon, N \right) = P^{(1,2),\mu\nu}_{g,ab} \hat{G}^{ab}_{Qg,\mu\nu} \,, \tag{104}$$

$$\hat{\hat{A}}_{gg,Q} \left(\frac{\hat{m}^2}{\mu^2}, \varepsilon, N \right) = P^{(1,2),\mu\nu}_{g,ab} \hat{G}^{ab}_{gg,Q,\mu\nu} \,, \tag{105}$$

$$\hat{\hat{A}}_{gq,Q}\left(\frac{\hat{m}^2}{\mu^2},\varepsilon,N\right) = P_q^{ij}\hat{G}_{gq,Q,ij}\,, \tag{106}$$

$$\hat{\hat{A}}^{\rm S}_{qq,Q}\left(\frac{\hat{m}^2}{\mu^2},\varepsilon,N\right) = P_q^{ij}\hat{G}^{\rm S}_{qq,Q,ij}\,, \tag{107}$$

$$\hat{\hat{A}}^{\rm NS}_{qq,Q}\left(\frac{\hat{m}^2}{\mu^2},\varepsilon,N\right) = P_q^{ij}\hat{G}^{\rm NS}_{qq,Q,ij}\,, \tag{108}$$

$$\hat{\hat{A}}^{\rm PS}_{Qq}\left(\frac{\hat{m}^2}{\mu^2},\varepsilon,N\right) = P_q^{ij}\hat{G}^{\rm S}_{Qq,ij}\,, \tag{109}$$

where the double hat indicates that these quantities are unrenormalized. The Feynman rules for the operators are summarized in Appendix E.

Note that again a pure singlet contribution is defined such that

$$A^S_{qq,Q} = A^{\rm PS}_{qq,Q} + A^{\rm NS}_{qq,Q}\,. \tag{110}$$

4.2 Renormalization of the Massive OMEs

Feynman integrals are in general divergent quantities, which have to be regularized due to a consistent prescription. In the calculations of the present thesis, dimensional regularization [89–92] is used. Later, it is the purpose of the renormalization to remove the singularities, that occur in the limit $\varepsilon \to 0$, such that the predictive power of the theory is regained.

In dimensional regularization, instead of 4 spacetime dimensions, one formulates the theory in $D = 4 + \varepsilon$ spacetime dimensions. All Feynman integrals therefore represent functions of the parameter ε. These functions are analytically continued, such that a Laurent series expansion around $\varepsilon = 0$ can be performed. The momentum integrals in D dimensions are always traced back to the integral:

$$\int \frac{d^Dk}{(2\pi)^D}\frac{(k^2)^r}{(k^2+R^2)^m} = \frac{1}{(4\pi)^{D/2}}\frac{\Gamma(r+D/2)\Gamma(m-r-D/2)}{\Gamma(D/2)\Gamma(m)(R)^{m-r-D/2}}\,, \tag{111}$$

for euclidean momenta k. Additionally, within dimensional regularization, scaleless integrals of the type

$$\int \frac{d^Dk}{(2\pi)^D}\frac{1}{(k^2)^m} \tag{112}$$

vanish.

Noting that the action of the theory has mass dimension 0, the coupling constant in the D-dimensional theory $\hat{g}'_s$ acquires a nonzero mass dimension. Therefore a dimensionless coupling constant $\hat{g}_s$ is defined, introducing an arbitrary scale μ:

$$\hat{g}'_s = \mu^{-\varepsilon/2}\hat{g}_s\,. \tag{113}$$

Also the Dirac algebra is continued to D spacetime dimensions, which causes a problem with γ_5 and the Levi-Civita symbol $\varepsilon_{\mu\nu\rho\sigma}$, since both are inherently four dimensional objects [89]. A useful prescription was given in [89, 230–232] leading to

$$\gamma_\mu\gamma_5 = \frac{1}{6}i\varepsilon_{\mu\nu\rho\sigma}\gamma^\nu\gamma^\rho\gamma^\sigma\,, \tag{114}$$

in axial vector couplings, and contracting the Levi-Civita symbols using the relation:

$$\varepsilon_{\alpha\beta\gamma\delta}\varepsilon_{\mu\nu\rho\sigma} = \left| \begin{array}{cccc} g_{\alpha\mu} & g_{\alpha\nu} & g_{\alpha\rho} & g_{\alpha\sigma} \\ g_{\beta\mu} & g_{\beta\nu} & g_{\beta\rho} & g_{\beta\sigma} \\ g_{\gamma\mu} & g_{\gamma\nu} & g_{\gamma\rho} & g_{\gamma\sigma} \\ g_{\delta\mu} & g_{\delta\nu} & g_{\delta\rho} & g_{\delta\sigma} \end{array} \right| . \tag{115}$$

The Lorentz contractions are performed in D dimensions. For higher order calculations the axial vector coupling needs a finite renormalization [232].

As mentioned above, the singularities represented in powers of $1/\varepsilon$, have to be absorbed by a redefinition of the parameters of the theory. A common scheme in which this is achieved is the $\overline{\rm MS}$ scheme [196, 233]. It combines two observations. First, absorbing only the singularities into the renormalization constants yields a consistent and unique prescription for rendering the theory predictions finite [233]. Second, a factor

$$S_\varepsilon = \exp\left[\frac{\varepsilon}{2}(\gamma_E - \ln(4\pi))\right] \tag{116}$$

appears for each loop integral. This can be checked from (111), with the relation:

$$\frac{\Gamma(1-\frac{\varepsilon}{2})}{(4\pi)^{\varepsilon/2}} = S_\varepsilon \exp\left(\sum_{i=2}^{\infty} \frac{\zeta_i}{i}\left(\frac{\varepsilon}{2}\right)^i\right) , \tag{117}$$

where $\zeta_k = \zeta(i)$ denotes Riemann's ζ-function. Therefore, the factor S_ε is an artefact of the regularization prescription, and can be removed along with the ε-poles. In the $\overline{\rm MS}$ scheme it is set to one at the end of the calculation.

The procedure for renormalizing the massive operator matrix elements includes, apart from the usual renormalization of theory parameters like masses and the coupling constants, also a renormalization of the operators themselves. A renormalization procedure presented in [228] with off-shell external lines, demands the calculation of additional unphysical contributions. These are stemming from the violation of the equations of motion as well as non-gauge invariant operators. These complications arise in the massless case, since the corresponding integrals are scaleless. Hence one has to keep the external momentum artificially off shell. For massive OMEs an internal scale is present and the external lines can be kept on shell.

Nevertheless, in order to keep the on-shell condition of the external line, mass and charge renormalization have to take place in a physical scheme. After the operator renormalization a finite scheme change is used to express mass and coupling in the $\overline{\rm MS}$ scheme. The consistent renormalization procedure was developed in [87], see also [229]. Essential relations are repeated in the following.

First, the mass is renormalized using the prescriptions in [234–238]

$$\hat{m} \;=\; Z_m m = m\left[1 + \hat{a}_s\left(\frac{m^2}{\mu^2}\right)^{\varepsilon/2}\delta m_1 + \hat{a}_s^2\left(\frac{m^2}{\mu^2}\right)^{\varepsilon}\delta m_2\right] + O(\hat{a}_s^3)\,, \tag{118}$$

where the coefficients are

$$\delta m_1 \;=\; C_F\left[\frac{6}{\varepsilon} - 4 + \left(4 + \frac{3}{4}\zeta_2\right)\varepsilon\right] \tag{119}$$

$$\equiv\; \frac{\delta m_1^{(-1)}}{\varepsilon} + \delta m_1^{(0)} + \delta m_1^{(1)}\varepsilon\,, \tag{120}$$

$$\delta m_2 \;=\; C_F\left\{\frac{1}{\varepsilon^2}\Big(18C_F - 22C_A + 8T_F(n_f + N_h)\Big) + \frac{1}{\varepsilon}\Big(-\frac{45}{2}C_F + \frac{91}{2}C_A\right.$$

$$
\begin{aligned}
&-14T_F(n_f+N_h)\Big) + C_F\Big(\frac{199}{8} - \frac{51}{2}\zeta_2 + 48\ln(2)\zeta_2 - 12\zeta_3\Big)\\
&+C_A\Big(-\frac{605}{8} + \frac{5}{2}\zeta_2 - 24\ln(2)\zeta_2 + 6\zeta_3\Big)\\
&+T_F\Big[n_f\Big(\frac{45}{2} + 10\zeta_2\Big) + N_h\Big(\frac{69}{2} - 14\zeta_2\Big)\Big]\Bigg\} \qquad (121)\\
\equiv\ & \frac{\delta m_2^{(-2)}}{\varepsilon^2} + \frac{\delta m_2^{(-1)}}{\varepsilon} + \delta m_2^{(0)}\,. \qquad (122)
\end{aligned}
$$

The formula is given for n_f light and N_h heavy flavors. In the rest of the thesis $N_h = 1$ will be needed.

Coupling constant renormalization in the desired $\overline{\rm MS}$ scheme is achieved by absorbing the ε-poles into the constant $Z_g^{\overline{\rm MS}}(\varepsilon, n_f)$:

$$
\begin{aligned}
\hat{a}_s &= Z_g^{\overline{\rm MS}^2}(\varepsilon, n_f) a_s^{\overline{\rm MS}}(\mu^2)\\
&= a_s^{\overline{\rm MS}}(\mu^2)\left[1 + \delta a_{s,1}^{\overline{\rm MS}}(n_f) a_s^{\overline{\rm MS}}(\mu^2) + \delta a_{s,2}^{\overline{\rm MS}}(n_f) a_s^{\overline{\rm MS}^2}(\mu^2)\right] + O(a_s^{\overline{\rm MS}^3})\,. \qquad (123)
\end{aligned}
$$

Here, the coefficients have the values [27, 28, 156, 239–241]

$$
\begin{aligned}
\delta a_{s,1}^{\overline{\rm MS}}(n_f) &= \frac{2}{\varepsilon}\beta_0(n_f)\,, \qquad (124)\\
\delta a_{s,2}^{\overline{\rm MS}}(n_f) &= \frac{4}{\varepsilon^2}\beta_0^2(n_f) + \frac{1}{\varepsilon}\beta_1(n_f)\,, \qquad (125)
\end{aligned}
$$

with the coefficients in the a_s-expansion of the $\overline{\rm MS}$ β-function:

$$
\begin{aligned}
\beta_0(n_f) &= \frac{11}{3}C_A - \frac{4}{3}T_F n_f\,, \qquad (126)\\
\beta_1(n_f) &= \frac{34}{3}C_A^2 - 4\left(\frac{5}{3}C_A + C_F\right)T_F n_f\,. \qquad (127)
\end{aligned}
$$

However in order to maintain the factorization property of the OMEs, a MOM scheme is introduced, by demanding that the heavy quark loop contribution to the gluon vacuum polarization vanishes at zero momentum, i.e. $\Pi_H(0, m^2) = 0$. This relation is conveniently stated in the background field formalism [242–244], see also [141], in which the background field renormalization constant Z_A is related to the renormalization constant of the coupling Z_g by

$$
Z_A = Z_g^{-2}\,. \qquad (128)
$$

Here Z_A is built from a light quark and a heavy quark part. The light quark part $Z_{A,l}$ is defined by the $\overline{\rm MS}$ prescription in the light quark sector and (128), i.e.

$$
Z_{A,l} = Z_g^{\overline{\rm MS}^{-2}}(\varepsilon, n_f)\,. \qquad (129)
$$

The heavy quark part is defined such that it absorbs the heavy quark loop contributions to the gluon vacuum polarization [87]:

$$
\Pi_{H,\rm BF}(0, m^2) + Z_{A,H} \equiv 0\,. \qquad (130)
$$

The renormalization constant for the coupling constant in the MOM scheme is then defined by (128):

$$Z_g^{\rm MOM}(\varepsilon, n_f+1, \mu^2, m^2) \equiv \frac{1}{(Z_{A,l}+Z_{A,H})^{1/2}}\,. \tag{131}$$

The calculation was performed in [87]. One finds:

$$\begin{aligned}\hat{a}_s &= Z_g^{\rm MOM^2}(\varepsilon, n_f+1, \mu^2, m^2) a_s^{\rm MOM}(\mu^2, m^2) \\ &= a_s^{\rm MOM}(\mu^2, m^2)\left[1 + a_s^{\rm MOM}(\mu^2, m^2)\delta a_{s,1}^{\rm MOM} + a_s^{\rm MOM}(\mu^2, m^2)^2 \delta a_{s,2}^{\rm MOM}\right]\,,\end{aligned} \tag{132}$$

with

$$\delta a_{s,1}^{\rm MOM} = \left[\frac{2\beta_0(n_f)}{\varepsilon} + \frac{2\beta_{0,Q}}{\varepsilon} f(\varepsilon)\right], \tag{133}$$

$$\begin{aligned}\delta a_{s,2}^{\rm MOM} &= \left[\frac{\beta_1(n_f)}{\varepsilon} + \left(\frac{2\beta_0(n_f)}{\varepsilon} + \frac{2\beta_{0,Q}}{\varepsilon} f(\varepsilon)\right)^2\right. \\ &\left. + \frac{1}{\varepsilon}\left(\frac{m^2}{\mu^2}\right)^{\varepsilon}\left(\beta_{1,Q} + \varepsilon\beta_{1,Q}^{(1)} + \varepsilon^2\beta_{1,Q}^{(2)}\right)\right] + O(\varepsilon^2)\,.\end{aligned} \tag{134}$$

The coefficients in the a_s-expansion of the QCD β-function in this MOM scheme are given by:

$$\beta_{1,Q} = \hat{\beta}_1(n_f) = -4\left(\frac{5}{3}C_A + C_F\right)T_F\,, \tag{135}$$

$$\beta_{1,Q}^{(1)} = -\frac{32}{9}T_F C_A + 15 T_F C_F\,, \tag{136}$$

$$\beta_{1,Q}^{(2)} = -\frac{86}{27}T_F C_A - \frac{31}{4}T_F C_F - \zeta_2\left(\frac{5}{3}T_F C_A + T_F C_F\right)\,. \tag{137}$$

After that, the operators are renormalized. In order not to confuse collinear poles and ultraviolet poles, which both are regularized by ε, the renormalization constants are derived from the ones of the massless OMEs. Knowing the anomalous dimensions, the Z-factors for the massless OMEs can be reconstructed from Eq. (87) order by order in perturbation theory.

These Z-factors are then the $\overline{\rm MS}$-renormalization constants, provided the mixture with unphysical terms can be neglected, so

$$A_{qq}^{\sf NS}\left(\frac{-p^2}{\mu^2}, a_s^{\overline{\sf MS}}, n_f, N\right) = Z_{qq}^{-1,{\sf NS}}(a_s^{\overline{\sf MS}}, n_f, \varepsilon, N)\hat{A}_{qq}^{\sf NS}\left(\frac{-p^2}{\mu^2}, a_s^{\overline{\sf MS}}, n_f, \varepsilon, N\right), \tag{138}$$

$$A_{ij}\left(\frac{-p^2}{\mu^2}, a_s^{\overline{\sf MS}}, n_f, N\right) = Z_{il}^{-1}(a_s^{\overline{\sf MS}}, n_f, \varepsilon, N)\hat{A}_{lj}\left(\frac{-p^2}{\mu^2}, a_s^{\overline{\sf MS}}, n_f, \varepsilon, N\right),\ i,j = q,g\,. \tag{139}$$

Adding another flavor carrying the mass m leads to operator matrix elements, which can be seen as a sum of the former ones plus the massive OMEs, which for the moment are also considered with slightly off-shell external legs:

$$\hat{A}_{ij}(p^2, m^2, \mu^2, a_s^{\rm MOM}, n_f+1) = \hat{A}_{ij}\left(\frac{-p^2}{\mu^2}, a_s^{\overline{\sf MS}}, n_f\right) + \hat{A}_{ij}^{Q}(p^2, m^2, \mu^2, a_s^{\rm MOM}, n_f+1)\,. \tag{140}$$

The massive OMEs are here indicated by the superscript Q. Note that the coupling constant renormalization had been performed in the MOM-scheme for the massive OMEs, while it was performed in the $\overline{\rm MS}$ scheme for the massless ones. Furthermore, the contribution δ_{ij} is considered part of the massless OME. Hence the renormalization is performed for the non-δ_{ij} part and both parts are combined afterwards.

The renormalization constants for these (n_f+1)-flavor OMEs are then derived from the ones of the massless n_f-flavor OMEs by the replacements $n_f \to n_f+1$, $a_s^{\overline{\rm MS}} \to a_s^{\rm MOM}$:

$$\hat{A}_{ij}(p^2,m^2,\mu^2,a_s^{\rm MOM},n_f+1) = Z_{il}(a_s^{\rm MOM},n_f+1,\varepsilon,N)\bar{A}_{lj}(p^2,m^2,\mu^2,a_s^{\rm MOM},n_f+1)\,. \quad (141)$$

This defines the renormalized (n_f+1)-flavor OME $\bar{A}_{lj}$. However, since one is interested in the renormalization of the heavy flavor part alone, the renormalized version is split again into a heavy flavor part and the $\overline{\rm MS}$-renormalized light flavor part from above:

$$\bar{A}_{ij}(p^2,m^2,\mu^2,a_s^{\rm MOM},n_f+1) = \bar{A}_{ij}^{Q^2}(p^2,m^2,\mu^2,a_s^{\rm MOM},n_f+1) + A_{ij}\left(\frac{-p^2}{\mu^2},a_s^{\overline{\rm MS}},n_f\right)\,. \quad (142)$$

So combining (140, 141), inserting (138, 139, 142), and solving for $\bar{A}_{lj}^{Q^2}$ yields:

$$\begin{aligned}\bar{A}_{ij}^{Q}(p^2,m^2,\mu^2,a_s^{\rm MOM},n_f+1) = {}& Z_{il}^{-1}(a_s^{\rm MOM},n_f+1,\mu^2)\hat{A}_{lj}^{Q}(p^2,m^2,\mu^2,a_s^{\rm MOM},n_f+1)\\ &+ Z_{il}^{-1}(a_s^{\rm MOM},n_f+1,\mu^2)\hat{A}_{lj}\left(\frac{-p^2}{\mu^2},a_s^{\overline{\rm MS}},n_f\right)\\ &- Z_{il}^{-1}(a_s^{\overline{\rm MS}},n_f,\mu^2)\hat{A}_{lj}\left(\frac{-p^2}{\mu^2},a_s^{\overline{\rm MS}},n_f\right)\,. \end{aligned} \quad (143)$$

In the limit $p^2 \to 0$, the scaleless integrals vanish. Hence for the massless contributions one is left with the Born contribution:

$$\hat{A}_{ij}\left(0,a_s^{\overline{\rm MS}},n_f\right) = \delta_{ij}\,. \quad (144)$$

With this prescription the ultraviolet poles can be removed. However collinear singularities of the massless lines remain, which have to be removed via mass factorization:

$$\bar{A}_{ij}^{Q}\left(\frac{m^2}{\mu^2},a_s^{\rm MOM},n_f+1\right) = A_{il}^{Q}\left(\frac{m^2}{\mu^2},a_s^{\rm MOM},n_f+1\right)\Gamma_{lj}(n_f)\,. \quad (145)$$

The operators on the right hand side will be called renormalized operators in the following. If only massless quarks were present, the transition functions and renormalization constants would be inverses of each other:

$$\Gamma_{ij} = Z_{ij}^{-1}\,. \quad (146)$$

However, since in this case heavy quark lines are present, the n_f-flavor transition function occurs. Also, due to the absence of the δ_{ij}-part from the very beginning of the renormalization procedure, the $O(\alpha_s^3)$ parts do not contribute. The δ_{ij}-part is added back to the finite OMEs.

The general structure of the renormalized massive OMEs was given in [87, 229] in terms of the coefficients in Eqs. (120, 122), the coefficients of the $\overline{\rm MS}$- and MOM-scheme β-functions in (126, 127, 135, 136, 137), as well as the anomalous dimensions in (86, 87).

5 Methodology of the Calculations

Perturbative quantum field theory provides on the one hand rules for expressing the Wilson coefficients given in previous Chapters in terms of Feynman diagrams. On the other hand it provides Feynman rules, which allow for translating these graphs into functions of kinematic quantities. After the reduction of color and spin traces, the momentum integrals of graphs contributing to the massive OME's have the following form, up to constant coefficients:

$$\int \prod_i \hat{d}k_i \frac{\prod_{j_1,j_2}(p_{j_1}.p_{j_2})^{\lambda_{j_1,j_2}}}{\prod_j (p_j^2 - m_j^2)} \mathrm{OP}_\alpha^{(N)}(\tilde{p}_1, ..., \tilde{p}_\alpha)\,, \tag{147}$$

where $\hat{d}k_i = \frac{d^D k_i}{(2\pi)^D}$ with k_i the independent internal momenta, p_j are the momenta of the internal lines, and p_{j_1}, p_{j_2} are internal and external momenta. Furthermore, $\lambda_{j_1,j_2} \in \mathbb{N}$ and $\mathrm{OP}_\alpha^{(N)}(\tilde{p}_1, ..., \tilde{p}_\alpha)$ are polynomials of Nth degree in scalar products $\Delta.\tilde{p}_i$ stemming from the operator insertion. For $\alpha = 1, 2, 3$ it has the form[2]:

$$\begin{aligned}
\mathrm{OP}_1^{(N)}(\tilde{p}_1) &= (\Delta.\tilde{p}_1)^N\,,\\
\mathrm{OP}_2^{(N)}(\tilde{p}_1, \tilde{p}_2) &= \sum_{j=0}^{N} (\Delta.\tilde{p}_1)^{N-j} (\Delta.\tilde{p}_2)^j\,,\\
\mathrm{OP}_3^{(N)}(\tilde{p}_1, \tilde{p}_2, \tilde{p}_3) &= \sum_{j=0}^{N} \sum_{l=0}^{j} (\Delta.\tilde{p}_1)^{N-j} (\Delta.\tilde{p}_2)^{j-l} (\Delta.\tilde{p}_3)^l\,.
\end{aligned} \tag{148}$$

The $\tilde{p}_j$ are combinations of internal and external momenta, that depend on the position of the operator insertion. Note that throughout the thesis $D = 4 + \varepsilon$ will be the spacetime dimension.

Using a Feynman parameterization, see e.g. [141],

$$\prod_{i=1}^{n} \frac{1}{A_i^{\lambda_i}} = \frac{\Gamma(\sum \lambda_i)}{\prod_{i=1}^n \Gamma(\lambda_i)} \int_{[0,1]^n} \left(\prod_{i=1}^{n} dx_i x_i^{\lambda_i - 1} \right) \left[\sum_{i=1}^{n} x_i A_i \right]^{-\sum \lambda_i} \delta\left(1 - \sum x_i\right)\,, \tag{149}$$

and using 111, one can map the Minkowski space integrals onto integrals over the unit hypercube $[0,1]^n$.

Similar to earlier analytic calculations of 3-loop massive OMEs, e.g. [79, 88], the parametrization is performed loop momentum per loop momentum, starting from simple sub-topologies and preferring peripheral ones to more central ones. In this way for each loop momentum a family of Feynman parameters is introduced.

The integral is then of the form

$$\int_{[0,1]^n} dx_1 \ \ldots dx_n \left(\prod_{\text{families } f} \delta^f \right) \underbrace{x_1^{\nu_1 - 1} \ldots x_n^{\nu_n - 1}}_{\text{monomial prefactor}} \underbrace{\prod_{i=1}^{n} x_i^{\alpha_i} (1 - x_i)^{\beta_i}}_{\text{non-monomial prefactor}} \frac{\overbrace{P_O(x_1, \ldots, x_n; N)}^{\text{operator polynomial}}}{\underbrace{[P_D(x_1, \ldots, x_n)]^\gamma}_{\substack{\text{denominator}\\ \text{polynomial}}}}\,, \tag{150}$$

where for each Feynman parameter family f we used the shorthand

$$\delta^f \equiv \delta\left(1 - \sum_{x \in f} x\right)\,, \tag{151}$$

[2]The value of N may vary due to shifts in different representations.

and ν_i are integers denoting the powers with which the propagators occur in (147). The exponents α_i, β_i are proportional to ε, N is the Mellin variable and γ has the form $\gamma = a+b\varepsilon$ where $a, b \in \mathbb{Q}$. The operator polynomial is not strictly a polynomial, but in all following cases the δ-distributions and Heaviside functions can be removed in such a way that the misnomer is corrected, and the operator polynomial is indeed a polynomial of maximum degree $N \in \mathbb{N}$.

In the case, where the operator polynomial has the simple form

$$P_O(x_1, \ldots, x_n; N) = [\bar{P}_O(x_1, \ldots, x_n)]^N \,, \tag{152}$$

with a polynomial $\bar{P}_O(x_1, \ldots, x_n)$ which is linear in each Feynman parameter, it will also be referred to as N-bracket.

Applying the δ-distributions one obtains

$$\int_0^1 dx\, \delta(1-x-Y) f(x) = \theta(Y)\theta(1-Y) f(1-Y) \,, \tag{153}$$

where Y is either a sum of Feynman parameters or a single one. In this way Heaviside θ-functions are introduced:

$$\theta(x) = \left\{ \begin{array}{ll} 1, & x \geq 0 \\ 0, & x < 0 \end{array} \right. . \tag{154}$$

These Heaviside functions are then removed applying the relation

$$\int_0^1 dx\, \theta(1-x-Y) f(x) = \int_0^1 dx\, \theta(1-Y)(1-Y) f(x(1-Y)) \,, \tag{155}$$

where Y is again either a sum of Feynman parameters or a single one. These procedures still offer the freedom in the choice of the order in which the above relations are applied to the Feynman parameters within one family. Rules for choosing this order effectively will be developed in Chapters 8 and 9.

Furthermore, the above relations can be read from right to left, giving the freedom to build θ-functions and δ-distributions, which are then removed again applying the same relations differently. These ideas are used in Chapter 9 systematically in Feynman integral calculations. In a different view, these relations imply coordinate transformations of the set of Feynman parameters, which map the integration region to itself. An example for such a derivation is given in Appendix B.

The routes of momenta through the graph are assigned in such a way, that the average number of loop momenta flowing through a line is minimal.

5.1 Harmonic Polylogarithms and Harmonic Sums

The results of higher order perturbative calculations in QED showed the occurrence of special numbers like $\zeta_2, \zeta_3, \ln(2)$ [120, 121, 123, 245]. These numbers were discovered calculating long tables of integrals over products of logarithms. Similar integrals carrying a dependence on a real variable were found in perturbative QCD calculations, e.g. [83, 86]. A systematic study of these integrals was made possible through the rediscovery of a certain type of Poincaré iterated integrals called harmonic polylogarithm [122, 246–248], and the harmonic sums [104–107, 128].

The construction of the harmonic polylogarithms begins with the choice of an alphabet $\mathfrak{A}$, which is a set of simple rational functions. In massless perturbative QCD the alphabet [122]

$$\mathfrak{A} = \left\{ f_0(x) := \frac{1}{x}, f_1(x) := \frac{1}{1-x}, f_{-1}(x) := \frac{1}{1+x} \right\} \tag{156}$$

is sufficient for various calculations, e.g. the 3-loop splitting functions and light flavor Wilson coefficients of [64, 126, 127]. The $f_i(x)$ are called letters.

A harmonic polylogarithm (HPL) is then constructed recursively setting

$$H_{\underbrace{0,\ldots,0}_{n\text{-times}}}(x) = \frac{1}{n!}\ln^n(x)\,,$$
$$H_i(x) = \int_0^x dy\; f_i(y), \quad \text{for } i \neq 0\,, \tag{157}$$

and iterating

$$H_{i,\vec{a}}(x) = \int_0^x dy\; f_i(y) H_{\vec{a}}(y) \tag{158}$$

if either $\vec{a} \neq (0,\ldots,0)$ or $i \neq 0$. The length of the index list $\vec{a}$ of a HPL $H_{\vec{a}}(x)$ is then called its weight.

Many properties of these functions can be traced back to the properties of rational functions exploiting the combinatorics of the iterated integrals. A central role is played by the property of the product of two integrals

$$\int_0^x dy f(y) \int_0^x dz g(z) = \int_0^x dy f(y) \int_0^y dz g(z) + \int_0^x dz g(z) \int_0^z dy f(y) \tag{159}$$

which induces a set of relations, called shuffle relations. They can be generated recursively in the following way:

$$H_{a_1,\ldots,a_k}(x) H_{b_1,\ldots,b_l}(x) = \int_0^x dy\; f_{a_1}(y) H_{a_2,\ldots,a_k}(y) H_{b_1,\ldots,b_l}(y)$$
$$+ \int_0^x dy\; f_{b_1}(y) H_{a_1,\ldots,a_k}(y) H_{b_2,\ldots,b_l}(y)\,. \tag{160}$$

Due to these relations one can choose for each given weight a certain number of basis functions, and express all other HPLs by these basis elements and polynomials of functions of lower weight. The construction of such a basis as well as the corresponding reductions are automated in the Mathematica package HarmonicSums [108–111] by J. Ablinger. The package also allows for the extension of the above alphabet, which will be necessary for the calculations in Chapter 9.

For the numerical evaluation of the functions defined above, FORTRAN routines were given in [124].

When calculating QCD corrections using the light cone expansion, the results depend on a positive integer variable N denoting the operator spin, cf. [47]. These results are related to the momentum space via the Mellin transformation

$$\mathbf{M}[f](N) = \int_0^1 dx\; x^{N-1} f(x)\,. \tag{161}$$

Here, in context of leading twist quantities, x corresponds to the Bjorken scaling variable (5). One therefore speaks of representations of functions in x-space and Mellin space (or Mellin N-space). The inverse of this transformation is given by the Mellin inversion theorem

$$f(x) = \frac{1}{2\pi i} \int_{c-i\infty}^{c+i\infty} ds\; x^{-s}\; \mathbf{M}[f](s)\,, \tag{162}$$

where c is chosen such, that the contour lies to the right of the rightmost singularity of $\mathbf{M}[f](s)$. However, in order to apply the inversion, a unique analytic continuation to complex values of N has to exist, which is subject to conditions, stated in Carlson's theorem [249, 250], for a precise formulation and detailed discussion of this aspect in the present context, see [111].

The Mellin transformation maps the HPLs from above, onto the class of harmonic sums [104–106, 186, 187], which are recursively defined via:

$$S_{a,\vec{b}}(N) = \sum_{i=1}^{N} \frac{(\mathrm{sign}(a))^i}{i^{|a|}} S_{\vec{b}}(i)\,, \quad S_\emptyset = 1\,, \tag{163}$$

where $a, b_1, \ldots, b_{d-1} \in \mathbb{Z} \setminus \{0\}$, and d is called (nesting) depth of $S_{a,\vec{b}}(N)$.

In larger formulae, the shorthand notation

$$S_{\vec{a}} \equiv S_{\vec{a}}(N)\,, \tag{164}$$

is used. To a sum $S_{\vec{a}}$ of depth d one assigns a weight w defined by

$$w = \sum_{i=1}^{d} a_i\,. \tag{165}$$

The harmonic sums obey relations which have the structure of a quasi-shuffle relation [251], and which are known as stuffel relations [104–106, 123]. They follow from splitting the product of two sums into parts in the following way:

$$\sum_{k=1}^{N} \frac{1}{k^a} \sum_{l=1}^{N} \frac{1}{l^b} = \sum_{k=1}^{N} \frac{1}{k^a} \sum_{l=1}^{k} \frac{1}{l^b} + \sum_{l=1}^{N} \frac{1}{l^b} \sum_{k=1}^{l} \frac{1}{k^a} + \sum_{l=1}^{N} \frac{1}{l^{a+b}}\,. \tag{166}$$

The relations are constructed recursively from

$$\begin{aligned} S_{a_1,\ldots,a_k}(N) S_{b_1,\ldots,b_l}(N) = & \sum_{i=1}^{N} \frac{\mathrm{sign}(a_1)^i}{i^{|a_1|}} S_{a_2,\ldots,a_k}(i) S_{b_1,\ldots,b_l}(i) \\ & + \sum_{i=1}^{N} \frac{\mathrm{sign}(b_1)^i}{i^{|b_1|}} S_{a_1,\ldots,a_k}(i) S_{b_2,\ldots,b_l}(i) \\ & - \sum_{i=1}^{N} \frac{(\mathrm{sign}(a_1)\,\mathrm{sign}(b_1))^i}{i^{|a_1|+|b_1|}} S_{a_2,\ldots,a_k}(i) S_{b_2,\ldots,b_l}(i)\,. \end{aligned} \tag{167}$$

These algebraic relations can be used to reduce sets of harmonic sums to smaller sets of basis sums. This method was developed in [104–106, 128] and finally implemented into the Mathematica package HarmonicSums. Furthermore, this package generates asymptotic expansions of these sums, which are needed for precise numerical representations of their analytic continuations, cf. also [105–107, 252, 253].

This machinery is, however, not sufficient for 3-loop QCD calculations, for in intermediate steps generalized harmonic sums may occur as was realized in [64], see also Chapter 8 and [133].

The generalized harmonic sums, also called S-sums, are defined [111, 254] via

$$S_{a_1,\ldots,a_n}(\xi_1,\ldots,\xi_n;N) = \sum_{i=1}^{N} \frac{\xi_1^i}{i^{a_1}} S_{a_2,\ldots,a_n}(\xi_2,\ldots,\xi_n;i)\,, \quad S_\emptyset(N) = 1\,, \tag{168}$$

with positive indices $a_1, \ldots, a_n \in \mathbb{N}$.

Furthermore, another generalization of harmonic sums will become important in Chapter 9, which is the class of cyclotomic harmonic sums [110]. These are built from the alphabet

$$\left\{ a_{\{l,m,n\}}(k) = \frac{(\mathrm{sign}(n))^k}{(lk+m)^{|n|}} \;\middle|\; l,m \in \mathbb{N} \setminus \{0\}, n \in \mathbb{Z} \setminus \{0\} \right\}. \tag{169}$$

For the omitted case $l = 1, m = 0$, the alphabet of the usual harmonic sums (163) emerges

$$\left\{ a_n(k) = \frac{(\mathrm{sign}(n))^k}{k^{|n|}} \;\middle|\; n \in \mathbb{Z} \setminus \{0\} \right\}. \tag{170}$$

Also cyclotomic S-sums [110] will be of interest, which are constructed from the alphabet

$$\left\{ a_{\{l,m,n\}}(\xi;k) = \frac{\xi^k}{(lk+m)^n} \;\middle|\; l,m,n \in \mathbb{N} \setminus \{0\},\ \xi \in \mathbb{C} \setminus \{0\} \right\}. \tag{171}$$

Here again the limiting case $l = 1, m = 0$ is not included. Instead, the alphabet for the generalized harmonic sums, or S-sums, is given by:

$$\left\{ a_n(\xi;k) = \frac{\xi^k}{k^n} \;\middle|\; n \in \mathbb{N} \setminus \{0\},\ \xi \in \mathbb{C} \setminus \{0\} \right\}. \tag{172}$$

It is worthwhile noting, that the cyclotomic harmonic sums are connected to cyclotomic harmonic polylogarithms [110], which are defined via the cyclotomic polynomials [255]

$$\Phi_n(x) := \prod_{\substack{1 \le k \le n \\ \gcd(k,n)=1}} \left(x - e^{2i\pi\frac{k}{n}} \right). \tag{173}$$

From this class only the following ones will be of relevance for the present thesis:

$$\begin{aligned} \Phi_0(x) &:= x \\ \Phi_1(x) &= x - 1 \\ \Phi_2(x) &= x + 1 \\ \Phi_4(x) &= x^2 + 1\,, \end{aligned} \tag{174}$$

where Φ_0 is included for convenience.

Corresponding iterated integrals, which are called cyclotomic harmonic polylogarithms [110], are constructed via the alphabet

$$\left\{ f_{(n,b)}(x) = \frac{x^b}{\Phi_n(x)} \;\middle|\; n,b \in \mathbb{N} \cup \{0\} \right\}. \tag{175}$$

The connection to (cyclotomic) harmonic sums via the Mellin transformation can be seen from the representation of a letter from the above alphabets by the relation, cf. [110],

$$\frac{(\pm 1)^k}{(lk+m)^n} = \int_0^1 \frac{dx_1}{x_1} \int_0^{x_1} \frac{dx_2}{x_2} \cdots \int_0^{x_{n-2}} \frac{dx_{n-1}}{x_{n-1}} \int_0^{x_{n-1}} dx_n x_n^{lk+m-1} (\pm 1)^k\,, \tag{176}$$

and the finite geometric sum

$$\sum_{k=1}^{N} x^{k-1} = \frac{x^N - 1}{x - 1}\,. \tag{177}$$

Furthermore, the (cyclotomic) S-sums with upper bound $N = \infty$ can be expressed in terms of (cyclotomic) HPLs. These relations are implemented in the package HarmonicSums [108–111] and are crucial for the calculations in Chapter 9.

5.2 The Beta Integral

In many calculations the following integral occurs:

$$I_\beta = \int_0^1 dx\; x^{a-1}(1-x)^{b-1} \tag{178}$$

If $a > 0$ and $b > 0$ the integral is well defined in the Riemann-Lebesgue sense, and it is equal to Euler's Beta functions

$$I_\beta \equiv B(a,b) \equiv \frac{\Gamma(a)\Gamma(b)}{\Gamma(a+b)}\,. \tag{179}$$

If the above conditions are not met, an analytic continuation of the above function has to be used. An analytic continuation of the Beta function, which is valid on the whole complex plane is given by the Pochhammer contour integral [256]:

$$(1-e^{2\pi i a})(1-e^{2\pi i b})B(a,b) = \int_C d\xi\; \xi^{a-1}(1-\xi)^{b-1}\,, \tag{180}$$

where the contour runs from close to 0 counterclockwise around 1 then clockwise around 0 then clockwise around 1, then counterclockwise around 0 and closes. The representation for B is restricted to non-integer values. What is important for practical purposes, is that the functional relation

$$B(a+1,b) = \frac{a}{a+b}B(a,b)\;, \quad B(a,b+1) = \frac{b}{a+b}B(a,b) \tag{181}$$

of the Beta function can be derived from the Pochhammer contour integral, and is thus valid for all non-integer values. From these relations we can infer that the relation between the Γ- and Beta functions is valid for all non-integers. Since the non-integers are dense in the complex plane, the representation of the Beta function in terms of Γ-functions is valid, whenever the right hand side of (179) is finite.

5.3 Hypergeometric Functions and Summation Theory

The methods used in this thesis to calculate Feynman integrals heavily rely on the knowledge of properties of hypergeometric functions such as Gauß' function and its generalizations as well as Appell functions and its generalizations. Most of what is known about these functions can be found in [257–264].

In the series expansions, often the Pochhammer symbol is used, which is defined as follows

$$\begin{aligned}&(a)_m \equiv a(a+1)\ldots(a+m-1),\; m\in\mathbb{N},\; a\in\mathbb{C}\,,\\ &(a)_0 \equiv 1\,.\end{aligned} \tag{182}$$

For $a \in \mathbb{C}\setminus(-\mathbb{N})$ and $m \neq a$ it may be written as

$$(a)_m = \frac{\Gamma(a+m)}{\Gamma(a)}\,. \tag{183}$$

From this relation, one can deduce the factorization property

$$(a)_m(a+m)_n = (a)_{m+n}\,. \tag{184}$$

The Gauß hypergeometric function has the following series representation [265]:

$$ {}_2F_1\left[\begin{array}{c} a,b;\\ c; \end{array} z\right] = \sum_{m=0}^{\infty} \frac{(a)_m (b)_m}{m!(c)_m} z^m \,. \tag{185} $$

The series converges if $|z| < 1$, or if $z = 1$ and $\mathrm{Re}(c-a-b) > 0$ [261, 265].

The Gauß function obeys the following integral representation:

$$ {}_2F_1\left[\begin{array}{c} a,b;\\ c; \end{array} z\right] = \frac{1}{B(b,c-b)} \int_0^1 dx\, x^{b-1}(1-x)^{c-b-1}(1-xz)^{-a} \,. \tag{186} $$

From the integral representation, one can immediately derive the Gauß summation theorem [261, 265]

$$ {}_2F_1\left[\begin{array}{c} a,b;\\ c; \end{array} 1\right] = \frac{\Gamma(c)\Gamma(c-a-b)}{\Gamma(c-a)\Gamma(c-b)} \,. \tag{187} $$

Since in practical applications also integrals of this kind occur, in which $|z| > 1$, one is also interested in series representations for these integrals. They can be obtained from analytic continuation fomulae of the Gauß function to domains for z, for which the series representation given above does not converge. These formulae are obtained studying solutions of the Gauß equation, a linear differential equation which is satisfied by the Gauß function [261, 266]. An example for such a relation is [267]:

$$ {}_2F_1\left[\begin{array}{c} a,b;\\ c; \end{array} z\right] = (1-z)^{-a} {}_2F_1\left[\begin{array}{c} a,c-b;\\ c; \end{array} \frac{z}{z-1}\right] \,. \tag{188} $$

These relations span the complete set of transformations, which are isomorphic to permutations of the set $\{0,1,\infty\}$ of singularities of the Gauß differential equation [256, 268]:

$$ x \to \frac{x}{x-1} \quad \widehat{=} \quad \{0,\infty,1\} \,, \tag{189} $$

$$ x \to \frac{1}{x} \quad \widehat{=} \quad \{\infty,1,0\} \,, \tag{190} $$

$$ x \to 1-x \quad \widehat{=} \quad \{1,0,\infty\} \,. \tag{191} $$

These transformations are important to allow for a convergent series representation of the occurring hypergeometric functions.

To find more general series representations for parameter integrals, we briefly show how the series representation for the Gauß function can be obtained from its integral representation. The main input is Newton's binomial theorem [269, 270] in the following form:

$$ (1-a)^b = \sum_{m=0}^{\infty} \frac{(-b)_m}{m!} a^m \,. \tag{192} $$

It reduces to the finite version of the binomial theorem by the properties of the Pochhammer symbol

$$ \frac{(-b)_m}{m!} = \left(\begin{array}{c} b \\ m \end{array}\right) (-1)^m \,, \tag{193} $$

and

$$ b, m \in \mathbb{N}, m \geq b \Rightarrow (-b)_m = 0 \,. \tag{194} $$

The above series converges whenever $a < 1$ or $b \in \mathbb{N}$. Furthermore, the series may be interchanged with integration, where the convergence of the sum of integrals is equivalent to the convergence of the series in (185). For more general situations the analysis of the convergence may become a difficult task, cf. [259, 264].

The so called generalized hypergeometric functions or generalized Gauß functions ${}_{A+1}F_A$ are constructed recursively from the Gauß function via [261]:

$$ {}_{A+1}F_A\left[\begin{array}{c} a_1,\ldots,a_A,c; \\ b_1\ldots,b_{A-1},d; \end{array} z\right] = \frac{1}{B(c,d-c)}\int_0^1 dx x^{c-1}(1-x)^{d-c-1}\,{}_AF_{A-1}\left[\begin{array}{c} a_1,\ldots,a_A; \\ b_1\ldots,b_{A-1}; \end{array} xz\right] . \tag{195}$$

Their series representation is

$$ {}_{A+1}F_A\left[\begin{array}{c} a_1,\ldots,a_{A+1}; \\ b_1\ldots,b_A; \end{array} z\right] = \sum_{m=0}^{\infty}\frac{(a_1)_m\ldots(a_{A+1})_m}{m!(b_1)_m\ldots(b_A)_m}z^m\,, \tag{196}$$

with the regions of convergence

$$ |z|<1, \quad \text{and} \quad z=1,\ \mathrm{Re}\left(\sum_{i=1}^{A}b_i-\sum_{i=1}^{A+1}a_i\right)>0\,. \tag{197}$$

Furthermore, for the calculation of 3-loop ladder graphs in Chapter 8, the Appell function F_1 [257, 261] is useful. It has the following integral representations

$$\begin{aligned} F_1[a,b,b',c;x,y] &= \Gamma\left[\begin{array}{c} c \\ b,b',c-b-b' \end{array}\right]\int_0^1 du\int_0^1 dv\,\theta(1-u-v) \\ &\quad u^{b-1}v^{b'-1}(1-u-v)^{c-b-b'-1}(1-ux-vy)^{-a} \qquad (198) \\ &= \frac{1}{B(a,c-a)}\int_0^1 du\,u^{a-1}(1-u)^{c-a-1}(1-ux)^{-b}(1-uy)^{-b'}\,. \qquad (199) \end{aligned}$$

For $|x|<1$ and $|y|<1$, this function has the convergent series representation

$$ F_1[a,b,b',c;x,y] = \sum_{m=0}^{\infty}\sum_{n=0}^{\infty}\frac{(a)_{m+n}(b)_m(b')_n}{m!\,n!\,(c)_{m+n}}x^m y^n\,. \tag{200}$$

The function may be analytically continued using the argument mapping relation

$$ F_1\left[a,b,b',c;\frac{x-1}{x},\frac{y-1}{y}\right] = x^b y^{b'}F_1[c-a,b,b',c;1-x,1-y]\,. \tag{201}$$

Since similar relations for the full set of Möbius transformations, which permute the singular points $\{0,1,\infty\}$, is not known, we may find the following representation useful:

$$ F_1[a,b,b',c;x,y] = \sum_{m=0}^{\infty}\frac{(a)_m(b)_m}{m!(c)_m}x^m\,{}_2F_1\left[\begin{array}{c} a+m,b'; \\ c+m; \end{array} y\right], \tag{202}$$

which, in case of convergence, allows for using the transformation formulae of the Gauß function.

The representations of integrals using hypergeometric series are useful, when combined with modern techniques of (multi) summation algorithms implemented in the Package Sigma [93–101]. For the efficient application to the calculations presented in this thesis, limit procedures and heuristic strategies for the application of the latter algorithms were developed and implemented in the package EvaluateMultiSums [101–103]. This development is not part of the thesis. Nevertheless, a considerable part of the work that led to the present thesis was concerned with generating series representations, or in general, sum representations, that were treatable by the methods cited above. The exchange of specific examples and many discussions, on the other hand, led to improvements in the packages.

5.4 The Mellin-Barnes Representation

It is known for a long time, that hypergeometric functions can be represented via complex contour integrals which are called Mellin-Barnes (MB) representations [114, 115, 261, 268]. The Mellin-Barnes representation of the Gauß hypergeometric function, for example, has the form

$$ {}_2F_1\left[\begin{array}{c} a,b; \\ c; \end{array} z\right] = \frac{\Gamma(c)}{2\pi i \Gamma(a)\Gamma(b)} \int_{-i\infty}^{i\infty} d\xi \frac{\Gamma(a+\xi)\Gamma(b+\xi)\Gamma(-\xi)}{\Gamma(c+\xi)} (-z)^{\xi} \,. \tag{203} $$

Since these representations are well defined for a large set of values of z, a, b, c, it was found useful for Feynman diagram calculations [116, 117, 271–273]. The representation is introduced either on the momentum integral level, or on Feynman parameter representations, using the formula:

$$ \frac{1}{(X+Y)^{\lambda}} = \frac{1}{\Gamma(\lambda)} \frac{1}{2\pi i} \int_{-i\infty}^{i\infty} d\xi \Gamma(-\xi)\Gamma(\xi+\lambda) \frac{X^{\xi}}{Y^{\lambda+\xi}} \,, \tag{204} $$

where the integration contour is indented such that all poles of $\Gamma(-\xi)$ lie to the right of the contour.

If further Feynman parameter integrals are performed, they are commuted into the MB integral. These Feynman parameter integrals are performed in terms of Euler's Beta function using (178), and represented via Euler's Γ-function using (179). In order to commute the Feynman parameter integrals with the Mellin-Barnes integral, the contour of the Mellin-Barnes integral in ξ has to lie such, that the integrand of the Feynman parameter integral in question is integrable. This amounts to the following rule of thumb, cf. [271]:

- $\mathrm{Re}(\xi) < A$ if $\Gamma(A-\xi)$ occurs in the numerator of the result,
- $\mathrm{Re}(\xi) > -A$ if $\Gamma(A+\xi)$ occurs in the numerator of the result.

However, this condition is usually too strict, and one may want to make use of the observation, that Γ-functions are regular on the complex plane except for a countable number of isolated poles on the non-positive real axis. In fact, for a single Γ-function of type $\Gamma(A \pm \xi)$ the above rule can be relaxed to: "allow" all contours, which are homotopic to the above contours on the complex plane from which all singular points have been removed. Having this in mind, we see that for an integral resulting in many Γ-functions in the numerator all contours in the intersection of the "allowed" contours of individual Γ-functions yield correct contour integrals. Denoting regions, which contain only left poles by open circles and regions with only right poles by solid circles, the contour in the complex plane is sketched in the following Figure.

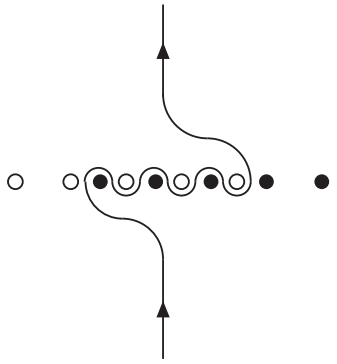

The Mellin-Barnes representation allows to perform the ε expansion [116, 117, 271–273], and to evaluate the coefficients numerically, or analytically. In such a way we can check numerically, that Mellin-Barnes representations derived for certain Feynman parameter integrals are valid representations.

Since with EvaluateMultiSums [101–103] and Sigma [93–101] we have algorithms at hand, which allow for an automated ε-expansion together with the symbolic summation, we will not make use of the former methods as means for analytic calculation.

Nevertheless, a Mellin-Barnes representation is necessary, if the analytic continuation formulae for the occurring hypergeometric functions are not known, since the complex contour integrals allow much flexibility to derive convergent series representations.

In many applications of these representations, the goal is to analytically continue the function in ε, such that the resulting integrand may be expanded in ε [116, 117, 271–273]. After that the integrals are performed applying corollaries of the Barnes Lemmas [115, 261, 274] :

$$\frac{1}{2\pi i}\int_{-i\infty}^{i\infty} d\xi \Gamma(\lambda_1+\xi)\Gamma(\lambda_2+\xi)\Gamma(\lambda_3-\xi)\Gamma(\lambda_4-\xi) = \frac{\Gamma(\lambda_1+\lambda_3)\Gamma(\lambda_1+\lambda_4)\Gamma(\lambda_2+\lambda_3)\Gamma(\lambda_2+\lambda_4)}{\Gamma(\lambda_1+\lambda_2+\lambda_3+\lambda_4)}\,, \tag{205}$$

$$\frac{1}{2\pi i}\int_{-i\infty}^{i\infty} d\xi \frac{\Gamma(\lambda_1+\xi)\Gamma(\lambda_2+\xi)\Gamma(\lambda_3+\xi)\Gamma(\lambda_4-\xi)\Gamma(\lambda_5-\xi)}{\Gamma(\lambda_6+\xi)} = \frac{\Gamma(\lambda_1+\lambda_4)\Gamma(\lambda_2+\lambda_4)\Gamma(\lambda_3+\lambda_4)\Gamma(\lambda_1+\lambda_5)\Gamma(\lambda_2+\lambda_5)\Gamma(\lambda_3+\lambda_5)}{\Gamma(\lambda_1+\lambda_2+\lambda_4+\lambda_5)\Gamma(\lambda_1+\lambda_3+\lambda_4+\lambda_5)\Gamma(\lambda_2+\lambda_3+\lambda_4+\lambda_5)}\,. \tag{206}$$

However, this method is not applicable in case of the integrals in Chapter 9, where a different method will be developed. This new method will use the afore mentioned summation algorithms as well as properties of the iterated integrals of the previous Sections.

6 Bubble Topologies Contributing to the Unpolarized OMEs $A_{gq,Q}$ and $A_{gg,Q}$

In this Chapter, the $O(\alpha_s^3 n_f T_F^2)$-contributions to the unpolarized OMEs $A_{gq,Q}$ and $A_{gg,Q}$ are computed. They are necessary for the construction of variable flavor number schemes, and for the definition of heavy quark PDFs. First, the relations of the fixed and variable flavor number schemes will be given. Then the calculation of the 3-loop contributions will be presented. These results are the first for general values of N for these quantities, and generalize the results for the moments for $N = 2, \ldots, 10$ in case of $A_{gg,Q}$ and up to 14 in $A_{gq,Q}$ [87].

6.1 Transition to the Variable Flavor Number Scheme

In the fixed flavor number scheme (FFNS), the heavy quark contributions are created purely radiatively. Thus there is no parton distribution for heavy partons. In the kinematic range of HERA, QCD analyses in the FFNS yield stable results [56, 223]. However, if Q^2 becomes very large, logarithms of the form $\ln(Q^2/m^2)$, $\ln(\mu^2/m^2)$ might eventually become large and spoil the convergence of the perturbation series. Furthermore, these logarithms prevent a naive transition to a description in a fixed flavor scheme, where the heavy quark is treated as a light quark.

These issues were discussed in the past [75, 205, 275, 276] and the correct definition of the VFNS was given at NLO in [75] and at NNLO in [87]. To cure the above problems for one heavy flavor, an explicit change in the renormalization and factorization schemes is necessary, which maps the occurring parton distribution functions onto an $(n_f + 1)$-flavor scheme for all light flavors, the heavy flavor and the gluon. These new PDFs are combinations of the PDFs defined in the n_f-flavor scheme, as well as perturbative coefficients, which are chosen such that the PDFs in the $(n_f + 1)$-flavor scheme obey renormalization group equations (RGEs) depending on $(n_f + 1)$ light flavors. As a consequence the light flavor Wilson coefficients become perturbatively stable again, but the matching conditions for the PDFs have to be evaluated at a scale, where the logarithms are sufficiently small. The scale evolution is then provided by the RGEs.

Adopting the nomenclature of [277], we will call such a prescription zero mass variable flavor number scheme (ZMVFNS). To comply with the renormalization group equations, the following relations between $(n_f + 1)$-flavor PDFs in the ZMVFNS and n_f-flavor PDFs of the FFNS follow [75]:

$$\begin{aligned}
f_k(n_f+1,\mu^2,m^2,N) + f_{\overline{k}}(n_f+1,\mu^2,m^2,N) = \\
&A_{qq,Q}^{\rm NS}\left(n_f+1,\frac{\mu^2}{m^2},N\right)\left[f_k(n_f,\mu^2,N) + f_{\overline{k}}(n_f,\mu^2,N)\right] \\
&+ \tilde{A}_{qq,Q}^{\rm PS}\left(n_f+1,\frac{\mu^2}{m^2},N\right)\Sigma(n_f,\mu^2,N) \\
&+ \tilde{A}_{qg,Q}\left(n_f+1,\frac{\mu^2}{m^2},N\right) G(n_f,\mu^2,N)\,, \qquad (207) \\
f_Q(n_f+1,\mu^2,m^2,N) + f_{\overline{Q}}(n_f+1,\mu^2,m^2,N) = \\
&A_{Qq}^{\rm PS}\left(n_f+1,\frac{\mu^2}{m^2},N\right)\Sigma(n_f,\mu^2,N) \\
&+ A_{Qg}\left(n_f+1,\frac{\mu^2}{m^2},N\right) G(n_f,\mu^2,N)\,. \qquad (208)
\end{aligned}$$

Here $f_Q(f_{\bar{Q}})$ are the heavy quark densities. The flavor singlet, non–singlet, and gluon densities for (n_f+1) flavors are given by

$$\begin{aligned}\Sigma(n_f+1,\mu^2,m^2,N) &= \left[A_{qq,Q}^{\rm NS}\left(n_f+1,\frac{\mu^2}{m^2},N\right)+n_f\tilde{A}_{qq,Q}^{\rm PS}\left(n_f+1,\frac{\mu^2}{m^2},N\right)\right.\\ &\left.+A_{Qq}^{\rm PS}\left(n_f+1,\frac{\mu^2}{m^2},N\right)\right]\Sigma(n_f,\mu^2,N)\\ &+\left[n_f\tilde{A}_{qg,Q}\left(n_f+1,\frac{\mu^2}{m^2},N\right)+A_{Qg}\left(n_f+1,\frac{\mu^2}{m^2},N\right)\right]G(n_f,\mu^2,N)\,, \end{aligned} \tag{209}$$

$$\begin{aligned}\Delta_k(n_f+1,\mu^2,m^2,N) &= f_k(n_f+1,\mu^2,N)+f_{\overline{k}}(n_f+1,\mu^2,m^2,N)\\ &-\frac{1}{n_f+1}\Sigma(n_f+1,\mu^2,m^2,N)\,, \end{aligned} \tag{210}$$

$$\begin{aligned}G(n_f+1,\mu^2,m^2,N) &= A_{gq,Q}\left(n_f+1,\frac{\mu^2}{m^2},N\right)\Sigma(n_f,\mu^2,N)\\ &+A_{gg,Q}\left(n_f+1,\frac{\mu^2}{m^2},N\right)G(n_f,\mu^2,N)\,. \end{aligned} \tag{211}$$

Here the gluonic and pure singlet OMEs are normalized such that only one light flavor flows through the operator, cf. Ref. [87]:

$$\tilde{A}_{ij}(n_f+1)\equiv\frac{1}{n_f}A_{ij}(n_f+1)\,. \tag{212}$$

It is worth noting that the relation between the process independent PDFs in different schemes is and can only be given by process independent quantities, i.e. the OMEs. Usually $\mu^2=m^2$ is chosen as matching point. However, in [278] it was shown, that preserving the value of the corresponding observable, much different scales may be requested.

The above description applies to a matching at scales at which both descriptions are valid. However, observables such as the deep-inelastic structure functions are measured to be continuous quantities, so it seems reasonable to expect a continuous theoretical description at all scales. The continuity might be spoiled by a scheme change as shown above so several definitions were given for so called general mass variable flavor number schemes (GMVFNS), where the description of the structure function continuously matches with the n_f-flavor description in the threshold region $\mu^2\sim m^2$ and matches the ZMVFNS description in the asymptotic region. Several of these schemes have been proposed in the past [75, 205, 275, 276, 279]. As an example the BMSN scheme [75, 277] is presented, which is defined via

$$F_2^{\rm BMSN}(n_f)=F_2^{\rm exact}(n_f)+F_2^{\rm ZMVFN}(n_f+1)-F_2^{\rm asympt}(n_f)\,, \tag{213}$$

where $F_2^{\rm exact}(n_f)$ is the exact heavy flavor contribution to F_2 in the n_f-flavor scheme, $F_2^{\rm asympt}(n_f)$ is its asymptotic representation omitting power corrections for $Q^2\gg m^2$ and $F_2^{\rm ZMVFN}(n_f+1)$ is the ZMVFNS description, with (n_f+1)-flavor PDFs and (n_f+1)-flavor evolution. As has been shown in [277] the GMVFNS description $F_2^{\rm BMSN}(n_f)$ is indeed a sufficiently smooth interpolation between the exact result and the ZMVFNS description, it is thus valid from the threshold region up to the asymptotic region.

The ranges of validity may now be stated formally as follows: The exact mass contributions implemented in the n_f-flavor scheme are valid, if $a_s\ln(Q^2/m^2)<1$. The ZMVFN scheme is

valid if $m^2/Q^2 \ll 1$. However, these considerations are only reasonable taking sufficiently high order in a_s into account, while to finite order the difference between the descriptions has to be checked numerically for the scales needed to describe the available experiments. In [277] the authors showed for the charm contributions to F_2 that the 3-flavor description with exact m_c-dependence does not differ significantly from the BMSN scheme, if compared to the experimental uncertainty.

The above considerations are, however, only valid, if one massive flavor is present; hence they can be used consecutively if the massive flavors obey a strict hierarchy $m_{H_1} \gg m_{H_2} \gg ....$ In case of the charm and the bottom quark, this hierarchy is not strictly given, since $m_b^2 \approx 10 m_c^2$. So here one has to check to which accuracy the hierarchy is a valid approximation. More likely, one will have to consider mass effects from two quark flavors [280].

6.2 The $O(\alpha_s^3 n_f T_F^2)$ Contributions to $A_{gg,Q}$ and $A_{gq,Q}$

The renormalization for $A_{gq,Q}$ and $A_{gg,Q}$ to $O(a_s^3)$ was derived in [87]. In the $\overline{\rm MS}$ scheme with the heavy quark mass m on shell, they are expressed in terms of lower order quantities as well as $a_{gq,Q}^{(1)}$ and $a_{gg,Q}^{(1)}$, which are calculated below:

$$\begin{aligned}
A_{gq,Q}^{(3),\overline{\rm MS}} &= -\frac{\gamma_{gq}^{(0)}}{24}\biggl\{\gamma_{gq}^{(0)}\hat{\gamma}_{qg}^{(0)} + \Bigl(\gamma_{qq}^{(0)} - \gamma_{gg}^{(0)} + 10\beta_0 + 24\beta_{0,Q}\Bigr)\beta_{0,Q}\biggr\}\ln^3\Bigl(\frac{m^2}{\mu^2}\Bigr) + \frac{1}{8}\biggl\{6\gamma_{gq}^{(1)}\beta_{0,Q} \\
&+\hat{\gamma}_{gq}^{(1)}\Bigl(\gamma_{gg}^{(0)} - \gamma_{qq}^{(0)} - 4\beta_0 - 6\beta_{0,Q}\Bigr) + \gamma_{gq}^{(0)}\Bigl(\hat{\gamma}_{qq}^{(1),\sf NS} + \hat{\gamma}_{qq}^{(1),\sf PS} - \hat{\gamma}_{gg}^{(1)} + 2\beta_{1,Q}\Bigr)\biggr\}\ln^2\Bigl(\frac{m^2}{\mu^2}\Bigr) \\
&+\frac{1}{8}\biggl\{4\hat{\gamma}_{gq}^{(2)} + 4a_{gq,Q}^{(2)}\Bigl(\gamma_{gg}^{(0)} - \gamma_{qq}^{(0)} - 4\beta_0 - 6\beta_{0,Q}\Bigr) + 4\gamma_{gq}^{(0)}\Bigl(a_{qq,Q}^{(2),\sf NS} + a_{Qq}^{(2),\sf PS} - a_{gg,Q}^{(2)} \\
&+\beta_{1,Q}^{(1)}\Bigr) + \gamma_{gq}^{(0)}\zeta_2\Bigl(\gamma_{gq}^{(0)}\hat{\gamma}_{qg}^{(0)} + \Bigl[\gamma_{qq}^{(0)} - \gamma_{gg}^{(0)} + 12\beta_{0,Q} + 10\beta_0\Bigr]\beta_{0,Q}\Bigr)\biggr\}\ln\Bigl(\frac{m^2}{\mu^2}\Bigr) \\
&+\overline{a}_{gq,Q}^{(2)}\Bigl(\gamma_{qq}^{(0)} - \gamma_{gg}^{(0)} + 4\beta_0 + 6\beta_{0,Q}\Bigr) + \gamma_{gq}^{(0)}\Bigl(\overline{a}_{gg,Q}^{(2)} - \overline{a}_{Qq}^{(2),\sf PS} - \overline{a}_{qq,Q}^{(2),\sf NS}\Bigr) - \gamma_{gq}^{(0)}\beta_{1,Q}^{(2)} \\
&-\frac{\gamma_{gq}^{(0)}\zeta_3}{24}\Bigl(\gamma_{gq}^{(0)}\hat{\gamma}_{qg}^{(0)} + \Bigl[\gamma_{qq}^{(0)} - \gamma_{gg}^{(0)} + 10\beta_0\Bigr]\beta_{0,Q}\Bigr) - \frac{3\gamma_{gq}^{(1)}\beta_{0,Q}\zeta_2}{8} + 2\delta m_1^{(-1)}a_{gq,Q}^{(2)} \\
&+\delta m_1^{(0)}\hat{\gamma}_{gq}^{(1)} + 4\delta m_1^{(1)}\beta_{0,Q}\gamma_{gq}^{(0)} + a_{gq,Q}^{(3)}\,, \qquad (214)
\end{aligned}$$

$$\begin{aligned}
A_{gg,Q}^{(3),\overline{\rm MS}} &= \frac{1}{48}\biggl\{\gamma_{gq}^{(0)}\hat{\gamma}_{qg}^{(0)}\Bigl(\gamma_{qq}^{(0)} - \gamma_{gg}^{(0)} - 6\beta_0 - 4n_f\beta_{0,Q} - 10\beta_{0,Q}\Bigr) - 4\Bigl(\gamma_{gg}^{(0)}\Bigl[2\beta_0 + 7\beta_{0,Q}\Bigr] \\
&+4\beta_0^2 + 14\beta_{0,Q}\beta_0 + 12\beta_{0,Q}^2\Bigr)\beta_{0,Q}\biggr\}\ln^3\Bigl(\frac{m^2}{\mu^2}\Bigr) + \frac{1}{8}\biggl\{\hat{\gamma}_{qg}^{(0)}\Bigl(\gamma_{gq}^{(1)} + (1-n_f)\hat{\gamma}_{gq}^{(1)}\Bigr) \\
&+\gamma_{gq}^{(0)}\hat{\gamma}_{qg}^{(1)} + 4\gamma_{gg}^{(1)}\beta_{0,Q} - 4\hat{\gamma}_{gg}^{(1)}[\beta_0 + 2\beta_{0,Q}] + 4[\beta_1 + \beta_{1,Q}]\beta_{0,Q} \\
&+2\gamma_{gg}^{(0)}\beta_{1,Q}\biggr\}\ln^2\Bigl(\frac{m^2}{\mu^2}\Bigr) + \frac{1}{16}\biggl\{8\hat{\gamma}_{gg}^{(2)} - 8n_f a_{gq,Q}^{(2)}\hat{\gamma}_{qg}^{(0)} - 16a_{gg,Q}^{(2)}(2\beta_0 + 3\beta_{0,Q}) \\
&+8\gamma_{gq}^{(0)}a_{Qg}^{(2)} + 8\gamma_{gg}^{(0)}\beta_{1,Q}^{(1)} + \gamma_{gq}^{(0)}\hat{\gamma}_{qg}^{(0)}\zeta_2\Bigl(\gamma_{gg}^{(0)} - \gamma_{qq}^{(0)} + 6\beta_0 + 4n_f\beta_{0,Q} + 6\beta_{0,Q}\Bigr) \\
&+4\beta_{0,Q}\zeta_2\Bigl(\gamma_{gg}^{(0)} + 2\beta_0\Bigr)\Bigl(2\beta_0 + 3\beta_{0,Q}\Bigr)\biggr\}\ln\Bigl(\frac{m^2}{\mu^2}\Bigr) + 2(2\beta_0 + 3\beta_{0,Q})\overline{a}_{gg,Q}^{(2)}
\end{aligned}$$

$$
+n_f\hat{\gamma}_{qg}^{(0)}\overline{a}_{gq,Q}^{(2)} - \gamma_{gq}^{(0)}\overline{a}_{Qg}^{(2)} - \beta_{1,Q}^{(2)}\gamma_{gg}^{(0)} + \frac{\gamma_{gq}^{(0)}\hat{\gamma}_{qg}^{(0)}\zeta_3}{48}\Big(\gamma_{qq}^{(0)} - \gamma_{gg}^{(0)} - 2[2n_f+1]\beta_{0,Q}
$$

$$
-6\beta_0\Big) + \frac{\beta_{0,Q}\zeta_3}{12}\Big([\beta_{0,Q} - 2\beta_0]\gamma_{gg}^{(0)} + 2[\beta_0 + 6\beta_{0,Q}]\beta_{0,Q} - 4\beta_0^2\Big)
$$

$$
-\frac{\hat{\gamma}_{qg}^{(0)}\zeta_2}{16}\Big(\gamma_{gq}^{(1)} + \hat{\gamma}_{gq}^{(1)}\Big) + \frac{\beta_{0,Q}\zeta_2}{8}\Big(\hat{\gamma}_{gg}^{(1)} - 2\gamma_{gg}^{(1)} - 2\beta_1 - 2\beta_{1,Q}\Big) + \frac{\delta m_1^{(-1)}}{4}\Big(8a_{gg,Q}^{(2)}
$$

$$
+24\delta m_1^{(0)}\beta_{0,Q} + 8\delta m_1^{(1)}\beta_{0,Q} + \zeta_2\beta_{0,Q}\beta_0 + 9\zeta_2\beta_{0,Q}^2\Big) + \delta m_1^{(0)}\Big(\beta_{0,Q}\delta m_1^{(0)} + \hat{\gamma}_{gg}^{(1)}\Big)
$$

$$
+\delta m_1^{(1)}\Big(\hat{\gamma}_{qg}^{(0)}\gamma_{gq}^{(0)} + 2\beta_{0,Q}\gamma_{gg}^{(0)} + 4\beta_{0,Q}\beta_0 + 8\beta_{0,Q}^2\Big) - 2\delta m_2^{(0)}\beta_{0,Q} + a_{gg,Q}^{(3)}\,. \tag{215}
$$

Here $\delta m_i^{(k)}$ are coefficients in the ε-expansion of the unrenormalized mass, $\beta_i, \beta_{i,Q}$ are coefficients of the β-functions (including mass effects), $a_{ij}^{(2)}, \overline{a}_{ij}^{(2)}$ are 2-loop contributions to order ε^0 and ε^1 respectively, and $\gamma_{ij}, \hat{\gamma}_{ij}$ are the anomalous dimensions. All contributions to (214, 215) but the constant terms $a_{ij,Q}^{(3)}$ are known [75, 76, 78–80, 127]. In particular, all the logarithmic contributions have already been obtained for general values of the Mellin variable N [281].

The unrenormalized OME $\hat{\hat{A}}_{gg,Q}^{(3)}$ also receives one particle reducible contributions from vacuum polarization insertions on external lines. The vacuum polarization tensor has the structure

$$
\hat{\Pi}_{\mu\nu}^{ab}(p^2, \hat{m}^2, \mu^2, \hat{a}_s^2) = i\delta^{ab}\left[-g_{\mu\nu}p^2 + p_\mu p_\nu\right]\sum_{k=1}^{\infty}\hat{a}_s^k\hat{\Pi}^{(k)}(p^2, \hat{m}^2, \mu^2)\,. \tag{216}
$$

The shorthand notation

$$
\hat{\Pi}^{(k)} \equiv \hat{\Pi}^{(k)}(0, \hat{m}^2, \mu^2) \tag{217}
$$

is used, such that

$$
\hat{\hat{A}}_{gg,Q}^{(3)} = \hat{\hat{A}}_{gg,Q}^{(3),1\mathrm{PI}} - \hat{\Pi}^{(3)} - \hat{\hat{A}}_{gg,Q}^{(2),1\mathrm{PI}}\hat{\Pi}^{(1)} - 2\hat{\hat{A}}_{gg,Q}^{(1)}\hat{\Pi}^{(2)} + \hat{\hat{A}}_{gg,Q}^{(1)}\hat{\Pi}^{(1)}\hat{\Pi}^{(1)} \tag{218}
$$

$$
\equiv \frac{a_{gg,Q}^{(3,0)}}{\varepsilon^3} + \frac{a_{gg,Q}^{(3,1)}}{\varepsilon^2} + \frac{a_{gg,Q}^{(3,2)}}{\varepsilon} + a_{gg,Q}^{(3)}\,. \tag{219}
$$

The expressions for $\hat{\Pi}^{(i)}$ can be found in [87].

In the following, the calculation of the contributions to $O(a_s^3 n_f T_F^2 C_{F,A})$ of the massive gluonic OMEs is given. The Feynman diagrams are generated by QGRAF [282] with the extension allowing to include local operators [87]. The color-algebra is reduced using the package color of [283]. For a large part of the calculation we use (T)FORM [284]. The momentum integrals are performed introducing a Feynman parameterization in the way described in Chapter 5. Using the integral representation in (195), the Feynman parameter integrals are then expressed in terms of hypergeometric functions ${}_3F_2$ and simpler objects, which allow for a representation in terms of absolutely convergent series (196). Additionally, some of the terms involve finite sums due to binomial expansions. These multi-sum expressions are then processed applying the symbolic summation technology, which is implemented in the package Sigma [93–101] and making use of a large number of algorithms for efficiently processing multi-sums using the package EvaluateMultiSums [101–103]. For additional speed up, it is very useful to reduce such sums to a smaller number of 'key sums', by synchronization of the summation ranges and algebraic reduction of the summands. This step helped to reduce the size of the terms from 2GByte to 7.6MByte and the number of sums from 2419 to 29. The algorithms for this step are implemented

in the package SumProduction [101]. The complexity of the resulting expressions are further reduced through mutual relations among nested sums. The corresponding methods for large classes of such sums are implemented in the package HarmonicSums [108–111]. The results for the individual diagrams have been checked by comparison to the moments which were obtained in [87] using the code MATAD [285]. The constant terms $a_{gj,Q}^{(3)}$, $j = q, g$ in the ε-expansion, which complete (214, 215) to $O(a_s^3 n_f T_F^2 C_{F,A})$ read:

$$
\begin{aligned}
a_{gq,Q}^{(3),n_f T_F^2} &= C_F T_F^2 n_f \Bigg\{ -\frac{16\,(N^2+N+2)}{9(N-1)N(N+1)} \left(\frac{1}{3} S_1^3 + S_2 S_1 + \frac{2}{3} S_3 + 14\zeta_3 + 3 S_1 \zeta_2 \right) \\
&+ \frac{16\,(8N^3+13N^2+27N+16)}{27(N-1)N(N+1)^2} \left(3\zeta_2 + S_1^2 + S_2 \right) \\
&- \frac{32\,(35N^4+97N^3+178N^2+180N+70)}{27(N-1)N(N+1)^3} S_1 \\
&+ \frac{32\,(1138N^5+4237N^4+8861N^3+11668N^2+8236N+2276)}{243(N-1)N(N+1)^4} \Bigg\}, \qquad (220) \\
a_{gg,Q}^{(3),n_f T_F^2} &= n_f T_F^2 \Bigg\{ C_A \frac{1}{(N-1)(N+2)} \Bigg[\frac{4P_1}{27N^2(N+1)^2} S_1^2 + \frac{8P_2}{729N^3(N+1)^3} S_1 \\
&+ \frac{160}{27}(N-1)(N+2)\zeta_2 S_1 - \frac{448}{27}(N-1)(N+2)\zeta_3 S_1 + \frac{P_3}{729N^4(N+1)^4} \\
&- \frac{2P_4}{27N^2(N+1)^2}\zeta_2 + \frac{56\,(3N^4+6N^3+13N^2+10N+16)}{27N(N+1)}\zeta_3 - \frac{4P_5}{27N^2(N+1)^2} S_2 \Bigg] \\
&+ C_F \frac{1}{(N-1)(N+2)} \Bigg[\frac{112\,(N^2+N+2)^2}{27N^2(N+1)^2} S_1^3 - \frac{16P_6}{27N^3(N+1)^3} S_1^2 \\
&+ \frac{32P_7}{81N^4(N+1)^4} S_1 + \frac{16\,(N^2+N+2)^2}{3N^2(N+1)^2}\zeta_2 S_1 + \frac{16\,(N^2+N+2)^2}{3N^2(N+1)^2} S_2 S_1 \\
&- \frac{32P_8}{243N^5(N+1)^5} - \frac{16P_9}{9N^3(N+1)^3}\zeta_2 + \frac{448\,(N^2+N+2)^2}{9N^2(N+1)^2}\zeta_3 + \frac{16P_{10}}{9N^3(N+1)^3} S_2 \\
&- \frac{160\,(N^2+N+2)^2}{27N^2(N+1)^2} S_3 \Bigg] \Bigg\}. \qquad (221)
\end{aligned}
$$

Here the polynomials P_i are given by

$$
\begin{aligned}
P_1 &= 16N^5 + 41N^4 + 2N^3 + 47N^2 + 70N + 32\,, \qquad (222) \\
P_2 &= 6944N^8 + 26480N^7 + 23321N^6 - 15103N^5 - 39319N^4 - 27001N^3 - 11178N^2 \\
&\quad - 2016N + 864\,, \qquad (223) \\
P_3 &= 4809N^{10} + 24045N^9 - 182720N^8 - 854414N^7 - 1522031N^6 - 1472927N^5 \\
&\quad - 758234N^4 - 126080N^3 - 1152N^2 - 50688N - 24192\,, \qquad (224) \\
P_4 &= 3N^6 + 9N^5 + 307N^4 + 599N^3 + 746N^2 + 448N + 96\,, \qquad (225) \\
P_5 &= 40N^6 + 112N^5 - 3N^4 - 166N^3 - 301N^2 - 210N - 96\,, \qquad (226) \\
P_6 &= 44N^6 + 123N^5 + 386N^4 + 543N^3 + 520N^2 + 248N + 24\,, \qquad (227) \\
P_7 &= 205N^8 + 856N^7 + 3169N^6 + 6484N^5 + 7310N^4 + 4722N^3 + 1534N^2 \\
&\quad + 48N - 72\,, \qquad (228)
\end{aligned}
$$

$$P_8 = 1976N^{10} + 9385N^9 + 24088N^8 + 38989N^7 + 50214N^6 + 53872N^5 + 35219N^4 + 6890N^3 - 4233N^2 - 2844N - 756\,, \tag{229}$$

$$P_9 = 14N^6 + 33N^5 + 59N^4 + 39N^3 + 55N^2 + 20N - 12\,, \tag{230}$$

$$P_{10} = 4N^6 + 3N^5 - 50N^4 - 129N^3 - 100N^2 - 56N - 24\,. \tag{231}$$

Only single harmonic sums contribute, which are given in the shorthand notation (164).

Sometimes the expressions with an $\overline{\rm MS}$-renormalized quark mass $\bar{m}$ are desired. Following [87] the expressions for $A_{gq,Q}^{(3),n_f T_F^2}$ and $A_{gg,Q}^{(3),n_f T_F^2}$ read:

$$\begin{aligned}
A_{gq,Q,C_F T_F^2 n_f}^{(3),\overline{\rm MS}} &= C_F n_f T_F^2 \Bigg\{ \frac{32\,(N^2+N+2)}{9(N-1)N(N+1)} \ln^3\left(\frac{\bar{m}^2}{\mu^2}\right) \\
&+ \Bigg[-\frac{16\,(N^2+N+2)}{3(N-1)N(N+1)} \left(S_1^2 + S_2\right) + \frac{32\,(8N^3+13N^2+27N+16)}{9(N-1)N(N+1)^2} S_1 \\
&+ \frac{32\,(19N^4+81N^3+86N^2+80N+38)}{27(N-1)N(N+1)^3} \Bigg] \ln\left(\frac{\bar{m}^2}{\mu^2}\right) \\
&+ \Bigg[\frac{32\,(N^2+N+2)}{27(N-1)N(N+1)} \left(S_1^3 + 3S_2S_1 + 2S_3 - 24\zeta_3\right) \\
&- \frac{32\,(8N^3+13N^2+27N+16)}{27(N-1)N(N+1)^2} \left(S_1^2 + S_2\right) \\
&+ \frac{64\,(4N^4+4N^3+23N^2+25N+8)}{27(N-1)N(N+1)^3} S_1 \\
&+ \frac{64\,(197N^5+824N^4+1540N^3+1961N^2+1388N+394)}{243(N-1)N(N+1)^4} \Bigg] \Bigg\}\,,
\end{aligned} \tag{232}$$

$$\begin{aligned}
A_{gg,Q}^{(3),n_f T_F^2,\overline{\rm MS}} &= n_f T_F^2 \Bigg\{ \Bigg(C_F \frac{64\,(N^2+N+2)^2}{9(N-1)N^2(N+1)^2(N+2)} \\
&+ C_A \left[\frac{128\,(N^2+N+1)}{27(N-1)N(N+1)(N+2)} - \frac{64}{27} S_1 \right] \Bigg) \ln^3\left(\frac{\bar{m}^2}{\mu^2}\right)
\end{aligned} \tag{233}$$

$$- C_F \frac{16}{3} \ln^2\left(\frac{\bar{m}^2}{\mu^2}\right) + \Bigg(C_A \frac{1}{(N-1)(N+2)} \Bigg[-\frac{4P_{11}}{81N^3(N+1)^3} \tag{234}$$

$$\begin{aligned}
&- \frac{16P_{12}}{81N^2(N+1)^2} S_1 \Bigg] + C_F \frac{1}{(N-1)(N+2)} \Bigg[\frac{16\,(N^2+N+2)^2}{N^2(N+1)^2} \left(S_1^2 - \frac{5}{3} S_2\right) \\
&- \frac{4P_{13}}{9N^4(N+1)^4} - \frac{32P_{14}}{3N^3(N+1)^3} S_1 \Bigg] \Bigg) \ln\left(\frac{\bar{m}^2}{\mu^2}\right) \\
&+ C_A \frac{1}{(N-1)(N+2)} \Bigg[-\frac{4P_{15}}{27N^2(N+1)^2} S_1^2 - \frac{8P_{16}}{729N^3(N+1)^3} S_1 \\
&+ \frac{512}{27}(N-1)(N+2)\zeta_3 S_1 - \frac{2P_{17}}{729N^4(N+1)^4} - \frac{1024\,(N^2+N+1)}{27N(N+1)} \zeta_3
\end{aligned}$$

$$+\frac{4P_{18}}{27N^2(N+1)^2}S_2\Bigg]$$
$$+C_F\frac{1}{(N-1)(N+2)}\Bigg[\frac{64\left(N^2+N+2\right)^2}{9N^2(N+1)^2}\left(-\frac{1}{3}S_1^3-8\zeta_3+\frac{4}{3}S_3\right)$$
$$+\frac{32P_{19}}{27N^3(N+1)^3}S_1^2-\frac{64P_{20}}{81N^4(N+1)^4}S_1-\frac{32P_{21}}{243N^5(N+1)^5}$$
$$-\frac{32P_{22}}{3N^3(N+1)^3}S_2\Bigg]\Bigg\}, \tag{235}$$

with the polynomials

$$\begin{aligned}
P_{11} &= 297N^8+1188N^7+640N^6-2094N^5-1193N^4+2874N^3+5008N^2 \\
&\quad +3360N+864\,, && (236)\\
P_{12} &= 136N^6+390N^5+19N^4-552N^3-947N^2-630N-288\,, && (237)\\
P_{13} &= 15N^{10}+75N^9-48N^8-866N^7-2985N^6-6305N^5-8206N^4-7656N^3 \\
&\quad -4648N^2-1600N-288\,, && (238)\\
P_{14} &= 5N^5+52N^4+109N^3+90N^2+48N+16\,, && (239)\\
P_{15} &= 4N^5+17N^4+14N^3+71N^2+70N+32\,, && (240)\\
P_{16} &= 3008N^8+11600N^7+9197N^6-10255N^5-27739N^4-24745N^3-12474N^2 \\
&\quad -2016N+864\,, && (241)\\
P_{17} &= 4185N^{10}+20925N^9+1892N^8-117118N^7-222151N^6-176863N^5-41446N^4 \\
&\quad +22304N^3-1296N^2-18432N-6912\,, && (242)\\
P_{18} &= 16N^6+52N^5-3N^4-106N^3-277N^2-210N-96\,, && (243)\\
P_{19} &= 10N^6+30N^5+109N^4+168N^3+155N^2+76N+12\,, && (244)\\
P_{20} &= 38N^8+206N^7+962N^6+2246N^5+2509N^4+1542N^3+509N^2+24N-36\,, && (245)\\
P_{21} &= 123N^{12}+738N^{11}+691N^{10}-3526N^9-14521N^8-29458N^7-39189N^6 \\
&\quad -37672N^5-21920N^4-3914N^3+2856N^2+1872N+432\,, && (246)\\
P_{22} &= 2N^6+4N^5+N^4-10N^3-5N^2-4N-4\,. && (247)
\end{aligned}$$

As has been noted before [87], the above results are free of ζ_2, which is common to all massive OMEs, and hence is a particular feature of representing also the mass in the $\overline{\rm MS}$ scheme. Furthermore, we note, that the $\ln^2\left(\bar{m}^2/\mu^2\right)$-contribution to $A^{(3),\overline{\rm MS}}_{gg,Q,C_FT_F^2n_f}$ is particularly simple, while the corresponding contribution to $A^{(3),\overline{\rm MS}}_{gq,Q,C_FT_F^2n_f}$ vanishes. This cancellation becomes complete in the former scheme involving the on-shell mass. However, this property was not yet checked to apply for all OMEs.

Since in the calculation all coefficients of the Laurent expansion up to the constant order are obtained, one may use them to determine the corresponding contributions to the anomalous dimensions from the single pole term $1/\varepsilon$ resp. the linear logarithmic contribution, cf. (214, 215),

$$\begin{aligned}
\hat{\gamma}_{gq}^{(2),n_f} &= n_fT_F^2C_F\Bigg(-\frac{64\left(N^2+N+2\right)}{3(N-1)N(N+1)}\left(S_1^2+S_2\right)+\frac{128\left(8N^3+13N^2+27N+16\right)}{9(N-1)N(N+1)^2}S_1 \\
&\quad -\frac{128\left(4N^4+4N^3+23N^2+25N+8\right)}{9(N-1)N(N+1)^3}\Bigg)\,, && (248)
\end{aligned}$$

$$\hat{\gamma}_{gg}^{(2),n_f} = n_f T_F^2 C_A \left[-\frac{32 P_{23}}{27(N-1)N^2(N+1)^2(N+2)} S_1 - \frac{8 P_{24}}{27(N-1)N^3(N+1)^3(N+2)} \right]$$
$$+ n_f T_F^2 C_F \left[\frac{64\left(N^2+N+2\right)^2}{3(N-1)N^2(N+1)^2(N+2)} \left(S_1^2 - 3S_2\right) \right.$$
$$\left. + \frac{128 P_{25}}{9(N-1)N^3(N+1)^3(N+2)} S_1 - \frac{16 P_{26}}{27(N-1)N^4(N+1)^4(N+2)} \right], \tag{249}$$

where

$$P_{23} = 8N^6 + 24N^5 - 19N^4 - 78N^3 - 253N^2 - 210N - 96\,, \tag{250}$$
$$P_{24} = 87N^8 + 348N^7 + 848N^6 + 1326N^5 + 2609N^4 + 3414N^3 + 2632N^2 + 1088N + 192\,, \tag{251}$$
$$P_{25} = 4N^6 + 3N^5 - 50N^4 - 129N^3 - 100N^2 - 56N - 24\,, \tag{252}$$
$$P_{26} = 33N^{10} + 165N^9 + 256N^8 - 542N^7 - 3287N^6 - 8783N^5 - 11074N^4 - 9624N^3 - 5960N^2 - 2112N - 288\,. \tag{253}$$

Equations (248, 249) confirm previous results in [127] by a first direct diagrammatic recalculation, here in the massive case.

A certain combination

$$\gamma_{gg}^{(2),n_f^2} + \frac{\gamma_{gq}^{(2),n_f^2} \gamma_{qg}^{(0)}}{\gamma_{gg}^{(0),n_f} n_f} \tag{254}$$

of the gluonic anomalous dimensions $\gamma_{gj}^{(2)}$, $j = q, g$, was calculated in [286] for the leading n_f contribution, $\propto n_f^2$. This result is also confirmed by a direct massive calculation.

The construction of structure functions proceeds most conveniently in N-space, as it is done in Chapter 10, by multiplying the massive OMEs, light flavor Wilson coefficients and PDFs analytically[3], cf. e.g. [287], while a single numerical contour integral around the singularities allows for a very fast numerical Mellin inversion into the physical x-space. The corresponding analytic continuations of harmonic sums up to weight $w = 8$ are given in [106, 107, 252, 253, 288].

Still, x-space codes are quite common, so the OMEs (232, 233) are also given in x-space:

$$A_{gq,Q}^{(3),n_f T_F^2,\overline{\rm MS}}(x) = C_F n_f T_F^2 \left\{ \left(\frac{32x}{9} + \frac{64}{9x} - \frac{64}{9}\right) \ln^3\left(\frac{\bar{m}^2}{\mu^2}\right) + \left[\left(-\frac{16x}{3} - \frac{32}{3x} + \frac{32}{3}\right) \mathrm{H}_1^2 \right.\right.$$
$$\left. + \left(\frac{256x}{9} + \frac{320}{9x} - \frac{320}{9}\right) \mathrm{H}_1 + \frac{608x}{27} + \frac{2176}{27x} - \frac{2176}{27} \right] \ln\left(\frac{\bar{m}^2}{\mu^2}\right)$$
$$+ \left(\frac{32x}{27} + \frac{64}{27x} - \frac{64}{27}\right) \mathrm{H}_1^3 + \left(-\frac{256x}{27} - \frac{320}{27x} + \frac{320}{27}\right) \mathrm{H}_1^2$$
$$+ \left(\frac{256x}{27} - \frac{128}{27x} + \frac{128}{27}\right) \mathrm{H}_1 + \left(-\frac{256x}{9} - \frac{512}{9x} + \frac{512}{9}\right) \zeta_3 + \frac{12608x}{243}$$
$$\left. + \frac{24064}{243x} - \frac{24064}{243} \right\}, \tag{255}$$

[3]For Mellin-space representations of a wide class of parton densities see [134].

$$A_{gg,Q}^{(3),n_f T_F^2,\overline{\rm MS}}(x) = \qquad r$$

$$- \frac{64x}{9} + \frac{128}{9}(1+x)\mathrm{H}_0 + \frac{64}{9} + \frac{256}{27x}\Bigg]\Bigg] \ln^3\left(\frac{\bar{m}^2}{\mu^2}\right)$$
$$- \frac{16}{3}C_F\delta(1-x)\ln^2\left(\frac{\bar{m}^2}{\mu^2}\right) + \Bigg[C_A\Bigg[-\frac{608x^2}{27} - \frac{16}{81}(144\zeta_2 - 85)x$$
$$+ \frac{32}{3}(1+x)\mathrm{H}_0^2 - \frac{44}{3}\delta(1-x) - \frac{16}{81}(144\zeta_2 + 149) + \Bigg(-\frac{832x^2}{27} + \frac{16x}{27}$$
$$- \frac{800}{27}\Bigg)\mathrm{H}_0 + \left(-\frac{832x^2}{27} + \frac{208x}{9} - \frac{176}{9} + \frac{832}{27x}\right)\mathrm{H}_1$$
$$+ \frac{256}{9}(1+x)\mathrm{H}_{0,1} - \frac{2176}{81(x-1)_+} + \frac{224}{27x}\Bigg] + C_F\Bigg[\frac{32}{3}(1+x)\mathrm{H}_0^3$$
$$+ \left(-\frac{256x^2}{9} - \frac{688x}{9} - \frac{592}{9}\right)\mathrm{H}_0^2 + \Bigg(-\frac{64x^2}{9} - \frac{64}{9}(12\zeta_2 + 5)x - \frac{64}{9}(12\zeta_2$$
$$- 41)\Bigg)\mathrm{H}_0 + \left(-\frac{512x^2}{9} - \frac{128x}{3} + \frac{128}{3} + \frac{512}{9x}\right)\mathrm{H}_1\mathrm{H}_0 + \frac{256}{3}(1+x)\mathrm{H}_{0,1}\mathrm{H}_0$$
$$+ \left(-\frac{64x^2}{3} - 16x + 16 + \frac{64}{3x}\right)\mathrm{H}_1^2 - \frac{20}{3}\delta(1-x) + \frac{64}{27}x^2(18\zeta_2 - 7) + \frac{64}{9}x(3\zeta_2$$
$$+ 3\zeta_3 - 28) + \frac{64}{9}(6\zeta_2 + 3\zeta_3 + 10) + \left(-\frac{64x^2}{9} - \frac{416x}{3} + \frac{736}{3} - \frac{896}{9x}\right)\mathrm{H}_1$$
$$+ \left(\frac{128x^2}{9} + \frac{64x}{3} - \frac{256}{3} - \frac{512}{9x}\right)\mathrm{H}_{0,1} - \frac{256}{3}(1+x)\mathrm{H}_{0,0,1} + 64(1+x)\mathrm{H}_{0,1,1}$$
$$+ \frac{3904}{27x}\Bigg]\Bigg]\ln\left(\frac{\bar{m}^2}{\mu^2}\right) + C_A\zeta_3\left(\frac{512x^2}{27} - \frac{512x}{27} + \frac{512}{27(x-1)_+} + \frac{1024}{27} - \frac{512}{27x}\right)$$
$$+ C_F\zeta_3\left(\frac{2048x^2}{27} + \frac{512x}{9} - \frac{1024}{9}(1+x)\mathrm{H}_0 - \frac{512}{9} - \frac{2048}{27x}\right) + C_A\Bigg[\frac{128}{81}(1+x)\mathrm{H}_0^3$$
$$+ \left(-\frac{208x^2}{81} + \frac{812x}{81} + \frac{320}{81}\right)\mathrm{H}_0^2 + \Bigg(-\frac{8624x^2}{243} - \frac{8}{81}(48\zeta_2 - 199)x - \frac{16}{27}(8\zeta_2 + 19)$$
$$- \frac{64}{27(x-1)}\Bigg)\mathrm{H}_0 + \left(-\frac{416x^2}{81} + \frac{56x}{27} - \frac{88}{27} + \frac{416}{81x}\right)\mathrm{H}_1\mathrm{H}_0 + \frac{128}{27}(1+x)\mathrm{H}_{0,1}$$
$$+ \left(\frac{64}{27}\zeta_2 - \frac{310}{27}\right)\delta(1-x)\mathrm{H}_0 + \left(\frac{208x^2}{81} - \frac{20x}{9} + \frac{44}{27} - \frac{208}{81x}\right)\mathrm{H}_1^2$$
$$- \frac{416}{729}x^2(9\zeta_2 + 113) - \frac{8}{729}(2088\zeta_2 - 864\zeta_3 + 6055) - \frac{8}{729}x(2601\zeta_2 - 864\zeta_3$$
$$- 4883) + \left(-\frac{8624x^2}{243} + \frac{2600x}{81} - \frac{872}{81} + \frac{4592}{243x}\right)\mathrm{H}_1 + \Big(\frac{832x^2}{81} + \frac{2144x}{81}$$

$$
\begin{aligned}
&+\frac{2120}{81}-\frac{416}{81x}\Big)\mathrm{H}_{0,1}-\frac{128}{27}(1+x)(\mathrm{H}_{0,0,1}+\mathrm{H}_{0,1,1})-\frac{24064}{729(x-1)_+}+\frac{32320}{729x}\Bigg]\\
&+C_F\Bigg[\frac{32}{27}(1+x)\mathrm{H}_0^4+\left(-\frac{128x^2}{81}+\frac{256x}{81}+\frac{64}{81}\right)\mathrm{H}_0^3+\Bigg(-\frac{2176x^2}{81}-\frac{32}{81}(18\zeta_2+107)x\\
&-\frac{32}{81}(18\zeta_2-1)\Bigg)\mathrm{H}_0^2+\left(-\frac{128x^2}{27}-\frac{32x}{9}+\frac{32}{9}+\frac{128}{27x}\right)\mathrm{H}_1\mathrm{H}_0^2+\frac{64}{9}(1+x)\mathrm{H}_{0,1}\mathrm{H}_0^2\\
&+\left(\frac{128x^2}{27}+\frac{32x}{9}-\frac{32}{9}-\frac{128}{27x}\right)\mathrm{H}_1^2\mathrm{H}_0+\Bigg(-\frac{128}{243}(18\zeta_2-1)x^2-\frac{64}{243}(333\zeta_2-108\zeta_3\\
&-410)x-\frac{64}{243}(225\zeta_2-108\zeta_3-1292)\Bigg)\mathrm{H}_0+\left(-\frac{1472x^2}{81}+\frac{64}{9}(x-1)+\frac{1472}{81x}\right)\mathrm{H}_1^2\\
&+\left(\frac{512x^2}{27}+\frac{2560x}{27}+\frac{1408}{27}-\frac{256}{27x}\right)\mathrm{H}_{0,1}\mathrm{H}_0-\frac{128}{9}(1+x)\left(\mathrm{H}_{0,0,1}\mathrm{H}_0+\mathrm{H}_{0,1,1}\mathrm{H}_0\right)\\
&+\left(\frac{256x^2}{81}+\frac{64}{27}(x-1)-\frac{256}{81x}\right)\mathrm{H}_1^3+\left(-\frac{4352x^2}{81}-\frac{320x}{9}+\frac{704}{9}+\frac{896}{81x}\right)\mathrm{H}_1\mathrm{H}_0\\
&+\left(\frac{1024}{9}\zeta_2^2-\frac{1312}{81}\right)\delta(1-x)-\frac{64}{405}x\left(63\zeta_2^2+145\zeta_2-120\zeta_3+1720\right)\\
&+\frac{64}{729}x^2(414\zeta_2-108\zeta_3-1165)-\frac{64}{405}\left(63\zeta_2^2-215\zeta_2-30\zeta_3-1675\right)\\
&-\left(\frac{128}{243}(18\zeta_2-1)x^2+\frac{64}{27}[(3\zeta_2+44)x-(3\zeta_2+80)]-\frac{128(18\zeta_2-163)}{243x}\right)\mathrm{H}_1\\
&+\left(\frac{1408x^2}{81}+\frac{128}{81}[(9\zeta_2+37)x+(9\zeta_2-71)]-\frac{896}{81x}\right)\mathrm{H}_{0,1}+\Bigg(-\frac{512x^2}{27}-\frac{2560x}{27}\\
&-\frac{1408}{27}+\frac{256}{27x}\Bigg)\mathrm{H}_{0,0,1}+\left(\frac{256x^2}{27}+\frac{1664x}{27}+\frac{1664}{27}+\frac{256}{27x}\right)\mathrm{H}_{0,1,1}\\
&+\frac{128}{9}(1+x)\left(\mathrm{H}_{0,0,0,1}+\mathrm{H}_{0,0,1,1}-2\mathrm{H}_{0,1,1,1}\right)+\frac{79744}{729x}\Bigg]\Bigg\}, \qquad (256)
\end{aligned}
$$

with the shorthand notation $\mathrm{H}_{\vec{a}} \equiv \mathrm{H}_{\vec{a}}(x)$ for the harmonic polylogarithms over the alphabet $\mathfrak{A} = \{0, 1, -1\}$ [122]. They can be expressed in terms of elementary functions and the Nielsen integrals [245, 289, 290]:

$$
\begin{aligned}
\mathrm{H}_0(x) &= \ln(x), && (257)\\
\mathrm{H}_1(x) &= -\ln(1-x), && (258)\\
\mathrm{H}_{0,1}(x) &= \mathrm{Li}_2(x), && (259)\\
\mathrm{H}_{0,0,1}(x) &= \mathrm{Li}_3(x), && (260)\\
\mathrm{H}_{0,1,1}(x) &= \mathrm{S}_{1,2}(x), && (261)\\
\mathrm{H}_{0,0,0,1}(x) &= \mathrm{Li}_4(x), && (262)\\
\mathrm{H}_{0,0,1,1}(x) &= \mathrm{S}_{2,2}(x), && (263)\\
\mathrm{H}_{0,1,1,1}(x) &= \mathrm{S}_{1,3}(x)\,, && (264)
\end{aligned}
$$

with

$$S_{n,p}(x) = \frac{(-1)^{(n+p-1)}}{(n-1)!p!} \int_0^1 \frac{dy}{y} \ln^{(n-1)}(y) \ln^p(1-xy)\,, \tag{265}$$

$$\mathrm{Li}_n(x) = S_{n-1,1}(x)\,. \tag{266}$$

Here $\mathrm{Li}_n(x)$ denotes the (classical) polylogarithm [245, 291–293]. All higher functions but $\mathrm{S}_{2,2}(x)$ can be reduced to polylogarithms by the argument relation $x \to (1-x)$. Numerical implementations of the functions $S_{n,p}(x)$ were given in [119].

At small values of x, the functions $A_{gq(g),Q}^{(3),n_f T_F^2,\overline{\mathsf{MS}}}(x)$ are singular as $\propto 1/x$, or in N-space like $\propto 1/(N-1)$, unlike the quarkonic contributions given in [88] with a leading pole $\propto 1/N$. One notices that the number of functions needed in x-space to express $A_{gq(g),Q}^{(3),n_f T_F^2,\overline{\mathsf{MS}}}$ is larger than in N-space, as has been found also in other analyses, cf. [78, 294, 295].

7 Bubble Topologies Contributing to the Polarized OMEs ΔA_{gq} and ΔA_{gg}

A key goal of deep-inelastic scattering with polarized particle beams and targets is the determination of the composition of the nucleon spin in terms of the quark and gluon spins, as well as the orbital angular momentum of these constituents, cf. [296] and references therein.

In QCD analyses of data from these experiments, polarized parton distributions $q_\pm$ are determined, which give the unpolarized PDFs in the combination $q = q_+ + q_-$. For longitudinally polarized nucleons they have a simple partonic interpretation: $q_\pm$ measure the probability of finding a quark with the same (opposite) polarization as compared to the nucleon, respectively. Therefore, the combination $\delta q = q_+ - q_-$ measures the contribution of the nucleon spin carried by the quark species q.

The differential cross section of the polarized DIS contribution due to photon exchange [144–146, 296] takes the following form for longitudinal nucleon polarization

$$\frac{d^2\sigma(\lambda,\pm S_L)}{dx\,dy} = \pm 2\pi s\frac{\alpha^2}{Q^4}\left[-2\lambda y\left(2-y-\frac{2xyM^2}{s}xg_1^\gamma(x,Q^2)\right)+8\lambda\frac{yx^2M^2}{s}g_2^\gamma(x,Q^2)\right], \quad (267)$$

and for transverse nucleon polarization

$$\frac{d^3\sigma(\lambda,\pm S_T)}{dx\,dy\,d\theta} = \pm s\frac{\alpha^2}{Q^4}\sqrt{\frac{M^2}{s}}\sqrt{xy\left[1-y-\frac{xyM^2}{s}\right]} \cos(\alpha-\theta)\left[-2\lambda yxg_1^\gamma(x,Q^2)-4\lambda xg_2^\gamma(x,Q^2)\right]. \quad (268)$$

In the nucleon's rest frame, the nucleon spin vector is parameterized by

$$S_L = (0,0,0,M), \quad (269)$$
$$S_T = M(0,\cos(\alpha),\sin(\alpha),0), \quad (270)$$

in case of the longitudinal and transverse polarizations, respectively. The helicity of the incoming electron is denoted by λ, and θ is the azimuthal angle of the final state lepton. The structure functions contain both light and heavy flavor contributions. Due to the Wandzura-Wilczek relation [297], at twist 2, g_2 is determined by g_1:

$$g_2(x,Q^2) = -g_1(x,Q^2) + \int_x^1 \frac{dz}{z} g_1(z,Q^2). \quad (271)$$

This relation also holds for target mass and initial and final state quark mass corrections [144, 298], as well as in case of non-forward [299] and diffractive scattering [300–302].

The leading order heavy flavor Wilson coefficients are known completely [69, 303, 304]. To next-to-leading order, heavy quark corrections in the asymptotic representation were given in [229, 305, 306], taking into account, that the factorization formulae for these quantities can be constructed from the ones for unpolarized DIS by one photon exchange, where Wilson coefficients and OMEs are replaced by their polarized counterparts, cf. [305].

The polarized counterparts to the twist-2 composite operators (54–56) read:

$$O^{\sf NS}_{q,r;\mu_1,\ldots,\mu_N} = i^{N-1}\mathbf{S}[\overline{\psi}\gamma_5\gamma_{\mu_1}D_{\mu_2}\ldots D_{\mu_N}\frac{\lambda_r}{2}\psi] - \text{trace terms}, \quad (272)$$
$$O^{\sf S}_{q;\mu_1,\ldots,\mu_N} = i^{N-1}\mathbf{S}[\overline{\psi}\gamma_5\gamma_{\mu_1}D_{\mu_2}\ldots D_{\mu_N}\psi] - \text{trace terms}, \quad (273)$$

$$O^{\mathsf{S}}_{g;\mu_1,\ldots,\mu_N} = 2i^{N-2}\mathbf{SSp}[\frac{1}{2}\varepsilon^{\mu_1\alpha\beta\gamma}F^a_{\beta\gamma}D^{\mu_2}\ldots D^{\mu_{N-1}}F^{\mu_N}_{\alpha,a}] - \text{trace terms}\,. \tag{274}$$

The corresponding Feynman rules are given in [229, 306, 307].

The 2-loop contributions to the massive OMEs $\Delta A_{Qg}, \Delta A^{\rm PS}_{Qq}, \Delta A^{\rm NS}_{qq,Q}$ are given in [229, 306, 308]. Since $\Delta A_{qg,Q}$ and $A^{\rm PS}_{qq,Q}$ start at 3-loop order, the following calculation of the 2-loop contributions to $\Delta A_{gq,Q}$ and $\Delta A_{gg,Q}$ complete the set of massive OMEs at 2-loops.

The calculation proceeds similar to the calculation of the unpolarized OMEs in Chapter 6, except for the occurrence of the antisymmetric Levi-Civita tensor, which are absent in the former case. Following the earlier calculations [229, 305, 306], products of Levi-Civita tensors are written via the determinant of metric tensors in (115). Contractions with these metric tensors are then evaluated in D dimensions.

The renormalization procedure is analogous to the unpolarized case as described in Section 4.2, replacing the anomalous dimensions with their polarized counter parts. However, due to the treatment of the genuinely four dimensional Levi-Civita tensor in D dimensions, the result may not be that of the $\overline{\rm MS}$ scheme, and a finite renormalization of the operators is still required [307].

The renormalization procedure allows for a prediction of the pole terms of the OMEs in terms of polarized anomalous dimensions at 2-loop order. The unrenormalized massive OMEs read:

$$\Delta\hat{\hat{A}}^{(2)}_{gq,Q} = \left(\frac{\hat{m}^2}{\mu^2}\right)^{\varepsilon}\left[\frac{2\beta_{0,Q}}{\varepsilon^2}\Delta\gamma^{(0)}_{gq} + \frac{\Delta\hat{\gamma}^{(1)}_{gq}}{2\varepsilon} + \Delta a^{(2)}_{gq,Q} + \Delta\overline{a}^{(2)}_{gq,Q}\varepsilon\right], \tag{275}$$

$$\begin{aligned}\Delta\hat{\hat{A}}^{(2)}_{gg,Q} = \left(\frac{\hat{m}^2}{\mu^2}\right)^{\varepsilon}\Bigg[&\frac{1}{2\varepsilon^2}\Big\{\Delta\gamma^{(0)}_{gq}\Delta\hat{\gamma}^{(0)}_{qg} + 2\beta_{0,Q}\Big(\Delta\gamma^{(0)}_{gg} + 2\beta_0 + 4\beta_{0,Q}\Big)\Big\} + \frac{\Delta\hat{\gamma}^{(1)}_{gg} + 4\delta m_1^{(-1)}\beta_{0,Q}}{2\varepsilon}\\ &+ \Delta a^{(2)}_{gg,Q} + 2\delta m^{(0)}_1\beta_{0,Q} + \beta^2_{0,Q}\zeta_2 + \varepsilon\Big[\Delta\overline{a}^{(2)}_{gg,Q} + 2\delta m^{(1)}_1\beta_{0,Q} + \frac{\beta^2_{0,Q}\zeta_3}{6}\Big]\Bigg].\end{aligned} \tag{276}$$

The renormalized OMEs are given by

$$\Delta A^{(2),\overline{\rm MS}}_{gq,Q} = \frac{\beta_{0,Q}\Delta\gamma^{(0)}_{gq}}{2}\ln^2\left(\frac{m^2}{\mu^2}\right) + \frac{\Delta\hat{\gamma}^{(1)}_{gq}}{2}\ln\left(\frac{m^2}{\mu^2}\right) + \Delta a^{(2)}_{gq,Q} - \frac{\beta_{0,Q}\Delta\gamma^{(0)}_{gq}}{2}\zeta_2\,, \tag{277}$$

$$\begin{aligned}\Delta A^{(2),\overline{\rm MS}}_{gg,Q} = &\frac{1}{8}\left\{2\beta_{0,Q}\Big(\Delta\gamma^{(0)}_{gg} + 2\beta_0\Big) + \Delta\gamma^{(0)}_{gq}\Delta\hat{\gamma}^{(0)}_{qg} + 8\beta^2_{0,Q}\right\}\ln^2\left(\frac{m^2}{\mu^2}\right) + \frac{\Delta\hat{\gamma}^{(1)}_{gg}}{2}\ln\left(\frac{m^2}{\mu^2}\right)\\ &- \frac{\zeta_2}{8}\Big[2\beta_{0,Q}\Big(\Delta\gamma^{(0)}_{gg} + 2\beta_0\Big) + \Delta\gamma^{(0)}_{gq}\Delta\hat{\gamma}^{(0)}_{qg}\Big] + \Delta a^{(2)}_{gg,Q}\,,\end{aligned} \tag{278}$$

using the pole mass m. All logarithmic term are predicted in the $\overline{\rm MS}$ scheme, referring to the anomalous dimensions, which are known to 2-loop order [307, 309, 310].

7.1 The $O(\alpha_s^2)$ Contributions to $\Delta\hat{\hat{A}}_{gq,Q}$ and $\Delta\hat{\hat{A}}_{gg,Q}$

The $O(\alpha_s^2)$ contributions to the unrenormalized OMEs $\Delta\hat{\hat{A}}_{gq,Q}$ and $\Delta\hat{\hat{A}}_{gg,Q}$ are evaluated analogously to the 2-loop contributions to the corresponding unpolarized OMEs [80]. The emerging sum representations contain at most finite single sums which were identified with single harmonic sums in a Maple program.

The following results are given up to linear order in ε, since these parts contribute to the 3-loop corrections through renormalization in later calculations:

$$\Delta\hat{\hat{A}}^{(2)}_{gq,Q} = \frac{1-(-1)^N}{2}\left(\frac{\hat{m}^2}{\mu^2}\right)^{\varepsilon} S^2_\varepsilon C_F T_F\left\{\frac{16(N+2)}{3\varepsilon^2 N(N+1)} + \frac{1}{\varepsilon}\left[\frac{8\left(N^2+4N+2\right)}{3N(N+1)^2} - \frac{8(N+2)S_1}{3N(N+1)}\right]\right.$$

$$
\begin{aligned}
&- \frac{4\left(N^2+4N+2\right)S_1}{3N(N+1)^2} + \frac{2(N+2)S_1^2}{3N(N+1)} + \frac{2(N+2)S_2}{3N(N+1)} + \frac{4\left(22N^3+97N^2+110N+44\right)}{27N(N+1)^3} \\
&+ \frac{4(N+2)\zeta_2}{3N(N+1)} + \varepsilon\left[\frac{\left(N^2+4N+2\right)S_1^2}{3N(N+1)^2} + \frac{\left(N^2+4N+2\right)S_2}{3N(N+1)^2}\right. \\
&- \frac{2\left(22N^3+97N^2+110N+44\right)S_1}{27N(N+1)^3} - \frac{2(N+2)\zeta_2 S_1}{3N(N+1)} - \frac{(N+2)S_1^3}{9N(N+1)} - \frac{(N+2)S_2S_1}{3N(N+1)} \\
&- \frac{2(N+2)S_3}{9N(N+1)} + \frac{2\left(N^2+4N+2\right)\zeta_2}{3N(N+1)^2} + \frac{2\left(40N^4+222N^3+395N^2+302N+80\right)}{27N(N+1)^4} \\
&\left.+ \frac{4(N+2)\zeta_3}{9N(N+1)}\right]\Bigg\}, \qquad (279)
\end{aligned}
$$

$$
\begin{aligned}
\Delta\hat{\hat{A}}^{(2)}_{gg,Q} = {}& \frac{1-(-1)^N}{2}\left(\frac{\hat{m}^2}{\mu^2}\right)^{\varepsilon} S_\varepsilon^2 \Bigg\{ \frac{1}{\varepsilon^2}\left[C_A T_F\left(\frac{64}{3N(N+1)} - \frac{32}{3}S_1\right)\right. \\
&\left. + C_F T_F \frac{16(N-1)(N+2)}{N^2(N+1)^2} + T_F^2\frac{64}{9}\right] \\
&+ \frac{1}{\varepsilon}\left[C_A T_F\left(\frac{16\left(3N^4+6N^3+16N^2+13N-3\right)}{9N^2(N+1)^2} - \frac{80}{9}S_1\right) - C_F T_F \frac{4P_{27}}{N^3(N+1)^3}\right] \\
&+ C_A T_F\left(\frac{2P_{28}}{27N^3(N+1)^3} - \frac{8}{3}\zeta_2 S_1 - \frac{4(56N+47)}{27(N+1)}S_1 + \frac{16}{3N(N+1)}\zeta_2\right) \\
&+ C_F T_F\left(\frac{4(N-1)(N+2)}{N^2(N+1)^2}\zeta_2 - \frac{P_{29}}{3N^4(N+1)^4}\right) + T_F^2\frac{16}{9}\zeta_2 \\
&+ \varepsilon\left[C_A T_F\left(-\frac{2\left(328N^2+584N+283\right)}{81(N+1)^2}S_1 + \frac{4\left(3N^4+6N^3+16N^2+13N-3\right)}{9N^2(N+1)^2}\zeta_2\right.\right. \\
&+ \frac{P_{30}}{81N^4(N+1)^4} - \frac{20}{9}\zeta_2 S_1 - \frac{8}{9}\zeta_3 S_1 - \frac{1}{3(N+1)}S_1^2 + \frac{2N+1}{3(N+1)}S_2 \\
&\left.+ \frac{16}{9N(N+1)}\zeta_3\right) + C_F T_F\left(\frac{4(N-1)(N+2)}{3N^2(N+1)^2}\zeta_3 - \frac{P_{27}}{N^3(N+1)^3}\zeta_2 - \frac{P_{31}}{12N^5(N+1)^5}\right) \\
&\left.+ T_F^2\frac{16}{27}\zeta_3\right]\Bigg\}, \qquad (280)
\end{aligned}
$$

with

$$
\begin{aligned}
P_{27} &= 3N^6+9N^5+7N^4+3N^3+8N^2-2N-4\,, && (281)\\
P_{28} &= 15N^6+45N^5+374N^4+601N^3+161N^2-24N+36\,, && (282)\\
P_{29} &= 13N^8+52N^7+54N^6+4N^5+13N^4+12N^2+36N+24\,, && (283)\\
P_{30} &= 3N^8+12N^7+2080N^6+5568N^5+4602N^4+1138N^3-3N^2-36N-108\,, && (284)\\
P_{31} &= 35N^{10}+175N^9+254N^8+62N^7+55N^6+347N^5+384N^4+72N^3 \\
&\quad -96N^2-120N-48\,. && (285)
\end{aligned}
$$

Due to the necessity of a finite renormalization, the calculation does not deliver the terms predicted by the $\overline{\rm MS}$ renormalization constants. Rather shifts occur between the calculation,

which are given for the coefficients of the expansion in ε:

$$\Delta\hat{\hat{A}}_{ij}^{(2)} = \sum_{i=-2}^{1} \varepsilon^i \Delta\hat{\hat{A}}_{ij}^{(2,i)}\,, \tag{286}$$

$$\Delta\hat{\hat{A}}_{ij}^{(2)} = \sum_{i=-2}^{1} \varepsilon^i \Delta\hat{\hat{A}}_{ij}^{(2,i)}\,. \tag{287}$$

For the pole-terms one obtains

$$\Delta\hat{\hat{A}}_{gq,Q}^{(2,-2)} = \Delta\hat{\hat{A}}_{gq,Q}^{(2,-2)}\,, \tag{288}$$

$$\Delta\hat{\hat{A}}_{gq,Q}^{(2,-1)} = \Delta\hat{\hat{A}}_{gq,Q}^{(2,-1)} - C_F T_F \frac{32(N-1)}{9\varepsilon N(N+1)}\,, \tag{289}$$

$$\Delta\hat{\hat{A}}_{gg,Q}^{(2,-2)} = \Delta\hat{\hat{A}}_{gg,Q}^{(2,-2)}\,, \tag{290}$$

$$\Delta\hat{\hat{A}}_{gg,Q}^{(2,-1)} = \Delta\hat{\hat{A}}_{gg,Q}^{(2,-1)}\,. \tag{291}$$

Comparing with (275), the shift can be attributed to the 2-loop anomalous dimension $\Delta\hat{\hat{\gamma}}_{gq,Q}$, which is subject to the shift

$$\Delta\hat{\hat{\gamma}}_{gq,Q} = \Delta\hat{\gamma}_{gq,Q} - C_F T_F \frac{64(N-1)}{9\varepsilon N(N+1)}\,. \tag{292}$$

Taking this into account, the logarithmic contributions follow from (277, 278):

$$\begin{aligned}
\Delta A_{gq,Q}^{(2)} =\; & \ln^2\!\left(\frac{m^2}{\mu^2}\right) C_F T_F \frac{8(N+2)}{3N(N+1)} \\
& + \ln\!\left(\frac{m^2}{\mu^2}\right) C_F T_F \frac{1}{2}\left(\frac{32(N+2)(5N+2)}{9N(N+1)^2} - \frac{32(N+2)}{3N(N+1)} S_1\right) + \text{const.}\,,
\end{aligned} \tag{293}$$

$$\begin{aligned}
\Delta A_{gg,Q}^{(2)} =\; & \ln^2\!\left(\frac{m^2}{\mu^2}\right)\left[C_A T_F\left(\frac{16}{3N(N+1)} - \frac{8}{3}S_1\right) + C_F T_F \frac{4(N-1)(N+2)}{N^2(N+1)^2} + T_F^2 \frac{16}{9}\right] \\
& + \ln\!\left(\frac{m^2}{\mu^2}\right)\left[C_A T_F\left(\frac{32\left(3N^4+6N^3+16N^2+13N-3\right)}{9N^2(N+1)^2} - \frac{160}{9}S_1\right)\right. \\
& \left. + C_F T_F \frac{8\left(N^6+3N^5+5N^4+N^3-8N^2+2N+4\right)}{N^3(N+1)^3}\right] + \text{const.}\,.
\end{aligned} \tag{294}$$

In order to determine the constant parts and linear contributions in ε, the finite renormalization has yet to be developed fully for the massive OMEs. Similarly, also the unrenormalized $O(\alpha_s^3 n_f T_F^2)$ contributions $\Delta\hat{\hat{A}}_{gq,Q}^{(3),n_f T_F^2}$ and $\Delta\hat{\hat{A}}_{gg,Q}^{(3),n_f T_F^2}$ were calculated, which are, however, subject to a later publication, together with the finite renormalization of the massive OMEs at 2-loop order [306].

8 3-Loop Ladder Graphs

In order to study the behavior of the deep-inelastic scattering heavy flavor structure functions one has to calculate the 3-loop corrections to the operator matrix elements. However, at the moment a general algorithm is not known, which computes all contributing graphs. Therefore, it is necessary to study the integrals in question in greater detail, and develop specific mathematical tools for an automated calculation of them. The genuine 3-loop topologies are ladder, benz, crossed box and V-graphs. In this Chapter, we address the ladder and V-graphs in a case study of the most complicated situations formed by the scalar graphs.

While recalculating the two loop massive OMEs and extending the results to linear order in the dimensional regularization parameter ε, the authors of [77–79] realized, that representing the Feynman integrals via generalized hypergeometric functions leads to a great reduction in size compared to earlier calculations [76], which were based on specific integration by parts reductions [113]. Furthermore, representations of hypergeometric functions via convergent power series expansions may in many cases be simplified using summation theory [93–101].

In the following we study scalar prototypes of 3-loop ladder diagrams with six massive lines contributing to $A_{Qg}^{(3)}$. These graphs are of the same topology as the tadpole graph shown in Figure 2, which has been computed [133, 229]. We start repeating the calculation of this particular

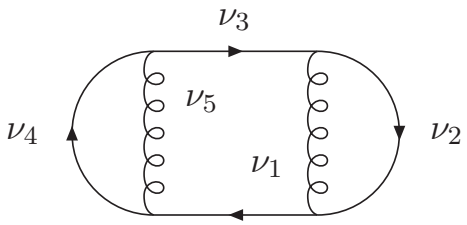

Figure 2: Massive tadpole graph with 3 loops.

graph. Using the scalar Feynman rules in Appendix F, one finds the following D-dimensional integral for arbitrary propagator powers ν_i :

$$T_1 = \iiint \frac{d^Dq d^Dk d^Dl}{(2\pi)^{3D}} \frac{i(-1)^{\nu_{12345}} (m^2)^{\nu_{12345}-3D/2} (4\pi)^{3D/2}}{(k^2)^{\nu_1}((k-l)^2-m^2)^{\nu_2}(l^2-m^2)^{\nu_3}((q-l)^2-m^2)^{\nu_4}(q^2)^{\nu_5}}, \quad (295)$$

where $\nu_{i_1,\ldots,i_l} = \sum_{k=1}^{l} \nu_{i_k}$, and the integral has been conveniently normalized. The loop integrals are performed in the order k, q, l, parameterizing each loop momentum according to Eq. (149). In this way the momentum integrals can be performed using (111), and leave us with

$$\begin{aligned} T_1 = {} & \Gamma\left[\begin{array}{c} \nu_{12345} - 6 - 3\varepsilon/2 \\ \nu_1, \nu_2, \nu_3, \nu_4, \nu_5 \end{array}\right] \\ & \int_0^1 dw_1 \ldots \int_0^1 dw_4 \frac{\theta(1-w_1-w_2) w_1^{-3-\varepsilon/2+\nu_{12}} w_2^{-3-\varepsilon/2+\nu_{45}} (1-w_1-w_2)^{\nu_3-1}}{\left(1 + w_1 \frac{w_3}{1-w_3} + w_2 \frac{w_4}{1-w_4}\right)^{\nu_{12345}-6-3\varepsilon/2}} \\ & w_3^{1+\varepsilon/2-\nu_1} (1-w_3)^{1+\varepsilon/2-\nu_2} w_4^{1+\varepsilon/2-\nu_5} (1-w_4)^{1+\varepsilon/2-\nu_4}, \end{aligned} \quad (296)$$

which is symmetric under the permutation $\binom{w_3}{\nu_3} \leftrightarrow \binom{w_4}{\nu_4}, \binom{w_1}{\nu_1} \leftrightarrow \binom{w_2}{\nu_2}$. Furthermore, the integrals over w_1, w_2 have the form of the double integral representation (199) of the Appell function

F_1 [257, 261]. However, the arguments of this Appell function become arbitrarily large. In order to obtain a convergent series representation, we therefore have to make use of the analytic continuation relation (201) in the form

$$F_1\left[a;b,b';c;\frac{x}{x-1},\frac{y}{y-1}\right] = (1-x)^b(1-y)^{b'}F_1[c-a;b,b';c;x,y]\,. \tag{297}$$

The convergent series representation (200) allows to perform the remaining (w_3, w_4) integrals. As a result, one obtains a double infinite series

$$\begin{aligned} T_1 &= \Gamma\left[\begin{array}{c} -2-\frac{\varepsilon}{2}+\nu_{12}, -2-\frac{\varepsilon}{2}+\nu_{45}, -6-\frac{3}{2}\varepsilon+\nu_{12345} \\ \nu_2, \nu_4, -4-\varepsilon+\nu_{12345} \end{array}\right] \\ &\quad \sum_{m,n=0}^{\infty} \Gamma\left[\begin{array}{c} 2+m+\frac{\varepsilon}{2}-\nu_1, 2+n+\frac{\varepsilon}{2}-\nu_5 \\ 1+m, 1+n, 2+m+\frac{\varepsilon}{2}, 2+n+\frac{\varepsilon}{2} \end{array}\right] \\ &\quad \frac{\left(2+\frac{\varepsilon}{2}\right)_{n+m}\left(-2-\frac{\varepsilon}{2}+\nu_{12}\right)_m\left(-2-\frac{\varepsilon}{2}+\nu_{45}\right)_n}{\left(-4-\varepsilon+\nu_{12345}\right)_{n+m}}\,, \end{aligned} \tag{298}$$

which can be cast into the form of a Kampé-De-Feriet series [258, 263, 264]:

$$\begin{aligned} T_1 &= \Gamma\left[\begin{array}{c} -6-\frac{3}{2}\varepsilon+\nu_{12345}, -2-\frac{\varepsilon}{2}+\nu_{12}, 2+\frac{\varepsilon}{2}-\nu_1, -2-\frac{\varepsilon}{2}+\nu_{45}, 2+\frac{\varepsilon}{2}-\nu_5 \\ -4-\varepsilon+\nu_{12345}, \nu_2, \nu_4, 2+\frac{\varepsilon}{2}, 2+\frac{\varepsilon}{2} \end{array}\right] \\ &\quad F^{1;2,2}_{1;1,1}\left[\begin{array}{c} 2+\frac{\varepsilon}{2}; -2-\frac{\varepsilon}{2}+\nu_{12}, 2+\frac{\varepsilon}{2}-\nu_1; -2-\frac{\varepsilon}{2}+\nu_{45}, 2+\frac{\varepsilon}{2}-\nu_5; \\ -4-\varepsilon+\nu_{12345}; 2+\frac{\varepsilon}{2}; 2+\frac{\varepsilon}{2}; \end{array} 1,1\right]. \end{aligned} \tag{299}$$

Now the paradigm proposed in [229] states that the general structure of the integral will remain when the diagram is dressed with external lines and an operator insertion. Therefore, in all these cases, one might seek an Appell function representation in order to make use of the analytic continuation. Finally one obtains finite sums over Kampé-De-Feriet series with the index structure $F^{1;2,2}_{1;1,1}$. However, it is not obvious whether the double series representation converges. The question of convergence will be a general issue when manipulating the quite delicate structures of multi sums, multi integrals and expansions in the following calculations.

In [229], see also [133], one example is given following the ideas above, namely the 3-loop ladder graph with external gluon lines attached to the exterior bubbles, and with an operator insertion on one of the central massive lines, which is shown in Fig. 3. The external lines refer to

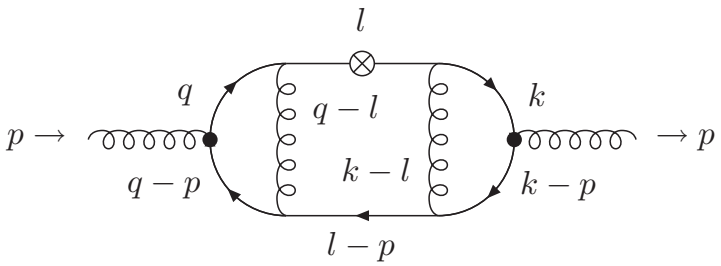

Figure 3: The 3–loop ladder graph containing a central local operator insertion. The momentum flow indicated here is used for all ladder diagrams in the following.

an external momentum flow entering at this point, but are no propagators. The momentum flow indicated by the vectors q, p, k, l is universal for all ladder graphs considered in this Chapter.

The momentum integral is parameterized using (149) loop momentum for loop momentum, starting with the exterior (triangle) loops. The resulting Feynman parameter integral has the form

$$\begin{aligned}\hat{I}_{1a} &= -\exp\left(-\frac{3}{2}\varepsilon\gamma_E\right)\Gamma\left(2-\frac{3}{2}\varepsilon\right)\prod_{i=1}^{7}\int_0^1 dw_i\,\frac{\theta(1-w_1-w_2)w_1^{-\varepsilon/2}w_2^{-\varepsilon/2}(1-w_1-w_2)}{\left(1+w_1\dfrac{1-w_3}{w_3}+w_2\dfrac{1-w_4}{w_4}\right)^{2-3\varepsilon/2}}\\ &\quad w_3^{-1+\varepsilon/2}(1-w_3)^{\varepsilon/2}w_4^{-1+\varepsilon/2}(1-w_4)^{\varepsilon/2}(w_5w_1+w_6w_2+(1-w_1-w_2)w_7)^N\,.\end{aligned} \tag{300}$$

Here and in the following scalar calculations, we omit a factor

$$I_{1a} \equiv \frac{i(\Delta.p)^N a_s^3 S_\varepsilon^3}{(m^2)^{2-3\frac{\varepsilon}{2}}}\hat{I}_{1a}, \tag{301}$$

where S_ε was defined in (116). Furthermore, we already removed all δ-distributions and θ-functions, which are not needed to make symmetries evident.

Similarly to the 2-loop case [77, 311], the integrand of this diagram is found to be equal to the integrand of the tadpole with the appropriate propagator powers, multiplied with a multilinear polynomial[4] raised to the power N:

$$[w_5w_1+w_6w_2+(1-w_1-w_2)w_7]^N\,. \tag{302}$$

This polynomial originates in the operator insertion and it will be called operator polynomial, operator insertion or simply operator, if no confusion is to be expected. The parameters w_5, w_6, w_7 occur due to the external momentum p, which flows through the diagram. Here one notes, that since $p^2 = 0$, these additional parameters do not occur in the integrand except for the operator insertion. Therefore, the integrals over these parameters can be performed using:

$$\int_0^1 dx\,(A+xB)^C = \frac{[(A+B)^{C+1}-A^{C+1}]}{(C+1)B}\,. \tag{303}$$

However, this step has to be handled with some care, since B will depend on further Feynman parameters, and hence for $B \to 0$ the individual parts $\frac{[(A+B)^{C+1}]}{(C+1)B}$ and $-\frac{[A^{C+1}]}{(C+1)B}$ may develop spurious poles which cancel in the sum.

Another approach consists in turning the power of the linear polynomial into a product of simpler polynomials and monomials using a binomial expansion, e.g.

$$(w_5w_1+w_6w_2+(1-w_1-w_2)w_7)^N = \sum_{i=0}^{N}\binom{N}{i}w_5^{N-i}w_1^{N-i}\sum_{j=0}^{i}\binom{i}{j}w_6^{i-j}w_2^{i-j}(1-w_1-w_2)^j w_7^j\,. \tag{304}$$

However, this method may introduce unnecessary sums. Therefore it will be most efficient to integrate the operator polynomial as far as possible, but introduce binomial sums only if necessary to cancel spurious poles at the integrand level.

In this way the operator polynomial is reduced to terms, that fit into the integral representation of the Appell function F_1, which delivers the following sum representation:

$$\hat{I}_{1a} = \frac{\exp\left(-\frac{3}{2}\varepsilon\gamma_E\right)\Gamma(2-3\varepsilon/2)}{(N+1)(N+2)(N+3)}\sum_{m,n=0}^{\infty}\Bigg\{$$

[4]Note that the triple integral over w_5, w_6, w_7 yields the same result for the polynomial (302), as for $(1-w_5w_1-w_6w_2-(1-w_1-w_2)w_7)^N$

$$
\sum_{t=1}^{N+2} \binom{3+N}{t} \frac{(t-\varepsilon/2)_m \, (2+N+\varepsilon/2)_{n+m} \, (3-t+N-\varepsilon/2)_n}{(4+N-\varepsilon)_{n+m}}
$$
$$
\times \Gamma \left[\begin{array}{c} t, t-\varepsilon/2, 1+m+\varepsilon/2, 1+n+\varepsilon/2, 3-t+N, 3-t+N-\varepsilon/2 \\ 4+N-\varepsilon, 1+m, 1+n, 1+t+m+\varepsilon/2, 4-t+n+N+\varepsilon/2 \end{array} \right]
$$
$$
- \sum_{s=1}^{N+3} \sum_{r=1}^{s-1} \binom{s}{r} \binom{3+N}{s} (-1)^s \frac{(r-\varepsilon/2)_m \, (-1+s+\varepsilon/2)_{n+m} \, (s-r-\varepsilon/2)_n}{(1+s-\varepsilon)_{n+m}}
$$
$$
\times \Gamma \left[\begin{array}{c} r, r-\varepsilon/2, s-r, 1+m+\varepsilon/2, 1+n+\varepsilon/2, s-r-\varepsilon/2 \\ 1+m, 1+n, 1+r+m+\varepsilon/2, 1+s-r+n+\varepsilon/2, 1+s-\varepsilon \end{array} \right] \Bigg\} . \tag{305}
$$

One now expands (305) in ε and applies the summation packages Sigma [93–101] and EvaluateMultiSums [101–103] by C. Schneider. The result may be expressed in terms of harmonic Sums:

$$
\begin{aligned}
\hat{I}_{1a} \;=\; & -\frac{4(N+1)S_1+4}{(N+1)^2(N+2)}\zeta_3 + \frac{2S_{2,1,1}}{(N+2)(N+3)} + \frac{1}{(N+1)(N+2)(N+3)} \Bigg\{ \\
& -2(3N+5)S_{3,1} - \frac{S_1^4}{4} + \frac{4(N+1)S_1 - 4N}{N+1} S_{2,1} + 2\left[(2N+3)S_1 + \frac{5N+6}{N+1}\right] S_3 \\
& + \frac{9+4N}{4} S_2^2 + \left[2\frac{7N+11}{(N+1)(N+2)} + \frac{5N}{N+1} S_1 - \frac{5}{2} S_1^2\right] S_2 + \frac{2(3N+5)S_1^2}{(N+1)(N+2)} \\
& + \frac{N}{N+1} S_1^3 + \frac{4(2N+3)S_1}{(N+1)^2(N+2)} - \frac{(2N+3)S_4}{2} + 8\frac{2N+3}{(N+1)^3(N+2)} \Bigg\} \\
& + O(\varepsilon) \,.
\end{aligned} \tag{306}
$$

Here the arguments of the harmonic sums were omitted, cf. (164). Equation (306) was checked against moments for $N = 1, ..., 10$ obtained with MATAD [285].

Noting that an operator insertion on the line can be decomposed in the following way:

$$
\begin{aligned}
\xrightarrow[p]{} \!\!\otimes\!\!\rightarrow \;\; &= \frac{i(\not{p}+m)\not{\Delta}(\Delta.p)^{N-1} i(\not{p}+m)}{(p^2-m^2)^2} \\
&= -2(\Delta.p)^N \frac{\not{p}+m}{(p^2-m^2)^2} + 2(\Delta.p)^{N-1} \frac{\not{\Delta}}{(p^2-m^2)} \,,
\end{aligned} \tag{307}
$$

so that there is one part in which the denominator is raised to the second power, and another with a first power, one is left with two cases to study in the scalar case.

The scalar integral from above is also considered with a higher power of the propagator carrying the operator insertion. The corresponding integral can be calculated analogously to the one above and yields:

$$
I_{1b} \;\equiv\; \frac{i(\Delta.p)^N a_s^3 S_\varepsilon^3}{(m^2)^{3-3\frac{\varepsilon}{2}}} \hat{I}_{1b} \,, \tag{308}
$$

$$
\begin{aligned}
\hat{I}_{1b} \;=\; & \frac{\exp\left(-\frac{3}{2}\varepsilon\gamma_E\right)}{(N+1)(N+2)(N+3)} \Gamma\left(3-\frac{3}{2}\varepsilon\right) \Bigg\{ - \sum_{m=0}^{\infty} \sum_{n=0}^{\infty} \sum_{l=1}^{N+2} \binom{N+3}{l} \\
& \times B\left(l, m+1+\frac{\varepsilon}{2}\right) B\left(N+3-l, n+1+\frac{\varepsilon}{2}\right)
\end{aligned}
$$

$$
\begin{aligned}
&\times\Gamma\left[\begin{array}{c} N+2+\frac{\varepsilon}{2}+m+n \\ m+1,n+1,N+2+\frac{\varepsilon}{2} \end{array}\right] \frac{B\left(l+m-\frac{\varepsilon}{2},N+3-l+n-\frac{\varepsilon}{2}\right)}{(N+4+m+n-\varepsilon)(N+3+m+n-\varepsilon)} \\
&+\frac{1}{N+4}\Bigg[\sum_{m=1}^{\infty}\sum_{n=1}^{\infty}\sum_{l=1}^{N+4}\binom{N+4}{l}\sum_{j=1}^{N+4-l}\binom{N+4-l}{j}(-1)^{j+l}B\left(j,m+1+\frac{\varepsilon}{2}\right) \\
&\times B\left(l,n+1+\frac{\varepsilon}{2}\right)\Gamma\left[\begin{array}{c} j+l-2+m+n+\frac{\varepsilon}{2} \\ m+1,n+1,j+l-2+\frac{\varepsilon}{2} \end{array}\right] \frac{B\left(j+m-\frac{\varepsilon}{2},l+n-\frac{\varepsilon}{2}\right)}{j+l+m+n-\varepsilon} \\
&+\sum_{m=1}^{\infty}\sum_{l=1}^{N+4}\binom{N+4}{l}\sum_{j=1}^{N+4-l}\binom{N+4-l}{j}(-1)^{j+l}B\left(j,m+1+\frac{\varepsilon}{2}\right)B\left(l,1+\frac{\varepsilon}{2}\right) \\
&\times\Gamma\left[\begin{array}{c} j+l-2+m+\frac{\varepsilon}{2} \\ m+1,j+l-2+\frac{\varepsilon}{2} \end{array}\right] \frac{B\left(j+m-\frac{\varepsilon}{2},l-\frac{\varepsilon}{2}\right)}{j+l+m-\varepsilon} \\
&+\sum_{n=1}^{\infty}\sum_{l=1}^{N+4}\binom{N+4}{l}\sum_{j=1}^{N+4-l}\binom{N+4-l}{j}(-1)^{j+l}B\left(j,1+\frac{\varepsilon}{2}\right)B\left(l,n+1+\frac{\varepsilon}{2}\right) \\
&\times\Gamma\left[\begin{array}{c} j+l-2+n+\frac{\varepsilon}{2} \\ n+1,j+l-2+\frac{\varepsilon}{2} \end{array}\right] \frac{B\left(j-\frac{\varepsilon}{2},l+n-\frac{\varepsilon}{2}\right)}{j+l+n-\varepsilon} \\
&+\sum_{l=1}^{N+4}\binom{N+4}{l}\sum_{j=1}^{N+4-l}\binom{N+4-l}{j}(-1)^{j+l}B\left(j,1+\frac{\varepsilon}{2}\right)B\left(l,1+\frac{\varepsilon}{2}\right)\frac{B\left(j-\frac{\varepsilon}{2},l-\frac{\varepsilon}{2}\right)}{j+l-\varepsilon} \\
&-\sum_{m=0}^{\infty}\sum_{n=0}^{\infty}\sum_{l=1}^{N+3}\binom{N+4}{l}B\left(l,m+1+\frac{\varepsilon}{2}\right)B\left(N+4-l,n+1+\frac{\varepsilon}{2}\right) \\
&\times\Gamma\left[\begin{array}{c} N+2+m+n+\frac{\varepsilon}{2} \\ m+1,n+1,N+2+\frac{\varepsilon}{2} \end{array}\right] \frac{B\left(l+m-\frac{\varepsilon}{2},N+4-l+n-\frac{\varepsilon}{2}\right)}{N+4+m+n-\varepsilon}\Bigg]\Bigg\} \qquad (309)
\end{aligned}
$$

$$
\begin{aligned}
= \;& \frac{1}{(N+1)(N+2)(N+3)(N+4)}\Bigg\{\frac{1}{2}S_1^4-\frac{3N+1}{N+1}S_1^3 \\
&-\frac{N^5+8N^4+45N^3+154N^2+234N+122}{(N+1)^2(N+2)(N+3)}S_1^2+\frac{4\left(5N^3+22N^2+23N+3\right)}{(N+1)^2(N+2)(N+3)}S_1 \\
&-\frac{1}{2}\left(2N^2+14N+21\right)S_2^2-\frac{2\left(6N^5+46N^4+170N^3+411N^2+575N+324\right)}{(N+1)^3(N+2)^2(N+3)} \\
&+4(N+3)(N+4)\left[S_1+\frac{1}{N+1}\right]\zeta_3+\Bigg[5S_1^2-\frac{5(3N+1)}{(N+1)}S_1 \\
&-\frac{3N^5+28N^4+151N^3+458N^2+638N+318}{(N+1)^2(N+2)(N+3)}\Bigg]S_2+\Bigg[-\frac{2\left(2N^3+16N^2+51N+43\right)}{(N+1)} \\
&-4\left(N^2+7N+9\right)S_1\Bigg]S_3+\left(N^2+7N+9\right)S_4+\Bigg[\frac{2\left(N^3+7N^2+20N+10\right)}{(N+1)} \\
&-8S_1\Bigg]S_{2,1}+2\left(3N^2+21N+28\right)S_{3,1}-2\left(N^2+7N+8\right)S_{2,1,1}\Bigg\}+O(\varepsilon)\,. \qquad (310)
\end{aligned}
$$

This integral has a similar structure as the one for Diagram 1a concerning the set of harmonic sums appearing, but the rational functions in N are of higher degree.

In the following, we perform the calculation of ladder-type diagrams of different complexity,

which is both due to the number of massive lines and the corresponding local operator insertions. At first, the computation of diagrams with six massive lines is presented, and after that a set of scalar Feynman integrals is solved, which constitute the class of graphs with three massive lines. The Feynman rules used for the calculation are given in Appendix F.

8.1 Further Diagrams with Six Fermion Propagators

Let us consider the diagrams in Figure 4. In Table 1 we summarize a series of Mellin moments

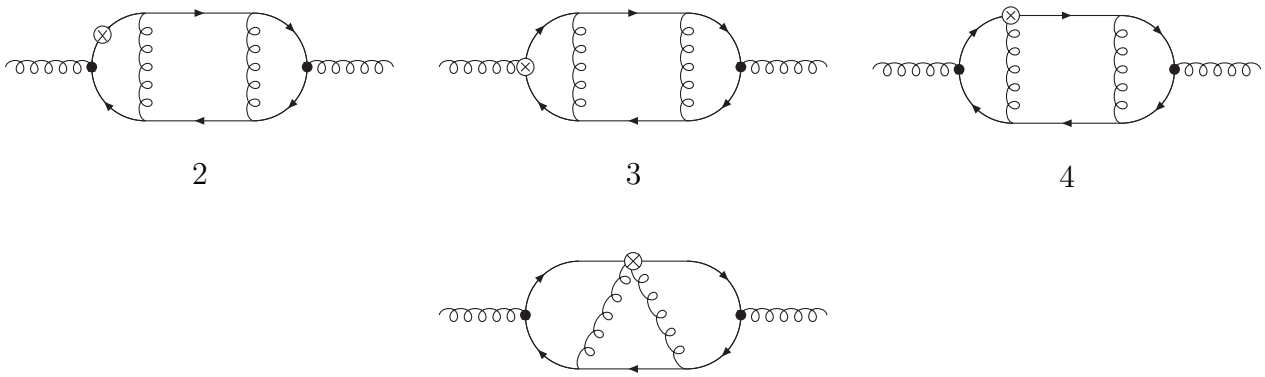

Figure 4: Diagrams with 6 fermion propagators

for the diagrams calculated using the code MATAD [285] for comparison to the general-N results.

Diagram	N		Diagram	N	
$\hat{I}_{1a}$	0	$2-2\zeta_3$	$\hat{I}_{2b}$	0	$\frac{1}{8}$
	1	$1-\zeta_3$		1	$\frac{5}{108}$
	2	$\frac{199}{324}-\frac{11}{18}\zeta_3$		2	$\frac{731}{1728}-\frac{1}{3}\zeta_3$
	3	$\frac{91}{216}-\frac{5}{12}\zeta_3$		3	$\frac{2142253}{5184000}-\frac{1}{3}\zeta_3$
$\hat{I}_{1b}$	0	$-\frac{9}{4}+2\zeta_3$	$\hat{I}_3$	0	$2-2\zeta_3$
	1	$-\frac{247}{216}+\zeta_3$		1	0
	2	$-\frac{1831}{2592}+\frac{11}{18}\zeta_3$		2	$\frac{967}{432}-2\zeta_3$
	3	$-\frac{1257637}{2592000}+\frac{5}{12}\zeta_3$		3	0
$\hat{I}_{2a}$	0	$2-2\zeta_3$	$\hat{I}_4$	0	$2\zeta_3$
	1	$1-\zeta_3$		1	$2-2\zeta_3$
	2	$\frac{1399}{1296}-\zeta_3$		2	$\frac{29}{12}-\frac{83}{36}\zeta_3$
	3	$\frac{967}{864}-\zeta_3$		3	$\frac{17}{6}-\frac{47}{18}\zeta_3$

Table 1: Mellin Moments for the Integrals $\hat{I}_{1a}-\hat{I}_4$.

Diagram 2a has the following Feynman parameter representation:

$$\hat{I}_{2a} = \exp\left(-\frac{3}{2}\varepsilon\gamma_E\right)\Gamma\left(2-\frac{3}{2}\varepsilon\right)\int_{[0,1]^7} dx\,dz\,du\,dw\,ds\,dt\,da\; z^{\frac{\varepsilon}{2}-1}(1-z)^{\frac{\varepsilon}{2}}w^{-1+\frac{\varepsilon}{2}}(1-w)^{\frac{\varepsilon}{2}}$$

$$\theta(1-s-t)s^{-\frac{\varepsilon}{2}}t^{-\frac{\varepsilon}{2}}(1-s-t)[u(1-w)+w(tu+sx+a(1-s-t))]^N$$
$$\left(1-s\frac{z-1}{z}-t\frac{w-1}{w}\right)^{-2+\frac{3}{2}\varepsilon} . \tag{311}$$

The calculation of the sum representation shall be shown in detail in the following, since it involves several details, which are necessary to maintain convergence or finiteness of the result. The Feynman parameters u, x, a only occur in the operator polynomial, so their integral will be performed first:

$$I_{uxa} \equiv \int_{[0,1]^3} du\, dx\, da\ [u(1-w)+tu+sx+a(1-s-t)]^N . \tag{312}$$

The integrals over a and x are straightforwardly performed using (303). One finds:

$$\begin{aligned} I_{uxa} = \frac{1}{(N+1)(N+2)w^2s(1-s-t)} \int_0^1 du \Big\{ & [(1-w)u+wtu+ws+w(1-s-t)]^{N+2} \\ & - [(1-w)u+wtu+w(1-s-t)]^{N+2} - [(1-w)u+wtu+ws]^{N+2} \\ & + [(1-w)u+wtu]^{N+2} \Big\} . \end{aligned} \tag{313}$$

Now the integral over u could be performed in the same way, but it would introduce a factor $(1-w+wt)$ in the denominator. Since this polynomial would introduce further complication, e.g. another infinite sum at a later stage, we first introduce a binomial sum:

$$\begin{aligned} I_{uxa} = \frac{1}{(N+1)(N+2)w^2s(1-s-t)} \int_0^1 du \sum_{l=0}^{N+2} \binom{N+2}{l} u^{N+2-l} w^l \Big\{ & (1-u)^l(1-t)^l \\ & - [-u(1-t)+1-s-t]^l - [-u(1-t)+s]^l + (-1)^l u^l (1-t)^l \Big\} . \end{aligned} \tag{314}$$

In order to make cancellations between different terms evident, the u integral is kept again, while another binomial sum is introduced:

$$\begin{aligned} I_{uxa} = \frac{1}{(N+1)(N+2)w^2s(1-s-t)} \int_0^1 du \sum_{l=0}^{N+2} \binom{N+2}{l} u^{N+2-l} w^l \Big\{ & \sum_{j=0}^{l} \binom{l}{j} (-1)^{l-j} u^{l-j} \\ & \Big[(1-t)^l - (1-t)^{l-j}(1-s-t)^j - (1-t)^{l-j} s^j \Big] + (-1)^l u^l (1-t)^l \Big\} . \end{aligned} \tag{315}$$

Now obviously the term $j=0$ cancels the last term, and the contribution for $j=1$ vanishes. Cancellations of this kind are important, since the integrations of the parameters a, x often introduce spurious singularities in individual terms, which cancel in the sum, and which correspond to boundary points in the summation ranges.

As a next step, a binomial sum is introduced in the following way:

$$(1-s-t)^j = \sum_{k=0}^{j} \binom{j}{k} (-1)^k (1-t)^{j-k} s^k . \tag{316}$$

This leads to a cancellation of the term $k=1$ with the first term in the square bracket of (315):

$$I_{uxa} = \frac{1}{(N+1)(N+2)w^2s(1-s-t)} \int_0^1 du \sum_{l=0}^{N+2} \binom{N+2}{l} u^{N+2-l} w^l \sum_{j=0}^{l} \binom{l}{j} (-1)^{l-j} u^{l-j}$$

$$(1-t)^{l-j}\left\{-\sum_{k=1}^{j}\binom{l}{j}(-1)^k(1-t)^{j-k}s^k - s^j\right\}. \tag{317}$$

Since the factors $(1-t)^\alpha$ are not part of the integral representation of the Appell function (198), they are subject to another binomial sum:

$$I_{uxa} = \frac{1}{(N+1)(N+2)w^2 s(1-s-t)}\int_0^1 du\ \sum_{l=0}^{N+2}\binom{N+2}{l}u^{N+2-l}w^l\sum_{j=0}^{l}\binom{l}{j}(-1)^{l-j}u^{l-j}$$
$$\left\{-\sum_{k=1}^{j}\binom{l}{j}(-1)^k\sum_{r=0}^{l-k}\binom{l-k}{r}(-1)^r s^k t^r - \sum_{r=0}^{l-j}\binom{l-j}{r}(-1)^r s^j t^r\right\}. \tag{318}$$

Now the u-integral is performed and the result is inserted into the complete expression for I_{2a}:

$$\hat{I}_{2a} = \exp\left(-\frac{3}{2}\varepsilon\gamma_E\right)\frac{\Gamma\left(2-\frac{3}{2}\varepsilon\right)}{(N+1)(N+2)}\int_{[0,1]^7} dz\,dw\,ds\,dt\,\theta(1-s-t)z^{\frac{\varepsilon}{2}-1}(1-z)^{\frac{\varepsilon}{2}}$$
$$\left(1-s\frac{z-1}{z}-t\frac{w-1}{w}\right)^{-2+\frac{3}{2}\varepsilon}\sum_{l=0}^{N+2}\binom{N+2}{l}(-1)^l w^{l-3+\frac{\varepsilon}{2}}(1-w)^{\frac{\varepsilon}{2}}\sum_{j=0}^{l}\binom{l}{j}(-1)^j\frac{1}{N+3-j}$$
$$\left\{-\sum_{k=1}^{j}\binom{l}{j}(-1)^k\sum_{r=0}^{l-k}\binom{l-k}{r}(-1)^r s^{k-1-\frac{\varepsilon}{2}}t^{r-\frac{\varepsilon}{2}} - \sum_{r=0}^{l-j}\binom{l-j}{r}(-1)^r s^{j-1-\frac{\varepsilon}{2}}t^{r-\frac{\varepsilon}{2}}\right\}. \tag{319}$$

The integrals over s and t then represent an Appell function:

$$\hat{I}_{2a} = \exp\left(-\frac{3}{2}\varepsilon\gamma_E\right)\frac{\Gamma\left(2-\frac{3}{2}\varepsilon\right)}{(N+1)(N+2)}\int_{[0,1]^7} dz\,dw\,z^{\frac{\varepsilon}{2}-1}(1-z)^{\frac{\varepsilon}{2}}\sum_{l=0}^{N+2}\binom{N+2}{l}(-1)^l$$
$$w^{l-3+\frac{\varepsilon}{2}}(1-w)^{\frac{\varepsilon}{2}}\sum_{j=0}^{l}\binom{l}{j}(-1)^j\frac{1}{N+3-j}\left\{-\sum_{k=1}^{j}\binom{l}{j}(-1)^k\sum_{r=0}^{l-k}\binom{l-k}{r}(-1)^r\right.$$
$$\frac{\Gamma(k-\frac{\varepsilon}{2})\Gamma(r+1-\frac{\varepsilon}{2})}{\Gamma(r+k+2-\varepsilon)}F_1\left[2-\frac{3}{2}\varepsilon; k-\frac{\varepsilon}{2}, r+1-\frac{\varepsilon}{2}; r+k+2-\varepsilon; \frac{z-1}{z}, \frac{w-1}{w}\right]$$
$$-\sum_{r=0}^{l-j}\binom{l-j}{r}(-1)^r\frac{\Gamma(j-\frac{\varepsilon}{2})\Gamma(r+1-\frac{\varepsilon}{2})}{\Gamma(r+j+2-\varepsilon)}$$
$$\left.F_1\left[2-\frac{3}{2}\varepsilon; j-\frac{\varepsilon}{2}, r+1-\frac{\varepsilon}{2}; r+j+2-\varepsilon; \frac{z-1}{z}, \frac{w-1}{w}\right]\right\}. \tag{320}$$

The arguments of the Appell function F_1 become infinitely large. If a series expansion shall be used, the arguments have to run in the interval $[0,1]$. This is achieved by the analytic continuation formula (201). Diagram 2a then takes the form:

$$\hat{I}_{2a} = \frac{\exp\left(-\frac{3}{2}\varepsilon\gamma_E\right)\Gamma\left(2-\frac{3}{2}\varepsilon\right)}{(N+1)(N+2)}\int_{[0,1]^7} dz\,dw\,z^{\frac{\varepsilon}{2}-1}(1-z)^{\frac{\varepsilon}{2}}\sum_{l=0}^{N+2}\binom{N+2}{l}(-1)^l w^{l-3+\frac{\varepsilon}{2}}(1-w)^{\frac{\varepsilon}{2}}$$
$$\sum_{j=0}^{l}\binom{l}{j}(-1)^j\frac{1}{N+3-j}\left\{-\sum_{k=1}^{j}\binom{l}{j}(-1)^k\sum_{r=0}^{l-k}\binom{l-k}{r}(-1)^r\frac{\Gamma(k-\frac{\varepsilon}{2})\Gamma(r+1-\frac{\varepsilon}{2})}{\Gamma(r+k+2-\varepsilon)}\right.$$
$$\left.z^{k-\frac{\varepsilon}{2}}w^{r+1-\frac{\varepsilon}{2}}F_1\left[r+k+\frac{\varepsilon}{2}; k-\frac{\varepsilon}{2}, r+1-\frac{\varepsilon}{2}; r+k+2-\varepsilon; 1-z, 1-w\right]\right.$$

$$
-\sum_{r=0}^{l-j}\binom{l-j}{r}(-1)^r\frac{\Gamma(j-\frac{\varepsilon}{2})\Gamma(r+1-\frac{\varepsilon}{2})}{\Gamma(r+j+2-\varepsilon)}
$$

$$
z^{j-\frac{\varepsilon}{2}}w^{r+1-\frac{\varepsilon}{2}}F_1\left[r+j+\frac{\varepsilon}{2};j-\frac{\varepsilon}{2},r+1-\frac{\varepsilon}{2};r+j+2-\varepsilon;1-z,1-w\right]\Bigg\}. \tag{321}
$$

In this form the series representation (200) is applied, and the remaining integrals are performed in terms of Beta functions. The result is the desired sum representation:

$$
I_{2a} \equiv \frac{i(\Delta.p)^N a_s^3 S_\varepsilon^3}{(m^2)^{2-3\frac{\varepsilon}{2}}}\hat{I}_{2a}, \tag{322}
$$

$$
\begin{aligned}
\hat{I}_{2a} &= \exp\left(-3\frac{\varepsilon}{2}\gamma_E\right)\Gamma\left(2-\frac{3}{2}\varepsilon\right)\frac{1}{(N+1)(N+2)}\sum_{m=0}^{\infty}\sum_{n=0}^{\infty}\sum_{l=2}^{N+2}\binom{N+2}{l}\sum_{j=2}^{l}\binom{l}{j}\Bigg\{\\
&\sum_{k=1}^{j}\binom{j}{k}\sum_{r=0}^{l-k}\binom{l-k}{r}(-1)^{l+j+k+r}\,\Gamma\left[\begin{array}{c}k+r+m+n+\frac{\varepsilon}{2}\\ m+1,n+1,k+r+\frac{\varepsilon}{2}\end{array}\right]\\
&\times B\left(k,m+1+\frac{\varepsilon}{2}\right)\frac{B\left(k+m-\frac{\varepsilon}{2},r+1+n-\frac{\varepsilon}{2}\right)B\left(r+l-1,n+1+\frac{\varepsilon}{2}\right)}{(k+r+1+m+n-\varepsilon)(N+3-j)}\\
&+\sum_{r=0}^{l-j}\binom{l-j}{r}(-1)^{l+j+r}\,\Gamma\left[\begin{array}{c}j+r+m+n+\frac{\varepsilon}{2}\\ m+1,n+1,j+r+\frac{\varepsilon}{2}\end{array}\right]B\left(j,m+1+\frac{\varepsilon}{2}\right)\\
&\times\frac{B\left(j+m-\frac{\varepsilon}{2},r+1+n-\frac{\varepsilon}{2}\right)B\left(r+l-1,n+1+\frac{\varepsilon}{2}\right)}{(j+r+1+m+n-\varepsilon)(N+3-j)}\Bigg\}.
\end{aligned} \tag{323}
$$

These sums can be reduced by Sigma and yield

$$
\begin{aligned}
\hat{I}_{2a} &= \frac{1}{(N+1)(N+2)(N+3)}\Bigg\{2^{N+4}S_{1,2}\left(\frac{1}{2},1\right)+2^{N+3}S_{1,1,1}\left(\frac{1}{2},1,1\right)+\frac{(N^2+12N+16)}{2(N+1)(N+2)}S_1^2\\
&+\frac{3N^2+40N+56}{2(N+1)(N+2)}S_2+\frac{1}{6}S_1^3+\frac{4(2N+3)}{(N+1)^2(N+2)}S_1-\frac{1}{2}S_2S_1-(-1)^NS_{-3}\\
&+\frac{1}{3}(-3N-17)S_3-2(-1)^NS_{-2,1}+(-N-3)S_{2,1}-2(-1)^N\zeta_3-2\left(2^{N+3}-3\right)\zeta_3\\
&+\frac{8(2N+3)}{(N+1)^3(N+2)}\Bigg\}+O(\varepsilon).
\end{aligned} \tag{324}
$$

In this diagram, for the first time generalized harmonic sums (S-sums) [254] occur in the final result. Their definition is given in (168) and their algebraic properties were studied in [111]. The algebra and many relations are implemented in the Package HarmonicSums by J. Ablinger [108–111].

The generalized harmonic sums emerge with $\xi \in \{\frac{1}{2},1\}$ together with powers 2^N. In the limit $N\to\infty$ the generalized harmonic sums approach finite values given below. Still $\hat{I}_{2a}$ does not diverge exponentially, which is due to relations among these special generalized harmonic sums, [111, 133]. The asymptotic series of $\hat{I}_{2a}$ was computed using HarmonicSums [108–111] and is given by

$$
\hat{I}_{2a}(N) \simeq \left[\left(-\frac{1}{2N^3}+\frac{3}{N^4}-\frac{25}{2N^5}+\frac{45}{N^6}-\frac{301}{2N^7}+\frac{483}{N^8}-\frac{3025}{2N^9}+\frac{4665}{N^{10}}\right)\ln(\bar{N})\right.
$$

$$
\begin{aligned}
&+\frac{3}{2N^3}-\frac{55}{4N^4}+\frac{2029}{24N^5}-\frac{903}{2N^6}+\frac{185923}{80N^7}-\frac{495179}{40N^8}+\frac{73442819}{1008N^9}-\frac{84311831}{168N^{10}}\Bigg]\zeta_2\\
&+\Big(\frac{1}{6N^3}-\frac{1}{N^4}+\frac{25}{6N^5}-\frac{15}{N^6}+\frac{301}{6N^7}-\frac{161}{N^8}+\frac{3025}{6N^9}-\frac{1555}{N^{10}}\Big)\ln^3(\bar{N})\\
&+\Big(\frac{1}{2N^3}-\frac{9}{4N^4}+\frac{227}{24N^5}-\frac{97}{2N^6}+\frac{22877}{80N^7}-\frac{72181}{40N^8}+\frac{12331933}{1008N^9}-\frac{15557449}{168N^{10}}\Big)\ln^2(\bar{N})\\
&+\Big(\frac{1}{N^3}-\frac{5}{2N^4}-\frac{145}{24N^5}+\frac{2897}{24N^6}-\frac{1509931}{1440N^7}+\frac{470549}{60N^8}-\frac{3304037}{56N^9}\\
&+\frac{116332471}{240N^{10}}\Big)\ln(\bar{N})+\frac{1}{N^3}-\frac{15}{4N^4}+\frac{1429}{72N^5}-\frac{7771}{48N^6}+\frac{1226359}{900N^7}-\frac{158319577}{14400N^8}\\
&+\frac{1140112957301}{12700800N^9}-\frac{334237263613}{423360N^{10}}+\Big(-\frac{3}{N^2}+\frac{37}{3N^3}-\frac{41}{N^4}+\frac{385}{3N^5}-\frac{393}{N^6}+\frac{3577}{3N^7}\\
&-\frac{3601}{N^8}+\frac{32545}{3N^9}-\frac{32633}{N^{10}}\Big)\zeta_3+O\left(\frac{1}{N^{11}}\right), \qquad (325)
\end{aligned}
$$

where $\ln(\bar{N})=\ln(N)+\gamma_E$.

For Diagram 2b, i.e. the corresponding graph with a squared propagator of the line carrying the operator insertion, the Feynman parameterization reads

$$
\begin{aligned}
\hat{I}_{2b}=\;&\exp\left(-\frac{3}{2}\varepsilon\gamma_E\right)\Gamma\left(3-\frac{3}{2}\varepsilon\right)\int_{[0,1]^7}dx\,dz\,du\,dw\,ds\,dt\,da\;z^{\frac{\varepsilon}{2}-1}(1-z)^{\frac{\varepsilon}{2}}(1-u)w^{-2+\frac{\varepsilon}{2}}(1-w)^{\frac{\varepsilon}{2}}\\
&\theta(1-s-t)s^{-\frac{\varepsilon}{2}}t^{1-\frac{\varepsilon}{2}}(1-s-t)\left(1-s\frac{z-1}{z}-t\frac{w-1}{w}\right)^{-3+\frac{3}{2}\varepsilon}\\
&[u(1-w)+w(tu+sx+a(1-s-t))]^{N-1}, \qquad (326)
\end{aligned}
$$

and one obtains a sum representation in a similar way:

$$
\begin{aligned}
I_{2b}\;&\equiv\;\frac{i(\Delta.p)^N a_s^3 S_\varepsilon^3}{(m^2)^{3-3\frac{\varepsilon}{2}}}\hat{I}_{2b}, \qquad (327)\\
\hat{I}_{2b}\;&=\;-\exp\left(-3\frac{\varepsilon}{2}\gamma_E\right)\Gamma\left(3-\frac{3}{2}\varepsilon\right)\frac{1}{(N+1)(N+2)}\sum_{m=0}^{\infty}\sum_{n=0}^{\infty}\sum_{l=2}^{N+2}\binom{N+2}{l}\sum_{j=2}^{l}\binom{l}{j}\Bigg[\\
&\sum_{k=1}^{j}\binom{j}{k}\sum_{r=0}^{l-k}\binom{l-k}{r}(-1)^{l+j+k+r}\,\Gamma\left[\begin{array}{c}k+r+m+n+\frac{\varepsilon}{2}\\ m+1,n+1,k+r+\frac{\varepsilon}{2}\end{array}\right]B\left(k,m+1+\frac{\varepsilon}{2}\right)\\
&\times B(N+3-j,2)\frac{B\left(k+m-\frac{\varepsilon}{2},r+2+n-\frac{\varepsilon}{2}\right)B\left(r+l-1,n+1+\frac{\varepsilon}{2}\right)}{k+r+2+m+n-\varepsilon}\\
&+\sum_{r=0}^{l-j}\binom{l-j}{r}(-1)^{l+j+r}\,\Gamma\left[\begin{array}{c}j+r+m+n+\frac{\varepsilon}{2}\\ m+1,n+1,j+r+\frac{\varepsilon}{2}\end{array}\right]B\left(j,m+1+\frac{\varepsilon}{2}\right)\\
&\times B(N+3-j,2)\frac{B\left(j+m-\frac{\varepsilon}{2},r+2+n-\frac{\varepsilon}{2}\right)B\left(r+l-1,n+1+\frac{\varepsilon}{2}\right)}{j+r+2+m+n-\varepsilon}\Bigg\} \qquad (328)\\
&=\;\frac{1}{(N+1)(N+2)(N+3)(N+4)}\Bigg\{2^{N+4}NS_{1,2}\left(\frac{1}{2},1\right)+2^{N+3}NS_{1,1,1}\left(\frac{1}{2},1,1\right)\\
&+(-1)^N(N^2+4N+2)\left(-S_{-3}-2S_{-2,1}-2\zeta_3\right)+\frac{1}{3}\left(-6N^2-33N-20\right)S_3\\
&+\frac{(8N^3+31N^2+17N-18)}{2(N+1)(N+2)(N+3)}S_1^2+\frac{2\left(9N^3+43N^2+58N+21\right)}{(N+1)^2(N+2)(N+3)}S_1
\end{aligned}
$$

$$+\frac{3\left(12N^3+55N^2+61N+6\right)}{2(N+1)(N+2)(N+3)}S_2 - \frac{1}{3}S_1^3 + S_2S_1 + (N+4)S_{2,1}$$
$$+2\left(N^2 - 2^{N+3}N + 6N + 2\right)\zeta_3$$
$$+\frac{-6N^5-14N^4+68N^3+247N^2+225N+36}{(N+1)^3(N+2)^2(N+3)}\Bigg\} + O(\varepsilon)\,. \tag{329}$$

Again the sum-structure of the integrals remains the same. Unlike the case for the massless 3-loop Wilson coefficients [64] and massive integrals in [100], the generalized harmonic sums do not vanish diagram by diagram. We remark that sums of this type even emerge in massive 2-loop integrals, if diagrams are simply separated into individual terms in a mathematical manner, e.g. in a fully automated computation to $O(\varepsilon)$ [79], while they are absent if the diagrams are considered as whole entities being mapped to various final sums [78, 79]. The presence of these generalized harmonic sums does not alter the structure of the diagrams significantly in the special way they appear, as we will outline below.

For Diagram 3 a general relation for the operator insertions on external lines can be used. The idea is to sum up the operator part:

$$\sum_{j=0}^{N}(\Delta.k - \Delta.p)^j(\Delta.k)^{N-j} = \frac{(\Delta.k)^{N+1} - (\Delta.k - \Delta.p)^{N+1}}{\Delta.p}\,, \tag{330}$$

where the denominator is trivial, due to the gluon line carrying the external momentum p only. Then the symmetry of the diagram is used:

$$\begin{aligned} I_3 =& \int \hat{d}k\hat{d}r\hat{d}s \frac{\sum_{j=0}^{N}(\Delta.k - \Delta.p)^j(\Delta.k)^{N-j}}{((k-p)^2-m^2)((r-p)^2-m^2)((s-p)^2-m^2)(s^2-m^2)(r^2-m^2)} \\ & \times \frac{1}{(k^2-m^2)(k-r)^2(s-r)^2} \\ =:& \int \hat{d}k\hat{d}r\hat{d}s \frac{1}{\Delta.p}\frac{(\Delta.k)^{N+1} - (\Delta.k - \Delta.p)^{N+1}}{D(k,r,s)}\,, \end{aligned} \tag{331}$$

where the propagators obviously obey $D(p-k, p-r, p-s) = D(k,r,s)$, so that one can cast the second term in the numerator into the same simple form as the first one:

$$I_3 = \int \hat{d}k\hat{d}r\hat{d}s \frac{1}{\Delta.p}\frac{(\Delta.k)^{N+1} + (-1)^N(\Delta.k)^{N+1}}{D(k,r,s)}\,. \tag{332}$$

From this, a relation to Diagram 2a follows:

$$I_3 = \left[1 + (-1)^N\right] I_{2a}(N+1)\,. \tag{333}$$

Diagrams with a gluon-quark-quark operator insertion on an external vertex can always be related to diagrams with the operator insertion on the fermion lines next to this vertex, due to the sum (330) occurring in the Feynman rule for the operators [87], cf. also Appendix F and [77, 311].

For Diagram 4, the Feynman parameter representation has the form

$$I_4 \equiv \frac{i(\Delta.p)^N a_s^3 S_\varepsilon^3}{(m^2)^{2-\frac{3}{2}\varepsilon}}\hat{I}_4\,, \tag{334}$$

$$\hat{I}_4 = \exp\left(-\frac{3}{2}\varepsilon\gamma_E\right)\Gamma\left(2-\frac{3}{2}\varepsilon\right)\sum_{j=0}^{N}\int_{[0,1]^7} dx\,dz\,du\,dw\,da\,ds\,dt\; w^{-1+\frac{\varepsilon}{2}}(1-w)^{\frac{\varepsilon}{2}}z^{-1+\frac{\varepsilon}{2}}(1-z)^{\frac{\varepsilon}{2}}$$
$$\theta(1-s-t)(1-s-t)s^{-\frac{\varepsilon}{2}}t^{-\frac{\varepsilon}{2}}\left(1-s\frac{z-1}{z}-t\frac{w-1}{w}\right)^{-2+\frac{3}{2}\varepsilon}$$
$$[(1-s-t)a+sx+tu]^{N-j}[(1-w)u+wa(1-s-t)+wsx+wtu]^{j}\,. \tag{335}$$

For this diagram, however, the derived sum representations in view of the paradigm from above, turned out not to be suitable for the summation algorithms of [93–101]. Instead the scalar prototype was solved by a completely different method [133] involving the method of hyperlogarithms [312] in an extended version. Nevertheless, the latter algorithm can only deal with graphs, which are free of ε poles. As a consequence it cannot be applied to all the QCD graphs.

The methods used for the calculations of Diagrams 1a-2b, however, is applicable to ε-singular graphs. Therefore it is worthwhile to study the integral in some detail in the present context.

For an approach using the multivariate Almkvist-Zeilberger algorithm (see the discussion below), the Feynman parameter representation was transformed such that the arguments of the (potential) Appell function have values in the unit hypercube:

$$\hat{I}_4 = \exp\left(-\frac{3}{2}\varepsilon\gamma_E\right)\Gamma\left(2-\frac{3}{2}\varepsilon\right)\int_{[0,1]^7} dx\,dz\,du\,dw\,da\,ds\,dt\;\theta(1-s-t)(1-w)^{\frac{\varepsilon}{2}}(1-z)^{\frac{\varepsilon}{2}}s^{-\frac{\varepsilon}{2}}t^{-\frac{\varepsilon}{2}}$$
$$(1-s-t)(1-s(1-z)-t(1-w))^{-N-2-\frac{\varepsilon}{2}}\sum_{j=0}^{N}\left[a(1-s-t)+wut+zxs\right]^{N-j}$$
$$\left[(1-w)u(1-s(1-z)-t(1-w))+w(a(1-s-t)+wut+zxs)\right]^{j}\,. \tag{336}$$

This is achieved by

1. expanding the operator polynomial in binomial sums,
2. identifying the Appell functions,
3. using the analytic continuation relation (201) to map the arguments into the unit hypercube and
4. going back to the (double) integral representation of the Appell function and reconstructing the polynomials by removing the binomial sums.

Due to the larger operator polynomial in Diagram 4 as compared to previous diagrams in this Chapter, there are more possibilities of introducing binomial expansions. Hence the minimum depth of the (definite) sum representation appears to be 6. This can be seen by partitioning the operator polynomial $[(1-w)u+wa(1-s-t)+wsx+wtu]$ into completely factorizing parts, e.g. $\{(1-w)u, wa(1-s-t), wsx, wtu\}$, where every splitting of the polynomial corresponds to introducing one binomial sum. Additionally, there is one finite sum from the Feynman rule of the operator insertion and two infinite ones from the series representation of the Appell function.

The following sum representation is obtained:

$$\hat{I}_4 = \sum_{k=0}^{N}\sum_{j=0}^{k}\binom{N+1}{j}\binom{N-j}{k-j}(-1)^{j-k}\sum_{l_3=0}^{k}\binom{k}{l_3}\sum_{l_2=0}^{l_3}\binom{l_3}{l_2}$$
$$\sum_{m=0}^{\infty}\sum_{n=0}^{\infty}\frac{(2+k+\frac{\varepsilon}{2})_{m+n}(l_2+1-\frac{\varepsilon}{2})_m(k+1-l_3-\frac{\varepsilon}{2})_n}{m!\;n!\;(k+4-\varepsilon)_{m+n}}$$

$$\Gamma\left[\begin{array}{c} l_2+1-\frac{\varepsilon}{2}, k+1-l_3-\frac{\varepsilon}{2}, l_3-l_2+2 \\ k+4-\varepsilon \end{array}\right]$$
$$B\left(k+1-l_3, N+1-j+n+\frac{\varepsilon}{2}\right) \frac{B(l_2+1, m+1-\frac{\varepsilon}{2})}{(N+1-l_3)(l_3-l_2+1)(l_2+1)}\,. \tag{337}$$

Due to the external momentum p being light like, for each internal momentum k one of the Feynman parameters associated to momenta $k, k-p$ is not contained in the numerator polynomial (the reason for this is shown formally in (403)). This uncouples these Feynman parameters from any non-integer parameter, such as the dimensional regulator ε. As a consequence the integrals in these parameters can be performed using an implementation of the multivariate Almkvist-Zeilberger algorithm [109, 313, 314]. The result is a four dimensional integral involving S-sums:

$$\hat{I}_4 = \exp\left(-\frac{3}{2}\varepsilon\gamma_E\right)\Gamma\left(2-\frac{3}{2}\varepsilon\right)\int_{[0,1]^7} dx\,dz\,du\,dw\,da\,ds\,dt\,\theta(1-s-t)(1-w)^{-1+\frac{\varepsilon}{2}}(1-z)^{\frac{\varepsilon}{2}}$$
$$s^{-\frac{\varepsilon}{2}}t^{-\frac{\varepsilon}{2}}(1-s-t)(1-s(1-z)-t(1-w))^{-N-2-\frac{\varepsilon}{2}} f_4(s,t,z,w)\,, \tag{338}$$

with

$$f_4(s,t,z,w) = \frac{(1-t(1-w)-s(1-z))^{N+1}}{(N+2)(N+3)}\Bigg\{\frac{(1-s-t)^{N+2}}{sz(1-t-s(1-z))^{N+2}}$$
$$\times S_1\left(\frac{(1-s-t(1-w))(1-t-s(1-z))}{(1-s-t)(1-t(1-w)-s(1-z))};N\right) + \Bigg[\frac{(sz)^{N+2}}{(1-s-t)(1-t-s(1-z))^{N+2}}$$
$$+\frac{(1-s-t)^{N+2}}{sz(1-t-s(1-z))^{N+2}} - \frac{(1-t-s(1-z))}{sz(1-s-t)}\Bigg] S_1\left(\frac{w(1-t-s(1-z))}{1-t(1-w)-s(1-z)};N\right)$$
$$+\Bigg[-\frac{(sz)^{N+2}}{(1-s-t)(1-t-s(1-z))^{N+2}} - \frac{(1-s-t)^{N+2}}{sz(1-t-s(1-z))^{N+2}}$$
$$+\frac{(1-t-s(1-z))}{sz(1-s-t)}\Bigg] S_1\left(\frac{1-t-s(1-z)}{1-t(1-w)-s(1-z)};N\right)$$
$$+\frac{(sz)^{N+2}}{(1-s-t)(1-t-s(1-z))^{N+2}} S_1\left(\frac{(1-t-s(1-z))(tw+sz)}{sz(1-t(1-w)-s(1-z))};N\right)$$
$$-\frac{(sz)^{N+2}}{(1-s-t)(1-t-s(1-z))^{N+2}} S_1\left(\frac{(1-t-s(1-z))((1-s-t)(1-w)+tw+sz)}{sz(1-t(1-w)-s(1-z))};N\right)$$
$$-\frac{(1-s-t)^{N+2}}{sz(1-t-s(1-z))^{N+2}} S_1\left(\frac{(1-t-s(1-z))(1-t(1-w)-s(1-(1-w)z))}{(1-s-t)(1-t(1-w)-s(1-z))};N\right)$$
$$-\frac{(N+2)(1-t-s(1-z))}{sz(1-s-t)} S_1\left(\frac{tw}{1-t(1-w)-s(1-z)};N\right)$$
$$+\frac{(N+2)(1-t-s(1-z))}{sz(1-s-t)} S_1\left(\frac{(1-s-t)(1-w)+sz(1-w)+tw}{1-t(1-w)-s(1-z)};N\right)$$
$$-\frac{(1-s-t-(N+2)zs)}{sz(1-s-t)} S_1\left(\frac{1-s-t(1-w)}{1-t(1-w)-s(1-z)};N\right)$$
$$-\frac{(sz-(N+2)(1-s-t))}{sz(1-s-t)} S_1\left(\frac{tw+sz}{1-t(1-w)-s(1-z)};N\right)$$
$$+\frac{(sz-(N+2)(1-s-t))}{sz(1-s-t)} S_1\left(\frac{(1-s-t)(1-w)+tw+sz}{1-t(1-w)-s(1-z)};N\right)$$

$$
+\frac{(1-s-t-(N+2)zs)}{sz(1-s-t)}S_1\left(\frac{1-t(1-w)-s(1-(1-w)z)}{1-t(1-w)-s(1-z)};N\right)\Bigg\}
$$
$$
-\frac{w^{N+1}(1-t-s(1-z))^{N+2}}{(N+1)(N+2)(N+3)s(1-s-t)z}+\frac{(1-t-s(1-z))^{N+2}}{(N+1)(N+2)(N+3)sz(1-s-t)}
$$
$$
+\frac{((1-s-t)(1-w)+sz(1-w)+tw)^{N+1}(1-t-s(1-z))}{(N+1)(N+3)sz(1-s-t)}
$$
$$
+\frac{(1-s-t-(N+2)zs)(1-t(1-w)-s(1-(1-w)z))^{N+1}}{(N+1)(N+2)(N+3)sz(1-s-t)}
$$
$$
-\frac{((1-s-t)(1-w)+tw+sz)^{N+2}}{(N+2)(N+3)swz(1-s-t)}+\frac{((1-s-t)(1-w)+sz(1-w)+tw)^{N+2}}{(N+2)(N+3)swz(1-s-t)}
$$
$$
+\frac{(1-s-t(1-w))^{N+1}(tw+2sz+N(1-s(1-z)-t(1-w)))}{(N+1)(N+2)(N+3)sz(1-s-t)}
$$
$$
+\frac{(1-w)(1-t(1-w)-s(1-z))^{N+2}}{(N+2)(N+3)swz(1-s-t)}-\frac{(tw)^{N+1}\left((N+2)(1-t(1-w)-s(1-z))-tw\right)}{(N+1)(N+2)(N+3)sz(1-s-t)}
$$
$$
+\frac{\left((1-s-t)^2+(N+1)(1-t-s(1-z))(1-t(1-w)-s(1-z))\right)(tw+sz)^{N+1}}{(N+1)(N+2)(N+3)sz(1-s-t)(1-t-s(1-z))}
$$
$$
-\frac{((N+2)(1-t-s(1-z))-sz)((1-s-t)(1-w)+tw+sz)^{N+1}}{(N+1)(N+2)(N+3)sz(1-t-s(1-z))}
$$
$$
+\frac{sz(swz)^{N+1}}{(N+1)(N+2)(N+3)(1-s-t)(1-t-s(1-z))}
$$
$$
-\frac{(sz)^{N+2}}{(N+1)(N+2)(N+3)(1-s-t)(1-t-s(1-z))}
$$
$$
-\frac{(w(1-s-t)^2+(N+1)(1-t-s(1-z))(1-t(1-w)-s(1-(1-w)z)))}{(N+1)(N+2)(N+3)swz(1-s-t)(1-t-s(1-z))}
$$
$$
\times(1-t(1-w)-s(1-(1-w)z))^{N+1}+\frac{(1-s-t)(1-s-t(1-w))^{N+1}}{(N+1)(N+2)(N+3)sz(1-t-s(1-z))}
$$
$$
+\frac{(1-s-t)^{N+2}w^{N+1}}{(N+1)(N+2)(N+3)sz(1-t-s(1-z))}
$$
$$
-\frac{(1-s-t)^{N+2}}{(N+1)(N+2)(N+3)sz(1-t-s(1-z))}\,. \tag{339}
$$

The structure of the expression is governed by the interplay of the (non-factorizing) polynomials:

$$
\begin{aligned}
1-t-s(1-z),\\
1-s-t(1-w),\\
1-t(1-w)-s(1-z),\\
1-t(1-w)-s(1-(1-w)z),\\
(1-s-t)(1-w)+tw+sz,\\
(1-s-t)(1-w)+sz(1-w)+tw,
\end{aligned}\tag{340}
$$

which map the region $s,t,w,z\in[0,1], s+t<1$ onto $[0,1]$, while the structures $s,t,w,z,(1-s-t),(1-w),(1-z)$ are considered atomic. Now let us have a look onto the number of infinite sums implied by the appearance of non-atomic polynomials: All the S-sums in (339) contain the non-atomic polynomial $(1-t(1-w)-s(1-z))$ as denominator of their first arguments. Due to

its connection to the Appell function, the presence of this polynomial implies a twofold infinite sum. Some of the coefficients contain even another integer power of a non-atomic polynomial in the denominator, which is in all cases $1-t-s(1-z)$. As a result the maximum nesting depth of infinite sums is 3. It turns out, that these triple infinite sums pose hard problems, particularly since an inner sum can spoil the convergence of an outer one.

For Diagram 5

$$I_5 \equiv \frac{i(\Delta.p)^N a_s^3 S_\varepsilon^3}{(m^2)^{1-\frac{3}{2}\varepsilon}} \hat{I}_5 \,, \tag{341}$$

$$\begin{aligned}
\hat{I}_5 = {} & \exp\left(-\frac{3}{2}\varepsilon\gamma_E\right)\Gamma\left(1-\frac{3}{2}\varepsilon\right)\int_{[0,1]^6} dx\,dz\,du\,dw\,ds\,dt\; z^{\frac{\varepsilon}{2}-1}(1-z)^{\frac{\varepsilon}{2}} w^{\frac{\varepsilon}{2}-1}(1-w)^{\frac{\varepsilon}{2}} \\
& \theta(1-s-t) s^{-\frac{\varepsilon}{2}} t^{-\frac{\varepsilon}{2}} \left(1 - s\frac{z-1}{z} - t\frac{w-1}{w}\right)^{-1+\frac{3}{2}\varepsilon} \sum_{j=0}^{N}\sum_{l=0}^{N-j} \\
& [(1-z)x + z(1-s-t) + zsx + ztu]^{N-j-l} [(1-w)u + w(1-s-t) + wsx + wtu]^j \\
& \{[1-s-t+sx+tu]^l \\
& + [u(1-w) - (1-z-w)(1-s-t) - (1-z-w)sx - (1-z-w)tu + x(1-z)]^l\}
\end{aligned} \tag{342}$$

one derives the following sum representation :

$$\begin{aligned}
I_5 = {} & (N+1)(N+2)\Gamma\left(1-\frac{3}{2}\varepsilon\right) \sum_{j=0}^{N} \binom{N}{j} \sum_{k=0}^{N-j} \binom{N-j}{k} \sum_{l=0}^{j} \binom{j}{l} \sum_{q=0}^{j} \binom{j}{q} \\
& \sum_{r=0}^{l} \binom{l}{r} \sum_{a=0}^{q} \binom{q}{a} \sum_{m=0}^{\infty}\sum_{n=0}^{\infty} \frac{(2+j+\frac{\varepsilon}{2})_{m+n} (1+q-a-\frac{\varepsilon}{2})_m (1+a-\frac{\varepsilon}{2})_n}{m!n!(3+j-\varepsilon)_{m+n}} \\
& \Gamma\left[\begin{array}{c} 1+q-a-\frac{\varepsilon}{2}, 1+a-\frac{\varepsilon}{2}, 1+j-q \\ 3+j-\varepsilon \end{array}\right] \Bigg\{ (-1)^r \frac{B(2+k+l, N+1-j-k)}{(1+k+q+a)(N+1-j-k+a)} \\
& \frac{B(1+q-a, 1+k+r+m+\frac{\varepsilon}{2})}{(1+k+r)} B(1+a+j-l, N+1-j-k+l-r+n+\frac{\varepsilon}{2}) \\
& + (-1)^{l+r} [B(r+1,k+1) - B(N+2-j-k-n+l, k+1)] \\
& \frac{B(1+q-a, N+1-j-k+l-r+\frac{\varepsilon}{2}+m)}{(N+1-j-k+q-a)(N+1-j-k+l-r)} \frac{B(1+a+j-l, k+r+1+n+\frac{\varepsilon}{2})}{(1+k+a)} \Bigg\}.
\end{aligned} \tag{343}$$

The solution of integrals I_4 and I_5 with tools of summation theory still remains an important research topic for the future. At the moment, the number of sums occurring is too large, needing a more detailed understanding. We not that I_5 for $\varepsilon \to 0$ has been solved using a combination of the hyperlogarithmic algorithm [312], and summation techniques [108–111] in [315]. The further work concerns the calculation of these graph topologies in the presence of poles implied by numerator structures, which is beyond the technology in Ref. [312].

8.2 Diagrams with Three Massive Fermion Propagators

In this section scalar diagrams with three massive propagators as given in Figure 5 are calculated. Again we first give a number of fixed moments in Table 2. Unlike the former case, the scalar diagrams contain poles down to $1/\varepsilon^2$.

Diagram	N	
$\hat{I}_{6a}$	0	$\frac{1}{6}\frac{1}{\varepsilon^2} + \frac{1}{9}\frac{1}{\varepsilon} + \frac{13}{54} + \frac{1}{16}\zeta_2$
	1	$\frac{1}{12}\frac{1}{\varepsilon^2} + \frac{1}{18}\frac{1}{\varepsilon} + \frac{13}{108} + \frac{1}{32}\zeta_2$
	2	$\frac{13}{270}\frac{1}{\varepsilon^2} + \frac{121}{3600}\frac{1}{\varepsilon} + \frac{138911}{1944000} + \frac{13}{720}\zeta_2$
	3	$\frac{11}{360}\frac{1}{\varepsilon^2} + \frac{163}{7200}\frac{1}{\varepsilon} + \frac{60911}{1296000} + \frac{11}{960}\zeta_2$
$\hat{I}_{6b}$	0	$-\frac{1}{10}\frac{1}{\varepsilon^2} + \frac{1}{600}\frac{1}{\varepsilon} - \frac{869}{9000} - \frac{3}{80}\zeta_2$
	1	$-\frac{1}{24}\frac{1}{\varepsilon^2} + \frac{1}{180}\frac{1}{\varepsilon} - \frac{223}{5400} - \frac{1}{64}\zeta_2$
	2	$-\frac{13}{630}\frac{1}{\varepsilon^2} + \frac{127}{33075}\frac{1}{\varepsilon} - \frac{2371837}{111132000} - \frac{13}{1680}\zeta_2$
	3	$-\frac{11}{960}\frac{1}{\varepsilon^2} + \frac{1919}{806400}\frac{1}{\varepsilon} - \frac{8361911}{677376000} - \frac{11}{2560}\zeta_2$
$\hat{I}_7$	0	$\frac{1}{6}\frac{1}{\varepsilon^2} + \frac{1}{9}\frac{1}{\varepsilon} + \frac{13}{54} + \frac{1}{16}\zeta_2$
	1	0
	2	$\frac{11}{180}\frac{1}{\varepsilon^2} + \frac{163}{3600}\frac{1}{\varepsilon} + \frac{60911}{648000} + \frac{11}{480}\zeta_2$
	3	0
$\hat{I}_{8a}$	0	$\frac{1}{6}\frac{1}{\varepsilon^2} + \frac{1}{9}\frac{1}{\varepsilon} + \frac{13}{54} + \frac{1}{16}\zeta_2$
	1	0
	2	$\frac{1}{54}\frac{1}{\varepsilon^2} + \frac{1}{360}\frac{1}{\varepsilon} + \frac{1189}{48600} + \frac{1}{144}\zeta_2$
	3	0
$\hat{I}_{8b}$	0	$-\frac{2}{15}\frac{1}{\varepsilon^2} + \frac{11}{450}\frac{1}{\varepsilon} - \frac{1643}{13500} - \frac{1}{20}\zeta_2$
	1	0
	2	$-\frac{2}{189}\frac{1}{\varepsilon^2} + \frac{19}{2205}\frac{1}{\varepsilon} - \frac{225079}{16669800} - \frac{1}{252}\zeta_2$
	3	0
$\hat{I}_9$	0	$\frac{1}{6}\frac{1}{\varepsilon^2} + \frac{1}{9}\frac{1}{\varepsilon} + \frac{13}{54} + \frac{1}{16}\zeta_2$
	1	$\frac{1}{12}\frac{1}{\varepsilon^2} + \frac{1}{18}\frac{1}{\varepsilon} + \frac{13}{108} + \frac{1}{32}\zeta_2$
	2	$\frac{151}{2160}\frac{1}{\varepsilon^2} + \frac{1783}{43200}\frac{1}{\varepsilon} + \frac{785701}{7776000} + \frac{151}{5760}\zeta_2$
	3	$\frac{31}{720}\frac{1}{\varepsilon^2} + \frac{1249}{43200}\frac{1}{\varepsilon} + \frac{166801}{2592000} + \frac{31}{1920}\zeta_2$
$\hat{I}_{10a}$	0	$\frac{1}{\varepsilon^2} + \frac{3}{2}\frac{1}{\varepsilon} + \frac{13}{4} + \frac{3}{8}\zeta_2$
	1	$\frac{3}{4}\frac{1}{\varepsilon^2} + \frac{59}{48}\frac{1}{\varepsilon} + \frac{1375}{576} + \frac{9}{32}\zeta_2$
	2	$\frac{47}{54}\frac{1}{\varepsilon^2} + \frac{73}{54}\frac{1}{\varepsilon} + \frac{2695}{972} + \frac{47}{144}\zeta_2$
	3	$\frac{155}{216}\frac{1}{\varepsilon^2} + \frac{2035}{1728}\frac{1}{\varepsilon} + \frac{1424773}{622080} + \frac{155}{576}\zeta_2$
$\hat{I}_{10b}$	0	$\frac{1}{\varepsilon^2} + \frac{3}{2}\frac{1}{\varepsilon} + \frac{13}{4} + \frac{3}{8}\zeta_2$
	1	$\frac{1}{2}\frac{1}{\varepsilon^2} + \frac{13}{24}\frac{1}{\varepsilon} + \frac{413}{288} + \frac{3}{16}\zeta_2$
	2	$\frac{37}{54}\frac{1}{\varepsilon^2} + \frac{101}{108}\frac{1}{\varepsilon} + \frac{8333}{3888} + \frac{37}{144}\zeta_2$
	3	$\frac{5}{12}\frac{1}{\varepsilon^2} + \frac{139}{288}\frac{1}{\varepsilon} + \frac{14297}{11520} + \frac{5}{32}\zeta_2$

Table 2: Mellin Moments for Integrals $\hat{I}_{6a} - \hat{I}_{10b}$.

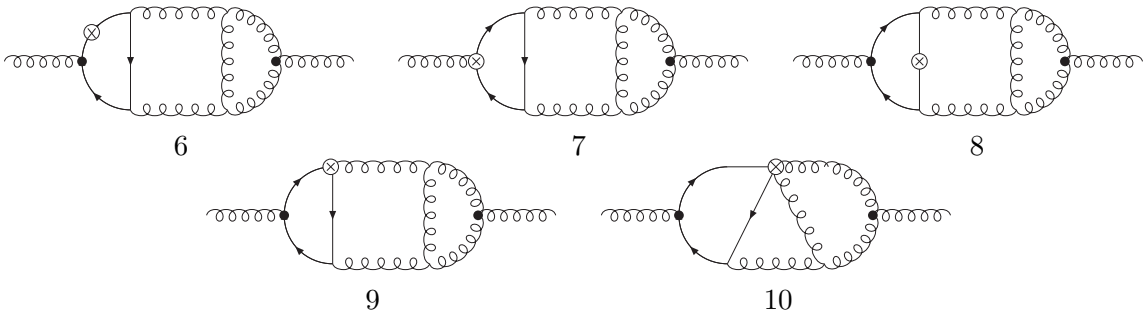

Figure 5: Diagrams with three fermion propagators.

In a first, step the different integrals are represented in finite sums keeping the general ε-dependence. After expanding in ε, evanescent poles in summation parameters may appear, which have to be dealt with. The resulting indefinite nested sums can again be simplified and reduced by Sigma.

Diagram 6a has the Feynman parameter representation

$$\begin{aligned}\hat{I}_{6a} = & -\exp\left(-\frac{3}{2}\varepsilon\gamma_E\right)\Gamma\left(2-\frac{3}{2}\varepsilon\right)\int_{[0,1]^7} dx\,dz\,du\,dw\,da\,ds\,dt\; z^{-1+\frac{\varepsilon}{2}}(1-z)^{\frac{\varepsilon}{2}}w^{1-\varepsilon}(1-w)^{2-\varepsilon} \\ & \theta(1-s-t)(1-s-t)s^{-\frac{\varepsilon}{2}}t^{\varepsilon-2} \\ & [(1-w)u+wa(1-s-t)+wsx+wtu]^N\,, \end{aligned} \tag{344}$$

and can thus be transformed into the following double sum:

$$I_{6a(b)} \equiv \frac{i(\Delta.p)^N a_s^3 S_\varepsilon^3}{(m^2)^{2-3\frac{\varepsilon}{2}}}\hat{I}_{6a(b)}\,, \tag{345}$$

$$\begin{aligned}\hat{I}_{6a} = & \exp\left(-3\frac{\varepsilon}{2}\gamma_E\right)\Gamma\left(2-\frac{3}{2}\varepsilon\right)B\left(\frac{\varepsilon}{2},1+\frac{\varepsilon}{2}\right)\sum_{j=0}^{N}\binom{N}{j}\sum_{l=0}^{j}\binom{j}{l}(-1)^{j+l} \\ & \frac{B(-\varepsilon+j+2,3-\varepsilon)}{(l+1)(l+2)(N+1-l)}B\left(\varepsilon-1,-\frac{\varepsilon}{2}+j+3\right)\left[\frac{2}{\varepsilon}+\frac{1}{l+2-\frac{\varepsilon}{2}}+B\left(-\frac{\varepsilon}{2},l+3\right)\right] \\ = & \frac{1}{(N+1)(N+3)(N+4)}\Bigg\{4\left[S_1-\frac{N^2+N-1}{(N+1)(N+2)}\right]\frac{1}{\varepsilon^2} \\ & +\Bigg[\frac{5}{2}S_1^2-\frac{1}{2}S_2+\frac{-5N^4-18N^3+62N^2+289N+244}{(N+1)(N+2)(N+3)(N+4)}S_1 \\ & +\frac{P_{32}}{(N+1)^2(N+2)^2(N+3)(N+4)}\Bigg]\frac{1}{\varepsilon} \\ & +\Bigg[\frac{11}{12}S_1^3+\frac{(-8N^4+3N^3+335N^2+994N+736)}{4(N+1)(N+2)(N+3)(N+4)}S_1^2 \\ & +\left(\frac{P_{33}}{2(N+1)^2(N+2)^2(N+3)^2(N+4)^2}+\frac{11}{4}S_2\right)S_1 \\ & +\frac{P_{34}}{(N+1)^3(N+2)^3(N+3)^2(N+4)^2}+\frac{3}{2}\left(S_1-\frac{(N^2+N-1)}{(N+1)(N+2)}\right)\zeta_2 \\ & +\frac{-2N^4+9N^3+185N^2+580N+472}{4(N+1)(N+2)(N+3)(N+4)}S_2-\frac{8}{3}S_3+6S_{2,1}\Bigg]\Bigg\}+O(\varepsilon), \end{aligned} \tag{346}$$

$$
\begin{aligned}
P_{32} &= -3N^6 - 65N^5 - 415N^4 - 1109N^3 - 1276N^2 - 468N + 64, && (347)\\
P_{33} &= -12N^8 - 311N^7 - 2943N^6 - 13584N^5 - 32101N^4 - 32407N^3 + 7542N^2 \\
&\quad +40744N + 22784, && (348)\\
P_{34} &= -24N^9 - 604N^8 - 6089N^7 - 32820N^6 - 104549N^5 - 202546N^4 \\
&\quad -232976N^3 - 143560N^2 - 32816N + 3328\,. && (349)
\end{aligned}
$$

Diagram 6b takes the form

$$
\begin{aligned}
\hat{I}_{6b} = \exp\left(-\frac{3}{2}\varepsilon\gamma_E\right)\Gamma\left(3-\frac{3}{2}\varepsilon\right)\int_{[0,1]^7} dx\,dz\,du\,dw\,da\,ds\,dt\; z^{-1+\frac{\varepsilon}{2}}(1-z)^{\frac{\varepsilon}{2}}w^{1-\varepsilon}(1-w)^{3-\varepsilon}(1-u) \\
\theta(1-s-t)(1-s-t)s^{-\frac{\varepsilon}{2}}t^{\varepsilon-2}[(1-w)u + wa(1-s-t) + wsx + wtu]^N\,, \qquad (350)
\end{aligned}
$$

which can be solved via the following sum representation

$$
\begin{aligned}
\hat{I}_{6b} &= \exp\left(-3\frac{\varepsilon}{2}\gamma_E\right)\Gamma\left(3-\frac{3}{2}\varepsilon\right)\sum_{l=0}^{N}\binom{N}{l}\sum_{j=0}^{l}\binom{l}{j}\frac{(-1)^{j+l}}{(j+1)(j+2)}B\left(\frac{\varepsilon}{2},1+\frac{\varepsilon}{2}\right) \\
&\quad \times B(N+1-j,2)B(l+2-\varepsilon,4-\varepsilon) \\
&\quad \times B\left(\varepsilon-1,l+3-\frac{\varepsilon}{2}\right)\left[-\frac{2}{\varepsilon}-B\left(-\frac{\varepsilon}{2},j+3\right)-\frac{1}{j+2-\frac{\varepsilon}{2}}\right] && (351)\\
&= \frac{1}{(N+1)(N+3)(N+4)(N+5)}\Bigg\{12\left[\frac{(N^2+N-1)}{(N+1)(N+2)}-S_1\right]\frac{1}{\varepsilon^2} \\
&\quad +\Bigg[-6S_1^2+\frac{(25N^5+261N^4+775N^3+3N^2-2744N-2496)}{(N+1)(N+2)(N+3)(N+4)(N+5)}S_1 \\
&\quad +\frac{-N^7+104N^6+1497N^5+7703N^4+18378N^3+20465N^2+8566N+24}{(N+1)^2(N+2)^2(N+3)(N+4)(N+5)}\Bigg]\frac{1}{\varepsilon} \\
&\quad +\Bigg[-2S_1^3+\frac{(10N^5+87N^4+97N^3-915N^2-2699N-1908)}{(N+1)(N+2)(N+3)(N+4)(N+5)}S_1^2 \\
&\quad +\left[\frac{P_{35}}{2(N+1)^2(N+2)^2(N+3)^2(N+4)^2(N+5)^2}-12S_2\right]S_1 \\
&\quad +\frac{P_{36}}{2(N+1)^3(N+2)^3(N+3)^2(N+4)^2(N+5)^2} \\
&\quad +\frac{9}{2}\left[\frac{(N^2+N-1)}{(N+1)(N+2)}-S_1\right]\zeta_2+\frac{(11N^2-39N-74)}{2(N+1)(N+2)}S_2+5S_3-12S_{2,1}\Bigg]\Bigg\}+O(\varepsilon), \qquad (352)
\end{aligned}
$$

$$
\begin{aligned}
P_{35} &= 5N^{10}+605N^9+12811N^8+124145N^7+674565N^6+2189463N^5+4196977N^4 \\
&\quad +4214683N^3+1030490N^2-1666304N-1086816, && (353)\\
P_{36} &= -15N^{12}-497N^{11}-5910N^{10}-27570N^9+35363N^8+1069961N^7+5838492N^6 \\
&\quad +17154824N^5+30447858N^4+32466210N^3+18880180N^2 \\
&\quad +4223536N-333696. && (354)
\end{aligned}
$$

Again both results show a similar structure.

Integral I_7 obeys a relation in analogy to I_3:

$$
I_7(N) = \left[1+(-1)^N\right]I_{6a}(N+1)\,. \qquad (355)
$$

Turning to Diagram 8a, one obtains a parameter integral

$$\hat{I}_{8a} = \exp\left(-\frac{3}{2}\varepsilon\gamma_E\right)\Gamma\left(2-\frac{3}{2}\varepsilon\right)\int_{[0,1]^7} dx\,dz\,du\,dw\,da\,ds\,dt\; z^{-1+\frac{\varepsilon}{2}}(1-z)^{\frac{\varepsilon}{2}}w^{1-\varepsilon}(1-w)^{2-\varepsilon}$$
$$\theta(1-s-t)(1-s-t)s^{-\frac{\varepsilon}{2}}t^{\varepsilon-2}(1-w)^N[u-a(1-s-t)-sx-tu]^N\,. \tag{356}$$

For the Diagrams 8a,b, an all-ε representation without any sums may be obtained. As a result only single harmonic sums occur after expanding in ε. One finds

$$I_{8a(b)} \equiv \frac{i(\Delta.p)^N a_s^3 S_\varepsilon^3}{(m^2)^{2-3\frac{\varepsilon}{2}}}\hat{I}_{8a(b)}\,, \tag{357}$$

$$\begin{aligned}\hat{I}_{8a} &= -\exp\left(-3\frac{\varepsilon}{2}\gamma_E\right)\Gamma\left(2-\frac{3\varepsilon}{2}\right)B\left(\frac{\varepsilon}{2},\frac{\varepsilon}{2}+1\right)\frac{[1+(-1)^N]}{(N+1)(N+2)(N+3)}\\
&\left\{-\frac{2}{\varepsilon}-\frac{1}{N+3-\frac{\varepsilon}{2}}-B\left(-\frac{\varepsilon}{2},N+4\right)\right\}\\
&\Gamma\left[\begin{array}{c}-1+\varepsilon,3+N-\varepsilon,2-\varepsilon,N+3-\frac{\varepsilon}{2}\\ N+2+\frac{\varepsilon}{2},N+5-2\varepsilon\end{array}\right]\end{aligned} \tag{358}$$

$$\begin{aligned}&= \frac{\left[1+(-1)^N\right]}{(N+1)(N+3)^2(N+4)}\Bigg\{2\left[S_1+\frac{2N+3}{(N+1)(N+2)}\right]\frac{1}{\varepsilon^2}\\
&+\left[\frac{1}{2}\left[S_1^2+S_2\right]-\frac{(3\,N^4+18\,N^3+21\,N^2-28\,N-40)}{(N+4)(N+3)(N+2)(N+1)}S_1\right.\\
&\left.-2\,\frac{3\,N^5+23\,N^4+53\,N^3+21\,N^2-57\,N-48}{(N+1)^2(N+2)^2(N+3)(N+4)}\right]\frac{1}{\varepsilon}\\
&+\left[\frac{1}{12}S_1^3+\frac{1}{6}S_3+\frac{13}{4}S_1S_2-\frac{1}{4}\frac{(3\,N^4-6\,N^3-183\,N^2-568\,N-472)}{(N+1)(N+2)(N+3)(N+4)}S_2\right.\\
&-\frac{(3\,N^4+18\,N^3+21\,N^2-28\,N-40)}{4(N+1)(N+2)(N+3)(N+4)}S_1^2+\frac{3}{4}\left[S_1+\frac{(2\,N+3)}{(N+1)(N+2)}\right]\zeta_2\\
&-\frac{P_{37}}{2(N+1)^2(N+2)^2(N+3)^2(N+4)^2}S_1\\
&\left.-\frac{P_{38}}{2(N+3)^2(N+4)^2(N+1)^3(N+2)^3}\right]\Bigg\}+O(\varepsilon)\,,\end{aligned} \tag{359}$$

with

$$\begin{aligned}P_{37} &= 36\,N^7+511\,N^6+2878\,N^5+8037\,N^4+10942\,N^3+4576\,N^2\\
&-4128\,N-3648\,,\end{aligned} \tag{360}$$

$$\begin{aligned}P_{38} &= 69\,N^8+1082\,N^7+6983\,N^6+23746\,N^5+44608\,N^4+41876\,N^3+7768\,N^2\\
&-17008\,N-9984\,.\end{aligned} \tag{361}$$

Similarly Diagram 8b takes the form

$$\hat{I}_{8b} = \exp\left(-\frac{3}{2}\varepsilon\gamma_E\right)\Gamma\left(3-\frac{3}{2}\varepsilon\right)\int_{[0,1]^7} dx\,dz\,du\,dw\,da\,ds\,dt\; z^{-1+\frac{\varepsilon}{2}}(1-z)^{\frac{\varepsilon}{2}}w^{2-\varepsilon}(1-w)^{2-\varepsilon}$$
$$\theta(1-s-t)(1-s-t)s^{-\frac{\varepsilon}{2}}t^{\varepsilon-2}(1-w)^N[u-a(1-s-t)-sx-tu]^N \tag{362}$$

and thus yields

$$
\begin{aligned}
\hat{I}_{8b} &= \exp\left(-3\frac{\varepsilon}{2}\gamma_E\right)\frac{[1+(-1)^N]}{(N+1)(N+2)(N+3)}\Gamma\left(3-\frac{3}{2}\varepsilon\right)B\left(3-\varepsilon,N+3-\varepsilon\right)\\
&\quad\times B\left(\frac{\varepsilon}{2},1+\frac{\varepsilon}{2}\right)B\left(\varepsilon-1,N+3-\frac{\varepsilon}{2}\right)\left[-B\left(-\frac{\varepsilon}{2},N+4\right)-\frac{1}{N+3-\frac{\varepsilon}{2}}-\frac{2}{\varepsilon}\right]\\
&= \frac{[1+(-1)^N]}{(N+1)(N+3)^2(N+4)(N+5)}\Bigg\{-8\left[S_1+\frac{(3+2\,N)}{(N+1)(N+2)}\right]\frac{1}{\varepsilon^2}\\
&\quad+2\Bigg[-\left(S_1^2+S_2\right)+\frac{11\,N^5+133\,N^4+567\,N^3+999\,N^2+610\,N+8}{(N+1)(N+2)(N+3)(N+4)(N+5)}S_1\\
&\quad+\frac{22\,N^6+301\,N^5+1563\,N^4+3869\,N^3+4667\,N^2+2394\,N+264}{(N+1)^2(N+2)^2(N+3)(N+4)(N+5)}\Bigg]\frac{1}{\varepsilon}\\
&\quad+\Bigg[-\frac{2}{3}S_3-\frac{1}{3}S_1^3-13S_1S_2-3S_1\zeta_2-3\,\frac{(3+2\,N)}{(N+1)(N+2)}\zeta_2\\
&\quad+\frac{11\,N^5+133\,N^4+567\,N^3+999\,N^2+610\,N+8}{2(N+1)(N+2)(N+3)(N+4)(N+5)}S_1^2\Bigg]\\
&\quad+\frac{11\,N^5+85\,N^4-81\,N^3-2121\,N^2-5654\,N-4312}{2(N+1)(N+2)(N+3)(N+4)(N+5)}S_2\\
&\quad-2\,\frac{P_{39}}{(N+1)^2(N+2)^2(N+3)^2(N+4)^2(N+5)^2}S_1\\
&\quad-\frac{P_{40}}{(N+1)^3(N+2)^3(N+3)^2(N+4)^2(N+5)^2}\Bigg\}+O(\varepsilon),
\end{aligned}
\tag{363}
$$

where

$$
\begin{aligned}
P_{39} &= 9\,N^{10}+182\,N^9+1388\,N^8+4103\,N^7-4913\,N^6-72860\,N^5-225446\,N^4\\
&\quad-327313\,N^3-198070\,N^2+17240\,N+52416, \qquad (364)\\
P_{40} &= 36\,N^{11}+793\,N^{10}+6942\,N^9+28237\,N^8+28250\,N^7-224189\,N^6\\
&\quad-1079534\,N^5-2213865\,N^4-2276462\,N^3-830640\,N^2\\
&\quad+388496\,N+315456\,. \qquad (365)
\end{aligned}
$$

Diagram 9 has a more complicated operator insertion

$$
\begin{aligned}
\hat{I}_9 = &-\exp\left(-\frac{3}{2}\varepsilon\gamma_E\right)\Gamma\left(2-\frac{3}{2}\varepsilon\right)\sum_{j=0}^{N}\int_{[0,1]^7}dx\,dz\,du\,dw\,da\,ds\,dt\\
&z^{-1+\frac{\varepsilon}{2}}(1-z)^{\frac{\varepsilon}{2}}w^{1-\varepsilon}(1-w)^{2-\varepsilon-j}\theta(1-s-t)(1-s-t)s^{-\frac{\varepsilon}{2}}t^{-2+\varepsilon}\\
&[u-a(1-s-t)-sx-tu]^j\\
&[u(1-w)+wa(1-s-t)+wsx+stu]^{N-j}
\end{aligned}
\tag{366}
$$

and can be represented by a threefold sum

$$
I_9 \equiv \frac{i(\Delta.p)^N a_s^3 S_\varepsilon^3}{(m^2)^{2-3\frac{\varepsilon}{2}}}\hat{I}_9\,, \tag{367}
$$

$$
\begin{aligned}
\hat{I}_9 &= -\exp\left(-3\frac{\varepsilon}{2}\gamma_E\right)\Gamma(\varepsilon-1)\Gamma\left(2-\frac{3}{2}\varepsilon\right)B\left(\frac{\varepsilon}{2},1+\frac{\varepsilon}{2}\right)\sum_{i=0}^{N}\sum_{j=0}^{N-i}\binom{N-i}{j}(-1)^j \\
&\times\sum_{l=0}^{i+j}\binom{i+j}{l}(-1)^l\Gamma\left[\begin{array}{c}3+j+i-\frac{\varepsilon}{2},3+i-\varepsilon,2+j-\varepsilon\\5+i+j-2\varepsilon,2+i+j+\frac{\varepsilon}{2}\end{array}\right] \\
&\times\frac{1}{(l+1)(l+2)(N+1-l)}\left[B\left(-\frac{\varepsilon}{2},1\right)-B\left(l+2-\frac{\varepsilon}{2},1\right)-B\left(-\frac{\varepsilon}{2},l+3\right)\right] \qquad (368)\\
&= \frac{1}{(N+2)(N+4)(N+5)}\left\{\left[\left(\frac{2(-1)^N\left(N^2+5N+7\right)}{(N+2)(N+3)^2}\right.\right.\right. \\
&+\left.\frac{2\left(2N^3+13N^2+27N+20\right)}{(N+1)(N+3)^2}\right)S_1+S_1^2+3S_2+\frac{2(-1)^N(2N^3+13N^2+29N+21)}{(N+1)(N+2)^2(N+3)^2} \\
&\left.\left.-\frac{2\left(2N^6+18N^5+57N^4+60N^3-53N^2-163N-99\right)}{(N+1)^2(N+2)^2(N+3)^2}\right]\frac{1}{\varepsilon^2}\right. \\
&+\frac{1}{N+3}\left[\frac{1}{2}(N+3)S_1^3+\left(\frac{(-1)^N\left(N^2+5N+7\right)}{2(N+2)(N+3)}\right.\right. \\
&\left.+\frac{2N^6+43N^5+360N^4+1529N^3+3524N^2+4218N+2048}{2(N+1)(N+2)(N+3)(N+4)(N+5)}\right)S_1^2 \\
&+\left(\frac{P_{41}}{(N+1)^2(N+2)(N+3)^2(N+4)(N+5)}\right. \\
&+\frac{(-1)^N P_{42}}{(N+1)^2(N+2)^2(N+3)^2(N+4)(N+5)} \\
&\left.+4S_{-2}\right)S_1+\left(\frac{7}{2}(N+3)S_1+\frac{(-1)^N\left(N^2+5N+7\right)}{2(N+2)(N+3)}\right. \\
&\left.+\frac{-10N^6-133N^5-612N^4-915N^3+1052N^2+4246N+3104}{2(N+1)(N+2)(N+3)(N+4)(N+5)}\right)S_2 \\
&+\frac{4(2N+3)}{(N+1)(N+2)}S_{-2}+2(N+5)S_3-4(N+3)S_{2,1} \\
&+\frac{(-1)^N P_{43}}{(N+1)^3(N+2)^3(N+3)^2(N+4)(N+5)} \\
&\left.+\frac{P_{44}}{(N+1)^3(N+2)^3(N+3)^2(N+4)(N+5)}\right]\frac{1}{\varepsilon} \\
&+\frac{1}{N+3}\left[\frac{7}{48}(N+3)S_1^4+\left(\frac{(-1)^N\left(N^2+5N+7\right)}{12(N+2)(N+3)}\right.\right. \\
&\left.+\frac{2N^6+59N^5+588N^4+2805N^3+7040N^2+8974N+4544}{12(N+1)(N+2)(N+3)(N+4)(N+5)}\right)S_1^3 \\
&+\left(\frac{(-1)^N P_{45}}{4(N+1)^2(N+2)^2(N+3)^2(N+4)(N+5)}\right.
\end{aligned}
$$

$$
+\frac{P_{46}}{4(N+1)^2(N+2)^2(N+3)^2(N+4)^2(N+5)^2}+7S_{-2}\Bigg)S_1^2
$$
$$
+\Bigg(\frac{(-1)^N P_{47}}{2(N+1)^3(N+2)^3(N+3)^3(N+4)^2(N+5)^2}
$$
$$
+\frac{P_{48}}{2(N+1)^3(N+2)^2(N+3)^3(N+4)^2(N+5)^2}+5S_{-3}
$$
$$
-\frac{2\left(5N^5+49N^4+104N^3-285N^2-1213N-1036\right)S_{-2}}{(N+1)(N+2)(N+3)(N+4)(N+5)}\Bigg)S_1+\frac{(55N+141)}{16}S_2^2
$$
$$
+\frac{(-1)^N P_{49}}{2(N+1)^4(N+2)^4(N+3)^3(N+4)^2(N+5)^2}
$$
$$
+\frac{P_{50}}{2(N+1)^4(N+2)^4(N+3)^3(N+4)^2(N+5)^2}+\frac{5(2N+3)}{(N+1)(N+2)}S_{-3}
$$
$$
-\frac{4\left(5N^6+63N^5+275N^4+425N^3-160N^2-1004N-684\right)S_{-2}}{(N+1)^2(N+2)^2(N+3)(N+4)(N+5)}
$$
$$
+\Bigg(\frac{3(9N+31)}{8}S_1^2+\Bigg(\frac{13(-1)^N\left(N^2+5N+7\right)}{4(N+2)(N+3)}
$$
$$
+\frac{-10N^6-65N^5+420N^4+5213N^3+18860N^2+29514N+16976}{4(N+1)(N+2)(N+3)(N+4)(N+5)}\Bigg)S_1
$$
$$
+\frac{(-1)^N P_{51}}{4(N+1)^2(N+2)^2(N+3)^2(N+4)(N+5)}
$$
$$
+\frac{P_{52}}{4(N+1)^2(N+2)^2(N+3)^2(N+4)^2(N+5)^2}+S_{-2}\Bigg)S_2+\zeta_2\Bigg(\frac{3}{8}(N+3)S_1^2
$$
$$
+\Bigg(\frac{3(-1)^N\left(N^2+5N+7\right)}{4(N+2)(N+3)}+\frac{3\left(2N^3+13N^2+27N+20\right)}{4(N+1)(N+3)}\Bigg)S_1
$$
$$
-\frac{3\left(2N^6+18N^5+57N^4+60N^3-53N^2-163N-99\right)}{4(N+1)^2(N+2)^2(N+3)}
$$
$$
+\frac{3(-1)^N\left(2N^3+13N^2+29N+21\right)}{4(N+1)(N+2)^2(N+3)}+\frac{9}{8}(N+3)S_2\Bigg)+\Bigg(\frac{(-1)^N\left(N^2+5N+7\right)}{6(N+2)(N+3)}
$$
$$
+\frac{-34N^5-383N^4-1379N^3-1280N^2+1830N+2632}{6(N+1)(N+2)(N+3)(N+4)}+\frac{(13N+105)}{6}S_1\Bigg)S_3
$$
$$
+\frac{(53-N)}{8}S_4+\left(-\frac{6(2N+3)}{(N+1)(N+2)}-6S_1\right)S_{-2,1}
$$
$$
+\left(\frac{12N^5+140N^4+546N^3+725N^2-93N-532}{(N+1)(N+2)(N+4)(N+5)}+(-4N-15)S_1\right)S_{2,1}
$$
$$
+(N-11)S_{3,1}+(N+9)S_{2,1,1}\Bigg]\Bigg\}+O(\varepsilon)\,. \tag{369}
$$

Here the following polynomials occur :

$$
P_{41} \;=\; -5N^8-68N^7-264N^6+410N^5+6293N^4+20720N^3+32900N^2
$$

$$
\begin{aligned}
& +26206N + 8440, && (370)\\
P_{42} &= -3N^8 - 49N^7 - 321N^6 - 1069N^5 - 1863N^4 - 1559N^3 - 773N^2 \\
& -1199N - 1108, && (371)\\
P_{43} &= -6N^9 - 108N^8 - 810N^7 - 3288N^6 - 7855N^5 - 11456N^4 - 11282N^3 \\
& -10300N^2 - 9171N - 4164, && (372)\\
P_{44} &= -3N^{11} - 112N^{10} - 1610N^9 - 12443N^8 - 58690N^7 - 178509N^6 - 355289N^5 \\
& -451853N^4 - 334491N^3 - 98371N^2 + 31775N + 23364, && (373)\\
P_{45} &= -3N^8 - 49N^7 - 321N^6 - 1069N^5 - 1863N^4 - 1559N^3 - 773N^2 \\
& -1199N - 1108, && (374)\\
P_{46} &= -8N^{11} - 189N^{10} - 1643N^9 - 4234N^8 + 32416N^7 + 340621N^6 + 1490447N^5 \\
& +3864842N^4 + 6329756N^3 + 6460920N^2 + 3775088N + 971008, && (375)\\
P_{47} &= -42N^{12} - 1213N^{11} - 15525N^{10} - 115864N^9 - 557609N^8 - 1804421N^7 - 3966084N^6 \\
& -5845058N^5 - 5625111N^4 - 3597908N^3 - 2035597N^2 - 1373344N - 553968, && (376)\\
P_{48} &= -12N^{13} - 523N^{12} - 9558N^{11} - 98647N^{10} - 644321N^9 - 2799010N^8 - 8183392N^7 \\
& -15639871N^6 - 17214281N^5 - 4125073N^4 + 17049900N^3 + 25968164N^2 \\
& +16422416N + 4131840, && (377)\\
P_{49} &= -81N^{13} - 2458N^{12} - 33378N^{11} - 267579N^{10} - 1405780N^9 - 5075289N^8 \\
& -12828559N^7 - 22692458N^6 - 27711081N^5 - 23127963N^4 - 14102081N^3 \\
& -8182893N^2 - 4780496N - 1528944, && (378)\\
P_{50} &= -60N^{15} - 2640N^{14} - 51484N^{13} - 594504N^{12} - 4564031N^{11} - 24724313N^{10} \\
& -97683496N^9 - 286337829N^8 - 626024531N^7 - 1014709686N^6 - 1194939874N^5 \\
& -978463105N^4 - 504961532N^3 - 120080691N^2 + 14776800N + 11512944, && (379)\\
P_{51} &= -3N^8 - 25N^7 + 147N^6 + 2723N^5 + 14685N^4 + 40381N^3 + 60691N^2 \\
& +46645N + 14012, && (380)\\
P_{52} &= -2N^{11} - 177N^{10} - 3713N^9 - 36850N^8 - 204686N^7 - 647555N^6 - 952035N^5 \\
& +618266N^4 + 5332620N^3 + 9769044N^2 + 8340336N + 2862784\,. && (381)
\end{aligned}
$$

Diagram 10 has an operator insertion with a contracted fermion line, as a result the Feynman rule already introduces two sums:

$$
\begin{aligned}
\hat{I}_{10} = {} & \exp\left(-\frac{3}{2}\varepsilon\gamma_E\right)\Gamma\left(1-\frac{3}{2}\varepsilon\right)\sum_{j=0}^{N}\sum_{l=0}^{N-j}\int_{[0,1]^6} dx\,dz\,du\,dw\,ds\,dt\,(-1)^j s^{\varepsilon-1}t^{-\frac{\varepsilon}{2}}(1-t)^{\varepsilon} \\
& w^{\frac{\varepsilon}{2}-1}(1-w)^{\frac{\varepsilon}{2}}z^{-\varepsilon}(1-z)^{-\varepsilon+j+1}(1-x-s(1-x)(1-t)-t(1-u))^j \\
& (x+z-xz-sz(1-x)(1-t)-tz(1-u))^{-j-l+N} \\
& \Big\{\Big[1+s(1-x)(1-w)(1-t)-(1-t)(1-u)(1-w) \\
& \quad -(1-x)(1-z)-sz(1-x)(1-t)-tz(1-u)\Big]^l \\
& +\Big[(1-u)(1-w)-(1-z)(1-x)+sw(1-x)(1-t)- \\
& \quad sz(1-x)(1-t)+tw(1-u)-tz(1-u)\Big]^l\Big\}\,. \qquad (382)
\end{aligned}
$$

Hence the sum representation contains sixfold nested sums, that can be simplified using EvaluateMultiSums. This leads to

$$
\begin{aligned}
I_{10a,b} &\equiv \frac{i(\Delta.p)^N a_s^3 S_\varepsilon^3}{(m^2)^{1-3\frac{\varepsilon}{2}}} \hat{I}_{10a,b}, \qquad (383)\\
\hat{I}_{10a} &= \exp\left(-3\frac{\varepsilon}{2}\gamma_E\right)\Gamma\left(1-3\frac{\varepsilon}{2}\right)\sum_{j=0}^{N}\binom{N+2}{j+2}\sum_{k=0}^{j}\binom{j+1}{k+1}\sum_{l=0}^{k}\binom{k}{l}(-1)^{k+l}\\
&\sum_{q=0}^{N-j}\binom{N-j}{q}(-1)^{N-j-q}\sum_{r_2=0}^{N-l-q}\binom{N-l-q}{r_2}\\
&\sum_{r_1=0}^{N-l-q-r_2}\binom{N-l-q-r_2}{r_1}\frac{B(1-\varepsilon,N+2-j-\varepsilon)B(\frac{\varepsilon}{2},k+1+\frac{\varepsilon}{2})}{(N+1-q-r_1-r_2)(q+r_2+1)}\\
&B(r_2+\varepsilon,r_1+1)B\left(N+1-l-q-r_1-r_2-\frac{\varepsilon}{2},r_1+r_2+1+\varepsilon\right) \qquad (384)\\
&= \frac{1}{(N+3)(N+4)}\Bigg\{\Bigg[-\frac{4\left(N^3+3N^2-N-5\right)}{(N+1)(N+2)(N+3)}S_1+2S_1^2+\frac{4(-1)^N}{N+3}S_1+4S_{-2}\\
&+2(2N+5)S_2+\frac{4(-1)^N\left(2N^3+7N^2+4N-3\right)}{(N+1)^2(N+2)^2(N+3)}+\frac{4\left(6N^3+34N^2+63N+39\right)}{(N+1)^2(N+2)^2(N+3)}\Bigg]\frac{1}{\varepsilon^2}\\
&+\Bigg[\frac{\left(-4N^4-25N^3-30N^2+49N+76\right)}{(N+1)(N+2)(N+3)(N+4)}S_1^2-\frac{4\left(2N^4+14N^3+27N^2+5N-16\right)}{(N+1)(N+2)(N+3)(N+4)}S_{-2}\\
&+\frac{\left(10N^4+73N^3+158N^2+73N-52\right)}{(N+1)(N+2)(N+3)(N+4)}S_2\\
&+\frac{2(-1)^N\left(12N^5+127N^4+538N^3+1177N^2+1354N+648\right)}{(N+1)^2(N+2)^2(N+3)^2(N+4)}S_1\\
&-\frac{2\left(8N^6+51N^5-72N^4-1330N^3-4062N^2-5151N-2436\right)}{(N+1)^2(N+2)^2(N+3)^2(N+4)}S_1\\
&+S_1^3+\frac{(-1)^N}{N+3}\left(S_1^2-S_2\right)+4S_{-2}S_1-5S_2S_1+2(4N+15)S_{-3}+2(N-1)S_3\\
&-12S_{-2,1}+8(N+4)S_{2,1}\\
&+\frac{2(-1)^N\left(11N^6+60N^5-160N^4-1837N^3-5005N^2-5801N-2508\right)}{(N+1)^3(N+2)^3(N+3)^2(N+4)}\\
&+\frac{2\left(70N^6+893N^5+4640N^4+12626N^3+19074N^2+15269N+5100\right)}{(N+1)^3(N+2)^3(N+3)^2(N+4)}\Bigg]\frac{1}{\varepsilon}\\
&+\frac{7}{24}S_1^4+\frac{\left(-10N^4-61N^3-68N^2+129N+188\right)}{6(N+1)(N+2)(N+3)(N+4)}S_1^3\\
&+\frac{(-1)^N\left(12N^5+127N^4+538N^3+1177N^2+1354N+648\right)}{2(N+1)^2(N+2)^2(N+3)^2(N+4)}S_1^2\\
&+\frac{P_{53}}{2(N+1)^2(N+2)^2(N+3)^2(N+4)^2}S_1^2+\frac{3}{4}\zeta_2 S_1^2-4S_{-2}S_1^2-\frac{13}{4}S_2S_1^2\\
&+\frac{(-1)^N P_{54}}{(N+1)^3(N+2)^3(N+3)^3(N+4)^2}S_1+\frac{P_{55}}{(N+1)^3(N+2)^3(N+3)^3(N+4)^2}S_1
\end{aligned}
$$

$$
\begin{aligned}
&-\frac{3\,(N^3+3N^2-N-5)}{2(N+1)(N+2)(N+3)}\zeta_2 S_1 - 2S_{-3}S_1 \\
&-\frac{4\,(4N^4+41N^3+155N^2+254N+148)}{(N+1)(N+2)(N+3)(N+4)}S_{-2}S_1 \\
&+\frac{(-1)^N}{N+3}\left(-4S_{-2}S_1+\frac{9}{2}S_2S_1+\frac{3}{2}\zeta_2 S_1+\frac{1}{6}S_1^3-2S_{-3}+\frac{10}{3}S_3+2S_{2,1}+12S_{-2,1}\right) \\
&+\frac{(-14N^4-201N^3-936N^2-1715N-1044)}{2(N+1)(N+2)(N+3)(N+4)}S_2S_1-\frac{119}{3}S_3S_1 \\
&-12S_{-2,1}S_1+22S_{2,1}S_1-2S_{-2}^2+\frac{1}{8}(32N+119)S_2^2 \\
&+\frac{(-1)^N P_{56}}{(N+1)^4(N+2)^4(N+3)^3(N+4)^2}+\frac{P_{57}}{(N+1)^4(N+2)^4(N+3)^3(N+4)^2} \\
&+\frac{3(-1)^N\,(2N^3+7N^2+4N-3)}{2(N+1)^2(N+2)^2(N+3)}\zeta_2+\frac{3\,(6N^3+34N^2+63N+39)}{2(N+1)^2(N+2)^2(N+3)}\zeta_2 \\
&+(8N+39)S_{-4}+\frac{2\,(8N^5+108N^4+558N^3+1365N^2+1553N+640)}{(N+1)(N+2)(N+3)(N+4)}S_{-3} \\
&-\frac{4(-1)^N\,(2N^3+7N^2+4N-3)}{(N+1)^2(N+2)^2(N+3)}S_{-2}-\frac{4P_{58}}{(N+1)^2(N+2)^2(N+3)^2(N+4)^2}S_{-2} \\
&+\frac{3}{2}\zeta_2 S_{-2}+\frac{(-1)^N\,(8N^5+79N^4+186N^3-279N^2-1426N-1224)}{2(N+1)^2(N+2)^2(N+3)^2(N+4)}S_2 \\
&+\frac{P_{59}}{2(N+1)^2(N+2)^2(N+3)^2(N+4)^2}S_2+\frac{3}{4}(2N+5)\zeta_2 S_2+8S_{-2}S_2 \\
&+\frac{(-18N^5-229N^4-1498N^3-5558N^2-10017N-6460)}{3(N+1)(N+2)(N+3)(N+4)}S_3 \\
&+\frac{1}{4}(20N-29)S_4-14S_{-3,1}+\frac{4\,(4N^4+22N^3+11N^2-85N-96)}{(N+1)(N+2)(N+3)(N+4)}S_{-2,1} \\
&-14S_{-2,2}+\frac{2\,(11N^4+107N^3+397N^2+640N+361)}{(N+1)(N+2)(N+3)}S_{2,1}+2(N+36)S_{3,1} \\
&+28S_{-2,1,1}+2(2N-7)S_{2,1,1}\Bigg\}+O(\varepsilon)\,, \qquad (385)
\end{aligned}
$$

with the polynomials

$$
\begin{aligned}
P_{53} &= -6N^8-164N^7-1613N^6-7762N^5-19526N^4-22888N^3-2137N^2 \\
&\quad +19968N+13264\,, \qquad (386)\\
P_{54} &= 119N^8+2250N^7+18755N^6+90365N^5+275464N^4+542281N^3+668958N^2 \\
&\quad +469072N+142112\,, \qquad (387)\\
P_{55} &= 16N^{11}+448N^{10}+5568N^9+41171N^8+204092N^7+720291N^6+1858328N^5 \\
&\quad +3504939N^4+4712624N^3+4272331N^2+2335952N+581072\,, \qquad (388)\\
P_{56} &= 78N^9+937N^8+2466N^7-17638N^6-155141N^5-538674N^4-1047495N^3 \\
&\quad -1197445N^2-757472N-206256\,, \qquad (389)\\
P_{57} &= 568N^9+11297N^8+98332N^7+492027N^6+1561688N^5+3266831N^4 \\
&\quad +4516420N^3+3994885N^2+2061840N+475824\,, \qquad (390)\\
P_{58} &= 4N^8+96N^7+942N^6+4995N^5+15753N^4+30351N^3+34903N^2
\end{aligned}
$$

$$+21844N + 5648\,, \tag{391}$$

$$P_{59} = -32N^9 - 730N^8 - 7180N^7 - 40057N^6 - 139918N^5 - 317434N^4 - 466820N^3 - 426421N^2 - 216416N - 45040\,. \tag{392}$$

In a similar way, for the Diagram 10b one obtains

$$\begin{aligned}
\hat{I}_{10b} &= \exp\left(-3\frac{\varepsilon}{2}\gamma_E\right)\Gamma\left(1-\frac{3}{2}\varepsilon\right)\sum_{j=0}^{N}\binom{N+2}{j+2}\sum_{k=0}^{j}\binom{j+1}{k+1}\sum_{l=0}^{k}\binom{k}{l} \\
&\times\sum_{q=0}^{N-j}\binom{N-j}{q}(-1)^{N-j-q+k}\sum_{r_1=0}^{N-l-q}\binom{N-l-q}{r_1}\sum_{r_2=0}^{N-l-q-r_1}\binom{N-l-q-r_1}{r_2} \\
&\times B(1-\varepsilon, N+2-j-\varepsilon)B\left(k-l+\frac{\varepsilon}{2}, l+1+\frac{\varepsilon}{2}\right)B(r_2+\varepsilon, r_1+1) \\
&\times B\left(N+1-l-q-r_1-r_2-\frac{\varepsilon}{2}, r_1+r_2+1+\varepsilon\right) \\
&\frac{1}{(q+r_2+1)(N+1-q-r_1-r_2)} \qquad (393) \\
&= \frac{1}{(N+3)(N+4)}\Bigg\{\Bigg[4S_1^2+\frac{8(2N+3)}{(N+1)(N+2)}S_1-4(-1)^N S_{-2}+\frac{8(2N+3)}{(N+1)^2(N+2)}\Bigg]\frac{1}{\varepsilon^2} \\
&+\Bigg[\frac{2(-1)^N(2N^2+14N+17)}{(N+1)^2(N+2)^2}S_1+\frac{2(14N^3+103N^2+235N+164)}{(N+1)(N+2)(N+3)(N+4)}S_1^2 \\
&-\frac{4(-1)^N(6N^3+43N^2+95N+64)}{(N+1)(N+2)(N+3)(N+4)}S_{-2} \\
&+\frac{2(44N^4+376N^3+1135N^2+1445N+660)}{(N+1)^2(N+2)^2(N+3)(N+4)}S_1 \\
&+2S_1^3-4(-1)^N S_{-2}S_1+8S_{-2}S_1-2(-1)^N S_2S_1-2(-1)^N S_{-3}+8S_{-3}+4(-1)^N S_{2,1} \\
&+\frac{2(2N+3)}{(N+1)(N+2)}\Big(4S_{-2}-(-1)^N S_2\Big)-2(-1)^N S_3+4(-1)^N S_{-2,1}-16S_{-2,1} \\
&+\frac{2(42N^4+355N^3+1056N^2+1319N+588)}{(N+1)^3(N+2)^2(N+3)(N+4)}-\frac{2(-1)^N(8N+13)}{(N+1)^2(N+2)^2}\Bigg]\frac{1}{\varepsilon}+\frac{7}{12}S_1^4 \\
&+10S_{-2}S_1^2+\frac{(38N^3+275N^2+615N+420)}{3(N+1)(N+2)(N+3)(N+4)}S_1^3+\frac{(-1)^N(2N^2+14N+17)}{2(N+1)^2(N+2)^2}S_1^2 \\
&+\frac{(260N^6+3844N^5+23111N^4+72230N^3+123747N^2+110376N+40304)}{2(N+1)^2(N+2)^2(N+3)^2(N+4)^2}S_1^2 \\
&+\frac{3}{2}\zeta_2 S_1^2+\frac{13}{2}S_2S_1^2+\frac{(-1)^N(-3N^5+8N^4+197N^3+631N^2+647N+148)}{(N+1)^3(N+2)^3(N+3)(N+4)}S_1 \\
&+\frac{P_{60}}{(N+1)^3(N+2)^3(N+3)^2(N+4)^2}S_1+\frac{4(18N^3+137N^2+325N+236)}{(N+1)(N+2)(N+3)(N+4)}S_{-2}S_1 \\
&+\frac{(-1)^N(2N+7)}{(N+3)(N+4)}(-8S_{-2}S_1-4S_2S_1+8S_{-2,1})-4(-1)^N S_{-3}S_1+26S_{-3}S_1 \\
&+\frac{(2N+3)}{(N+1)(N+2)}\left(3\zeta_2 S_1+13S_2S_1+\frac{29}{3}S_3+2S_{2,1}\right)+\frac{29}{3}S_3S_1-28S_{-2,1}S_1 \\
&+2S_{2,1}S_1+(-1)^N S_3S_1-2(-1)^N S_{2,1}S_1+2(-1)^N S_{-2}^2-(-1)^N S_2^2+\frac{3}{4}S_2^2
\end{aligned}$$

$$
+\frac{(-1)^N\left(-127N^6-1569N^5-7862N^4-20557N^3-29733N^2-22680N-7168\right)}{(N+1)^4(N+2)^4(N+3)(N+4)}
$$
$$
+\frac{P_{61}}{(N+1)^4(N+2)^4(N+3)^2(N+4)^2}+\frac{3(2N+3)}{(N+1)^2(N+2)}\zeta_2-7(-1)^N S_{-4}+14S_{-4}
$$
$$
-\frac{8(-1)^N\left(2N^3+15N^2+35N+25\right)}{(N+1)(N+2)(N+3)(N+4)}S_{-3}+\frac{2\left(42N^3+325N^2+785N+580\right)}{(N+1)(N+2)(N+3)(N+4)}S_{-3}
$$
$$
+\frac{4\left(25N^4+216N^3+656N^2+831N+372\right)}{(N+1)^2(N+2)^2(N+3)(N+4)}S_{-2}
$$
$$
-\frac{16(-1)^N\left(6N^6+86N^5+500N^4+1508N^3+2491N^2+2145N+760\right)}{(N+1)^2(N+2)^2(N+3)^2(N+4)^2}S_{-2}
$$
$$
-\frac{3}{2}(-1)^N S_{-2}\zeta_2+\frac{\left(64N^2+216N+183\right)}{2(N+1)^2(N+2)^2}S_2
$$
$$
+\frac{(-1)^N\left(-30N^4-212N^3-437N^2-177N+156\right)}{2(N+1)^2(N+2)^2(N+3)(N+4)}S_2-8(-1)^N S_{-2}S_2
$$
$$
-2S_{-2}S_2+\frac{(-1)^N\left(-6N^3-35N^2-55N-20\right)}{(N+1)(N+2)(N+3)(N+4)}S_3
$$
$$
+2(-1)^N S_4+\frac{19}{2}S_4+4(-1)^N S_{-3,1}-24S_{-3,1}
$$
$$
-\frac{4\left(30N^3+223N^2+515N+364\right)}{(N+1)(N+2)(N+3)(N+4)}S_{-2,1}+2(-1)^N S_{-2,2}-20S_{-2,2}
$$
$$
+\frac{2(-1)^N\left(6N^3+35N^2+55N+20\right)}{(N+1)(N+2)(N+3)(N+4)}S_{2,1}-13(-1)^N S_{3,1}-17S_{3,1}
$$
$$
\left.+32S_{-2,1,1}+5(-1)^N S_{2,1,1}+3S_{2,1,1}\right\}+O(\varepsilon)\,, \tag{394}
$$

with

$$
\begin{aligned}
P_{60} &= 367N^7+5827N^6+38741N^5+139834N^4+296246N^3+369049N^2 \\
&\quad +251056N+72240\,, \qquad (395)\\
P_{61} &= 373N^8+6728N^7+52275N^6+228755N^5+617580N^4+1055293N^3 \\
&\quad +1117044N^2+671360N+175872\,. \qquad (396)
\end{aligned}
$$

In the results of the above diagrams, the harmonic sums of maximum depth 3 and maximum weight 4 appear:

$$
S_1,\ S_2,\ S_3,\ S_4,\ S_{-2},\ S_{-3},\ S_{-4},\ S_{2,1},\ S_{-2,1},\ S_{-2,2},\ S_{3,1},\ S_{-3,1},\ S_{2,1,1},\ S_{-2,1,1}. \tag{397}
$$

This set is the same as for the $O(\alpha_s^2\varepsilon)$ contributions to the massive OMEs, which contribute at the 3-loop order via renormalization [79] and for a wide class of other processes, see [316, 317]. In addition, in the case of the diagrams with six massive propagators also the following generalized harmonic sums [111, 254] contribute:

$$
S_{1,1,1}\left(\frac{1}{2},1,1\right), S_{1,2}\left(\frac{1}{2},1\right)\,. \tag{398}
$$

These functions do not emerge in case of the diagrams with only three massive propagators.

Representations for the analytic continuations of the harmonic sums as functions in the complex plane were calculated in [106, 107, 252, 253]. The sums can further be represented via Mellin transforms of HPLs:

$$S_{1,2}\left(\frac{1}{2},1;N\right) = \frac{5}{8}\zeta_3 + \frac{1}{2^N}\int_0^1 dx\,\frac{x^N}{2-x}H_{1,0}(x)\,, \tag{399}$$

$$S_{1,1,1}\left(\frac{1}{2},1,1;N\right) = \frac{3}{4}\zeta_3 - \frac{1}{2^N}\int_0^1 dx\,\frac{x^N}{2-x}H_{1,1}(x)\,. \tag{400}$$

It was shown, that the representation of 3-loop ladder and V-diagrams in case of a lower number of massive lines does not pose a problem in calculating these topologies. Here the representation of the graphs in terms of sums and the corresponding higher transcendental functions provides the correct starting point. This will allow to compute as well all diagrams with numerator structures, without any further complication and thus solve a further wide class of graphs contributing to different OMEs at the 3-loop order.

8.3 Functions from Moments

Since the integrals I_1–I_{10} satisfy linear difference equations with polynomial coefficients in N, the analytic form of their results can be reconstructed from a finite number of initial values, provided that sufficiently many values can be calculated analytically. The method, known as "guessing", was described in [318–320], which is used to construct a recurrence equation from a sufficiently large number of points. The recurrences can then be solved using Sigma [93–101]. This method has been used successfully before in Ref. [295] in case of very large recurrences.

In [133] the results from above were used to compute the moments efficiently, and then guess appropriate recurrences. Tables 3 and 4 summarize properties of the results for diagrams I_{1a} to I_4 and I_{6a} to I_{10b}, respectively. Here prefactors of the form $[1+(-1)^N]$ were dropped, which can always be identified in the analytic calculation, and the remainder part was used to evaluate the moments. Leaving this factor out is more efficient, since lower moments have to be computed to establish the corresponding recurrences, provided a valid representation for odd values of N is given.

	rational			ζ_3		
Diagram	# Moments	Degree	Order	# Moments	Degree	Order
I_{1a}	203	26	8	15	3	2
I_{1b}	269	36	9	15	3	2
I_{2a}	215	31	8	19	3	3
I_{2b}	269	42	9	35	6	3
I_4	623	90	13	131	24	6

Table 3: Complexity of the smallest recurrences describing the integrals I_{1a}–I_4.

The number of moments needed to determine the corresponding expressions ranges from $N = 142$ to 1199, except of the simpler pole- and ζ_3-terms. On the other hand, the most involved recurrence is of order 16 only, with larger polynomial coefficients of a degree up to 210. For comparison, in Ref. [295] the authors handled far larger recurrences of order 35 and degree

	ε^{-2}			ε^{-1}			ε^0 rat.			$\varepsilon^0\zeta_2$		
Diagram	#	Deg.	Ord.	#	Deg.	Ord.	#	Deg.	Ord.	#	Deg.	Ord.
I_{6a}	15	3	2	55	11	3	142	25	5	15	3	2
I_{6b}	15	3	2	55	12	3	142	27	5	15	3	2
I_{8a}	19	4	2	69	14	3	164	30	5	19	4	2
I_{8b}	19	4	2	79	16	3	175	34	5	19	4	2
I_9	142	26	9	463	83	10	1199	210	16	142	26	5
I_{10a}	47	6	4	341	57	10	949	156	16	109	17	6
I_{10b}	109	17	6	323	53	10	911	152	16	47	6	4

Table 4: Complexity of the smallest recurrences describing the integrals I_{6a}–I_{10b}.

~ 1000 have been handled. Still there is no thorough algorithm known producing the number of moments needed directly from the integrals given above.

9 Graphs with Two Lines of Equal Mass

In this Chapter the calculation of graphs with two distinct fermion lines with the same mass m is presented. In these topologies, new mathematical quantities will emerge in the results. A calculation along the lines of the previous Chapter suffers from the emergence of divergent series representations of generalized hypergeometric functions of type ${}_{p+1}F_p$ ($p > 1$), of which no suitable analytic continuation relation is known. In order to find a convergent series representation the integral is cast into the form of a Mellin-Barnes [114, 115] integral and one of the Feynman parameter integrals will be left unintegrated. This representation will allow to transform the convergence condition of the series representation into a condition for how to close the contour depending on the values of the remaining Feynman parameter.

Fulfilling this condition the sum of residues can be checked to be absolutely convergent allowing for an exchange of the Laurent expansion with the summation operator. The coefficients of this expansion are then simplified using symbolic summation supplied with suitable limit procedures [93–101] leading to S-sums (168) [111, 254] and cyclotomic S-sums [110] evaluated at infinity, which correspond to (cyclotomic) harmonic polylogarithms depending on the remaining integration variable.

Since at this point it appears most natural to perform the last integral inside a family of iterated integrals over an alphabet of rational functions, we will consider the generating function of the Mellin moments. In this picture the remaining Feynman parameter integration is performed in the alphabet of (cyclotomic) harmonic polylogarithms with an extended alphabet. Finally the N-th Taylor coefficient of this series has to be determined analytically.

In the following the calculation is presented in detail, following the calculation of an example graph.

9.1 Method of Calculation

Feynman Parametrization

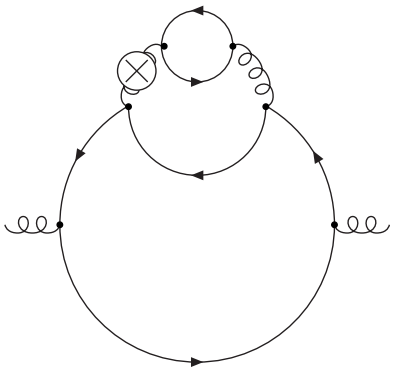

Figure 6: An example graph with a strict nesting : graph 4

The graph serving as an example in this section is shown in Figure 6. The list of graphs is generated with QGRAF [282] and written as momentum integrals using the Feynman rules of Appendix F. The momenta are integrated at the cost of introducing a Feynman parameterization, as described in Chapter 5.

For arbitrary propagator powers the parameterized form of the example reads :

$$\hat{I}_{\rm ex} = -e^{-\frac{3}{2}\varepsilon\gamma_E}\Gamma\left[\begin{array}{c} -6-\frac{3}{2}\varepsilon+\nu_{1,2,3,4,5,6} \\ \nu_1,\nu_2,\nu_3,\nu_4,\nu_5,\nu_6 \end{array}\right]\int_{[0,1]^7} dx_0\,dy_0\,dy_1\,dy_2\,dz_0\,dz_1\,dz_2$$

$$\delta\left(1-y_0-y_1-y_2\right)\delta\left(1-z_0-z_1-z_2\right)z_1^{\nu_2-1}x_0^{-\varepsilon+\nu_{1,2,3,4,6}-5}\left(1-x_0\right)^{-\varepsilon+\nu_{1,2,3,4,5}-5}$$
$$\left(1-y_0-y_2\right)^{\nu_4-1}\left(1-y_0\right)^{-\frac{\varepsilon}{2}+\nu_{1,2}-2}y_0^{-\frac{\varepsilon}{2}+\nu_{1,2,3}-3}y_2^{-\frac{\varepsilon}{2}+\nu_{5,6}-3}\left(1-z_1-z_2\right)^{\nu_1-1}z_2^{-\varepsilon+\nu_{3,4,5,6}-5}$$
$$\left(y_0z_1\right)^N\left(\left(1-x_0\right)x_0y_0\left(1-y_0+y_0z_2\right)+y_2z_2\right)^{\frac{3}{2}\varepsilon-\nu_{1,2,3,4,5,6}+6}\,, \tag{401}$$

where we made use of the shorthand notation

$$\nu_{i_1,..,i_n}=\nu_{i_1}+\cdots+\nu_{i_n}\,.$$

For better readability, a common factor of

$$i\;a_s\,S_\varepsilon^3(m^2)^{-3+\frac{3}{2}\varepsilon}(\Delta.p)^N$$

is omitted throughout the calculation.

The δ-distributions can be removed using the relations (154) and (155). However, the choice of which Feynman parameter to remove by virtue of the Dirac δ-distributions and in which order to successively remove the Heaviside θ-functions has to follow rules that will be developed in the following.

External Vertices

Let us consider a loop to which an external momentum p with $p^2=0$ is attached, schematically it has the form:

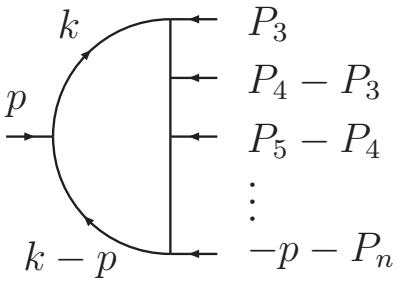

Its momentum integral reads

$$L_E=\int\hat{d}k\frac{1}{(k^2+m^2)^{\nu_1}((k-p)^2+m^2)^{\nu_2}}\prod_{i=3}^{n}\frac{1}{((k+P_i)^2+\delta_i m^2)^{\nu_i}}\,, \tag{402}$$

where n is the number of edges of the loop, P_i are some linear combinations of internal and external momenta, δ_i are either 1 or 0, depending on whether the ith propagator is massive or not, and all momenta are Euclidean due to an earlier Wick rotation. The Feynman parameterization of this loop yields

$$L_E=\frac{1}{(4\pi)^{D/2}}\frac{\Gamma\left(-\frac{D}{2}+\sum\nu_i\right)}{\prod\Gamma(\nu_i)}\int_{[0,1]^n}dx_1\;\ldots\;dx_n\left(\prod_{i=1}^{n}x_i^{\nu_i-1}\right)\delta\left(1-\sum_{i=1}^{n}x_i\right)$$
$$\left[\left(\sum_{i=3}^{n}2x_2\;x_i\;p.P_i\right)+\left(\sum_{i=3}^{n}x_i(1-x_i)\;P_i.P_i\right)-\left(\sum_{\substack{i,j=3\\ j\neq i}}^{n}2x_i\;x_j\;P_i.P_j\right)\right.$$

$$+ m^2 \sum_{i=1}^{n} \delta_i x_i \Bigg]^{\frac{D}{2} - \sum \nu_i} . \tag{403}$$

Here x_2 only occurs in the coefficient of scalar products linear in p. Therefore, in the integration of the last internal momentum, when all the P_i are proportional to p, x_2 drops out from the denominator polynomial. Therefore, it only occurs in the monomial prefactor and the operator polynomial, and can hence always be integrated once it is removed from the δ-distributions and Heaviside functions and the corresponding values of the propagator power is inserted.

Principle of the Minimal Operator Polynomial and δ-Reconstruction

Now some δ-distributions and Heaviside functions are removed, for the others one can follow a set of rules, which aim at keeping the operator polynomial as simple as possible. The goal of the rules is to determine the parameter which is either eliminated by virtue of a δ-distribution, or rescaled and removed from a Heaviside θ-function:

1. If all but one of the variables occurring in the δ-distribution occur also in the N-bracket, then choose one of the variables from the N-bracket applying principle 3. E.g. let $X = x_1 + \cdots + x_k$ be a sum of Feynman parameters and y a single Feynman parameter, then the rule implies

$$\delta(1 - X - y)(f(X))^N dy\, dx_1 \dots dx_k = \theta(1 - x_2 - \cdots - x_k)(f(1-y))^N dy\, dx_2 \dots dx_k .$$

2. Otherwise do not eliminate or rescale parameters which occur in the N-bracket.

3. Prefer parameters, which do not occur in the non-monomial prefactor (to avoid complication of the denominator polynomial).

4. There should never be factors $(1-x)^a, a \in \mathbb{R} \setminus \mathbb{N}$, for which x occurs in the θ-function.

Rule 4 is not really used for picking a parameter, but rather to indicate whether the set of rules 1-3 is sufficient, which turns out to be the case for the diagrams of this Chapter. For the example graph we get $y_1 = 1 - y_0 - y_2$, $y_2 \to y_2(1-y_0)$, $z_0 = 1 - z_1 - z_2$ and $z_1 \to z_1(1-z_2)$.

There might be θ-functions left, but they contain the same variables as the operator polynomial. In this case it is useful to reconstruct a δ-distribution by

$$\begin{aligned} \theta(1-X) f(1-X) &= \int_0^1 dy \delta(1-X-y) f(1-X) \\ &\stackrel{1.}{=} \int_0^1 dy \delta(1-X-y) f(y) , \end{aligned} \tag{404}$$

and then follow again the rules 1 to 4 to get a hypercubic integration region. Note that this reconstruction step can be used to construct coordinate transformations of Feynman parameter integrals. This will be shown in Appendix B.

The above procedure is applied, in order to avoid the proliferation of N. In fact, together with later steps one achieves, that N only occurs in the exponent of one of the Feynman parameters, allowing to effectively decouple N from the solution of infinite sums. This property of the calculation is of crucial importance[5].

[5]These considerations also carry over to the case of two lines of unequal masses.

Mellin-Barnes (MB) Representation

The remaining parameters still occur in the denominator polynomial. This polynomial has the form $(A+B)$ where A, B are products of elements x_i or $(1-x_i)$, for Feynman parameters x_i. Only in the cases of graphs with a massive line that runs through four edges of the graph, e.g. graphs 4 and 5 in Section 9.3, a factor $(1-x(1-y))$ occurs. A Mellin-Barnes integral [114, 115] is then introduced by the substitution, see also [271],

$$(A+B)^{-\gamma} = \frac{1}{\Gamma(\gamma)} \frac{1}{2\pi i} \int_{-i\infty}^{i\infty} d\xi \Gamma(-\xi)\Gamma(\gamma+\xi) \frac{A^\xi}{B^{\gamma+\xi}}\,, \tag{405}$$

which in the present example leads to the form

$$\begin{aligned}
\hat{I}_{\rm ex} = & -\frac{e^{-\frac{3}{2}\varepsilon\gamma_E} B\left(N+\nu_2,\nu_1\right)}{2\pi i\,\Gamma\left(\nu_1\right)\Gamma\left(\nu_2\right)\Gamma\left(\nu_3\right)\Gamma\left(\nu_4\right)\Gamma\left(\nu_5\right)\Gamma\left(\nu_6\right)} \int_{[0,1]^4} dx_0\, dy_0\, dy_2\, dz_2 \\
& \int_{-i\infty}^{i\infty} d\xi \Gamma\left(-\xi\right)\Gamma\left(-\frac{3D}{2}+\nu_{1,2,3,4,5,6}+\xi\right) y_2^{-\nu_{1,2,3,4}-\xi+D-1} \left(1-y_2\right)^{\nu_4-1} \\
& z_2^{-\nu_{1,2}-\xi+\frac{D}{2}-1} \left(1-z_2\right)^{\nu_{1,2}+N-1} y_0^{\nu_{1,2,3}+\xi+N-\frac{D}{2}-1} \left(1-y_0\right)^{-\nu_3-\xi+\frac{D}{2}-1} \\
& x_0^{\nu_{1,2,3,4,6}+\xi-D-1} \left(1-x_0\right)^{\nu_{1,2,3,4,5}+\xi-D-1} \left(1-y_0(1-z_2)\right)^{\xi}\,.
\end{aligned} \tag{406}$$

This procedure is equivalent to splitting the mass-term off the propagator like part that occurs in the Feynman parameter representation of a massive vacuum polarization diagram, before proceeding with successive parameterization and momentum integration.

In the cases that the products A, B from above factorize completely, all integrals can be performed in terms of Beta functions. In the remaining two cases, in which a factor $(1-x(1-y))$ remains, the integrals represent a generalized hypergeometric function ${}_3F_2$, which is already given in a form, such that it reduces to a ratio of Γ-functions.

In the example graph one finds for arbitrary propagator exponents ν_1, ν_2, ν_3:

$$\begin{aligned}
{}_3F_2\left[\begin{array}{c} -\xi, N+\nu_{1,2}, N+\nu_{1,2,3}+\xi-\frac{D}{2} \\ N-\xi+\frac{D}{2}, N+\nu_{1,2} \end{array}; 1\right] = & {}_2F_1\left[\begin{array}{c} -\xi, N+\nu_{1,2,3}+\xi-\frac{D}{2} \\ N-\xi+\frac{D}{2} \end{array}; 1\right] \\
= & \frac{\Gamma\left(D-\nu_{1,2,3}-\xi\right)}{\Gamma\left(\xi\right)\Gamma\left(D-\nu_{1,2,3}-2\xi\right)} B\left(N+\frac{D}{2}-\xi,\xi\right)\,.
\end{aligned} \tag{407}$$

Furthermore, the remaining Γ-functions may be combined to Beta functions and due to the relation

$$B\left(N+\frac{D}{2}-\xi,\xi\right) B\left(N+\nu_{1,2},\frac{D}{2}-\nu_{1,2}-\xi\right) = B\left(N+\nu_{1,2},\frac{D}{2}-\nu_{1,2}\right) B\left(\xi,\frac{D}{2}-\nu_{1,2}-\xi\right)\,, \tag{408}$$

the number of Beta functions containing N and ξ is reduced.

Closing the Contour

At this point in all the diagrams only one Beta function remains, that contains both N and ξ. This function is rewritten in terms of a Feynman parameter integral, i.e. in the example

$$B\left(N-\frac{D}{2}+\nu_{1,2,3}+\xi,\frac{D}{2}-\nu_3-\xi\right) = \int_0^1 dx\, x^{N-\frac{D}{2}+\nu_{1,2,3}+\xi-1} (1-x)^{\frac{D}{2}-\nu_3-\xi-1}\,. \tag{409}$$

The reason is, that the contour of the Mellin-Barnes integral can not be closed to one side. One can see this from two representations. On the one hand, the Beta function which contains N and ξ has the form

$$B(N+\xi+\alpha,-\xi+\beta) = \frac{\Gamma(N+\xi+\alpha)\Gamma(-\xi+\beta)}{\Gamma(N+\alpha+\beta)}\,, \tag{410}$$

so that the denominator drops out of the MB-integral. Hence if the contour is closed to one side and written as the sum of residues, then, due to the convergence condition (197), for every set of values of the propagator powers there is an N_0 so that for $N > N_0$ the sum is divergent.

On the other hand, when the Beta function is written down as a Feynman parameter integral over x, then the combination

$$\left(\frac{1-x}{x}\right)^{\xi} \tag{411}$$

demands that to which direction to close the contour depends on whether $(1-x)/x$ is greater or less than one. Here a splitting is necessary, between values $x < \frac{1}{2}$ for which the contour may be closed towards $\xi \to \infty$, and values $x > \frac{1}{2}$ for which $\xi \to -\infty$ is the convergent choice. For simplicity, we change the order of the ξ-integration such that the contour can be closed to the right in all cases.

After that the quantity raised to the power ξ is mapped onto a single integration variable T:

$$\begin{aligned} T \equiv \frac{x}{1-x} \in [0,1] \quad &\Leftrightarrow \quad x \equiv \frac{T}{1+T} \in \left[0,\frac{1}{2}\right]\,, \\ T \equiv \frac{1-x}{x} \in [0,1] \quad &\Leftrightarrow \quad x \equiv \frac{1}{1+T} \in \left[\frac{1}{2},1\right]\,, \\ &\text{with } dx = \frac{1}{(1+T)^2} dT\,. \end{aligned} \tag{412}$$

Now it is obvious that all contours have to be closed to the right, if the residue theorem is applied.

To make this procedure more explicit, an example will be given in the following. Let $a \in \mathbb{R}\setminus\mathbb{N}, 0 \le A \le 1, N \in \mathbb{N}$ and consider the following integral

$$I \;=\; \Gamma(a) \int_0^1 dx\, \frac{x^N}{(x+(1-x)A)^a}\,, \tag{413}$$

where one may introduce a Mellin-Barnes representation

$$I \;=\; \int_0^1 dx\, \frac{1}{2\pi i} \int_{-i\infty}^{i\infty} d\xi\, \Gamma(-\xi)\Gamma(\xi+a)\, x^{N-a} \left(\frac{1-x}{x}A\right)^{\xi}\,. \tag{414}$$

Here the contour may be closed depending on the value of x:

- if $(1-x)A/x < 1 \Leftrightarrow A/(1+A) < x$, close for $\xi > 0$,
- if $(1-x)A/x > 1 \Leftrightarrow A/(1+A) > x$, close for $\xi < 0$.

So if we first integrate x to form Beta functions, we mess up these regions and the series of residues will in general not converge. Thus the integral over x has to be split, so as to separate these regions

$$I \;=\; \int_0^{A/(A+1)} dx\, \frac{1}{2\pi i} \int_{-i\infty}^{i\infty} d\xi\, \Gamma(-\xi)\Gamma(\xi+a)\, x^{N-a} \left(\frac{1-x}{x}A\right)^{\xi}$$

$$+\int_{A/(A+1)}^{1} dx\,\frac{1}{2\pi i}\int_{-i\infty}^{i\infty} d\xi\,\Gamma(-\xi)\Gamma(\xi+a)\,x^{N-a}\left(\frac{1-x}{x}A\right)^{\xi}. \tag{415}$$

The mappings $\xi \to -\xi$ and $x \to 1-x$ for the first part make it possible to close both contours in an analogous manner:

$$\begin{aligned} I &= \frac{1}{2\pi i}\int_{-i\infty}^{i\infty} d\xi\,\int_{1/(A+1)}^{1} dx\,\Gamma(\xi)\Gamma(-\xi+a)\,(1-x)^{N-a}\left(\frac{1-x}{xA}\right)^{\xi} \\ &\quad +\frac{1}{2\pi i}\int_{-i\infty}^{i\infty} d\xi\,\int_{A/(A+1)}^{1} dx\,\Gamma(-\xi)\Gamma(\xi+a)\,x^{N-a}\left(\frac{1-x}{x}A\right)^{\xi}, \end{aligned} \tag{416}$$

and further assimilate the two parts. The ξ integral of the first term may be shifted yielding

$$\begin{aligned} I &= A^{-a}\int_{1/(A+1)}^{1} dx\,\frac{1}{2\pi i}\int_{-i\infty}^{i\infty} d\xi\,\Gamma(\xi+a)\Gamma(-\xi)\,x^{-a}(1-x)^{N}\left(\frac{1-x}{xA}\right)^{\xi} \\ &\quad +\int_{A/(A+1)}^{1} dx\,\frac{1}{2\pi i}\int_{-i\infty}^{i\infty} d\xi\,\Gamma(-\xi)\Gamma(\xi+a)\,x^{N-a}\left(\frac{1-x}{x}A\right)^{\xi}. \end{aligned} \tag{417}$$

Now the contour integral may be performed, such that the integral commutes with the summation,

$$\begin{aligned} I &= -A^{-a}\sum_{k=0}^{\infty}\frac{\Gamma(k+a)}{k!}(-\frac{1}{A})^{k}\int_{1/(A+1)}^{1} dx\,x^{-a-k}(1-x)^{N+k} \\ &\quad -\sum_{k=0}^{\infty}\frac{\Gamma(k+a)}{k!}(-A)^{k}\int_{A/(A+1)}^{1} dx\,x^{N-a-k}(1-x)^{k}. \end{aligned} \tag{418}$$

In order to evaluate the Feynman parameter integrals, we map $x \to (1-x)$ and rescale the upper integration limit to 1:

$$\begin{aligned} I &= -A^{-a}\sum_{k=0}^{\infty}\frac{\Gamma(k+a)}{k!}\left(-\frac{1}{A}\right)^{k}\left(\frac{A}{A+1}\right)^{N+k+1}\int_{0}^{1} dx\,\left(1-\frac{A}{A+1}x\right)^{-a-k}x^{N+k} \\ &\quad -\sum_{k=0}^{\infty}\frac{\Gamma(k+a)}{k!}(-A)^{k}\left(\frac{1}{A+1}\right)^{k+1}\int_{0}^{1} dx\,\left(1-\frac{1}{A+1}x\right)^{N-a-k}x^{k}. \end{aligned} \tag{419}$$

Then the binomial theorem helps to integrate the parameter x

$$\begin{aligned} I &= -A^{-a}\sum_{k=0}^{\infty}\sum_{m=0}^{\infty}\frac{\Gamma(a+k+m)}{k!\,m!\,(N+1+k+m)}\left(-\frac{1}{A}\right)^{k}\left(\frac{A}{A+1}\right)^{N+1+k+m} \\ &\quad -\sum_{k=0}^{\infty}\sum_{m=0}^{\infty}\frac{\Gamma(k+a)(a-N+k)_{m}}{k!\,m!\,(1+k+m)}(-A)^{k}\left(\frac{1}{A+1}\right)^{1+k+m}. \end{aligned} \tag{420}$$

Due to $0 \le A/(A+1) \le 1/2$, the integral can be performed in terms of a ${}_2F_1$, and the resulting double series is absolutely convergent. Using Sigma, the infinite sums are performed one after the other. This, however, reorganizes the summand of the second sum in such a way, that individual parts diverge linearly or polynomially, although the whole sum is expected to converge. A treatment for these divergent sums is not known. Therefore, the x-integral will be kept until it can be performed within the algebra of iterated integrals at a later stage.

For the graphs considered in this Chapter, A contains further integration variables, which are integrated already at the stage of (414). The splitting of the x-integral can therefore be performed assuming $A = 1$.

Convergence of the MB-integral

It is worthwhile having a look onto convergence issues of the procedure described so far. First, the Mellin-Barnes integral is introduced in the integrand of the multiple Feynman parameter integral of Eq. (401). The contour follows the requirements stated in Chapter 5.4.

Of course, contours of the above kind can only be found, if the right-poles are separated from left-poles. In cases where this is not obviously the case, we enforce such a separation by introducing a regularization parameter. The introduction of such artificial parameters has to be consistent throughout the expression. So it is most convenient to keep symbolic propagator powers from the beginning, and to use substitutions of these symbolic quantities.

We will see later at which point the expansion into a Laurent series in these parameters can be performed most conveniently. Furthermore, there might be points in the complex plane at which several right poles are located. These are also separated by introducing further artificial regularization parameters. In contrast to the parameters separating left from right poles, the expansion in these parameters is equivalent to the calculation of the residue of multiple poles. So here no correspondence with other terms has to be obeyed.

Calculating the MB-Integral via the Residue Theorem

The classical procedure for calculating Mellin-Barnes integrals in particle physics proceeds by deforming the contour and subtracting finitely many residues, such that the remaining contour integral represents a regular function in ε [117, 271–273]. In that case the expansion can be performed on the integrand level. However, since factors of T^ξ occur in the arguments of the contour integrals, cf. (409, 412), no Barnes lemmas [115, 274] can be applied[6]. Furthermore, calculations involving Barnes lemmas are not well suited for a completely automated calculation procedure, since usually they are not applied directly, but rather through corollaries, which are recognized to be needed by individual inspection.

In the present calculation, it appears more automatic to rather write down the sums of residues and generate the necessary simplifications and algebraic relations by symbolic summation methods implemented in the package Sigma [93–101], equipped with suitable limit procedures for infinite sums.

Distinction of Special Cases on Γ-Functions

When residues are calculated and the corresponding sums are written down, one has to perform a Laurent expansion in the regularization parameters. Here it is important to observe the singularity structure.

One therefore brings the Γ-function arguments to a standard form, such that all of them are positive for vanishing regulators:

$$\Gamma(x) = \theta(\lfloor x \rfloor - 1)\Gamma(x) + \theta(-\lfloor x \rfloor)(-1)^{\lfloor x \rfloor + 1} \frac{\Gamma(\langle x \rangle)\Gamma(1 - \langle x \rangle)}{\Gamma(1 - x)} \,. \tag{421}$$

Here $\langle x \rangle$ and $\lfloor x \rfloor$ represent the fractional and integer parts of the variable x, respectively. The regulators are assumed to be chosen such, that they only contribute to the fractional part. The Heaviside θ-functions are defined in (154).

[6] For a list of corollaries see [271].

The Heaviside functions are removed by commuting them with summation operators, which can be done using the following relations:

$$\sum_{i=a}^{b} \theta(c+d\cdot i) = \theta\left(\left\lceil -\frac{c}{d}\right\rceil - a\right)\theta\left(b - \left\lceil -\frac{c}{d}\right\rceil\right) \sum_{i=\lceil c/d\rceil}^{b} + \theta\left(a - \left\lceil -\frac{c}{d}\right\rceil - 1\right)\sum_{i=a}^{b},$$

$$\sum_{i=a}^{b} \theta(c-d\cdot i) = \theta\left(\left\lfloor \frac{c}{d}\right\rfloor - a\right)\theta\left(b - \left\lfloor \frac{c}{d}\right\rfloor - 1\right) \sum_{i=a}^{\lfloor c/d\rfloor} + \theta\left(\left\lfloor \frac{c}{d}\right\rfloor - b\right)\sum_{i=a}^{b}. \tag{422}$$

Once the θ-functions do not contain any summation parameters, they can be evaluated. Note that they are also free from the Mellin variable N, since it had been separated from the sums by construction.

Expansion in Regulators and Summation

Once the Γ-functions have been reflected such that the integer parts of their arguments are positive, their expansion in the artificial regulators is straight forward. Finally, the expansion of the sums in the dimensional regulator ε can be done using the Package EvaluateMultiSums [101–103]. It also manages the call of Sigma-routines and performs limits of many expressions.

Yet one additional preparation is necessary for the expansion in the dimensional regulator ε, since the Feynman parameter integrals may not be well defined in the Lebesgue sense for $0 < \varepsilon < 1$, but rather as an analytic continuation in $\varepsilon \to 0$. The expressions are of the form

$$f(\varepsilon) = \int_0^1 dx\, x^{\varepsilon-a} g(x)\,, \tag{423}$$

which only converges as a Lebesgue integral if $\varepsilon > a - 1$. Nevertheless, using integration by parts, one can shift this integrand such that it is integrable for $0 < \varepsilon < 1$. For the form above with $a \geq 1$, the relation

$$\int_0^1 dx\, x^{\varepsilon-a} g(x) = \frac{g(1)}{\varepsilon - a + 1} - \frac{1}{\varepsilon - a + 1}\int_0^1 dx\, x^{\varepsilon-a+1} g'(x) \tag{424}$$

has to be iterated $(a-1)$-times. Here the function $g(x)$ must have sufficiently many regular derivatives on $[0,1]$, which is indeed the case in the integral in question. Then the integral represents a regular function in ε, the integrand is measurable for $0 \leq \varepsilon < 1$ and thus the Taylor expansion commutes with the integration.

The result of expansion and summation yields an expression, which still depends on one integration variable T, and which contains S-sums and cyclotomic S-sums of this variable. They can be converted into (cyclotomic) harmonic polylogarithms (HPL):

$$S_1(-T,\infty) = -H_{-1}(T)\,, \tag{425}$$

$$S_2(-T,\infty) = -H_{0,-1}(T)\,, \tag{426}$$

$$S_{1,1}(-T,1,\infty) = H_{-1,-1}(T) - H_{0,-1}(T)\,, \tag{427}$$

$$S_{(2,1,1)}(-T;\infty) = \frac{H_{(4,0)}\left(\sqrt{T}\right)}{\sqrt{T}} - 1\,, \tag{428}$$

$$S_{(2,1,2)}(-T;\infty) = \frac{H_{0,(4,0)}\left(\sqrt{T}\right)}{\sqrt{T}} - 1\,, \tag{429}$$

$$S_{(1,0,1),(2,1,1)}(-T,1;\infty) = -\frac{4H_{(4,0)}\left(\sqrt{T}\right)}{\sqrt{T}} + \frac{H_{(4,1)}\left(\sqrt{T}\right)}{2T} - \frac{3}{2}H_{(4,1)}\left(\sqrt{T}\right)$$

$$- 2H_{(4,0),(4,0)}\left(\sqrt{T}\right) + \frac{15}{4}\,, \tag{430}$$

$$S_{(2,1,1),(1,0,1)}(-T,1;\infty) = -\frac{H_{(4,0)}\left(\sqrt{T}\right)}{2T^{3/2}} + \frac{3H_{(4,0)}\left(\sqrt{T}\right)}{2\sqrt{T}} - \frac{2H_{(4,1)}\left(\sqrt{T}\right)}{T}$$
$$- \frac{2H_{(4,0),(4,1)}\left(\sqrt{T}\right)}{\sqrt{T}} + \frac{1}{2T}\,, \tag{431}$$

$$S_{(2,1,1),(2,1,1)}(-T,1;\infty) = \frac{H_{(4,0)}\left(\sqrt{T}\right)}{4T^{3/2}} - \frac{3H_{(4,0)}\left(\sqrt{T}\right)}{4\sqrt{T}} + \frac{H_{0,(4,0)}\left(\sqrt{T}\right)}{\sqrt{T}}$$
$$- \frac{H_{(4,1),(4,0)}\left(\sqrt{T}\right)}{\sqrt{T}} - \frac{1}{4T}\,. \tag{432}$$

The conversions to iterated integrals are performed using ideas of [110] and which are automated in J. Ablinger's package HarmonicSums [108–111].

In this conversion the iterated integrals first appear evaluated at 1, but with letters that depend on the remaining integration variable. They will be denoted by

$$f_{[\alpha,y]}(x) := f_\alpha(xy)\,, \tag{433}$$

where f_α is a letter from the alphabets (156, 175). Therefore a procedure is needed, that maps the class of iterated integrals appearing here onto (cyclotomic) HPLs with the integration variable in the argument. There is such a procedure which was used for deriving properties of two-dimensional HPLs [125] and in the method of hyperlogarithms [312]. It makes use of the fact, that differentiation of a certain type of iterated integrals with respect to variables appearing in the index leads to a drop in the transcendental weight of the function, e.g.:

$$\frac{\partial}{\partial x} H_{-x,-1}(1) = \frac{\partial}{\partial x}\int_0^1 \frac{dy}{x+y}\int_0^1 \frac{dz}{1+z} = -\frac{H_x(1)}{1-x} - \frac{2\ln(2)}{x^2-1}\,, \quad x > 0\,. \tag{434}$$

In this way the problem can be traced back to properties of rational functions, solving the problem recursively at a lower weight and integrating again over x, where in each recursive call a constant has to be determined.

However, in case of letters containing polynomials of degree 2 or more, this is not possible, since in general the weight does not drop due to differentiation, e.g.

$$\frac{\partial}{\partial x} H_{[(4,0),x],-1}(1) = -\frac{1}{x} H_{[(4,0),x],-1}(1) - \frac{x}{x^2+1} H_{[(4,1),x]}(1) - \frac{1}{x(x^2+1)} H_{[(4,0),x]}(1) + \frac{2\ln(2)}{x(x^2+1)}\,. \tag{435}$$

Here the following procedure will be useful. Let us distinguish the letters with indices α and denote the corresponding rational functions with $f_\alpha(x)$. One can form new letters by scaling the argument of the rational functions with a variable y, cf. (433). If one such letter is built into a cyclotomic HPL with argument $x = 1$, there is an algorithm for removing the parameter y from the index, such that it occurs in the argument.

At first, by virtue of the shuffle algebra, the weighted letter is brought to the rightmost position. Then indexing general rational letters with α_i, $i = 1, ..., n$, we find the algorithm:

$$\begin{aligned} H_{\alpha_1,...,\alpha_{n-1},[\alpha_n,y]}(1) &= \int_0^1 dx_1\, f_{\alpha_1}(x_1) ... \int_0^{x_{n-2}} dx_{n-1}\, f_{\alpha_{n-1}}(x_{n-1}) \int_0^{x_{n-1}} dx_n\, f_{\alpha_n}(yx_n) \\ &= \frac{1}{y}\int_0^y dx_n \int_0^1 dx_1 f_{\alpha_1}(x_1) ... \end{aligned}$$

$$
\begin{aligned}
&\ldots \int_0^{x_{n-2}} dx_{n-1} x_{n-1} f_{\alpha_{n-1}}(x_{n-1}) f_{\alpha_n}(x_{n-1} x_n) \\
&= \text{"cycl. HPLs"} + \frac{1}{y} \int_0^y dx_n \; f_{\beta_n}(x_n) H_{\alpha_1,\ldots,\alpha_{n-2},[\tilde{\alpha}_n,x_n]}(1) \,, \qquad (436)
\end{aligned}
$$

where a partial fraction decomposition is performed in the last step. After that the formula may be recursively applied where the terminal step is obviously

$$
H_{[\alpha_n,x_2]}(1) = \frac{1}{x_2} H_{\alpha_n}(x_2) \,. \qquad (437)
$$

So that the result is a multivariate polynomial in iterated integrals of arguments $1, y$. This procedure produces also letters $1/(x-1)$, which introduce branch points at $y = 1$. However, considering the integration contour of the iterated integrals infinitesimally away from the real axis does not affect the algorithm introduced above. In this sense the iterated integrals may be analytically continued, as described in [122] and implemented in HarmonicSums [108–111]. Thus they can always be expressed as iterated integrals with arguments in $[0, 1]$.

The Final Integral

Once the sums are performed, i.e. written in terms of iterated integrals, the remaining task is to perform the last integration, which carries the nontrivial dependence on N. However, the integral does not just represent a Mellin-transform, but it contains rational functions $R(T) \in \{1/(1+T^2), T^2/(1+T^2)\}$, which are raised to the power N. It therefore seems most natural to consider the generating function of the sequence in N, and to introduce the corresponding tracing parameter κ in the following way:

$$
\sum_{N=0}^{\infty} (\kappa R(T))^N = \frac{1}{1 - \kappa R(T)} \,. \qquad (438)
$$

The integral over T from 0 to 1 is performed in two steps: First a primitive is calculated for the integral in terms of iterated integrals. Then the limits $T \to 1$ and $T \to 0$ are calculated. This procedure introduces additional letters into the otherwise cyclotomic alphabet of HPLs, namely

$$
\frac{1}{1 + g(\kappa) T^2} = f_{(4,0)}\left(\sqrt{g(\kappa)} T\right), \quad \frac{T}{1 + g(\kappa) T^2} = \frac{1}{\sqrt{g(\kappa)}} f_{(4,1)}\left(\sqrt{g(\kappa)} T\right) , \qquad (439)
$$

with $g(\kappa) \in \{(1-\kappa), (1-\kappa)^{-1}\}$. Obviously this leads again to rescaled letters, and one can use the algorithm from above to transform the emerging cyclotomic HPLs at 1 with weighted letters into cyclotomic HPLs with unweighted letters, but a function of κ in the argument. It is not hard to see, that the functions occurring in the arguments of these HPLs are the functions $g(\kappa)$ from above.

The limit $T \to 0$ has to be taken carefully, since factors $1/T$ are present, which only cancel in the desired limit. Therefore a Taylor expansion is performed. In many cases relations similar to Eqs. (425–432) are used, reading them from right to left, in order to obtain the Taylor series. However, such relations are not implemented in HarmonicSums for the additional (weighted) letters of Eq. (439). This is due to the requirement of special assumptions on the values of $g(\kappa)$. We rather use an easy trick to obtain the Taylor series of cyclotomic HPLs extended by the above letter, using the fact that the above letter can be factorized over the complex numbers:

$$
\frac{1}{1 + g(\kappa) T^2} = \frac{1}{2} \left(\frac{1}{1 + i\sqrt{g(\kappa)} T} + \frac{1}{1 - i\sqrt{g(\kappa)} T} \right) . \qquad (440)
$$

Then these linear letters are treated like the letter

$$\frac{1}{a+T} \tag{441}$$

from the alphabet of multiple polylogarithms [111], treating a as real and positive. For the cyclotomic HPLs extended by one such letter, the Taylor series expansions can be derived [110, 111]. Finally the imaginary factors $i\sqrt{g(\kappa)}$ are re-substituted. The results are checked to be regular in $T = 0$ and thus the limit can be taken.

Regularity of the Generating Function

Once the last Feynman parameter integral is performed, we need to find the Nth coefficient of the Taylor expansion in κ. Since we want to make use of methods for finding the Nth Taylor coefficient for HPLs and cyclotomic HPLs which are implemented in the Package HarmonicSums [108–111], it is necessary to make sure that the dependence on $\ln(\kappa)$ cancels. This can be done using argument transformations and algebraic relations of the (cyclotomic) HPLs.

At first, the arguments are mapped back into the interval $[0, 1]$:

$$H_{\vec{\alpha}}\left(\frac{1}{\sqrt{1-\kappa}}\right) = \sum_{\vec{\beta}} a_{\vec{\beta}} H_{\vec{\beta}}\left(\sqrt{1-\kappa}\right) , \tag{442}$$

where the length of the list $\vec{\beta}$ is bounded by the length of $\vec{\alpha}$, and the $a_{\vec{\beta}}$ are integer coefficients. The relations of this kind can be obtained algorithmically and are implemented for all cyclotomic HPLs in the package HarmonicSums.

Then the square roots are removed from the arguments, as far as possible. For this step one makes use of the fact that all cyclotomic HPLs with arguments x^2 can be rewritten in terms of cyclotomic HPLs at arguments x. These transformations can be inverted, so that (cyclotomic) HPLs which contain the letter $f_{(1,0)}(x) = \frac{1}{x-1}$ and the argument $\sqrt{1-\kappa}$ are mapped onto (cyclotomic) HPLs with argument $1-\kappa$ and (cyclotomic) HPLs without the letter $f_{(1,0)}$, i.e.

$$H_{\vec{\alpha}}\left(\sqrt{1-\kappa}\right) = \sum_{\vec{\beta}} b_{\vec{\beta}} H_{\vec{\beta}}(1-\kappa) + \sum_{\vec{\gamma}} c_{\vec{\gamma}} H_{\vec{\gamma}}\left(\sqrt{1-\kappa}\right) , \tag{443}$$

where in the vector $\vec{\alpha}$ there is an index $(1, 0)$. The length of $\vec{\beta}$ is again bounded by the length of $\vec{\alpha}$ and $\vec{\gamma}$ is free of the index $(1, 0)$.

This reduction is, however, not complete, so it is introduced by constructing a basis of HPLs w.r.t. the shuffle relations as well the relations of squared arguments. It is a sign of a proper Laurent-series that after the reduction to such a basis the remaining (cyclotomic) HPLs involving the letter $f_{(1,0)}$ and with argument $\sqrt{1-\kappa}$ will cancel.

The last step to properly cancel logarithmic parts is to write all $\ln(\kappa)$ parts explicitly, using the flip relation

$$H_{\alpha}(1-\kappa) = \sum_{\vec{\eta}} d_{\vec{\eta}} H_{\vec{\eta}}(\kappa) . \tag{444}$$

In the present case, this relation only has to be applied to HPLs with letters from the alphabet

$$\left\{ f_0(x) = \frac{1}{x}, f_1(x) = \frac{1}{1-x}, f_{-1}(x) = \frac{1}{1+x} \right\} . \tag{445}$$

This subset is not closed under the flip $x \to (1-x)$, so the property

$$f_{-1}(1-x) = \frac{1}{2-x} =: f_2(x) \tag{446}$$

will lead to multiple polylogarithms [111] in the result.

Nevertheless, the representation is standardized so that indeed all dependencies on $\ln(\kappa)$ cancel. The remaining HPLs fit into the alphabet (156), enhanced by two cyclotomic letters $f_{(4,0)}, f_{(4,1)}$, and one letter from the multiple polylogarithms f_2. So in the alphabet the letters

$$\left\{ f_{(0,0)}(x) = \frac{1}{x}, f_{(2,0)}(x) = \frac{1}{1+x}, f_{(4,0)}(x) = \frac{1}{1+x^2}, f_{(4,1)}(x) = \frac{x}{1+x^2} \right\} \tag{447}$$

occur for HPLs with the argument $\sqrt{1-\kappa}$, as well as HPLs and multiple polylogarithms with letters f_1, f_0, f_{-1}, f_2 and argument κ.

Extraction of the Nth Taylor Coefficient

Since the result may be expanded into a Taylor series, the remaining step to obtain the all-N result is to extract the Nth coefficient of this Taylor series in κ. This can be done analytically term by term, using expansions of individual factors and calculating their Cauchy products, as well as by deriving difference equations which are solved in terms of indefinite nested sums. Also these methods are available through the packages HarmonicSums and Sigma.

As a result of this procedure one obtains a large expression in terms of sums of higher depth, involving definite and indefinite sums and products. To obtain a minimal representation, the package Sigma can be applied, in order to represent these objects in terms of indefinite nested sums, and in order to eliminate all relations among these indefinite nested sums and products.

9.2 Operator Insertions on External Vertices

The class of graphs with two massive fermion lines of the same mass also includes graphs with operator insertions on external gluon vertices. In the scalar case these graphs are directly related to graphs with operator insertions on a line, see the ladder graphs in Eqs. (333, 355).

The idea carries over to the non-scalar case, but there are not simply relations among graphs, but rather the statement, that if a method is known for the calculation of certain graphs with operator insertions on lines, then the same methods apply for the graphs with operator insertions on external gluon vertices.

The reason lies in the structure of the Feynman rule for the operator insertion of a gluon vertex, which can be taken from [87, 229], and is also given in Appendix E:

$$\begin{aligned} V^{abc}_{\mu\nu\lambda}(q_1,q_2,q_3) = & -ig\frac{1+(-1)^N}{2} f^{abc} \Bigg[\\ & t^{3g}_{\mu\nu\lambda}(q_1,q_2,q_3)(\Delta.q_1)^{N-2} + \tau^{3g}_{\mu\nu\lambda}(q_1,q_2,q_3) \sum_{j=0}^{N-3} (-\Delta.q_1)^j (\Delta.q_2)^{N-3-j} \\ & + t^{3g}_{\nu\lambda\mu}(q_2,q_3,q_1)(\Delta.q_2)^{N-2} + \tau^{3g}_{\nu\lambda\mu}(q_2,q_3,q_1) \sum_{j=0}^{N-3} (-\Delta.q_2)^j (\Delta.q_3)^{N-3-j} \\ & + t^{3g}_{\lambda\mu\nu}(q_3,q_1,q_2)(\Delta.q_3)^{N-2} + \tau^{3g}_{\lambda\mu\nu}(q_3,q_1,q_2) \sum_{j=0}^{N-3} (-\Delta.q_3)^j (\Delta.q_1)^{N-3-j} \Bigg], \end{aligned} \tag{448}$$

with

$$t^{3g}_{\mu\nu\lambda}(q_1,q_2,q_3) = (\Delta_\nu g_{\lambda\mu} - \Delta_\lambda g_{\mu\nu})\Delta.p_1 + \Delta_\mu(p_{1,\nu}\Delta_\lambda - p_{1,\lambda}\Delta_\nu)\,,$$
$$\tau^{3g}_{\mu\nu\lambda}(q_1,q_2,q_3) = \Delta_\lambda\Big[\Delta.p_1 p_{2,\mu}\Delta_\nu + \Delta.p_2 p_{1,\nu}\Delta_\mu - \Delta.p_1\Delta.p_2 g_{\mu\nu} - p_1.p_2\Delta_\mu\Delta_\nu\Big]\,. \tag{449}$$

In this notation the summands in the left column of Eq. (448) all behave like operator insertions on lines. Furthermore, if $q_1 = p$ is the external momentum then the first and last summand in the second column behave like insertions on lines too, but here in addition the result is subject to a finite sum of the form

$$\sum_{j=0}^{N-3}(-\Delta.p)^j(\Delta.p)^{N-3-j}f(N-3-j) = (\Delta.p)^{N-3}\sum_{j=0}^{N-3}(-1)^j f(N-3-j)$$
$$= (-\Delta.p)^{N-3}\sum_{j=0}^{N-3}(-1)^j f(j)\,. \tag{450}$$

The remaining summand (second term, right column) can be summed, and using $q_2 + q_3 = -q_1 = -p$ one finds:

$$\sum_{j=0}^{N-3}(-\Delta.q_2)^j(\Delta.q_3)^{N-3-j} = \frac{1}{\Delta.p}\Big[(-\Delta.q_2)^{N-2} - (\Delta.q_3)^{N-2}\Big]\,. \tag{451}$$

In this way the operator insertion on an external vertex is related to operator insertions on internal lines. However, a direct relation between a graph with a vertex insertion and the corresponding graphs with line insertions does not follow from this consideration, due to the presence of the tensors $t^{3g}_{\mu\nu\lambda}$ and $\tau^{3g}_{\mu\nu\lambda}$.

9.3 Results

In the following, the results for the scalar prototypes of the graphs contributing to the $O(T_F^2)$ part of the operator matrix element $A^{(3)}_{gg,Q}$ are summarized in the following. Graph 1 coincides with the scalar prototype for all graphs contributing to the $O(T_F^2)$ part of the operator matrix element $A^{(3)}_{gq,Q}$.

Additionally the asymptotic expansions for $N \to \infty$ are given, which are necessary for an analytic continuation to complex values of N. They are obtained with the package HarmonicSums [108–111].

The following convention was used:

$$\ln(\bar{N}) = \ln(N) + \gamma_E\,, \tag{452}$$

and all diagrams are normalized such, that the factor

$$ia_s^3 S_\varepsilon^3 (\frac{m^2}{\mu^2})^{\frac{3}{2}\varepsilon-3}(\Delta.p)^N \tag{453}$$

is omitted. The results for the diagrams, calculated as explained before, together with their asymptotic expansions are:

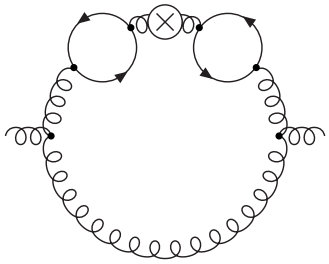

Graph 1

$$
\begin{aligned}
\mathrm{Res}_1 = \frac{(-1)^N+1}{2}\Bigg\{ & \frac{2}{105\varepsilon^2(N+1)} - \frac{1}{\varepsilon}\left[\frac{S_1(N)}{105(N+1)} + \frac{57N+127}{7350(N+1)^2}\right] \\
& + \frac{1}{420(N+1)}\left(S_1(N)^2 + S_2(N) + \zeta_2\right) + \frac{57N+127}{14700(N+1)^2}S_1(N) \\
& - \frac{75253N^2+78686N-84767}{18522000(N+1)^3}\Bigg\} \qquad (454) \\
= \frac{(-1)^N+1}{2}\Bigg\{ & \frac{1}{\varepsilon^2}\left[\frac{2}{105N} - \frac{2}{105N^2} + \frac{2}{105N^3} - \frac{2}{105N^4} + \frac{2}{105N^5} - \frac{2}{105N^6} + \frac{2}{105N^7}\right] \\
& + \frac{1}{\varepsilon}\Bigg[\left(-\frac{1}{105N} + \frac{1}{105N^2} - \frac{1}{105N^3} + \frac{1}{105N^4} - \frac{1}{105N^5} + \frac{1}{105N^6} - \frac{1}{105N^7}\right)\ln(\bar{N}) \\
& - \frac{19}{2450N} - \frac{8}{1225N^2} + \frac{743}{44100N^3} - \frac{1163}{44100N^4} + \frac{351}{9800N^5} - \frac{1333}{29400N^6} + \frac{14527}{264600N^7}\Bigg] \\
& + \left(+\frac{1}{420N} - \frac{1}{420N^2} + \frac{1}{420N^3} - \frac{1}{420N^4} + \frac{1}{420N^5} - \frac{1}{420N^6}\frac{1}{420N^7}\right)\ln(\bar{N})^2 \\
& + \Bigg(\frac{19}{4900N} + \frac{4}{1225N^2} - \frac{743}{88200N^3} + \frac{1163}{88200N^4} - \frac{351}{19600N^5} + \frac{1333}{58800N^6} \\
& - \frac{14527}{529200N^7}\Bigg)\ln(\bar{N}) - \frac{75253}{18522000N} + \frac{138883}{18522000N^2} - \frac{51313}{18522000N^3} - \frac{57871}{9261000N^4} \\
& + \frac{481169}{24696000N^5} - \frac{102331}{2744000N^6} + \frac{1110283}{18522000N^7} \\
& + \left(\frac{1}{105N} - \frac{1}{105N^2} + \frac{1}{105N^3} - \frac{1}{105N^4} + \frac{1}{105N^5} - \frac{1}{105N^6} + \frac{1}{105N^7}\right)\zeta_2\Bigg\} \\
& + O\left(\ln^2(\bar{N})\frac{1}{N^8}\right), \qquad (455)
\end{aligned}
$$

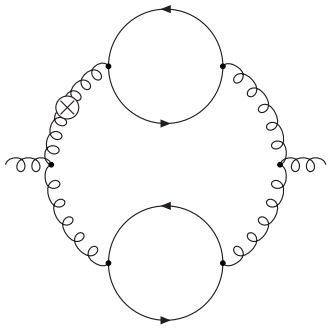

Graph 2

$$\begin{aligned}\mathrm{Res}_2 = \frac{(-1)^N+1}{2}\Bigg\{ & \frac{1}{105\varepsilon^2} + \frac{1}{\varepsilon}\left[\frac{74N^3-455N^2+381N-210}{44100(N-1)N(N+1)} - \frac{1}{210}S_1(N)\right] \\ & + \frac{8903N^3+39537N^2-114440N+36576}{2822400(N+1)(2N-3)(2N-1)}S_1(N) \\ & + \frac{P_{62}}{148176000(N-1)^2N^2(N+1)^2(2N-3)(2N-1)} \\ & + \frac{1}{840}\Big(S_1(N)^2+S_2(N)+3\zeta_2\Big) \\ & + \frac{(N-1)N(5N-6)}{1536(2N-3)(2N-1)4^N}\binom{2N}{N}\left[\sum_{j=1}^{N}\frac{4^jS_1(j)}{\binom{2j}{j}j^2} - \sum_{j=1}^{N}\frac{4^j}{\binom{2j}{j}j^3} - 7\zeta_3\right]\Bigg\}, \end{aligned} \tag{456}$$

$$\begin{aligned}P_{62} = {} & 1795487N^8 - 7087789N^7 + 10654130N^6 - 5797102N^5 + 6828839N^4 - 16594069N^3 \\ & + 9651144N^2 + 902160N - 1058400\,, \end{aligned} \tag{457}$$

$$\begin{aligned}\mathrm{Res}_2 = \frac{(-1)^N+1}{2}\Bigg\{ & \frac{1}{105\varepsilon^2} + \frac{1}{\varepsilon}\left[-\frac{\ln(\bar{N})}{210}\right. \\ & \left. + \frac{37}{22050} - \frac{4}{315N} + \frac{3}{280N^2} - \frac{19}{1260N^3} + \frac{37}{3600N^4} - \frac{19}{1260N^5} + \frac{547}{52920N^6} - \frac{19}{1260N^7}\right] \\ & + \left(-\frac{37}{44100} + \frac{2}{315N} - \frac{3}{560N^2} + \frac{1}{360N^3} - \frac{113}{16800N^4} + \frac{13}{27720N^5} - \frac{152981}{15135120N^6}\right. \\ & \left. - \frac{41}{9240N^7}\right)\ln(\bar{N}) + \frac{1}{840}\ln(\bar{N})^2 + \frac{1}{210}\zeta_2 - \frac{523}{2315250} - \frac{179}{33075N} + \frac{4411}{352800N^2} \\ & - \frac{29}{2205N^3} + \frac{1970701}{63504000N^4} - \frac{8084987}{384199200N^5} + \frac{3314839601}{67334467200N^6} - \frac{88780933}{3329726400N^7}\Bigg\} \\ & + O\left(\ln(\bar{N})\frac{1}{N^8}\right), \end{aligned} \tag{458}$$

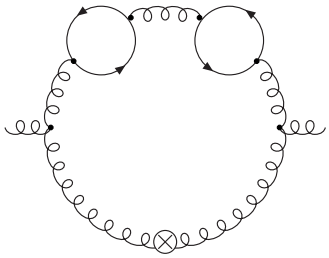

Graph 3

$$\mathrm{Res}_3 = \frac{(-1)^N+1}{2}\left\{\frac{1}{\varepsilon}\frac{1}{105N(N+1)} - \frac{57N^2+197N+70}{14700N^2(N+1)^2}\right\}, \tag{459}$$

$$\begin{aligned}\mathrm{Res}_3 = \frac{(-1)^N+1}{2}\Bigg\{&\frac{1}{\varepsilon}\left[\frac{1}{105N^2} - \frac{1}{105N^3} + \frac{1}{105N^4} - \frac{1}{105N^5} + \frac{1}{105N^6} - \frac{1}{105N^7}\right]\\ &- \frac{19}{4900N^2} - \frac{83}{14700N^3} + \frac{51}{4900N^4} - \frac{223}{14700N^5} + \frac{293}{14700N^6} - \frac{121}{4900N^7}\Bigg\}\\ &+ O\left(\frac{1}{N^8}\right), \end{aligned} \tag{460}$$

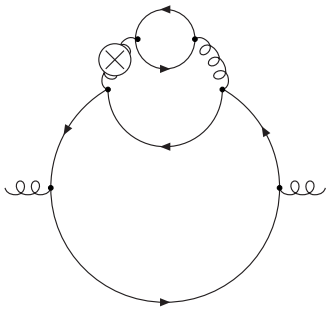

Graph 4

$$\begin{aligned}\mathrm{Res}_4 = \frac{(-1)^N+1}{2}\Bigg\{&-\frac{1}{\varepsilon}\frac{1}{5(N-1)N(N+1)^2(N+2)}\\ &- \frac{(3N^2-N+56)}{192(N+1)^2(N+2)(2N-3)(2N-1)}S_1(N)\\ &- \frac{(N-3)}{128(N+1)(2N-3)(2N-1)4^N}\binom{2N}{N}\left[\sum_{j=1}^{N}\frac{4^j}{\binom{2j}{j}j^2}S_1(j) - \sum_{j=1}^{N}\frac{4^j}{\binom{2j}{j}j^3} - 7\zeta_3\right]\\ &- \frac{P_{63}}{7200(N-1)^2N^2(N+1)^3(N+2)(2N-3)(2N-1)}\Bigg\}, \end{aligned} \tag{461}$$

$$P_{63} = 225N^7 - 325N^6 - 10398N^5 + 6806N^4 + 23517N^3 - 18721N^2 - 1824N + 2160\,, \tag{462}$$

$$\begin{aligned}\mathrm{Res}_4 = \frac{(-1)^N+1}{2}\Bigg\{&\frac{1}{\varepsilon}\left[-\frac{1}{5N^5} + \frac{3}{5N^6} - \frac{8}{5N^7}\right] + \left(-\frac{1}{10N^5} + \frac{13}{70N^6} - \frac{62}{105N^7}\right)\ln(\bar{N})\\ &+ \frac{91}{300N^5} - \frac{4027}{7350N^6} + \frac{386147}{264600N^7}\Bigg\} + O\left(\ln(\bar{N})\frac{1}{N^8}\right), \end{aligned} \tag{463}$$

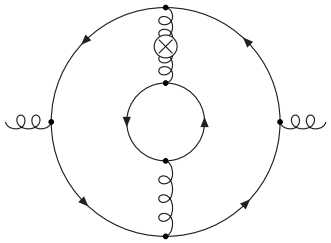

Graph 5

$$\begin{aligned}\mathrm{Res}_5 = \frac{(-1)^N+1}{2}\Bigg\{ & -\frac{1}{\varepsilon}\frac{4}{15(N-1)N(N+1)^2(N+2)} \\ & + \frac{N^2-3N+6}{64(N+1)(N+2)(2N-3)(2N-1)4^N}\binom{2N}{N}\left[\sum_{j=1}^{N}\frac{4^j}{\binom{2j}{j}j^2}S_1(j) - \sum_{j=1}^{N}\frac{4^j}{\binom{2j}{j}j^3} - 7\zeta_3\right] \\ & + \frac{(N-5)(3N+8)}{96(N+1)^2(N+2)(2N-3)(2N-1)}S_1(N) \\ & + \frac{P_{64}}{3600(N-1)^2N^2(N+1)^3(N+2)(2N-3)(2N-1)}\Bigg\}, \end{aligned} \tag{464}$$

$$P_{64} = 225N^7 - 775N^6 + 7702N^5 - 4194N^4 - 16783N^3 + 13129N^2 + 1176N - 1440\,, \tag{465}$$

$$\begin{aligned}\mathrm{Res}_5 = \frac{(-1)^N+1}{2}\Bigg\{ & \frac{1}{\varepsilon}\left[-\frac{4}{15N^5} + \frac{4}{5N^6} - \frac{32}{15N^7}\right] + \left(-\frac{2}{15N^5} + \frac{8}{35N^6} - \frac{26}{35N^7}\right)\ln(\bar{N}) \\ & + \frac{101}{225N^5} - \frac{3176}{3675N^6} + \frac{30631}{13230N^7}\Bigg\} \\ & + O\left(\ln(\bar{N})\frac{1}{N^8}\right), \end{aligned} \tag{466}$$

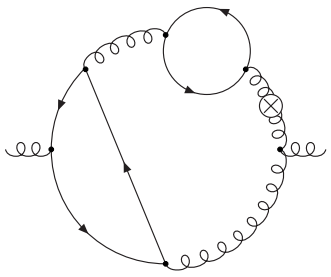

Graph 6

$$\begin{aligned}\mathrm{Res}_6 = \frac{(-1)^N+1}{2}\Bigg\{ & \frac{1}{45\varepsilon^2(N+1)} - \frac{1}{\varepsilon}\left[\frac{S_1(N)}{90(N+1)} + \frac{47N^3+20N^2-67N+40}{1800(N-1)N(N+1)^2}\right] \\ & + \frac{105N^3-175N^2+56N+96}{13440(N+1)^2(2N-3)(2N-1)4^N}\binom{2N}{N}\left[\sum_{j=1}^{N}\frac{4^jS_1(j)}{\binom{2j}{j}j^2} - \sum_{j=1}^{N}\frac{4^j}{\binom{2j}{j}j^3} - 7\zeta_3\right] \\ & + \frac{(5264N^3-2409N^2-12770N+3528)\,S_1(N)}{100800(N+1)^2(2N-3)(2N-1)} + \frac{S_1(N)^2+S_2(N)+3\zeta_2}{360(N+1)}\end{aligned}$$

$$+\frac{S_3(N)-S_{2,1}(N)+7\zeta_3}{420(N+1)}+\frac{P_{65}}{2268000(N-1)^2N^2(N+1)^3(2N-3)(2N-1)}\Bigg\}, \quad (467)$$

$$P_{65} = -257476N^8+682667N^7-144175N^6-586654N^5+615368N^4-948403N^3+592683N^2 +71190N-75600\,, \quad (468)$$

$$\begin{aligned}
\mathrm{Res}_6 = \frac{(-1)^N+1}{2}\Bigg\{&\frac{1}{\varepsilon^2}\left[\frac{1}{45N}-\frac{1}{45N^2}+\frac{1}{45N^3}-\frac{1}{45N^4}+\frac{1}{45N^5}-\frac{1}{45N^6}+\frac{1}{45N^7}\right]\\
&+\frac{1}{\varepsilon}\Bigg[\left(-\frac{1}{90N}+\frac{1}{90N^2}-\frac{1}{90N^3}+\frac{1}{90N^4}-\frac{1}{90N^5}+\frac{1}{90N^6}-\frac{1}{90N^7}\right)\ln(\bar{N})\\
&-\frac{47}{1800N}+\frac{17}{1800N^2}+\frac{7}{2700N^3}-\frac{97}{2700N^4}+\frac{169}{3600N^5}-\frac{289}{3600N^6}+\frac{20737}{226800N^7}\Bigg]\\
&+\left(\frac{1}{360N}-\frac{1}{360N^2}+\frac{1}{360N^3}-\frac{1}{360N^4}+\frac{1}{360N^5}-\frac{1}{360N^6}+\frac{1}{360N^7}\right)\ln(\bar{N})^2\\
&+\Bigg(\frac{47}{3600N}-\frac{17}{3600N^2}-\frac{7}{5400N^3}-\frac{23}{5400N^4}-\frac{67}{5600N^5}-\frac{373}{50400N^6}\\
&-\frac{140123}{4989600N^7}\Bigg)\ln(\bar{N})-\frac{64369}{2268000N}+\frac{25621}{567000N^2}-\frac{221873}{4536000N^3}\\
&+\frac{348923}{4536000N^4}-\frac{79297}{2646000N^5}+\frac{631847}{10584000N^6}+\frac{296889403}{7683984000N^7}\\
&+\left(\frac{1}{90N}-\frac{1}{90N^2}+\frac{1}{90N^3}-\frac{1}{90N^4}+\frac{1}{90N^5}-\frac{1}{90N^6}+\frac{1}{90N^7}\right)\zeta_2\\
&+\left(\frac{1}{70N}-\frac{1}{70N^2}+\frac{1}{70N^3}-\frac{1}{70N^4}+\frac{1}{70N^5}-\frac{1}{70N^6}+\frac{1}{70N^7}\right)\zeta_3\Bigg\}\\
&+O\left(\ln^2(\bar{N})\frac{1}{N^8}\right), \quad (469)
\end{aligned}$$

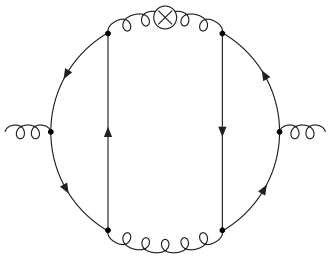

Graph 7

$$\begin{aligned}
\mathrm{Res}_7 = \frac{(-1)^N+1}{2}\Bigg\{&\frac{27N^2+49N+38}{2880(N+1)^2(N+2)4^N}\binom{2N}{N}\left[\sum_{j=1}^{N}\frac{4^j}{\binom{2j}{j}j^2}S_1(j)-\sum_{j=1}^{N}\frac{4^j}{\binom{2j}{j}j^3}-7\zeta_3\right]\\
&+\frac{1}{90(N+1)}\Big[S_3(N)-S_{2,1}(N)+7\zeta_3\Big]+\frac{1}{90N(N+1)^2(N+2)}\Big[S_2(N)-S_1(N)^2\Big]\\
&+\frac{60N^2+191N+120}{1440(N+1)^2(N+2)}S_1(N)-\frac{81N^3+194N^2+83N+60}{720N(N+1)^2(N+2)}
\end{aligned}$$

$$- \frac{1}{\varepsilon} \frac{1}{12(N+1)} \Bigg\}, \tag{470}$$

$$\begin{aligned}
\mathrm{Res}_7 = \frac{(-1)^N+1}{2} \Bigg\{ & \frac{1}{\varepsilon} \left[-\frac{1}{12N} + \frac{1}{12N^2} - \frac{1}{12N^3} + \frac{1}{12N^4} - \frac{1}{12N^5} + \frac{1}{12N^6} - \frac{1}{12N^7} \right] \\
& + \left(-\frac{1}{90N^4} + \frac{2}{45N^5} - \frac{11}{90N^6} + \frac{13}{45N^7} \right) \ln(\bar{N})^2 \\
& + \left(\frac{1}{24N} - \frac{1}{24N^2} + \frac{1}{24N^3} - \frac{91}{1800N^4} + \frac{281}{4200N^5} - \frac{3587}{37800N^6} + \frac{60377}{415800N^7} \right) \ln(\bar{N}) \\
& + \left(\frac{1}{90N^4} - \frac{2}{45N^5} + \frac{11}{90N^6} - \frac{13}{45N^7} \right) \zeta_2 \\
& + \left(\frac{1}{15N} - \frac{1}{15N^2} + \frac{1}{15N^3} - \frac{1}{15N^4} + \frac{1}{15N^5} - \frac{1}{15N^6} + \frac{1}{15N^7} \right) \zeta_3 \\
& - \frac{9}{80N} + \frac{7}{40N^2} - \frac{317}{1440N^3} + \frac{49273}{324000N^4} + \frac{4143619}{31752000N^5} - \frac{5330119}{6350400N^6} \\
& + \frac{5531737439}{2305195200N^7} \Bigg\} + O\left(\ln^2(\bar{N}) \frac{1}{N^8} \right),
\end{aligned} \tag{471}$$

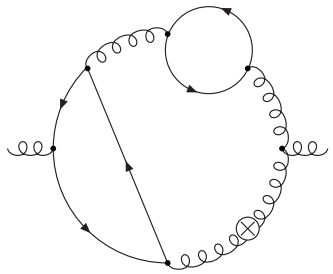

Graph 8

$$\begin{aligned}
\mathrm{Res}_8 = \frac{(-1)^N+1}{2} \Bigg\{ & \frac{1}{\varepsilon^2} \frac{N+2}{45(N+1)} + \frac{1}{\varepsilon} \left[\frac{(N-4)\left(8N^2+11N-5\right)}{1800N(N+1)^2} - \frac{N+2}{90(N+1)} S_1(N) \right] \\
& + \frac{25N^3+81N^2+72N+32}{13440(N+1)^2 4^N} \binom{2N}{N} \left[\sum_{j=1}^{N} \frac{4^j}{j^2 \binom{2j}{j}} S_1(j) - \sum_{j=1}^{N} \frac{4^j}{j^3 \binom{2j}{j}} - 7\zeta_3 \right] \\
& + \frac{151N^2+1678N+2072}{100800(N+1)^2} S_1(N) + \frac{7N^3+21N^2+14N-3}{2520N(N+1)^2} S_1(N)^2 \\
& + \frac{7N^3+21N^2+14N+3}{2520N(N+1)^2} S_2(N) + \frac{N+2}{120(N+1)} \zeta_2 \\
& + \frac{16091N^5+37499N^4+46885N^3-4133N^2-67410N-12600}{2268000N^2(N+1)^3} \Bigg\},
\end{aligned} \tag{472}$$

$$\begin{aligned}
\mathrm{Res}_8 = \frac{(-1)^N+1}{2} \Bigg\{ & \frac{1}{\varepsilon^2} \left[\frac{1}{45} + \frac{1}{45N} - \frac{1}{45N^2} + \frac{1}{45N^3} - \frac{1}{45N^4} + \frac{1}{45N^5} - \frac{1}{45N^6} + \frac{1}{45N^7} \right] \\
& + \frac{1}{\varepsilon} \Bigg[\left(-\frac{1}{90} - \frac{1}{90N} + \frac{1}{90N^2} - \frac{1}{90N^3} + \frac{1}{90N^4} - \frac{1}{90N^5} + \frac{1}{90N^6} - \frac{1}{90N^7} \right) \ln(\bar{N})
\end{aligned}$$

$$+\frac{1}{225}-\frac{47}{1800N}+\frac{13}{2700N^2}+\frac{13}{675N^3}-\frac{449}{10800N^4}+\frac{229}{3600N^5}-\frac{19457}{226800N^6}$$
$$+\frac{24517}{226800N^7}\Bigg]+\Bigg(\frac{1}{360}+\frac{1}{360N}-\frac{1}{360N^2}+\frac{1}{630N^3}-\frac{1}{2520N^4}-\frac{1}{1260N^5}+\frac{1}{504N^6}$$
$$-\frac{1}{315N^7}\Bigg)\ln(\bar{N})^2+\Bigg(-\frac{1}{450}+\frac{47}{3600N}-\frac{13}{5400N^2}-\frac{323}{52920N^3}+\frac{14117}{1058400N^4}$$
$$-\frac{79649}{3880800N^5}+\frac{506161}{18162144N^6}-\frac{4005779}{113513400N^7}\Bigg)\ln(\bar{N})$$
$$+\Bigg(\frac{1}{90}+\frac{1}{90N}-\frac{1}{90N^2}+\frac{31}{2520N^3}-\frac{17}{1260N^4}+\frac{37}{2520N^5}-\frac{1}{63N^6}+\frac{43}{2520N^7}\Bigg)\zeta_2$$
$$-\frac{7}{20250}-\frac{4717}{324000N}+\frac{8287}{324000N^2}-\frac{10467929}{222264000N^3}$$
$$+\frac{103409}{1975680N^4}-\frac{159482173}{3361743000N^5}+\frac{96644749931}{3030051024000N^6}-\frac{23737834423}{4545076536000N^7}\Bigg\}$$
$$+O\left(\ln^2(\bar{N})\frac{1}{N^8}\right). \tag{473}$$

The rather compact results contain harmonic sums of weight ≤ 3 as well as a new type of definite sum, which in the cases considered in this thesis occurs in the combination:

$$\frac{1}{4^N}\binom{2N}{N}\left[\sum_{j=1}^{N}\frac{4^j S_1(j)}{\binom{2j}{j}j^2}-\sum_{j=1}^{N}\frac{4^j}{\binom{2j}{j}j^3}-7\zeta_3\right]. \tag{474}$$

The sums are characterized by the occurrence of an inverse binomial $\binom{2j}{j}^{-1}$ in the summand, which makes them similar to a class of "inverse binomial sums" found in [321] and studied for infinite upper bounds in [322, 323]. Differences are the finite upper bound and the factor 4^j in the summand. The sums do not reduce to (cyclotomic) harmonic sums and are representants of a new class of nested sums which obey quasi-shuffle relations.

The upper bound N plays the role of the Mellin variable in the graphs under consideration, so it is worthwhile studying also the counter parts in the picture of iterated integrals. Here the inverse binomial contributions correspond to the letters, cf. [324],

$$f_{w_1}(x)=\frac{1}{\sqrt{x(1-x)}},\quad f_{w_2}(x)=\frac{1}{x\sqrt{1-x}}. \tag{475}$$

Along with the above combination of inverse binomial sums, a factor $1/(2N-3)$ occurs, which is not expected in physical calculations, since it introduces a pole at $N=3/2$ for the analytic continuations of the results. Such a pole corresponds to the property of the Wilson coefficients in x-space to diverge like $x^{-3/2}$ in the small-x region. However, it can be shown, that the diagrams are regular in the point $N=3/2$. This is done using an integral representation of the inverse binomial sums [324] in (474), which is obtained via:

$$\sum_{j=1}^{N}\frac{4^j S_1(j)}{\binom{2j}{j}j^2}-\sum_{j=1}^{N}\frac{4^j}{\binom{2j}{j}j^3}=\int_0^1 dx\,\frac{x^N-1}{x-1}\int_x^1 dy\,\frac{1}{y\sqrt{1-y}}\Big[\ln(1-y)-\ln(y)+2\ln(2)\Big]. \tag{476}$$

For $N=3/2$ this integral can be solved numerically. Furthermore, occurring harmonic sums at $N=3/2$ can be calculated via the duplication relations of harmonic sums, see [110] and references therein. Also the evanescent pole at $N=1/2$ cancels.

To obtain the asymptotic expansions, it is necessary to know the asymptotic expansion of the combination of inverse binomial sums

$$\sum_{j=1}^{N} \frac{4^j S_1(j)}{\binom{2j}{j} j^2} - \sum_{j=1}^{N} \frac{4^j}{\binom{2j}{j} j^3} - 7\zeta_3$$
$$= \sqrt{\pi}\sqrt{N}\Bigg\{\Bigg[-\frac{2}{N} + \frac{5}{12N^2} - \frac{21}{320N^3} - \frac{223}{10752N^4} + \frac{671}{49152N^5} + \frac{11635}{1441792N^6}$$
$$- \frac{1196757}{136314880N^7} - \frac{376193}{50331648N^8} + \frac{201980317}{18253611008N^9} + \frac{42437231395}{3427383902208N^{10}}$$
$$+ O(N^{-11})\Bigg] \ln(\bar{N}) - \frac{4}{N} + \frac{5}{18N^2} - \frac{263}{2400N^3} + \frac{579}{12544N^4} + \frac{10123}{1105920N^5}$$
$$- \frac{1705445}{71368704N^6} - \frac{27135463}{11164188672N^7} + \frac{197432563}{7927234560N^8} + \frac{405757489}{775778467840N^9}$$
$$- \frac{1845010417267}{418630462341l2N^{10}} + O(N^{-11})\Bigg\}. \tag{477}$$

Expansions of this kind are obtained from the integral representation 476 using HarmonicSums, and treated systematically in [324].

The graphs 1 and 3 are free of inverse binomial sums. Additionally, these are the only graphs, for which a convergent series representation could be derived, without splitting one of the Feynman parameter integrals into two parts. So there appears to be a relation between this splitting and the occurrence of the inverse binomial sums. The results for the corresponding graphs with numerator structure, and hence for the $O(\alpha_s^3 T_F^2)$ part of $A_{gg,Q}$ and $A_{gq,Q}$, are calculated in the same way, and will be given in an upcoming publication.

10 Structure Functions of Charged Current DIS to 2-Loop Order

Charged current deep-inelastic scattering, in contrast to DIS by photon exchange, depends on three structure functions named F_1, F_2, F_3. It comprises four reactions

$$\nu(\overline{\nu})p \to l(\bar{l}) + X\,, \tag{478}$$

$$l(\bar{l})p \to \nu(\overline{\nu}) + X\,, \tag{479}$$

whose scattering cross sections in the case of negligible target and lepton masses have the form

$$\frac{d\sigma^{\nu(\bar{\nu})}}{dxdy} = \frac{G_F^2 s}{4\pi}\left\{(1+(1-y)^2)F_2^{W^\pm} - y^2 F_L^{W^\pm} \pm (1-(1-y)^2)xF_3^{W^\pm}\right\}, \tag{480}$$

$$\frac{d\sigma^{e^-(e^+)}}{dxdy} = \frac{G_F^2 s}{4\pi}\left\{(1+(1-y)^2)F_2^{W^\mp} - y^2 F_L^{W^\mp} \pm (1-(1-y)^2)xF_3^{W^\mp}\right\}. \tag{481}$$

As has been defined before, $x = Q^2/yS$, $y = q.P/l.P$ are the Bjorken variables, l and P are the lepton and nucleon momentum and $S = 2l.P$. G_F denotes the Fermi constant, M_W the mass of the W-boson, and $F_i^{W^\pm}(x, Q^2)$ are the structure functions. The $\pm$ signs in (480, 481) refer to incoming neutrinos (anti-neutrinos) or charged leptons (anti-leptons), respectively. Due to the inclusive kinematics the dependence on quark masses is only implicit.

Current QCD analyses take these processes into account using x-space representations, see e.g. [56], for which Mellin convolutions with the PDFs have to be computed numerically, together with numerical solutions of the evolution equations of the PDFs, which are integro-differential equations.

In Mellin space, these calculations are more efficient, since the Mellin convolutions reduce to simple products, and the evolution equations reduce to ordinary differential equations. The map from moments back into the (physical) x-space proceeds via a single numerical contour integral in the complex plane, which can be performed very efficiently.

In the neutral current case, the light flavor Wilson coefficients [64] and anomalous dimensions [126, 127] up to third loop order are available in Mellin space. They are represented in terms of harmonic sums whose analytic continuations to complex values of N were studied in [252, 253]. A fast and precise Mellin-space implementation of the exact heavy flavor Wilson coefficients of [70–72] was given in [325].

Of the heavy quark corrections to charged current deep-inelastic scattering the 1-loop contributions in x-space are available in [73, 74].

In the first part of this Chapter, therefore Mellin space representations are derived for the 1-loop heavy flavor Wilson coefficients, together with fast and precise numerical implementations. These results have already been published in [134]. There also several Mellin space representations for PDF-shapes used in the literature were given.

Since large parts of available DIS data populate the region of large Q^2, an asymptotic description is appropriate, as it was worked out for electroproduction to two loops in [76] and to three loops in [87]. This representation is derived at first loop order from the exact representation. Furthermore, using the considerations in [76, 87], the asymptotic representation of heavy flavor Wilson coefficients up to two loops is constructed in terms of light flavor Wilson coefficients and massive OMEs, which are both available in the literature. For some of the heavy flavor Wilson coefficients the asymptotic representations were given in [86]. The complete set of representations will be given in Section 10.5, correcting errors in [86], also at $O(\alpha_s)$, which had to be clarified in relation to Ref. [74].

Note that in charged current DIS both odd- and even-N Mellin moments contribute at the same time. Since parts of the expressions contain factors $(-1)^N$, and these factors are not compatible with the uniqueness of the analytic continuation in N to complex values (see the careful discussion in [111] of the applicability of Carlson's theorem [249]), even and odd moments may lead to different functions in N. However, the corresponding graphs were identified in [81, 84], where it is obvious that they contribute only starting from two loops. Here it is important to consider the cross section combinations for $W^+ + W^-$ and $W^+ - W^-$, and perform the analytic continuation either from the even *or* from the odd moments, respectively, cf. [145, 146].

10.1 Heavy Quark Production at 1-Loop Order

The Born level contributions to the charged current deep-inelastic structure functions comprise the flavor excitation processes

$$s' = s\ |V_{cs}|^2 + d\ |V_{cd}|^2 \to c, \text{ and } \bar{s}' = \bar{s}\ |V_{cs}|^2 + \bar{d}\ |V_{cd}|^2 \to \bar{c}\,, \tag{482}$$

with V_{ij} denoting the CKM matrix elements [175, 176], and s and d the strange and down quark parton distributions. Here $\bar{d}$ and $\bar{s}$ denote the corresponding anti-quark distributions. For this transition the Bjorken variable x and the momentum fraction of the struck parton ξ are related by

$$x = \xi\lambda \leq \lambda\,, \tag{483}$$

with $\lambda = Q^2/(Q^2+m_c^2)$. So heavy quark production in neutrino scattering exhibits slow rescaling [137, 148–151]. The heavy quark structure functions and parton densities are Mellin convoluted as functions of $\xi \in [0,1]$, assuming the incoming lepton energy to be sufficiently high, cf. (36).

The $O(\alpha_s)$ charged current heavy-flavor Wilson coefficients were calculated in [73] and corrected in [74] later. Following Ref. [74] and working in the fixed flavor number scheme (FFNS), we define the parton level quantities

$$\mathcal{F}_{1,c}^{W^\pm} = F_{1,c}^{W^\pm}, \quad \mathcal{F}_{2,c}^{W^\pm} = F_{2,c}^{W^\pm}/2\xi, \quad \mathcal{F}_{3,c}^{W^\pm} = F_{3,c}^{W^\pm}/2\,. \tag{484}$$

To $O(\alpha_s)$ one obtains, after a Mellin transformation (161) over ξ,

$$\begin{aligned}\mathcal{F}_{i,c}^{W^+}(N,Q^2) &= s'(N,\mu^2) + a_s\Bigg[H_{i,q}^{W,\mathrm{NS},(1)}\left(N,\frac{m^2}{\mu^2},\frac{Q^2}{\mu^2}\right)s'(N,\mu^2)\\ &\quad + H_{i,g}^{W,(1)}\left(N,\frac{m^2}{\mu^2},\frac{Q^2}{\mu^2}\right)G(N,\mu^2)\Bigg]\,,\end{aligned} \tag{485}$$

$$\begin{aligned}\mathcal{F}_{i,c}^{W^-}(N,Q^2) &= b_i\bar{s}'(N,\mu^2) + a_s\Bigg[b_i H_{i,q}^{W,\mathrm{NS},(1)}\left(N,\frac{m^2}{\mu^2},\frac{Q^2}{\mu^2}\right)\bar{s}'(N,\mu^2)\\ &\quad + b_i H_{i,g}^{W,(1)}\left(N,\frac{m^2}{\mu^2},\frac{Q^2}{\mu^2}\right)G(N,\mu^2)\Bigg]\,.\end{aligned} \tag{486}$$

The emergence of the sign $b_1 = b_2 = -b_3 = 1$ is discussed in detail in the next Section, $a_s = \alpha_s/(4\pi)$ denotes the strong coupling constant, and G the gluon distribution. The massive

Wilson coefficients for charged current deep-inelastic scattering in Mellin space are expanded in a power series in a_s:

$$H_{i,q}^{W,\rm NS}\left(N,\frac{m^2}{\mu^2},\frac{Q^2}{\mu^2}\right) = 1+\sum_{k=1}^{\infty} a_s^k H_{i,q}^{W,{\rm NS},(k)}\left(N,\frac{m^2}{\mu^2},\frac{Q^2}{\mu^2}\right), \tag{487}$$

$$H_{i,g}^{W}\left(N,\frac{m^2}{\mu^2},\frac{Q^2}{\mu^2}\right) = \sum_{k=1}^{\infty} a_s^k H_{i,g}^{W,(k)}\left(N,\frac{m^2}{\mu^2},\frac{Q^2}{\mu^2}\right), \tag{488}$$

where the $O(a_s)$ contributions read:

$$H_{i,q}^{W,{\rm NS},(1)}\left(N,\frac{m^2}{\mu^2},\frac{Q^2}{\mu^2}\right) = \frac{1}{2}P_{qq}^{(0)}(N)\ln\left(\frac{Q^2+m_c^2}{\mu^2}\right)+h_i^q(\lambda,N),\ i=1,2,3, \tag{489}$$

$$H_{1(2),g}^{W,(1)}\left(N,\frac{m^2}{\mu^2},\frac{Q^2}{\mu^2}\right) = \frac{1}{4}P_{qg}^{(0)}(N)\ln\left(\frac{Q^2+m_c^2}{\mu^2}\right)+\frac{1}{4}\tilde{P}(\lambda,N)+h_{1,2}^g(\lambda,N), \tag{490}$$

$$H_{3,g}^{W,(1)}\left(N,\frac{m^2}{\mu^2},\frac{Q^2}{\mu^2}\right) = \frac{1}{4}P_{qg}^{(0)}(N)\ln\left(\frac{Q^2+m_c^2}{\mu^2}\right)-\frac{1}{4}\tilde{P}(\lambda,N)+h_3^g(\lambda,N). \tag{491}$$

Here the leading order splitting functions [32] are

$$P_{qq}^{(0)}(N) = 4C_F\left[\frac{3}{2}+\frac{1}{N(N+1)}-2S_1(N)\right], \tag{492}$$

$$P_{qg}^{(0)}(N) = 8T_F\frac{N^2+N+2}{N(N+1)(N+2)}, \tag{493}$$

with $T_F=1/2, C_F=(N_c^2-1)/(2N_c)$ for $SU(N_c)$ and $N_c=3$ for QCD. The function $\tilde{P}(\lambda,N)$ is given by

$$\begin{aligned}\tilde{P}(\lambda,N) &= \mathbf{M}\left[P_{qg}^{(0)}(z)\ln\frac{1-\lambda z}{(1-\lambda)z}\right](N)\\ &= 8T_F\left\{\frac{\left[\lambda^2\left(N^2+3N+2\right)-2\lambda\left(N^2+2N\right)+2N^2+2N\right]}{\lambda N(N+1)(N+2)}\left[f_2(\lambda,N)-\frac{1}{\lambda}\ln(1-\lambda)\right]\right.\\ &\left.+\frac{\lambda\left(N^2+3N+2\right)-2N^2}{\lambda N^2(N+1)(N+2)}\right\}.\end{aligned} \tag{494}$$

In the limit $\lambda\to 1$ it takes the form

$$\tilde{P}(1,N) = 8T_F\left\{\frac{N^2+N+2}{N(N+1)(N+2)}\left[\ln\left(\frac{Q^2}{m^2}\right)-S_1(N)\right]+\frac{-N^2+3N+2}{N^2(N+1)(N+2)}\right\}. \tag{495}$$

The functions $h_i^{q(g)}(\lambda,N)$ read:

$$\begin{aligned}h_1^q(\lambda,N) &= C_F\left[4f_1(\lambda,N)-\frac{\left[\lambda^2\left(N^3+N+2\right)-\lambda\left(N^3+3N^2+4N\right)+2N^2+2N\right]}{\lambda N(N+1)}f_2(\lambda,N)\right.\\ &+\frac{4\left(N^2+N-1\right)}{N(N+1)}S_1(N)-\frac{(1-\lambda)\left[\lambda\left(N^2+3N+4\right)-2N-2\right]}{\lambda^2(N+1)}\ln(1-\lambda)\\ &\left.+4S_1^2(N)-\frac{\left[\lambda(9N^3+8N^2-5N-2)-2N^2\right]}{\lambda N^2(N+1)}\right],\end{aligned} \tag{496}$$

$$
\begin{aligned}
h_2^q(\lambda,N) &= C_F\Bigg[4f_1(\lambda,N) + \frac{[4\lambda^2\left(N^2+N\right) - \lambda\left(N^3+2N^2+3N+2\right)+N^3-N^2]}{N(N+1)} f_2(\lambda,N) \\
&+\frac{4\left(N^2+N-1\right)}{N(N+1)} S_1(N) + 4S_1^2(N) + \frac{(1-\lambda)\left[4\lambda(N+1)-N^2+N\right]}{\lambda(N+1)}\ln(1-\lambda) \\
&+\frac{[4\lambda(N^2+N)-9N^3-6N^2+N+2]}{N^2(N+1)}\Bigg], \qquad (497)\\
h_3^q(\lambda,N) &= C_F\Bigg[4f_1(\lambda,N) - \frac{(N-1)\left[\lambda(N^2-N-2)-N^2\right]}{N(N+1)} f_2(\lambda,N) \\
&+\frac{4\left(N^2+N-1\right)}{N(N+1)} S_1(N) + 4S_1^2(N) - \frac{(1-\lambda)\left(N^2+N+2\right)}{\lambda(N+1)}\ln(1-\lambda) \\
&-\frac{(3N+2)\left(3N^2-1\right)}{N^2(N+1)}\Bigg], \qquad (498)\\
h_1^g(\lambda,N) &= -4T_F\Bigg[\frac{[\lambda^2(2N^3+3N^2+7N+2)-\lambda(2N^3+4N^2+8N)+2N^2+2N]}{2\lambda N(N+1)(N+2)} f_2(\lambda,N) \\
&+\frac{(N^2+N+2)}{N(N+1)(N+2)} S_1(N) + \frac{(1-\lambda)\left[\lambda(N^2+N+3)-N-1\right]}{\lambda^2(N+1)(N+2)}\ln(1-\lambda) \\
&+\frac{\lambda(2N^3+N^2+N-2)-2N^2}{2\lambda N^2(N+1)(N+2)}\Bigg], \qquad (499)\\
h_2^g(\lambda,N) &= -4T_F\Bigg\{\Bigg[\frac{[\lambda^3(2N^3-6N^2+4N)+\lambda^2(-2N^3+7N^2-N+2)-\lambda(2N^2+4N)]}{2\lambda N(N+1)(N+2)} \\
&+\frac{1}{\lambda(N+2)}\Bigg] f_2(\lambda,N) + \frac{(1-\lambda)\left[\lambda^2(N^2-3N+2)+\lambda-N-1\right]}{\lambda^2(N+1)(N+2)}\ln(1-\lambda) \\
&+\frac{(N^2+N+2)}{N(N+1)(N+2)} S_1(N) + \frac{\lambda^2(2N^3-6N^2+4N)-\lambda(N^2+3N)-2\lambda-2N^2}{2\lambda N^2(N+1)(N+2)}\Bigg\}, \qquad (500)\\
h_3^g(\lambda,N) &= -4T_F\Bigg[\frac{(\lambda^2(N^2-N+2)+\lambda(2N^2+4N)-2N^2-2N)}{2\lambda N(N+1)(N+2)} f_2(\lambda,N) \\
&+\frac{(N^2+N+2)}{N(N+1)(N+2)} S_1(N) - \ln(1-\lambda)\frac{(1-\lambda)(\lambda-N-1)}{\lambda^2(N+1)(N+2)} \\
&-\frac{\lambda(N^2+3N+2)-2N^2}{2\lambda N^2(N+1)(N+2)}\Bigg]. \qquad (501)
\end{aligned}
$$

Here single harmonic sums $S_k(N)$ occur [104, 105] which are analytically continued using their relations to the polygamma functions, cf. [105]:

$$
S_k(N) = \frac{(-1)^{k+1}}{(k-1)!}\psi^{(k-1)}(N+1) + \zeta_k, k \in \mathbb{N}\backslash\{0\}\,. \qquad (502)
$$

The functions $f_{1,2}(\lambda,N)$ are defined by

$$
f_1(\lambda,N) = \int_0^1 dx\, \frac{x^N-1}{x-1}\ln(1-\lambda x)\,, \qquad (503)
$$

$$f_2(\lambda, N) \;=\; \int_0^1 dx\, \frac{x^N - 1}{1-\lambda x}\,. \tag{504}$$

The expression $H_{2,g}^{W,(1)}$ for $Q^2 = \mu^2$ can also be cast into the form

$$\begin{aligned} H_2^{(1),g}(\lambda, N) = 4T_F \Bigg\{ & \frac{4 - 2N(N-3) - N(N^2+N+2)\{2S_1(N) + \ln[\lambda(1-\lambda)]\}}{2N^2(N+1)(N+2)} \\ & + \frac{8 - 18(1-\lambda) + 12(1-\lambda)^2}{(N+1)(N+2)} + \frac{(1-\lambda)\,{}_2F_1(1, N, N+1; \lambda)}{N} - \frac{1}{N} \\ & + 6\lambda(1-\lambda)\left[\frac{{}_2F_1(1, N+1, N+2; \lambda)}{(N+1)^2} - 2\frac{{}_2F_1(1, N+1, N+2; \lambda) - 1}{(N+1)(N+2)}\right]\Bigg\}, \end{aligned} \tag{505}$$

which corrects Eq. (70) in Ref. [61]. Here, ${}_2F_1$ denotes the Gauß hypergeometric function (185), which appears in the form

$${}_2F_1(\eta, N+\alpha+1, N+\alpha+\beta+2, \xi) = \frac{1}{B(N+\alpha+1, \beta+1)} \int_0^1 dz\, z^{N+\alpha}(1-z)^\beta (1-\xi z)^{-\eta}\,. \tag{506}$$

$k\backslash\lambda$	0.1	0.5	0.9
0	+9.99999999999999999	+1.99999999999954543	+1.111110872017648708
1	+0.821423460E-22	+0.1975123084486687E-10	+0.000098847800695649
2	−0.050000000000000000	−0.250000001423445310	−0.456776649795426910
3	−0.001666666666666666	−0.041666626227537189	+0.048001787041481484
4	−0.000083333333333336	−0.010417267014473893	−2.639926313632337045
5	−0.499999999997477753E-05	−0.003119649969153064	+21.74650303005800508
6	−0.333333333484935779E-06	−0.001072643292472726	−119.2024353694977123
7	−0.238095231857886535E-07	−0.000249816388951957	+442.8630812379568060
8	−0.178571609458723466E-08	−0.000477192766818736	−1147.492168730891145
9	−0.138885135219891312E-09	+0.000607438245655042	+2095.900562359927839
10	−0.111169685797600287E-10	−0.000939620170907808	−2688.830619105423874
11	−0.903191209860331475E-12	+0.000876266420390668	+2371.811788035594662
12	−0.800460593905461726E-13	−0.000571683728308967	−1370.383159208738358
13	−0.439528295242656941E-14	+0.000219008887781703	+467.1985539745224063
14	−0.107994848505839019E-14	−0.000041032031472769	−71.30766062862566906

Table 5: The expansion coefficients a_k, Eq. (513) for special values of λ.

Many of the contributing functions have known Mellin transforms given before in [104, 105]. Their analytic continuations to complex values of N are known, cf. [106, 107, 252, 253]. The

new functions (503, 504) are solely related to integrals of the kind (506) for $N \in \mathbb{N}$. They obey the following recursion relations

$$f_1(\lambda, N+1) = f_1(\lambda, N) + \frac{\lambda}{N+1} f_2(\lambda, N+1)\,, \tag{507}$$

$$f_2(\lambda, N+1) = \frac{1}{\lambda}\left[f_2(\lambda, N) - \frac{1}{N+1} - \frac{1-\lambda}{\lambda}\ln(1-\lambda)\right]. \tag{508}$$

The singularity structure of $f_{1,2}(\lambda, N)$ for $N \in \mathbb{C}$ can be seen using the representation

$$f_1(\lambda, N) = -\sum_{l=1}^{\infty} \frac{\lambda^l}{l} \left[\psi(l+N+1) - \psi(l+1)\right], \tag{509}$$

$$f_2(\lambda, N) = -N \sum_{l=0}^{\infty} \frac{\lambda^l}{(N+l+1)(l+1)}\,. \tag{510}$$

Both functions possess poles in N at negative integers.

For $f_1(\lambda, N)$ one may derive a sufficiently precise representation using a Minimax approximation, see e.g. [325–329]. The function f_1 can be written as

$$f_1(\lambda, N) = -\left\{\frac{1}{\lambda} - N\mathcal{E}(\lambda, 1) + \sum_{l=0}^{14} a_l \ \{N - 1 - l[S_1(N+l-1) - S_1(l)]\}\right\}, \tag{511}$$

$$\mathcal{E}(\lambda, x) \equiv \frac{1}{\lambda}(1-\lambda x)(1 - \ln(1-\lambda x))\,. \tag{512}$$

The function $\mathcal{E}$ under the integral is approximated by the adaptive polynomial, cf. Table 1,

$$\mathcal{E}(\lambda, x) = \sum_{k=0}^{14} a_k(\lambda)\ x^k\,. \tag{513}$$

Knowing the difference equations (507, 508) one may shift $f_{1,2}$ parallel to the real axis. Usually one attempts to shift towards the asymptotic region and applies an analytic representation there, cf. [252, 253]. However, one may also turn the view, and rather consider $f_{1,2}(\lambda, N)$ inside the unit circle, to obtain the following representation:

$$\begin{aligned} f_1(\lambda, N) &= -\frac{1}{2}\left[S_1^2(N) + S_2(N)\right] \\ &\quad - \sum_{k=1}^{\infty} (-N)^k \left\{\mathrm{Li}_{k+2}(\lambda) - \zeta_{k+2} + H_{1,k+1}(\lambda) - H_{1,k+1}(1)\right\} \end{aligned} \tag{514}$$

$$f_2(\lambda, N) = \frac{1}{\lambda}\left\{\sum_{k=1}^{\infty} (-N)^k \left[\mathrm{Li}_{k+1}(\lambda) - 1\right] - \frac{N}{N+1}\right\}, \tag{515}$$

for $|N| < 1$. Here, $\mathrm{Li}_k(x)$ denotes the classical polylogarithm [293], $H_{\vec{a}}(x)$ a harmonic polylogarithm [122],

$$H_{1,k}(x) := \int_0^x dz\ \frac{\mathrm{Li}_k(z) - \zeta_k}{1-z}\,, \tag{516}$$

and ζ_k, $k \geq 2$, Riemann's ζ-function at an integer argument. In the limit $\lambda \to 1$ one obtains

$$f_1(1, N) = -\frac{1}{2}\left[S_1^2(N) + S_2(N)\right], \tag{517}$$

$$f_2(1,N) \;=\; -S_1(N)\,. \tag{518}$$

The series representations (514, 515) are fast converging and deliver even more precise results than using (511, 513). The contour integral is performed along the line $(-\infty,-a)$, $(c,-a)$, (c,a), $(-\infty,a)$, with $a=0.5$. The choice of the parameter c depends also on the rightmost singularity of the non-perturbative distribution $f(x)$ and was chosen with $c=1.5$ in the figures given below. The inverse Mellin transform is obtained by, cf. [287, 330],

$$f(x) = \frac{1}{\pi}\left\{-\int_{-\infty}^{c} \mathsf{Im}\left[x^{-s-ia}\mathbf{M}[f](s+ia)\right] ds + \int_0^a \mathsf{Im}\left[ix^{-is-c}\mathbf{M}[f](is+c)\right] ds\right\}. \tag{519}$$

We extended the integral to 1000 units parallel to the real axis. The recursion relations (507, 508) together with the series (514, 515) allow to compute $f_{1,2}(\lambda,N)$ along the integration contour. Here usually the first 30 terms in the infinite sums (514, 515) provide sufficient accuracy.

10.2 The Heavy Flavor Wilson Coefficients in the Asymptotic Region

In many applications the value of λ becomes close to one. Within this kinematic region $Q^2 \gg m_c^2$, the Wilson coefficients take a simpler form, and the functions needed to express them are only harmonic sums. This has been shown up to 2-loop order in case of neutral current deep-inelastic scattering in [76, 78–80, 331]. To 3-loop order this was shown to be true in all available cases [88, 131], however, the scalar prototypes in Chapters 8 and 9 seem to imply larger classes of basic functions. At $O(\alpha_s)$ one obtains the following relations:

$$H_{i,q}^{W,\mathrm{NS},(1)}\left(N,\frac{Q^2}{m^2},\frac{m^2}{\mu^2}\right) \;=\; C_{i,q}^{W,\mathrm{NS},(1)}\left(N,\frac{Q^2}{\mu^2}\right),\; i=1,2,3\,, \tag{520}$$

$$H_{i,g}^{W,(1)}\left(N,\frac{Q^2}{m^2},\frac{m^2}{\mu^2}\right) \;=\; \frac{1}{2}A_{Qg}^{(1)}\left(N,\frac{m^2}{\mu^2}\right) + C_{i,g}^{W,\mathrm{NS},(1)}\left(N,\frac{Q^2}{\mu^2}\right),\; i=1,2\,, \tag{521}$$

$$H_{3,g}^{W,(1)}\left(N,\frac{Q^2}{m^2},\frac{m^2}{\mu^2}\right) \;=\; -\frac{1}{2}A_{Qg}^{(1)}\left(N,\frac{m^2}{\mu^2}\right). \tag{522}$$

with

$$A_{Qg}^{(1)}\left(N,\frac{m^2}{\mu^2}\right) = -\ln\left(\frac{m^2}{\mu^2}\right)\frac{P_{qg}(N)}{2}\,, \tag{523}$$

and $P_{qg}^{(0)}(N)$ given in (493). Here, $A_{lm}^{(1)}$ denote the 1–loop massive operator matrix elements from previous Chapters and $C_{i,g(q)}^{W,(\mathrm{NS}),(1)}$ are the massless 1-loop Wilson coefficients, [199]. Eqs. (520, 521) are derived by expanding (496–501) for $\lambda \to 1$. At $O(\alpha_s)$ there is no pure-singlet contribution. It turns out, that $A_{qq,Q}^{\mathrm{NS},(1)}$ vanishes as expected, because closed massive fermion loop contributions can occur at $O(\alpha_s^2)$ earliest. In the charged current case, the interaction transmutes the massless s'-quark into the massive c-quark. The massless quark-loop contribution to $A_{Qg}^{(1)}$ occurs with a combinatorial factor $1/2$ compared to the neutral current case. The "missing" terms vanish, because the corresponding diagrams are scaleless.

The massless Wilson coefficients are also expanded into a power series in a_s:

$$C_{i,j}\left(N,\frac{Q^2}{\mu^2}\right) = \delta_{jq} + \sum_{k=1}^{\infty} a_s^k C_{i,j}^{(k)}\left(N,\frac{Q^2}{\mu^2}\right), \tag{524}$$

where the leading QCD contributions are

$$C_{i,q}^{W,\rm NS,(1)}\left(N,\frac{Q^2}{\mu^2}\right) = \frac{1}{2}P_{qq}^{(0)}(N)\ln\left(\frac{Q^2}{\mu^2}\right) + c_{i,q}^{(1)}(N)\,, \tag{525}$$

$$C_{i,g}^{W,(1)}\left(N,\frac{Q^2}{\mu^2}\right) = \frac{1}{2}P_{qg}^{(0)}(N)\ln\left(\frac{Q^2}{\mu^2}\right) + c_{i,g}^{(1)}(N)\,, \tag{526}$$

and the massless Wilson coefficients are given by the Mellin transforms of the expressions in [199], yielding:

$$c_{1,q}^{(1)}(N) = c_{2,q}^{(1)}(N) - 4C_F\frac{1}{N+1}\,, \tag{527}$$

$$c_{2,q}^{(1)}(N) = C_F\left[\frac{(3N^2+3N-2)}{N(N+1)}S_1(N) + 2S_1^2(N) - 2S_2(N) - \frac{(9N^3+2N^2-5N-2)}{N^2(N+1)}\right], \tag{528}$$

$$c_{3,q}^{(1)}(N) = c_{2,q}^{(1)}(N) - C_F\frac{2(2N+1)}{N(N+1)}\,, \tag{529}$$

$$c_{1,g}^{(1)}(N) = c_{2,g}^{(1)}(N) - T_F\frac{16}{(N+1)(N+2)}\,, \tag{530}$$

$$c_{2,g}^{(1)}(N) = T_F\left[-\frac{4\,(N^2+N+2)}{N(N+1)(N+2)}S_1(N) - \frac{4(N^3-4N^2-N-2)}{N^2(N+1)(N+2)}\right], \tag{531}$$

$$c_{3,g}^{(1)}(N) = 0\,. \tag{532}$$

The form of Eqs. (520, 521) were predicted in [86] using mass factorization as described in Chapter 4, cf. [76]. There only expressions for $H_{i,g}^{W,(1)}$ were given. Eq. (521) confirms the corresponding prediction, while (522) differs in the sign from Eq. (A1.17) of [86]. In order to decide, which of the representations is correct, an independent recalculation of the gluonic Wilson coefficient was performed. It is presented in Section 10.4, where also an asymptotic calculation following the ideas of [34] is presented. This allows for a calculation of the logarithmic parts of Eq. (522). An a priori construction of the asymptotic representation is given in Section 10.5. The gluonic contribution in charged current heavy quark production has been calculated before, using two finite quark masses for e^-p scattering in Refs. [214–217] and both for e^-N and e^+N scattering in [214]. For calculations in case of neutrino-nucleon scattering see [332].

10.3 Numerical Results

We compare the Mellin space representation given in Section 10.1 with the representation in x-space of Ref. [74], using the reference distribution

$$xf(x) = x^{-0.1}(1-x)^5 \tag{533}$$

for both the quark and gluon densities, and determine the relative accuracies $|\delta F_{i,c}^{W^+}|/F_{i,c}^{W^+}$ for different values of Q^2 in the massive Wilson coefficients choosing $m_c = 1.5$ GeV and the corresponding values of $\alpha_s^{\rm NLO}(Q^2)$ [277]. If one employs the Minimax representation relative accuracies of better than 3×10^{-6} are reached below $x = 0.5$. For $x > 0.5$ the relative accuracy becomes worse. In this region, however, the charm contribution is very much suppressed, as shown in Figures 8 and 9. Using the representations (514, 515) the relative accuracy is improved

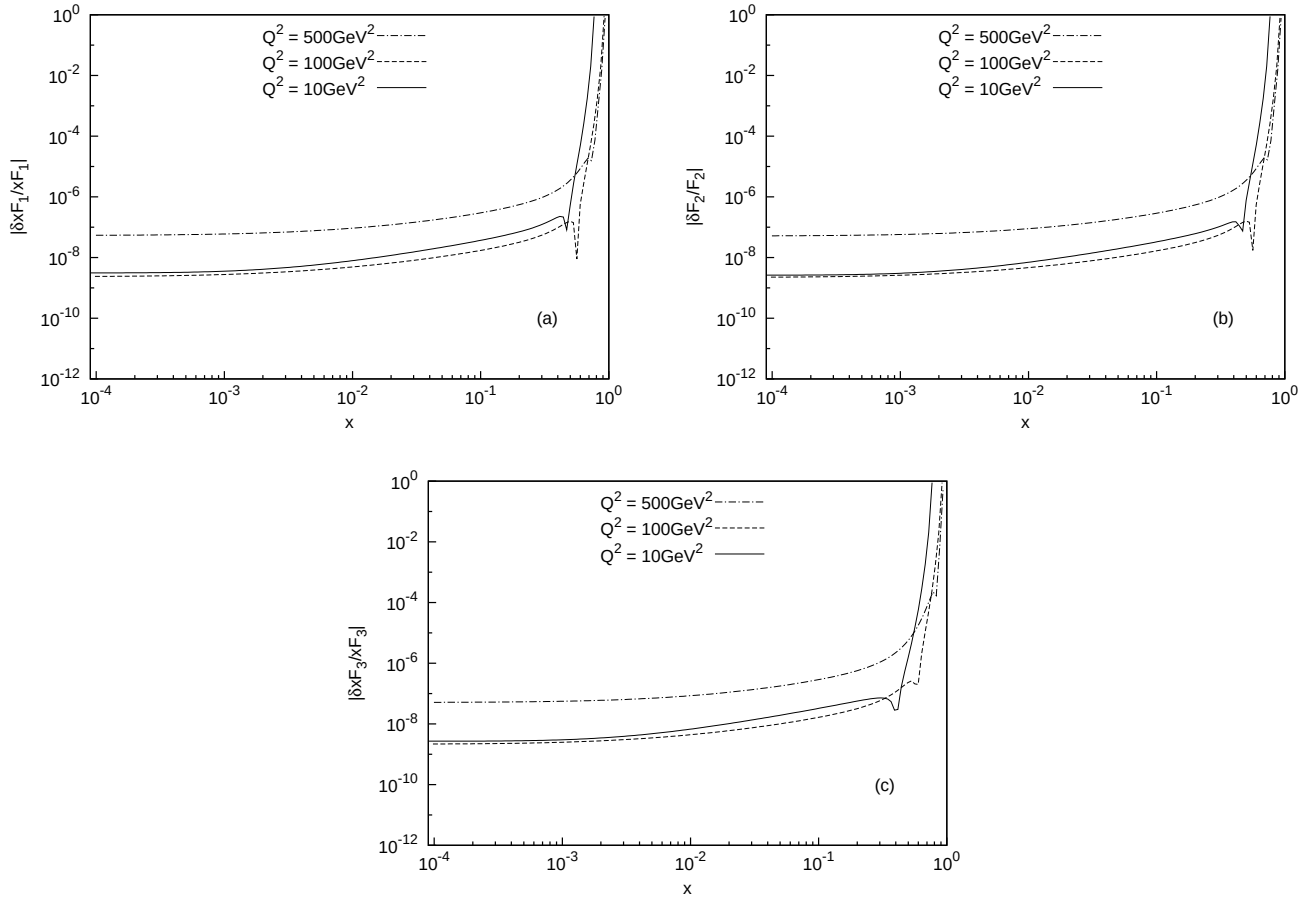

Figure 7: Relative accuracy of the charged current structure functions $F_{i,c}^{W^+}$ to $O(\alpha_s)$ at $Q^2 = 10, 100, 500$ GeV^2, comparing the implementation in Mellin- and z-space. Here both for $f_{1,2}(\lambda, N)$ the analytic representation (514, 515) and their recurrences were used; from [134].

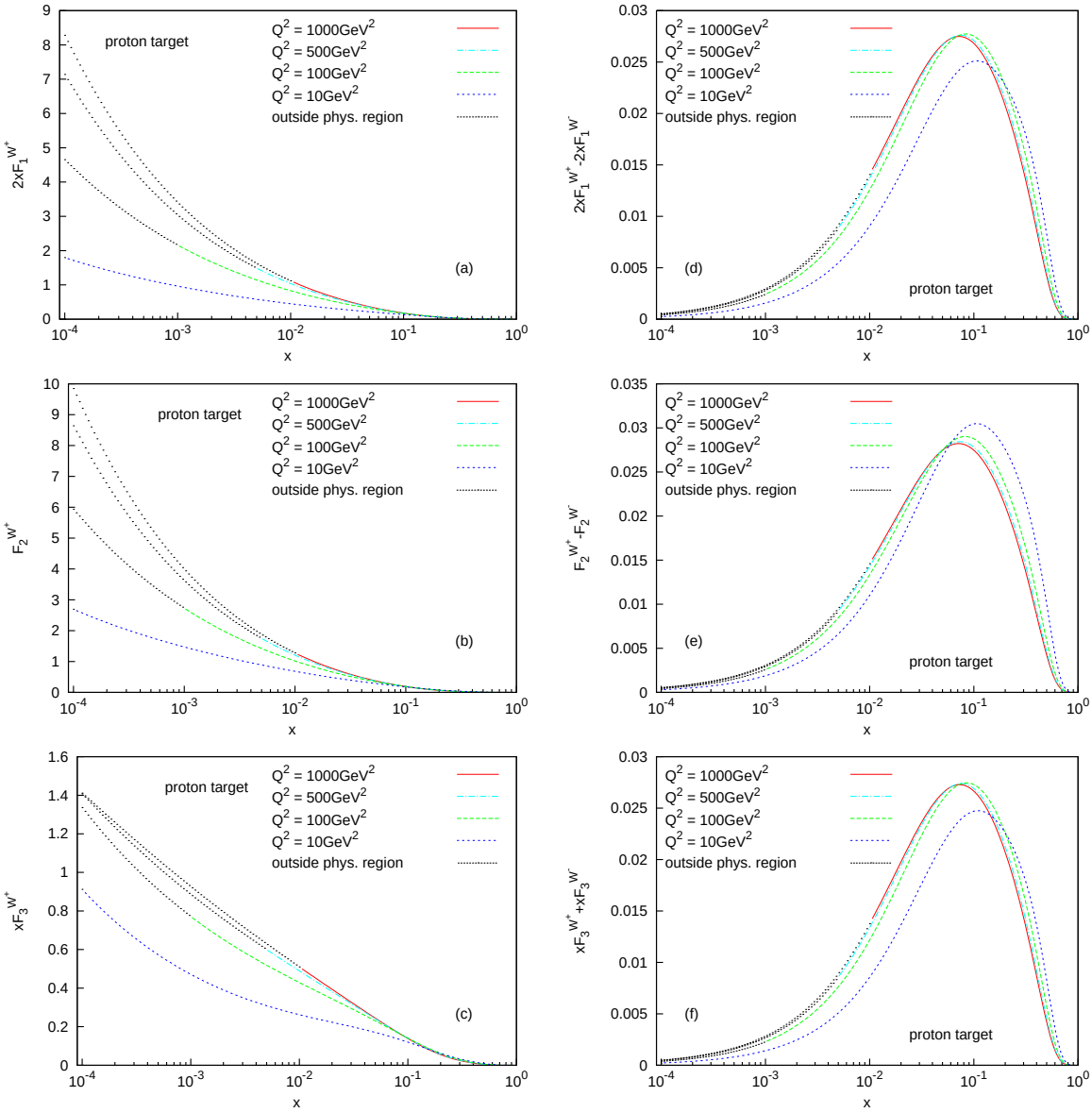

Figure 8: The charged current structure functions for charm production for different values of Q^2, using the ABKM09 parton parameterizations [277]. We indicated the kinematic range being accessible at HERA. (a)–(c) : the structure functions for W^+ exchange. (d)–(f) difference between the structure functions for W^+ and W^- exchange; from [134].

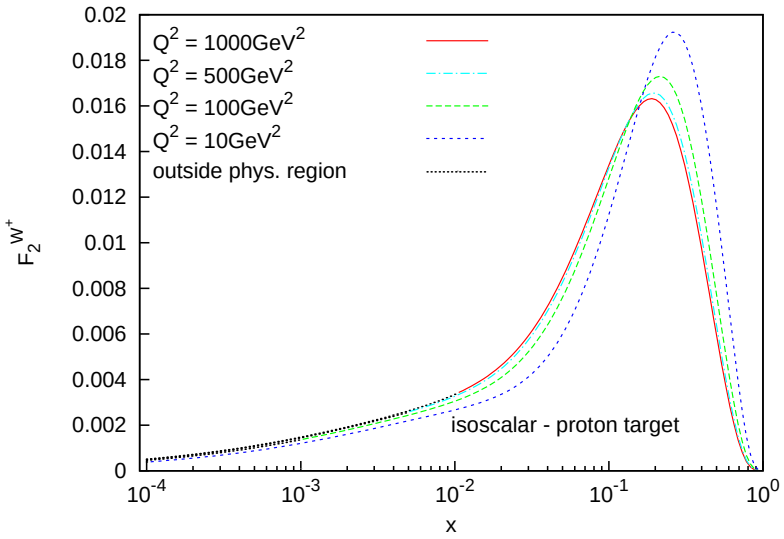

Figure 9: The difference of the structure function $F_{2,c}^{W^+}$ for an isoscalar and a proton target using the ABKM09 parton distribution functions [277] depending on x and Q^2, from [134].

and amounts to 5×10^{-8} or better at $x = 10^{-4}$ growing to $\sim 10^{-6}$ for $x \sim 0.4$, cf. Figure 7,a–c. Beyond this value the relative accuracy becomes worse, but also the sea quark distributions are very small in this region. For comparison we note that in [61] only accuracies of 0.015 to 0.002 were obtained.

In Figure 8, the charged current heavy flavor structure functions $2xF_{1,c}^{W^\pm}$, $F_{2,c}^{W^\pm}$, and $xF_{3,c}^{W^\pm}$ for deep-inelastic ep-scattering in the kinematic range of HERA are shown. Figures 8a–c show the structure functions for W^+ exchange, and Figs. 8d–f show structure function differences between W^+ and W^- scattering. In both cases $m_c = 1.5$ GeV, and the ABKM09 NLO parton distribution functions in the fixed flavor number scheme are used [277].

Results are shown for $Q^2 = 10, 100, 500$ and 1000 GeV^2, ($\alpha_s^{\rm NLO} = 0.2399, 0.1666, 0.1379, 0.1283$). The dominant contributions are those due to $W^\pm$–gluon fusion, which is the same for W^+ and W^- exchange. All structure functions rise towards small values of x. The difference between the W^+ and W^--exchange structure functions, on the other hand, receives its main contributions in the valence region with smaller scaling violations than in case of $W^\pm$–gluon fusion.

In Figure 9 the difference of the structure function $F_2^{W^+}$ for an isoscalar and proton target is shown, which is also clearly sensitive to the valence part of the PDFs. With the present precise Mellin space implementations at hand one may perform QCD fits including the charged current heavy flavor contributions in an efficient way.

10.4 Calculation of $H_g^{(1)}$ and the Leading Logarithmic Part of $H_q^{\rm PS,(2)}$

Since the sign in front of the OME in the gluonic heavy flavor Wilson coefficient of Eq. (522) contradicts the asymptotic representation given in Eq. (A.17) of [86], a recalculation of the full gluonic $O(\alpha_s)$ correction was performed which will be presented in the following.

As the minus sign was confirmed in this careful analysis, further changes in signs in the relations (A.18) and (A.19) of [86] are anticipated. The reasoning follows the idea of calculating leading logarithms in the Altarelli-Parisi picture of scaling violations [34], and will be presented later in this Section.

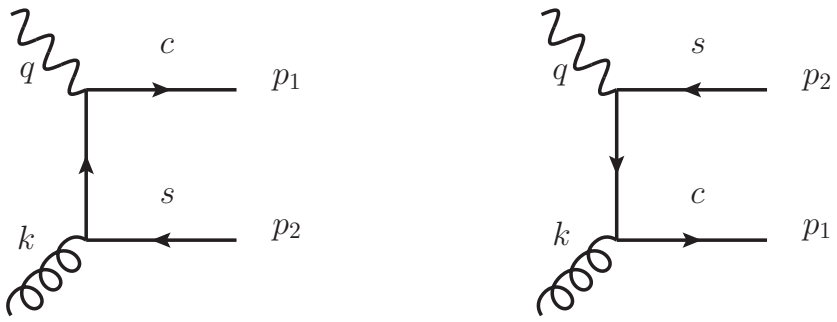

Figure 10: Graphs contributing to $H_g^{(2)}$

For the calculation of the heavy flavor Wilson coefficient H_g one has to calculate the diagrams in Figure 10 with the matrix element

$$\begin{aligned} M_a^\mu = & \bar{u}(p_1) i\gamma^\mu (1-\gamma_5) \frac{i(\not{p}_1 - \not{q})}{(p_1-q)^2} \gamma^\rho i g_s t^a v(p_2) \varepsilon_\rho^a(k) \\ & + \bar{u}(p_1) \gamma^\rho i g_s t^a \frac{i(\not{p}_1 - \not{k} + m)}{(p_1-k)^2 - m^2} i\gamma^\mu (1-\gamma_5) v(p_2) \varepsilon_\rho^a(k) \end{aligned} \tag{534}$$

contributing to the hadronic tensor. For the implementation of γ_5, the prescription of [232] was used, which amounts to the replacement

$$\gamma_\mu \gamma_5 = \frac{i}{6} \varepsilon_{\mu\nu\rho\sigma} \gamma_\nu \gamma_\rho \gamma_\sigma \,, \tag{535}$$

in the matrix element, where products of Levi-Civita symbols are evaluated by the determinant in (115) and Lorentz contractions are performed in D dimensions. Since $O(\alpha_s)$ is the leading order of the gluon channel, no finite renormalization is needed. The Lorentz-structure of the squared matrix element is projected onto the (unrenormalized) partonic versions of the structure functions $\hat{\mathcal{F}}_i$, $i = 1, 2, 3$ via the projectors:

$$\begin{aligned} \hat{P}_1 &= \frac{1}{2+\varepsilon} \frac{x}{Q^2} \left(4x P_\mu P_\nu + 2 P_\mu q_\nu + 2 P_\nu q_\mu - \frac{Q^2}{x} g_{\mu\nu} \right) , \\ \hat{P}_2 &= 2x \left(\frac{q_\mu q_\nu}{Q^2} - \frac{g_{\mu\nu}}{2+\varepsilon} \right) + 4 \frac{x^2}{Q^2} \frac{3+\varepsilon}{2+\varepsilon} \left(2x P_\mu P_\nu + P_\mu q_\nu + P_\nu q_\mu \right) , \\ \hat{P}_3 &= -\frac{4x}{Q^2} \frac{1}{(1+\varepsilon)(2+\varepsilon)} i \varepsilon_{\mu\nu\rho\sigma} P^\rho q^\sigma \,. \end{aligned} \tag{536}$$

The two particle phase space leads to one dimensional integrals which, after a partial fraction decomposition, can be solved in terms of ${}_2F_1$ functions, e.g.

$$\int_0^1 dy\, y^{\frac{\varepsilon}{2}} (1-y)^{\frac{\varepsilon}{2}} \frac{1}{(p_1-k)^2 - m^2} = -\frac{1}{s+Q^2} B\left(1+\frac{\varepsilon}{2}, 1+\frac{\varepsilon}{2}\right) {}_2F_1 \left[\begin{matrix} 1, 1+\frac{\varepsilon}{2} \\ 2+\varepsilon \end{matrix} ; \frac{s-m^2}{s} \right] , \tag{537}$$

with

$$y = \frac{1}{2}[1 + \cos \sphericalangle(p_1, q)], \quad (p_1-k)^2 - m^2 = -(s+Q^2) \left(1 - \frac{s-m^2}{s}(1-y) \right) . \tag{538}$$

This particular example is the source for the mass logarithms:

$$ {}_2F_1\left[\begin{array}{c} 1, 1+\frac{\varepsilon}{2} \\ 2+\varepsilon \end{array}; \frac{s-m^2}{s}\right] = -\frac{s}{s-m^2}\ln\left(\frac{m^2}{s}\right) + O(\varepsilon)\,, \tag{539} $$

and thus contributes to the OME in the asymptotic expansions (521, 522).

The t-channel exchange of the light s-quark in the first diagram of Fig. 10 introduces a collinear singularity, which has to be removed via mass factorization as described in Eq. (2.38) of [83]. In the present case it proceeds via:

$$ \hat{\mathcal{F}}_i = \Gamma_{qg}^{(1)} + H_{i,g}^{(1)}\,, \tag{540} $$

with the $\overline{\rm MS}$ transition function

$$ \Gamma_{qg}^{(1)} = S_\varepsilon \frac{1}{2\varepsilon} P_{qg}^{(0)}, \quad P_{qg}^{(0)}(z) = 8T_F[z^2 + (1-z)^2]\,. \tag{541} $$

In contrast to the electromagnetic case, the factor $2n_f$ in (2.38) of [83] is omitted, since the above calculation is performed for only one incoming light flavor, and only for one of the two graphs in Fig. 10 the quark propagator is massless and thus develops a collinear singularity. The results of this calculation agree with the results in [73, 74, 333].

In order to gain further confidence in the emergence of a minus sign in the asymptotic representation (522), as well as to understand how this observation relates to the pure singlet Wilson coefficients at 2-loop order, the calculation of leading logarithmic contributions is performed using the method also applied by Altarelli and Parisi [34], cf. also [334].

A Sudakov parameterization [335] is introduced for the t-channel momentum in the diagram in Fig. 10(a):

$$ k - p_2 = \alpha k + \beta q' + k_\perp\,, \tag{542} $$

denoting the gluon momentum by k, and the photon momentum by q. Furthermore, the vectors $k_\perp$ and q' are defined via

$$ q' = q + xk, \quad q'.k_\perp = k.k_\perp = 0\,. \tag{543} $$

This leads to the final state momenta

$$ p_1 = (\alpha - x)k + (\beta+1)q' + k_\perp\,, \tag{544} $$

$$ p_2 = (1-\alpha)k - \beta q' - k_\perp\,, \tag{545} $$

and the Mandelstam variables

$$ \begin{aligned} s &:= (q+k)^2 = 2k.q - Q^2\,, \\ t &:= (p_1 - q)^2\,, \\ u &:= (p_1 - k)^2 = -t + m^2 - Q^2 - s\,. \end{aligned} \tag{546} $$

With the approximation $q'^2 \approx k^2 \approx 0$ and $p.q' \approx p.q$, the phase space integral then takes the form

$$ \int dp_1\, dp_2\, \delta(p_1^2 - m^2)\delta(p_2^2) = \int d\beta\, d\alpha\, dk_\perp^2\, \frac{\pi}{2k.q(1-\alpha)} \delta\left(\beta - \frac{k_\perp^2}{2k.q(1-\alpha)}\right) $$

$$\times \delta\left(\alpha - x + \frac{1-x}{1-\alpha}\frac{k_\perp^2}{2k.q} - \frac{m^2}{2k.q}\right) . \tag{547}$$

Using the implication from the δ-distributions one finds

$$k_\perp^2 = (1-\alpha)t\,, \tag{548}$$

and thus defines the positive variable

$$r^2 := -t\,. \tag{549}$$

The physical region[7] is determined from the conditions

$$0 \le \cos\sphericalangle(q,p_1) \le 1 \text{ and } 0 \le \cos\sphericalangle(q,p_2) \le 1 \tag{550}$$

on the angles in the target system of coordinates. As a result one finds

$$2k^2\frac{s-m^2}{s+Q^2} \le r^2 \le \frac{(s-m^2)(s+Q^2)}{s}\,. \tag{551}$$

There are two integrals leading to logarithmic values:

$$\begin{aligned}\int dr^2 \frac{1}{(p_1-q)^2} &= -\int dr^2 \frac{1}{r^2} \\ &= \ln\left(\frac{2sk^2}{(s+Q^2)^2}\right) \approx \ln\left(\frac{k^2}{s}\right) , \end{aligned} \tag{552}$$

$$\begin{aligned}\int dr^2 \frac{1}{(p_1-k)^2-m^2} &= \int dr^2 \frac{1}{r^2-s-Q^2} \\ &= -\ln\left(\frac{s}{m^2} - 2\frac{k^2}{m^2}\frac{s}{s+Q^2}\frac{(s-m^2)}{s+Q^2}\right) \\ &\approx \ln\left(\frac{m^2}{s}\right) . \end{aligned} \tag{553}$$

Since the incoming gluon in massless, i.e. $k^2 = 0$, the first logarithm represents a collinear singularity, which was earlier regulated in $D = 4+\varepsilon$ dimensions and removed via mass factorization in Eq. (540). The second logarithm indeed constitutes the leading mass dependence of the process. Picking out this logarithmic part, one finds

$$H_{g,1}^{W,(1),\mathrm{LL}} = H_{g,2}^{W,(1),\mathrm{LL}} = -\frac{1}{2}P_{qg}^{(0)}(N)\ln\left(\frac{m^2}{Q^2}\right) , \tag{554}$$

$$H_{g,3}^{W,(1),\mathrm{LL}} = \frac{1}{2}P_{qg}^{(0)}(N)\ln\left(\frac{m^2}{Q^2}\right) . \tag{555}$$

The splitting functions derive from the fermion traces after applying the above approximations and canceling against denominators.

In order to obtain the 2-loop pure singlet contribution in leading logarithmic approximation, one has to include another ladder rung formed by a light quark line, as depicted in Fig. 11.

Then the Sudakov parameters are introduced as above:

$$k_1 = \alpha_1 k + \beta_1 q' + k_{\perp 1}\,, \tag{556}$$

[7]For a collection of kinematic formulae used here see [336].

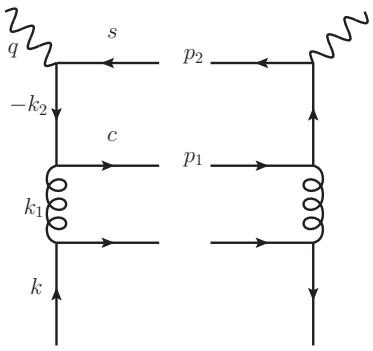

Figure 11: The leading logarithmic 2-loop PS-contribution $H_q^{\mathsf{PS},(2),\mathsf{LL}}$ can be built from the leading logarithmic 1-loop gluonic contribution by adding a splitting of a quark into a gluon.

$$k_2 = \alpha_2 k + \beta_2 q' + k_{\perp 2}\,. \tag{557}$$

The three-particle phase space can be treated similarly as before, assuming a strict hierarchy $k^2 \ll |k_{\perp 1}^2| \ll |k_{\perp 2}^2| \ll Q^2$. The δ-distributions introduced by the phase space integral then take the forms:

$$\begin{aligned}
\delta((k-k_1)^2) &= \frac{1}{2k.q(1-\alpha_1)}\delta\left(\beta_1 - \frac{k_{\perp 1}^2}{2k.q(1-\alpha_1)}\right)\,,\\
\delta((k_2-k_1)^2 - m^2) &= \frac{1}{2k.q(\alpha_1-\alpha_2)}\delta\left(\beta_2 - \frac{k_{\perp 2}^2 - m^2}{2k.q(\alpha_1-\alpha_2)}\right)\,,\\
\delta((k_2+q)^2) &= \frac{1}{2k.q}\delta\left(\alpha_2 - x + \frac{(\alpha_1-x)}{(\alpha_1-\alpha_2)}\frac{(k_\perp^2 - m^2)}{2k.q}\right)\,.
\end{aligned} \tag{558}$$

This again leads to the definition of positive squares of momenta:

$$\begin{aligned}
r_1^2 &= -\frac{k_{\perp 1}^2}{1-\alpha_1}\,,\\
r_2^2 &= -\frac{k_{\perp 2}^2}{\alpha_1-\alpha_2}\,.
\end{aligned} \tag{559}$$

Like in the case of purely massless ladder rungs [34], see also [334, 337], the integral becomes nested in both the momentum and the Sudakov variables α_1, α_2,

$$\begin{aligned}
H_{3,q}^{W,\mathrm{PS},(2)} = \frac{1}{8}\int_{k^2}^{\frac{(s-m^2)(s+Q^2)}{s}} \frac{dr_2^2}{r_2^2 - s - Q^2}\int_{k^2}^{|k_{\perp 2}^2|}\frac{d|k_{\perp 1}^2|}{-|k_{\perp 1}^2|}\\
\int_0^1 \frac{d\alpha_2}{\alpha_2}\delta\left(1-\frac{x}{\alpha_2}\right)\int_{\alpha_2}^1 \frac{d\alpha_1}{\alpha_1}P_{gq}^{(0)}\left(\frac{\alpha_1}{\alpha_2}\right)P_{qg}^{(0)}(\alpha_1)\,,
\end{aligned} \tag{560}$$

where the following splitting function occurs:

$$P_{gq}^{(0)}(x) = 4C_F\frac{1+(1-x)^2}{x}\,. \tag{561}$$

With the variable substitution $R^2 = s + Q^2 - r_2^2$, the integrals over the squared momenta can be performed:

$$\int_{k^2}^{\frac{(s-m^2)(s+Q^2)}{s}} \frac{dr_2^2}{r_2^2 - s - Q^2}\int_{k^2}^{|k_{\perp 2}^2|}\frac{d|k_{\perp 1}^2|}{-|k_{\perp 1}^2|} = \int_{m^2\frac{s+Q^2}{s}}^{s+Q^2-k^2}\frac{dR^2}{R^2}\int_{k^2}^{R^2\frac{\alpha_1-\alpha_2}{\alpha_1}-m^2}\frac{d|k_{\perp 1}^2|}{-|k_{\perp 1}^2|}$$

$$\approx \int_{m^2 \frac{s+Q^2}{s}}^{s+Q^2} \frac{dR^2}{R^2} \ln\left(\frac{R^2}{k^2}\frac{\alpha_1-\alpha_2}{\alpha_1}\right)$$
$$= \frac{1}{2}\ln^2\left(\frac{m^2}{Q^2}\right) + O(\ln(m^2/Q^2))\,. \tag{562}$$

Here the reference scale in the mass-logarithm was chosen to be Q^2. In Mellin space the convolutions of the splitting functions in (560) factorize, and one finds to $O(\ln^2(m^2/Q^2))$ the relation

$$H_{3,q}^{W,\mathrm{PS},(2)} = \frac{1}{16}P_{qg}^{(0)}(N)P_{gq}^{(0)}(N)\ln^2\left(\frac{m^2}{Q^2}\right) = -\frac{1}{2}A_{Qq}^{\mathrm{PS},(2)}\,, \tag{563}$$

which fixes the respective sign. The additional ladder rung has the effect of introducing another splitting function independently from the boson-quark coupling. Hence the minus sign from the one-loop heavy flavor Wilson coefficient in leading logarithmic approximation is simply translated to the 2-loop pure-singlet contribution. As in the gluonic heavy flavor Wilson coefficient at the 1-loop order, the result above disagrees with the asymptotic representation given in [86]. A correct derivation of the asymptotic representations at the 2-loop order is therefore necessary, carefully tracing the origin of these signs. This is the purpose of the next Chapter.

10.5 The Asymptotic Representation to the 2-Loop Order

In the following, the asymptotic representations of the heavy flavor Wilson coefficients at $O(\alpha_s^2)$ are derived. The derivation follows the ideas leading to asymptotic representations in the electromagnetic current case of Chapter 4, cf. [75, 87, 305]. Also for the charged current case asymptotic representations have been given in [86] for the heavy flavor Wilson coefficients $H_{2,g}^{W,(2)}$, $H_{2,q}^{\mathrm{PS},(2)}$, $H_{3,g}^{W,\mathrm{PS},(2)}$ and $H_{3,q}^{\mathrm{PS},(2)}$. But since this is not the complete set of heavy flavor Wilson coefficients at 2 loops, and the relations for the last two coefficients disagree with the results of the previous sections, a complete derivation of the $O(\alpha_s^2)$ asymptotic representations is performed. Special emphasis is put on the occurrence of factors (-1), which reflect the sensitivity to the direction of the fermion flow of certain contributing diagrams.

Thus, first the structure of the Born cross section is summarized. After that, the higher order QCD corrections are systematized, exploiting the combinatorics of W-quark couplings and PDFs. A study of the symmetries of the underlying Feynman diagrams leads to the construction of expressions for the structure functions in terms of heavy and light flavor Wilson coefficients, as well as the PDFs. Using the relations of 3- and 4-flavor PDFs due to the equivalence of variable flavor number schemes in the electromagnetic case, cf. Chapter 6, and the charged current case, the asymptotic representations of the heavy flavor Wilson coefficients are derived. The expressions are constructed from the light flavor Wilson coefficients at $O(\alpha_s)$ [184–191, 196] and $O(\alpha_s^2)$ [81–85], together with the $O(\alpha_s)$ and $O(\alpha_s^2)$ massive OMEs [76–80]. The results are given in Mellin space and x-space.

The derivations are specifically performed for charm production, hence the number of light flavors is $n_f = 3$. Nevertheless, the symbol n_f is used throughout for further transparency.

10.5.1 Structure Functions at Leading Order

The Born level cross sections are well known, cf. [135, 338], and have the forms:

$$\frac{d\sigma^{\nu(\bar{\nu})}}{dxdy} = \frac{G_F^2 s}{4\pi}\left\{(1+(1-y)^2)F_2^{W^\pm} \pm (1-(1-y)^2)xF_3^{W^\pm}\right\}\,, \tag{564}$$

$$\frac{d\sigma^{e^-(e^+)}}{dxdy} = \frac{G_F^2 s}{4\pi}\left\{(1+(1-y)^2)F_2^{W^\mp} \pm (1-(1-y)^2)xF_3^{W^\mp}\right\}, \tag{565}$$

with the structure functions

$$F_2^{W^+} = 2x[(|V_{ud}|^2+|V_{cd}|^2)d + (|V_{us}|^2+|V_{cs}|^2)s + (|V_{ud}|^2+|V_{us}|^2)\bar{u}], \tag{566}$$
$$F_2^{W^-} = 2x[(|V_{ud}|^2+|V_{cd}|^2)\bar{d} + (|V_{us}|^2+|V_{cs}|^2)\bar{s} + (|V_{ud}|^2+|V_{us}|^2)u], \tag{567}$$
$$xF_3^{W^+} = 2x[(|V_{ud}|^2+|V_{cd}|^2)d + (|V_{us}|^2+|V_{cs}|^2)s - (|V_{ud}|^2+|V_{us}|^2)\bar{u}], \tag{568}$$
$$xF_3^{W^-} = 2x[-(|V_{ud}|^2+|V_{cd}|^2)\bar{d} - (|V_{us}|^2+|V_{cs}|^2)\bar{s} + (|V_{ud}|^2+|V_{us}|^2)u]. \tag{569}$$

It is now worthwhile to study combinations of cross sections

$$\frac{d\sigma^\nu}{dxdy} + \frac{d\sigma^{\bar\nu}}{dxdy} =: \frac{G_F^2 s}{4\pi}\left\{(1+(1-y)^2)F_2^{W^+ + W^-} + (1-(1-y)^2)xF_3^{W^+ + W^-}\right\}, \tag{570}$$
$$\frac{d\sigma^\nu}{dxdy} - \frac{d\sigma^{\bar\nu}}{dxdy} =: \frac{G_F^2 s}{4\pi}\left\{(1+(1-y)^2)F_2^{W^+ - W^-} + (1-(1-y)^2)xF_3^{W^+ - W^-}\right\}, \tag{571}$$

which implies the definitions:

$$\begin{aligned} F_2^{W^+ + W^-} &:= F_2^{W^+} + F_2^{W^-} \\ &= 2x\left[(|V_{ud}|^2+|V_{cd}|^2)(d+\bar{d}) + (|V_{us}|^2+|V_{cs}|^2)(s+\bar{s}) + (|V_{ud}|^2+|V_{us}|^2)(u+\bar{u})\right], \end{aligned} \tag{572}$$

$$\begin{aligned} xF_3^{W^+ + W^-} &:= xF_3^{W^+} - xF_3^{W^-} \\ &= 2x\left[(|V_{ud}|^2+|V_{cd}|^2)(d+\bar{d}) + (|V_{us}|^2+|V_{cs}|^2)(s+\bar{s}) - (|V_{ud}|^2+|V_{us}|^2)(u+\bar{u})\right], \end{aligned} \tag{573}$$

$$\begin{aligned} F_2^{W^+ - W^-} &:= F_2^{W^+} - F_2^{W^-} \\ &= 2x\left[(|V_{ud}|^2+|V_{cd}|^2)(d-\bar{d}) + (|V_{us}|^2+|V_{cs}|^2)(s-\bar{s}) - (|V_{ud}|^2+|V_{us}|^2)(u-\bar{u})\right], \end{aligned} \tag{574}$$

$$\begin{aligned} xF_3^{W^+ - W^-} &:= xF_3^{W^+} + xF_3^{W^-} \\ &= 2x\left[(|V_{ud}|^2+|V_{cd}|^2)(d-\bar{d}) + (|V_{us}|^2+|V_{cs}|^2)(s-\bar{s}) + (|V_{ud}|^2+|V_{us}|^2)(u-\bar{u})\right]. \end{aligned} \tag{575}$$

10.5.2 Higher Order Corrections

In the following the partonic quantities

$$\mathcal{F}_2^{W^\pm} := \frac{1}{2x}F_2^{W^\pm}, \quad \mathcal{F}_3^{W^\pm} := \frac{1}{2}F_3^{W^\pm} \tag{576}$$

will be used. Exploiting the number of combinations of proton constituents $(u, \bar{u}, d, \bar{d}, s, \bar{s})$ and quark-boson couplings (du, dc, su, sc) the QCD corrections may be organized as follows:

$$\begin{aligned} \mathcal{F}_i^{W^\pm} = \; & \lambda_{du}^{W^\pm}\left[\sum_q \left(\mathcal{C}_{i,q}^{W^\pm:du}(x)\otimes q(x) + \mathcal{C}_{i,\bar{q}}^{W^\pm:du}(x)\otimes\bar{q}(x)\right) + \mathcal{C}_{i,G}^{W^\pm:du}(x)\otimes G(x)\right] \\ & + \lambda_{dc}^{W^\pm}\left[\sum_q \left(\mathcal{C}_{i,q}^{W^\pm:dc}(x)\otimes q(x) + \mathcal{C}_{i,\bar{q}}^{W^\pm:dc}(x)\otimes\bar{q}(x)\right) + \mathcal{C}_{i,G}^{W^\pm:dc}(x)\otimes G(x)\right] \end{aligned}$$

$$+ \lambda_{su}^{W^\pm} \left[\sum_q \left(\mathcal{C}_{i,q}^{W^\pm:su}(x) \otimes q(x) + \mathcal{C}_{i,\bar{q}}^{W^\pm:su}(x) \otimes \bar{q}(x) \right) + \mathcal{C}_{i,G}^{W^\pm:su}(x) \otimes G(x) \right]$$
$$+ \lambda_{sc}^{W^\pm} \left[\sum_q \left(\mathcal{C}_{i,q}^{W^\pm:sc}(x) \otimes q(x) + \mathcal{C}_{i,\bar{q}}^{W^\pm:sc}(x) \otimes \bar{q}(x) \right) + \mathcal{C}_{i,G}^{W^\pm:sc}(x) \otimes G(x) \right] . \qquad (577)$$

The symbol $\otimes$ denotes the Mellin convolution (67). With the Mellin transforms of the structure functions:

$$F_2^{W^\pm}(N) := \int_0^1 dx x^{N-2} F_2^{W^\pm}(x) = 2 \int_0^1 dx x^{N-1} \mathcal{F}_2^{W^\pm}(x) =: 2\mathcal{F}_2^{W^\pm}(N) ,$$
$$F_3^{W^\pm}(N) := \int_0^1 dx x^{N-1} F_3^{W^\pm}(x) = 2 \int_0^1 dx x^{N-1} \mathcal{F}_3^{W^\pm}(x) =: 2\mathcal{F}_3^{W^\pm}(N) . \qquad (578)$$

In the following formulae, we will work in Mellin space and drop the argument N.

There are diagrams in which the incoming fermion line runs through the W-boson-quark vertex, and others where these two fermion lines are separated, examples are given in Figure 12.

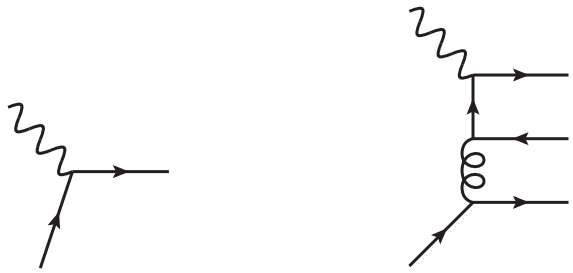

(a) (b)

Figure 12: A diagram where the incoming quark line and the one connected to the W-boson-quark vertex are the same, and one where these are separated.

It is useful to separate them into "valence" and "sea" contributions, respectively. The valence parts are flavor-diagonal while the sea parts do not distinguish different flavors, however, differences in the quark masses are detected, hence the c-quark is treated differently from u, d, s.

Obviously, all terms built from graphs like Fig. 12(a) (and QCD corrections) form valence contributions, and all sea contributions are built from graphs like Fig. 12(b). However there are interference contributions from the latter class of graphs, e.g. Fig. 13, which clearly form valence terms.

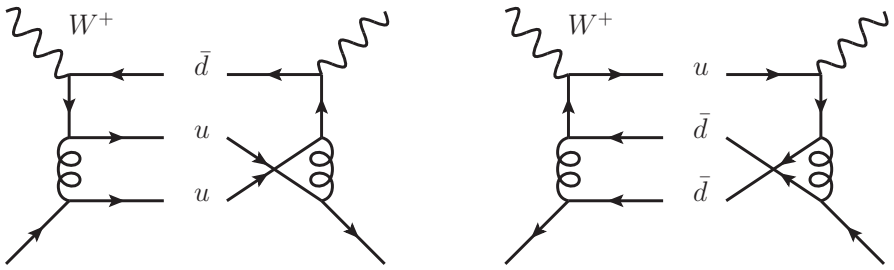

Figure 13: Valence like interference terms for W^+u-scattering and $W^+\bar{d}$-scattering, which have no counter parts on tree level.

In this way the parton structure functions can be written as

$$\begin{aligned}
\mathcal{F}_i^{W^+} = \quad & \lambda_{du}^{W^+}\Big[\mathcal{C}_{i,u}^{W^+:du,V}u + \mathcal{C}_{i,d}^{W^+:du,V}d + \mathcal{C}_{i,\bar{u}}^{W^+:du,V}\bar{u} + \mathcal{C}_{i,\bar{d}}^{W^+:du,V}\bar{d} \\
& \quad + \mathcal{C}_{i,q}^{W^+:du,S}(u+d+s) + \mathcal{C}_{i,\bar{q}}^{W^+:du,S}(\bar{u}+\bar{d}+\bar{s}) + \mathcal{C}_{i,G}^{W^+:du}G\Big] \\
& + \lambda_{dc}^{W^+}\Big[\mathcal{C}_{i,d}^{W^+:dc,V}d + \mathcal{C}_{i,\bar{d}}^{W^+:dc,V}\bar{d} \\
& \quad + \mathcal{C}_{i,q}^{W^+:dc,S}(u+d+s) + \mathcal{C}_{i,\bar{q}}^{W^+:dc,S}(\bar{u}+\bar{d}+\bar{s}) + \mathcal{C}_{i,G}^{W^+:dc}G\Big] \\
& + \lambda_{su}^{W^+}\Big[\mathcal{C}_{i,u}^{W^+:du,V}u + \mathcal{C}_{i,d}^{W^+:du,V}s + \mathcal{C}_{i,\bar{u}}^{W^+:du,V}\bar{u} + \mathcal{C}_{i,\bar{d}}^{W^+:du,V}\bar{s} \\
& \quad + \mathcal{C}_{i,q}^{W^+:du,S}(u+d+s) + \mathcal{C}_{i,\bar{q}}^{W^+:du,S}(\bar{u}+\bar{d}+\bar{s}) + \mathcal{C}_{i,G}^{W^+:du}G\Big] \\
& + \lambda_{sc}^{W^+}\Big[\mathcal{C}_{i,d}^{W^+:dc,V}s + \mathcal{C}_{i,\bar{d}}^{W^+:dc,V}\bar{s} \\
& \quad + \mathcal{C}_{i,q}^{W^+:dc,S}(u+d+s) + \mathcal{C}_{i,\bar{q}}^{W^+:dc,S}(\bar{u}+\bar{d}+\bar{s}) + \mathcal{C}_{i,G}^{W^+:dc}G\Big], \qquad (579)
\end{aligned}$$

$$\begin{aligned}
\mathcal{F}_i^{W^-} = \quad & \lambda_{du}^{W^-}\Big[\mathcal{C}_{i,u}^{W^-:du,V}u + \mathcal{C}_{i,d}^{W^-:du,V}d + \mathcal{C}_{i,\bar{u}}^{W^-:du,V}\bar{u} + \mathcal{C}_{i,\bar{d}}^{W^-:du,V}\bar{d} \\
& \quad + \mathcal{C}_{i,q}^{W^-:du,S}(u+d+s) + \mathcal{C}_{i,\bar{q}}^{W^-:du,S}(\bar{u}+\bar{d}+\bar{s}) + \mathcal{C}_{i,G}^{W^-:du}G\Big] \\
& + \lambda_{dc}^{W^-}\Big[\mathcal{C}_{i,d}^{W^-:dc,V}d + \mathcal{C}_{i,\bar{d}}^{W^-:dc,V}\bar{d} \\
& \quad + \mathcal{C}_{i,q}^{W^-:dc,S}(u+d+s) + \mathcal{C}_{i,\bar{q}}^{W^-:dc,S}(\bar{u}+\bar{d}+\bar{s}) + \mathcal{C}_{i,G}^{W^-:dc}G\Big] \\
& + \lambda_{su}^{W^-}\Big[\mathcal{C}_{i,u}^{W^-:du,V}u + \mathcal{C}_{i,d}^{W^-:du,V}s + \mathcal{C}_{i,\bar{u}}^{W^-:du,V}\bar{u} + \mathcal{C}_{i,\bar{d}}^{W^-:du,V}\bar{s} \\
& \quad + \mathcal{C}_{i,q}^{W^-:du,S}(u+d+s) + \mathcal{C}_{i,\bar{q}}^{W^-:du,S}(\bar{u}+\bar{d}+\bar{s}) + \mathcal{C}_{i,G}^{W^-:du}G\Big] \\
& + \lambda_{sc}^{W^-}\Big[\mathcal{C}_{i,\bar{d}}^{W^-:dc,V}s + \mathcal{C}_{i,\bar{d}}^{W^-:dc,V}\bar{s} \\
& \quad + \mathcal{C}_{i,q}^{W^-:dc,S}(u+d+s) + \mathcal{C}_{i,\bar{q}}^{W^-:dc,S}(\bar{u}+\bar{d}+\bar{s}) + \mathcal{C}_{i,G}^{W^-:dc}G\Big]. \qquad (580)
\end{aligned}$$

The constants $\lambda_{q(\bar{q}),i}^{W^\pm}$ can be read off from Eqs. (566–569), if the Born contribution of the valence part is normalized to

$$\mathcal{C}_{i,d}^{W^+:q'q'',V,(0)} = \mathcal{C}_{i,u}^{W^-:q'q'',V,(0)} = b_i\mathcal{C}_{i,\bar{u}}^{W^+:q'q'',V,(0)} = b_i\mathcal{C}_{i,\bar{d}}^{W^-:q'q'',V,(0)} = 1\,, \qquad (581)$$

while obviously

$$\mathcal{C}_{i,u}^{W^+:q'q'',V,(0)} = \mathcal{C}_{i,d}^{W^-:q'q'',V,(0)} = b_i\mathcal{C}_{i,\bar{d}}^{W^+:q'q'',V,(0)} = b_i\mathcal{C}_{i,\bar{u}}^{W^-:q'q'',V,(0)} = 0\,. \qquad (582)$$

In the same comparison, one finds:

$$\begin{aligned}
& \lambda_{du}^{W^+} = \lambda_{du}^{W^-} = |V_{du}|^2, \quad \lambda_{dc}^{W^+} = \lambda_{dc}^{W^-} = |V_{dc}|^2, \\
& \lambda_{su}^{W^+} = \lambda_{su}^{W^-} = |V_{su}|^2, \quad \lambda_{sc}^{W^+} = \lambda_{sc}^{W^-} = |V_{sc}|^2, \qquad (583) \\
& b_2 = 1, \quad b_3 = -1\,. \qquad (584)
\end{aligned}$$

Using the shorthand notation

$$V_u := |V_{du}|^2 + |V_{su}|^2\,, \quad V_d := |V_{du}|^2 + |V_{dc}|^2\,,$$
$$V_s := |V_{su}|^2 + |V_{sc}|^2\,, \quad V_c := |V_{dc}|^2 + |V_{sc}|^2\,, \tag{585}$$

and due to charge conjugation invariance of QCD, the coefficients are related in the following way:

$$\begin{aligned}
\mathcal{C}_{i,d}^{W^+:q'q'',V} &= b_i \mathcal{C}_{i,\bar{u}}^{W^+:q'q'',V} = \mathcal{C}_{i,u}^{W^-:q'q'',V} = b_i \mathcal{C}_{i,\bar{d}}^{W^-:q'q'',V} \equiv \mathcal{C}_{i,q}^{W:q'q'',V}\,,\\
\mathcal{C}_{i,u}^{W^+:q'q'',V} &= b_i \mathcal{C}_{i,\bar{d}}^{W^+:q'q'',V} = \mathcal{C}_{i,d}^{W^-:q'q'',V} = b_i \mathcal{C}_{i,\bar{u}}^{W^-:q'q'',V} \equiv \mathcal{C}_{i,m}^{W:q'q'',V}\,,\\
\mathcal{C}_{i,q}^{W^+:q'q'',S} &= \mathcal{C}_{i,\bar{q}}^{W^+:q'q'',S} = b_i \mathcal{C}_{i,q}^{W^-:q'q'',S} = b_i \mathcal{C}_{i,\bar{q}}^{W^-:q'q'',S} \equiv \mathcal{C}_{i,q}^{W:q'q'',S}\,,\\
\mathcal{C}_{i,G}^{W^+,q'q''} &= b_i \mathcal{C}_{i,G}^{W^-,q'q''} \equiv \mathcal{C}_{i,G}^{W,q'q''}\,.
\end{aligned} \tag{586}$$

This is true for the $C_{i,q(\bar{q})}^{W^\pm:dc,V}$ only up to power corrections in m^2/Q^2, which are disregarded here. The coefficient functions are brought into the following compact from:

$$\begin{aligned}
\mathcal{F}_i^{W^+} =& (V_u b_i \bar{u} + |V_{du}|^2 d + |V_{su}|^2 s)\mathcal{C}_{i,q}^{W:du,V} + (|V_{dc}|^2 d + |V_{sc}|^2 s)\mathcal{C}_{i,q}^{W:dc,V}\\
& (V_u u + |V_{du}|^2 b_i \bar{d} + |V_{su}|^2 b_i \bar{s})\mathcal{C}_{i,m}^{W:du,V} + (|V_{dc}|^2 b_i \bar{d} + |V_{sc}|^2 b_i \bar{s})\mathcal{C}_{i,m}^{W:dc,V}\\
& + V_u \left[\mathcal{C}_{i,q}^{W:du,S}\Sigma + \mathcal{C}_{i,G}^{W:du} G\right] + V_c \left[\mathcal{C}_{i,q}^{W:dc,S}\Sigma + \mathcal{C}_{i,G}^{W:dc} G\right]\,,
\end{aligned} \tag{587}$$

$$\begin{aligned}
\mathcal{F}_i^{W^-} =& (V_u u + b_i |V_{du}|^2 \bar{d} + b_i |V_{su}|^2 \bar{s})\mathcal{C}_{i,q}^{W:du,V} + (|V_{dc}|^2 \bar{d} + |V_{sc}|^2 \bar{s}) b_i \mathcal{C}_{i,q}^{W:dc,V}\\
& (b_i V_u \bar{u} + |V_{du}|^2 d + |V_{su}|^2 s)\mathcal{C}_{i,m}^{W:du,V} + (|V_{dc}|^2 d + |V_{sc}|^2 s)\mathcal{C}_{i,m}^{W:dc,V}\\
& + b_i V_u \left[\mathcal{C}_{i,q}^{W:du,S}\Sigma + \mathcal{C}_{i,G}^{W:du} G\right] + b_i V_c \left[\mathcal{C}_{i,q}^{W:dc,S}\Sigma + \mathcal{C}_{i,G}^{W:dc} G\right]\,,
\end{aligned} \tag{588}$$

where the singlet combination of quark PDFs is defined as

$$\Sigma = u + \bar{u} + d + \bar{d} + s + \bar{s}\,. \tag{589}$$

Note that the minus signs denoted by b_i are due to the minus signs in the Feynman rules of the $W^\pm q$-vertex, as well as due to the charge conjugation antisymmetry of the fermion line to which the W-boson is attached. This antisymmetry is due to the presence of a single γ_5 and hence only occurs in contributions to F_3.

The emergence of these minus signs is shortly illustrated in the following. In these considerations, factors of i or (-1) stemming from the Feynman rules are not of relevance, since expressions with the same number of vertices and propagators are compared.

The fermion trace of the digram in Fig. 14(a) can be written as

$$T_q^{W^+,V} = \sum_{\text{Spins}} \bar{u}(p')\Gamma_2 \frac{1+\gamma_5}{2}\gamma_\mu \Gamma_1 u(p) \bar{u}(p)\bar{\Gamma}_1 \frac{1+\gamma_5}{2}\gamma_\nu \bar{\Gamma}_2 u(p')\,, \tag{590}$$

where the Γ_i denote products of Dirac matrices, multiplied by real numbers which also include the denominators of the propagators, and $\bar{\Gamma}_i = \gamma_0 \Gamma_i^\dagger \gamma_0$ is just Γ_i with inverted order of the factors. Assuming an antifermion in the initial state, the same trace has the form

$$T_{\bar{q}}^{W^+,V} = \sum_{\text{Spins}} \bar{v}(p)\bar{\Gamma}_1 \frac{1+\gamma_5}{2}\gamma_\mu \bar{\Gamma}_2 v(p') \bar{v}(p')\Gamma_2 \frac{1+\gamma_5}{2}\gamma_\nu \Gamma_1 v(p)$$

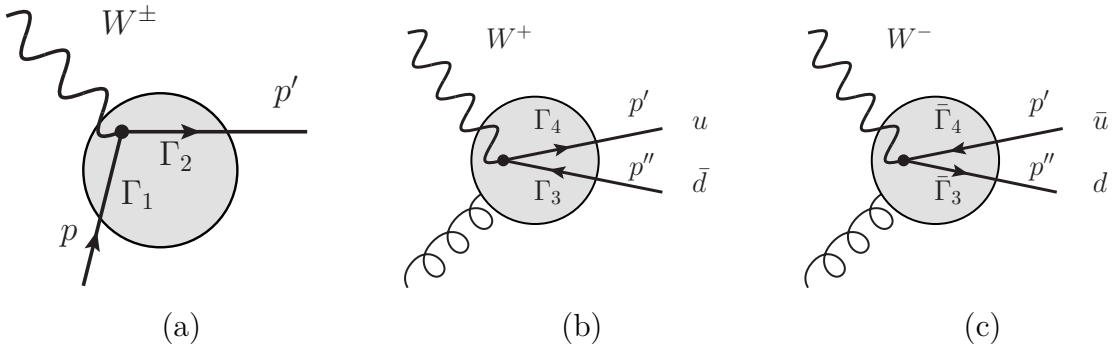

Figure 14: The QCD corrections, denoted by the gray area, are connected to the scattered quark line through gluon exchange.

$$= \sum_{\text{Spins}} \bar{v}(p')\Gamma_2 \frac{1+\gamma_5}{2}\gamma_\nu \Gamma_1 v(p)\bar{v}(p)\bar{\Gamma}_1 \frac{1+\gamma_5}{2}\gamma_\mu \bar{\Gamma}_2 v(p') \,. \tag{591}$$

Since the difference between fermion and antifermion spinors in the trace only affects the part $\propto m^2$, it contributes to the power corrections only, and due to antisymmetry of the γ_5 part, $T_{\bar{q}}^{W^+}$ and $T_q^{W^+}$ only differ by a minus sign in front of γ_5. This leads to the relations among the "valence" parts in Eqs. (586).

In case of the "sea"-contributions depicted in Figure 14(b) and (c) the traces read:

$$T^{W^+,S} = \sum_{\text{Spins}} \bar{u}_u(p')\Gamma_4 \frac{1+\gamma_5}{2}\gamma_\mu \Gamma_3 v_d(p'')\bar{v}_d(p'')\bar{\Gamma}_3 \frac{1+\gamma_5}{2}\gamma_\nu \bar{\Gamma}_4 u_u(p') \,, \tag{592}$$

$$\begin{aligned} T^{W^-,S} &= \sum_{\text{Spins}} \bar{u}_d(p'')\bar{\Gamma}_3 \frac{1+\gamma_5}{2}\gamma_\mu \bar{\Gamma}_4 v_u(p')\bar{v}_u(p')\Gamma_4 \frac{1+\gamma_5}{2}\gamma_\nu \Gamma_3 u_d(p'') \\ &= \sum_{\text{Spins}} \bar{v}_u(p')\Gamma_4 \frac{1+\gamma_5}{2}\gamma_\nu \Gamma_3 u_d(p'')\bar{u}_d(p'')\bar{\Gamma}_3 \frac{1+\gamma_5}{2}\gamma_\mu \bar{\Gamma}_4 v_u(p') \,. \end{aligned} \tag{593}$$

Here, bispinors of down-type (anti)quarks are marked by the subscript d and the ones of up-type (anti)quarks are marked by u. One notes, that the relation of the down-(up-)type line to the string $\Gamma_3(\Gamma_4)$ of γ-matrices is only strict, if the flavors differ in mass, which is dominantly related to the mass occurring in denominators of propagators. If this is not the case, Γ_3 and $\bar{\Gamma}_4$ are exchangeable and hence $T^{W^+,S} = T^{W^-,S}$. Generally one further notes, that $T^{W^+,S}$ and $T^{W^-,S}$ only differ by the order of the indices μ and ν which leads to the relations among "sea" contributions in Eqs. (586).

Note that combining the symmetry statement in the massless case and the antisymmetry of the part proportional to γ_5, leads to the vanishing of the corresponding "sea" contributions and thus to Eq. (597).

So the sum of partonic structure functions has the form

$$\begin{aligned} \mathcal{F}_i^{W^+} + \mathcal{F}_i^{W^-} = &\left(|V_{du}|^2(d+b_i\bar{d}) + |V_{su}|^2(s+b_i\bar{s}) + V_u(u+b_i\bar{u})\right)\left(\mathcal{C}_{i,q}^{W:du,V} + \mathcal{C}_{i,m}^{W:du,V}\right) \\ &+ \left(|V_{dc}|^2(d+b_i\bar{d}) + |V_{sc}|^2(s+b_i\bar{s})\right)\left(\mathcal{C}_{i,q}^{W:dc,V} + \mathcal{C}_{i,m}^{W:dc,V}\right) \\ &+ (1+b_i)V_u\left[\mathcal{C}_{i,q}^{W:du,S}\Sigma + \mathcal{C}_{i,G}^{W:du}G\right] + (1+b_i)V_c\left[\mathcal{C}_{i,q}^{W:dc,S}\Sigma + \mathcal{C}_{i,G}^{W:dc}G\right] \,, \end{aligned} \tag{594}$$

$$\mathcal{F}_i^{W^+} - \mathcal{F}_i^{W^-} = \left(|V_{du}|^2(d-b_i\bar{d}) + |V_{su}|^2(s-b_i\bar{s}) - V_u(u-b_i\bar{u})\right)\left(\mathcal{C}_{i,q}^{W:du,V} - \mathcal{C}_{i,m}^{W:du,V}\right)$$

$$
\begin{aligned}
&+ \left(|V_{dc}|^2(d-b_i\bar{d}) + |V_{sc}|^2(s-b_i\bar{s})\right)\left(\mathcal{C}_{i,q}^{W^+:dc,V} - \mathcal{C}_{i,m}^{W^+:dc,V}\right)\\
&+ (1-b_i)V_u\left[\mathcal{C}_{i,q}^{W:du,S}\Sigma + \mathcal{C}_{i,G}^{W:du}G\right] + (1-b_i)V_c\left[\mathcal{C}_{i,q}^{W:dc,S}\Sigma + \mathcal{C}_{i,G}^{W:dc}G\right]. \qquad (595)
\end{aligned}
$$

To make contact with the factorization of the heavy flavor Wilson coefficients [75, 76, 87], we further separate the contributions to the Wilson coefficients depending on whether they only consist of massless lines (C), whether they contain massive lines which do not couple to the W-boson (L), or whether the W-boson couples to a massive line (H):

$$
\begin{aligned}
\mathcal{C}_{i,q}^{W:du,V} + \mathcal{C}_{i,m}^{W:du,V} &\equiv C_{i,q}^{W^+ + W^-,\mathrm{NS}} + L_{i,q}^{W^+ + W^-,\mathrm{NS}},\\
\mathcal{C}_{i,q}^{W:du,V} - \mathcal{C}_{i,m}^{W:du,V} &\equiv C_{i,q}^{W^+ - W^-,\mathrm{NS}} + L_{i,q}^{W^+ - W^-,\mathrm{NS}},\\
\mathcal{C}_{i,q}^{W:dc,V} + \mathcal{C}_{i,m}^{W:dc,V} &\equiv H_{i,q}^{W^+ + W^-,\mathrm{NS}},\\
\mathcal{C}_{i,q}^{W:dc,V} - \mathcal{C}_{i,m}^{W:dc,V} &\equiv H_{i,q}^{W^+ - W^-,\mathrm{NS}},\\
\mathcal{C}_{i,q}^{W:du,S} &\equiv C_{i,q}^{W,\mathrm{PS}} + L_{i,q}^{W,\mathrm{PS}},\\
\mathcal{C}_{i,q}^{W:dc,S} &\equiv H_{i,q}^{W,\mathrm{PS}},\\
\mathcal{C}_{i,G}^{W:du} &\equiv C_{i,g}^{W} + L_{i,g}^{W},\\
\mathcal{C}_{i,G}^{W:dc} &\equiv H_{i,g}^{W}. \qquad (596)
\end{aligned}
$$

Due to charge conjugation invariance of QCD, the gluon and singlet coefficients associated to the third structure function vanish, cf. [86], as well as the comment below Eq. (592). One therefore finds

$$
C_{3,q}^{W,\mathrm{PS}} = C_{3,g}^{W} = 0 \text{ and } L_{3,q}^{W,\mathrm{PS}} = L_{3,g}^{W} = 0\,. \qquad (597)
$$

If not written explicitly, the light Wilson coefficients depend on n_f light flavors:

$$
C_{i,j} = C_{i,j}(n_f)\,. \qquad (598)
$$

The heavy flavor Wilson coefficients are always assumed to depend on n_f light flavors and the heavy flavor. Writing the contributions to the structure functions explicitly one finds:

$$
\begin{aligned}
\mathcal{F}_2^{W^+} + \mathcal{F}_2^{W^-} = &\left(|V_{du}|^2(d+\bar{d}) + |V_{su}|^2(s+\bar{s}) + V_u(u+\bar{u})\right)(C_{2,q}^{W^+ + W^-,\mathrm{NS}} + L_{2,q}^{W^+ + W^-,\mathrm{NS}})\\
&+ \left(|V_{dc}|^2(d+\bar{d}) + |V_{sc}|^2(s+\bar{s})\right)H_{2,q}^{W^+ + W^-,\mathrm{NS}}\\
&+ 2V_u\left[(C_{2,q}^{W,\mathrm{PS}} + L_{2,q}^{W,\mathrm{PS}})\Sigma + (C_{2,g}^{W} + L_{2,g}^{W})G\right]\\
&+ 2V_c\left[H_{2,q}^{W,\mathrm{PS}}\Sigma + H_{2,g}^{W}G\right], \qquad (599)
\end{aligned}
$$

$$
\begin{aligned}
\mathcal{F}_2^{W^+} - \mathcal{F}_2^{W^-} = &\left(|V_{du}|^2(d-\bar{d}) + |V_{su}|^2(s-\bar{s}) - V_u(u-\bar{u})\right)(C_{2,q}^{W^+ - W^-,\mathrm{NS}} + L_{2,q}^{W^+ - W^-,\mathrm{NS}})\\
&+ \left(|V_{dc}|^2(d-\bar{d}) + |V_{sc}|^2(s-\bar{s})\right)H_{2,q}^{W^+ - W^-,\mathrm{NS}}, \qquad (600)
\end{aligned}
$$

$$
\begin{aligned}
\mathcal{F}_3^{W^+} + \mathcal{F}_3^{W^-} = &\left(|V_{du}|^2(d-\bar{d}) + |V_{su}|^2(s-\bar{s}) + V_u(u-\bar{u})\right)(C_{3,q}^{W^+ - W^-,\mathrm{NS}} + L_{3,q}^{W^+ - W^-,\mathrm{NS}})\\
&+ \left(|V_{dc}|^2(d-\bar{d}) + |V_{sc}|^2(s-\bar{s})\right)H_{3,q}^{W^+ - W^-,\mathrm{NS}}, \qquad (601)
\end{aligned}
$$

$$
\mathcal{F}_3^{W^+} - \mathcal{F}_3^{W^-} = \left(|V_{du}|^2(d+\bar{d}) + |V_{su}|^2(s+\bar{s}) - V_u(u+\bar{u})\right)(C_{3,q}^{W^+ + W^-,\mathrm{NS}} + L_{3,q}^{W^+ + W^-,\mathrm{NS}})
$$

$$+ \left(|V_{dc}|^2(d+\bar{d}) + |V_{sc}|^2(s+\bar{s})\right) H_{3,q}^{W^+ + W^-,\mathrm{NS}}$$
$$+ 2V_c \left[H_{3,q}^{W,\mathrm{PS}}\Sigma + H_{3,g}^{W} G\right] . \tag{602}$$

Since the combinations of structure functions behave uniformly under crossing, either even or odd moments contribute to the combinations in Mellin space. One finds [33, 143–145] :

$$F_2^{W^+} + F_2^{W^-} \text{ : even N}, \tag{603}$$
$$F_2^{W^+} - F_2^{W^-} \text{ : odd N}, \tag{604}$$
$$F_3^{W^+} + F_3^{W^-} \text{ : odd N}, \tag{605}$$
$$F_3^{W^+} - F_3^{W^-} \text{ : even N}. \tag{606}$$

Now one can write the even-N combinations in terms of non-singlet combinations of PDFs

$$\Delta_q = q + \bar{q} - \frac{1}{n_f}\Sigma, \tag{607}$$

leading to

$$\begin{aligned}
\mathcal{F}_2^{W^+} + \mathcal{F}_2^{W^-} = \; & \left(|V_{du}|^2\Delta_d + |V_{su}|^2\Delta_s + V_u\Delta_u\right)(C_{2,q}^{W^+ + W^-,\mathrm{NS}} + L_{2,q}^{W^+ + W^-,\mathrm{NS}}) \\
& + \left(|V_{dc}|^2\Delta_d + |V_{sc}|^2\Delta_s\right) H_{2,q}^{W^+ + W^-,\mathrm{NS}} \\
& + \frac{V_u}{n_f}\left[(C_{2,q}^{W,\mathrm{S}} + L_{2,q}^{W,\mathrm{S}})\Sigma + 2n_f(C_{2,g}^{W} + L_{2,g}^{W})G\right] \\
& + \frac{V_c}{n_f}\left[H_{2,q}^{W,\mathrm{S}}\Sigma + 2n_f H_{2,g}^{W} G\right] ,
\end{aligned} \tag{608}$$

$$\begin{aligned}
\mathcal{F}_3^{W^+} - \mathcal{F}_3^{W^-} = \; & \left(|V_{du}|^2\Delta_d + |V_{su}|^2\Delta_s - V_u\Delta_u\right)(C_{3,q}^{W^+ + W^-,\mathrm{NS}} + L_{3,q}^{W^+ + W^-,\mathrm{NS}}) \\
& + \left(|V_{dc}|^2\Delta_d + |V_{sc}|^2\Delta_s\right) H_{3,q}^{W^+ + W^-,\mathrm{NS}} \\
& + \frac{V_c}{n_f}\left[\left(2n_f H_{3,q}^{W,\mathrm{PS}} + H_{3,q}^{W^+ + W^-,\mathrm{NS}}\right)\Sigma + 2n_f H_{3,g}^{W} G\right] ,
\end{aligned} \tag{609}$$

where a singlet combination of Wilson coefficients was defined analogously to the electromagnetic case [76] :

$$\begin{aligned}
C_{2,q}^{W^+ \pm W^-,\mathrm{S}} &:= 2n_f C_{2,q}^{W,\mathrm{PS}} + 2C_{2,q}^{W^+ \pm W^-,\mathrm{NS}} , \\
L_{2,q}^{W^+ \pm W^-,\mathrm{S}} &:= 2n_f L_{2,q}^{W,\mathrm{PS}} + 2L_{2,q}^{W^+ \pm W^-,\mathrm{NS}} , \\
H_{2,q}^{W^+ \pm W^-,\mathrm{S}} &:= 2n_f H_{2,q}^{W,\mathrm{PS}} + H_{2,q}^{W^+ \pm W^-,\mathrm{NS}} .
\end{aligned} \tag{610}$$

In order to derive factorization formulae, we choose to take a safe detour via the relations of parton distributions in the variable flavor number scheme $(q', \bar{q}')$ [75, 87], cf. (207–211) :

$$\begin{aligned}
q' + \bar{q}' &= A_{qq,Q}^{\mathrm{NS}}(q+\bar{q}) + \tilde{A}_{qq,Q}^{\mathrm{PS}}\Sigma + \tilde{A}_{qg,Q} G , \\
c' + \bar{c}' &= A_{Qq}^{\mathrm{PS}}\Sigma + A_{Qg} G , \\
\Sigma' &= (n_f \tilde{A}_{qq,Q}^{\mathrm{PS}} + A_{Qq}^{\mathrm{PS}} + A_{qq,Q}^{\mathrm{NS}})\Sigma + (n_f \tilde{A}_{qg,Q} + A_{Qg})G , \\
G' &= A_{gq,Q}\Sigma + A_{gg,Q} G ,
\end{aligned}$$

$$\Delta'_q + \frac{1}{n_f}\Delta'_c = A^{\rm NS}_{qq,Q}\Delta_q\,,$$
$$\Delta'_c = \frac{1}{n_f+1}\left(n_f A^{\rm PS}_{Qq} - n_f \tilde{A}^{\rm PS}_{qq,Q} - A^{\rm NS}_{qq,Q}\right)\Sigma + \frac{1}{n_f+1}\left(n_f A_{Qg} - n_f \tilde{A}_{qg,Q}\right) G\,. \quad (611)$$

Here the notation $\tilde{A}_{ij}$ defined in (212) was used. From this point on, the number of light flavors contributing to the light flavor Wilson coefficients is written explicitly as an argument. The four-flavor expressions read:

$$\mathcal{F}_2^{W^+} + \mathcal{F}_2^{W^-} = (V_d\Delta'_d + V_s\Delta'_s + V_u\Delta'_u + V_c\Delta'_c)C_{2,q}^{W^+ + W^-,{\rm NS}}(n_f+1) + \frac{V_u+V_c}{n_f+1}\left[C_{2,q,(n_f+1)}^{W^+ + W^-,{\rm S}}\Sigma' + 2(n_f+1)C_{2,g}^{W}(n_f+1)G'\right], \quad (612)$$

$$\mathcal{F}_2^{W^+} - \mathcal{F}_2^{W^-} = \left(V_d(d-\bar{d}) + V_s(s-\bar{s}) - V_u(u-\bar{u}) - V_c(c-\bar{c})\right) C_{2,q}^{W^+ - W^-,{\rm NS}}(n_f+1)\,, \quad (613)$$

$$\mathcal{F}_3^{W^+} - \mathcal{F}_3^{W^-} = (V_d\Delta'_d + V_s\Delta'_s - V_u\Delta'_u - V_c\Delta'_c)C_{3,q}^{W^+ + W^-,{\rm NS}}(n_f+1)\,, \quad (614)$$

$$\mathcal{F}_3^{W^+} + \mathcal{F}_3^{W^-} = \left(V_d(d-\bar{d}) + V_s(s-\bar{s}) + V_u(u-\bar{u}) + V_c(c-\bar{c})\right) C_{3,q}^{W^+ - W^-,{\rm NS}}(n_f+1)\,. \quad (615)$$

Comparing the coefficients of $\Sigma, G, \Delta_q, V_u, V_c$ in eqs. (612) and (608) one finds

$$\begin{aligned}
C_{2,q}^{W^+\pm W^-,{\rm NS}}(n_f) + L_{2,q}^{W^+\pm W^-,{\rm NS}} &= A^{\rm NS}_{qq,Q}C_{2,q}^{W^+\pm W^-,{\rm NS}}(n_f+1)\,,\\
H_{2,q}^{W^+\pm W^-,{\rm NS}} &= A^{\rm NS}_{qq,Q}C_{2,q}^{W^+\pm W^-,{\rm NS}}(n_f+1)\,,\\
C_{2,q}^{W,{\rm PS}}(n_f) + L_{2,q}^{W,{\rm PS}} &= \tilde{A}^{\rm PS}_{qq,Q}C_{2,q}^{W^+ + W^-,{\rm NS}}(n_f+1)\\
&\quad + C_{2,q}^{W,{\rm PS}}(n_f+1)\left(n_f\tilde{A}^{\rm PS}_{qq,Q} + A^{\rm PS}_{Qq} + A^{\rm NS}_{qq,Q}\right)\\
&\quad + A_{gq,Q}C_{2,g}^{W}(n_f+1)\,,\\
H_{2,q}^{W,{\rm PS}} &= \frac{1}{2}\left(\tilde{A}^{\rm PS}_{qq,Q} + A^{\rm PS}_{Qq}\right)C_{2,q}^{W^+ + W^-,{\rm NS}}(n_f+1)\\
&\quad + \left(n_f\tilde{A}^{\rm PS}_{qq,Q} + A^{\rm PS}_{Qq} + A^{\rm NS}_{qq,Q}\right)C_{2,q}^{W,{\rm PS}}(n_f+1)\\
&\quad + A_{gq,Q}C_{2,g}^{W}(n_f+1)\,,\\
C_{2,g}^{W}(n_f) + L_{2,g}^{W} &= \tilde{A}_{qg,Q}C_{2,q}^{W^+ + W^-,{\rm NS}}(n_f+1)\\
&\quad + \left(n_f\tilde{A}_{qg,Q} + A_{Qg}\right)C_{2,q}^{W,{\rm PS}}(n_f+1) + A_{gg,Q}C_{2,g}^{W}(n_f+1)\,,\\
H_{2,g}^{W} &= \frac{1}{2}\left(\tilde{A}_{qg,Q} + A_{Qg}\right)C_{2,q}^{W^+ + W^-,{\rm NS}}(n_f+1)\\
&\quad + \left(n_f\tilde{A}_{qg,Q} + A_{Qg}\right)C_{2,q}^{W,{\rm PS}}(n_f+1) + A_{gg,Q}C_{2,g}^{W}(n_f+1)\,,
\end{aligned} \quad (616)$$

where the odd-N combinations are included in analogy to the even-N ones. From eqs. (614) and (609) one can deduce similarly

$$\begin{aligned}
L_{3,q}^{W^+\pm W^-,{\rm NS}} &= A^{\rm NS}_{qq,Q}C_{3,q}^{W^+\pm W^-,{\rm NS}}(n_f+1) - C_{3,q}^{W^+\pm W^-,{\rm NS}}(n_f)\,,\\
H_{3,q}^{W^+\pm W^-,{\rm NS}} &= A^{\rm NS}_{qq,Q}C_{3,q}^{W^+\pm W^-,{\rm NS}}(n_f+1)\,,\\
H_{3,q}^{W,{\rm PS}} &= \frac{1}{2}(\tilde{A}^{\rm PS}_{qq,Q} - A^{\rm PS}_{Qq})C_{3,q}^{W^+ + W^-,{\rm NS}}(n_f+1)\,,\\
H_{3,g}^{W} &= \frac{1}{2}(\tilde{A}_{qg,Q} - A_{Qg})C_{3,q}^{W^+ + W^-,{\rm NS}}(n_f+1)\,.
\end{aligned} \quad (617)$$

By inserting the odd-N factorization relations into (600) and (602), and comparing with (613) and (615), respectively, one finds:

$$\begin{aligned} q' - \bar{q}' &= A^{\rm NS}_{qq,Q}(q - \bar{q})\,, \\ c' - \bar{c}' &= 0\,. \end{aligned} \tag{618}$$

Expanding the above relations up to order a_s^2,

$$f(a_s) = \sum_{l=0}^{\infty} a_s^l f^{(l)}\,, \tag{619}$$

one finds the asymptotic representations. The relations for the longitudinal structure function F_L are almost complete analogs to the ones for F_2, so they are included using the index $i = 2/L$, where the only structural difference, denoted by Kronecker symbols $\delta_{i,2}$, derives from the fact, that the coefficients $C_L^{\rm NS}$ do not have a Born contribution. On the Born level, one obviously has

$$\begin{aligned} H_{i,q}^{W^+\pm W^-,{\rm NS},(0)} &= \delta_{i,2}\,, \\ H_{3,q}^{W^+\pm W^-,{\rm NS},(0)} &= 1\,. \end{aligned} \tag{620}$$

At 1-loop level, one obtains

$$\begin{aligned} H_{i,q}^{W^+\pm W^-,{\rm NS},(1)} &= C_{i,q}^{W^+\pm W^-,{\rm NS},(1)}(n_f+1)\,, \\ H_{i,g}^{W,(1)} &= \frac{1}{2}\delta_{i,2}A_{Qg}^{(1)} + C_{i,g}^{W,(1)}(n_f+1)\,, \\ H_{3,q}^{W^+\pm W^-,{\rm NS},(1)} &= C_{3,q}^{W^+\pm W^-,{\rm NS},(1)}(n_f+1)\,, \\ H_{3,g}^{W,(1)} &= -\frac{1}{2}A_{Qg}^{(1)}\,, \end{aligned} \tag{621}$$

in accordance with (520–522). At 2-loop order, the asymptotic formulae take the form:

$$\begin{aligned} L_{i,q}^{W^+\pm W^-,{\rm NS},(2)} &= \delta_{i,2}A_{qq,Q}^{{\rm NS},(2)} + C_{i,q}^{W^+\pm W^-,{\rm NS},(2)}(n_f+1) - C_{i,q}^{W^+\pm W^-,{\rm NS},(2)}(n_f)\,, \\ H_{i,q}^{W^+\pm W^-,{\rm NS},(2)} &= \delta_{i,2}A_{qq,Q}^{{\rm NS},(2)} + C_{i,q}^{W^+\pm W^-,{\rm NS},(2)}(n_f+1)\,, \\ L_{i,q}^{W,{\rm PS},(2)} &= C_{i,q}^{W,{\rm PS},(2)}(n_f+1) - C_{i,q}^{W,{\rm PS},(2)}(n_f) = 0\,, \\ H_{i,q}^{W,{\rm PS},(2)} &= \frac{1}{2}\delta_{i,2}A_{Qq}^{{\rm PS},(2)} + C_{i,q}^{W,{\rm PS},(2)}(n_f+1)\,, \\ L_{i,g}^{W,(2)} &= A_{gg,Q}^{(1)}C_{i,g}^{W,(1)}(n_f+1) + C_{i,g}^{W,(2)}(n_f+1) - C_{i,g}^{W,(2)}(n_f)\,, \\ H_{i,g}^{W,(2)} &= A_{gg,Q}^{(1)}C_{i,g}^{W,(1)}(n_f+1) + C_{i,g}^{W,(2)}(n_f+1) \\ &\quad + \frac{1}{2}\left(\delta_{i,2}A_{Qg}^{(2)} + A_{Qg}^{(1)}C_{i,q}^{W^++W^-,{\rm NS},(1)}(n_f+1)\right)\,, \\ L_{3,q}^{W^+\pm W^-,{\rm NS},(2)} &= A_{qq,Q}^{{\rm NS},(2)} + C_{3,q}^{W^+\pm W^-,{\rm NS},(2)}(n_f+1) - C_{3,q}^{W^+\pm W^-,{\rm NS},(2)}(n_f)\,, \\ H_{3,q}^{W^+\pm W^-,{\rm NS},(2)} &= A_{qq,Q}^{{\rm NS},(2)} + C_{3,q}^{W^+\pm W^-,{\rm NS},(2)}(n_f+1)\,, \\ H_{3,q}^{W,{\rm PS},(2)} &= -\frac{1}{2}A_{Qq}^{{\rm PS},(2)}\,, \\ H_{3,g}^{W,(2)} &= \frac{1}{2}\left(-A_{Qg}^{(2)} - A_{Qg}^{(1)}C_{3,q}^{W^++W^-,{\rm NS},(1)}(n_f+1)\right)\,. \end{aligned} \tag{622}$$

Comparing with results given in [86], one finds that the abve relations agree for $H_{2,g}^{W,(1)}$ and $H_{2,q}^{W,\rm PS,(2)}$. They further correct $H_{2,g}^{W,(2)}$ with regard to heavy quark loop contributions on external lines, cf. [87], and correct signes in $H_{3,g}^{W,(1)}$, $H_{3,g}^{W,(2)}$ and $H_{3,g}^{W,\rm PS,(2)}$.

The non-singlet light flavor Wilson coefficients $c_{i,q}^{(i),\rm ns,\pm}$ defined in Eq. (94) of [85] are related to the ones used above via

$$C_{i,q}^{W^+\pm W^-,\rm NS,(i)} = c_{i,q}^{(i),\rm ns,+} \pm c_{i,q}^{(i),\rm ns,-}, \quad i = 2, 3\,, \tag{623}$$

where the $\pm$-signs correspond to each other on the left and right hand sides. The splitting denoted by superscripts $+$ or $-$ is the same as in Eq. (14) in [84]. The gluonic and pure singlet Wilson coefficients can be taken over from the electromagnetic case. Using $c_{i,\rm ps}^{(i)}$ and $c_{i,g}^{(i)}$ from [64], one finds

$$C_{i,q}^{W,\rm PS,(i)}(n_f) = \frac{1}{n_f} c_{i,\rm ps}^{(i)}, \quad C_{i,g}^{W,\rm PS,(i)}(n_f) = \frac{1}{n_f} c_{i,g}^{(i)}, \quad i = 2, L\,. \tag{624}$$

The contributions to the non-singlet Wilson coefficients of the structure functions $F_{2,3}$ were given in [81–84], and confirmed in [85] (see also [339], where also the even-odd-N difference for the Wilson coefficient of F_L is published).

Note that although the complete set of Wilson coefficients up to the third loop order was published as computer algebraic input in x- and N-space in [64] for the photon exchange case (see also [295], for more compact representations), the implied odd-N expressions are not correct. One either has to rederive the even-N combination with the correct $(-1)^N$-factors from the x-space representation of [64] and then use the differences given in [339] to obtain the odd-N expressions, or just use the even-/odd-N combinations from [81].

10.5.3 The Asymptotic Representations at $O(\alpha_s^2)$ in Mellin and x-Space

The heavy flavor Wilson coefficients are constructed as described above, and are given explicitly in Mellin space in the following. The appearing harmonic sums are reduced to the following basis:

$$\begin{aligned}&\{S_1(N), S_2(N), S_{-2}(N), S_3(N), S_{-3}(N), S_{2,1}(N), S_{-2,1}(N),\\ &S_4(N), S_{-4}(N), S_{3,1}(N), S_{-3,1}(N), S_{-2,2}(N), S_{2,1,1}(N)\}\,.\end{aligned} \tag{625}$$

For brevity, the arguments N will be omitted. The results are:

$$\begin{aligned}L_{2,q}^{W^+ + W^-,\rm NS,(2)} = C_F \Bigg\{ & \frac{8}{3} S_{2,1} - \frac{4}{9} {S_1}^3 + \frac{4}{3} S_2 S_1 - \frac{44 S_3}{9} - \frac{29N^2 + 29N - 6}{9N(N+1)} {S_1}^2 \\ & + \frac{85N^2 + 85N - 6}{9N(N+1)} S_2 - \frac{247N^4 + 620N^3 + 331N^2 + 66N + 72}{27N^2(N+1)^2} S_1 \\ & + \frac{P_{66}}{108N^3(N+1)^3} \Bigg\} \\ & + C_F T_F \ln^2\left(\frac{m^2}{Q^2}\right) \left\{ \frac{2(3N^2 + 3N + 2)}{3N(N+1)} - \frac{8}{3} S_1 \right\} \\ & + C_F T_F \ln\left(\frac{m^2}{Q^2}\right) \left\{ \frac{16}{3} S_2 - \frac{80}{9} S_1 + \frac{2(3N^4 + 6N^3 + 47N^2 + 20N - 12)}{9N^2(N+1)^2} \right\}\end{aligned}$$

$$+ C_F T_F \left\{ \frac{P_{67}}{54N^3(N+1)^3} - \frac{224}{27} S_1 + \frac{40}{9} S_2 - \frac{8}{3} S_3 \right\}, \tag{626}$$

$$P_{66} = 1371N^6 + 2517N^5 + 1397N^4 + 31N^3 + 140N^2 + 648N + 360\,, \tag{627}$$

$$P_{67} = 219N^6 + 657N^5 + 1193N^4 + 763N^3 - 40N^2 - 48N + 72\,, \tag{628}$$

$$\begin{aligned}
H_{2,q}^{W^+ + W^-,\mathrm{NS},(2)} = C_F^2 \Bigg\{ & 2{S_1}^4 + \frac{2(3N^2+3N-2)}{N(N+1)} {S_1}^3 - \frac{27N^4+26N^3-9N^2-40N-24}{2N^2(N+1)^2} {S_1}^2 \\
& - 16(-1)^N \zeta_2 {S_1}^2 + 16\zeta_2 {S_1}^2 - 32(-1)^N S_{-2} {S_1}^2 - 20 S_2 {S_1}^2 - \frac{P_{68}}{2N^3(N+1)^3} S_1 \\
& - \frac{8(-1)^N(4N-3)}{N(N+1)} S_1 \zeta_2 + \frac{8(4N-3)}{N(N+1)} S_1 \zeta_2 + 32(-1)^N \zeta_3 S_1 + 16\zeta_3 S_1 \\
& + 16(-1)^N S_{-3} S_1 - \frac{16(-1)^N(4N-3)}{N(N+1)} S_1 S_{-2} - \frac{2(9N^2+9N-10)}{N(N+1)} S_1 S_2 \\
& - 24 S_3 S_1 + 32(-1)^N S_{-2,1} S_1 + 16 S_{2,1} S_1 - \frac{64}{5}(-1)^N \zeta_2^2 + \frac{64\zeta_2^2}{5} + 24 {S_{-2}}^2 \\
& + 6 {S_2}^2 + \frac{P_{69}}{8(N-2)N^4(N+1)^4(N+3)} - \frac{4(-1)^N P_{70}}{(N-2)N^2(N+1)^2(N+3)} \zeta_2 \\
& + \frac{4P_{70}}{(N-2)N^2(N+1)^2(N+3)} \zeta_2 + \frac{4(-1)^N(4N-5)}{N(N+1)} \zeta_3 \\
& - \frac{4(18N^2-2N+7)}{N(N+1)} \zeta_3 + 40(-1)^N S_{-4} - \frac{32(-1)^N}{N+1} S_{-3} \\
& - \frac{8(-1)^N P_{70}}{(N-2)N^2(N+1)^2(N+3)} S_{-2} - 24(-1)^N \zeta_2 S_{-2} + 24\zeta_2 S_{-2} \\
& + \frac{95N^4+162N^3+35N^2-32N-16}{2N^2(N+1)^2} S_2 + 8(-1)^N \zeta_2 S_2 - 8\zeta_2 S_2 \\
& + 16(-1)^N S_{-2} S_2 - \frac{2(9N^2+25N-10)}{N(N+1)} S_3 + 12 S_4 - 32(-1)^N S_{-3,1} \\
& + \frac{32(-1)^N(2N-1)}{N(N+1)} S_{-2,1} - 16(-1)^N S_{-2,2} + \frac{4(3N^2+3N-2)}{N(N+1)} S_{2,1} \\
& + 40 S_{3,1} - 24 S_{2,1,1} \Bigg\} + C_F T_F \ln^2\left(\frac{m^2}{Q^2}\right) \left\{ \frac{2(3N^2+3N+2)}{3N(N+1)} - \frac{8}{3} S_1 \right\} \\
& + C_F T_F \ln\left(\frac{m^2}{Q^2}\right) \left\{ \frac{2(3N^4+6N^3+47N^2+20N-12)}{9N^2(N+1)^2} - \frac{80}{9} S_1 + \frac{16}{3} S_2 \right\} \\
& + C_F T_F \left\{ \frac{P_{71}}{54N^3(N+1)^3} - \frac{224}{27} S_1 + \frac{40}{9} S_2 - \frac{8}{3} S_3 \right\} \\
& + n_f C_F \Bigg\{ -\frac{4}{9} {S_1}^3 - \frac{29N^2+29N-6}{9N(N+1)} {S_1}^2 \\
& - \frac{247N^4+620N^3+331N^2+66N+72}{27N^2(N+1)^2} S_1 + \frac{4}{3} S_2 S_1 + \frac{P_{72}}{108N^3(N+1)^3}
\end{aligned}$$

$$
\begin{aligned}
&+\frac{85N^2+85N-6}{9N(N+1)}S_2-\frac{44}{9}S_3+\frac{8}{3}S_{2,1}\Bigg\}+C_F\Bigg\{-\frac{4}{9}{S_1}^3\\
&-\frac{29N^2+29N-6}{9N(N+1)}{S_1}^2-\frac{247N^4+620N^3+331N^2+66N+72}{27N^2(N+1)^2}S_1+\frac{4}{3}S_2S_1\\
&+\frac{P_{72}}{108N^3(N+1)^3}+\frac{85N^2+85N-6}{9N(N+1)}S_2-\frac{44}{9}S_3+\frac{8}{3}S_{2,1}\Bigg\}\\
&+C_AC_F\Bigg\{\frac{22}{9}{S_1}^3+\frac{(367N^2+367N-66)}{18N(N+1)}{S_1}^2+8(-1)^N\zeta_2{S_1}^2-8\zeta_2{S_1}^2\\
&+16(-1)^NS_{-2}{S_1}^2+4S_2{S_1}^2+\frac{P_{73}}{54N^2(N+1)^3}S_1+\frac{4(-1)^N(4N-3)}{N(N+1)}S_1\zeta_2\\
&-\frac{4(4N-3)}{N(N+1)}S_1\zeta_2-16(-1)^N\zeta_3S_1-32\zeta_3S_1-8(-1)^NS_{-3}S_1\\
&+\frac{8(-1)^N(4N-3)}{N(N+1)}S_1S_{-2}-\frac{2(11N^2+11N+6)}{3N(N+1)}S_1S_2+24S_3S_1\\
&-16(-1)^NS_{-2,1}S_1-16S_{2,1}S_1+\frac{32}{5}(-1)^N\zeta_2^2-\frac{32\zeta_2^2}{5}-12{S_{-2}}^2-4{S_2}^2\\
&-\frac{P_{74}}{216(N-2)N^3(N+1)^3(N+3)}+\frac{2(-1)^NP_{70}}{(N-2)N^2(N+1)^2(N+3)}\zeta_2\\
&-\frac{2P_{70}}{(N-2)N^2(N+1)^2(N+3)}\zeta_2-\frac{2(-1)^N(4N-5)}{N(N+1)}\zeta_3\\
&+\frac{2(27N^2+7N+13)}{N(N+1)}\zeta_3-20(-1)^NS_{-4}+\frac{16(-1)^N}{N+1}S_{-3}\\
&+\frac{4(-1)^NP_{70}}{(N-2)N^2(N+1)^2(N+3)}S_{-2}+12(-1)^N\zeta_2S_{-2}-12\zeta_2S_{-2}\\
&-\frac{(1067N^3+2134N^2+929N-66)}{18N(N+1)^2}S_2-4(-1)^N\zeta_2S_2+4\zeta_2S_2\\
&-8(-1)^NS_{-2}S_2+\frac{2(121N^2+193N-72)}{9N(N+1)}S_3-8S_4+16(-1)^NS_{-3,1}\\
&-\frac{16(-1)^N(2N-1)}{N(N+1)}S_{-2,1}+8(-1)^NS_{-2,2}-\frac{4(11N^2+11N-6)}{3N(N+1)}S_{2,1}\\
&-24S_{3,1}+24S_{2,1,1}\Bigg\}, \qquad (629)
\end{aligned}
$$

$$P_{68}=51N^6+203N^5+207N^4+33N^3+106N^2+160N+48\,, \qquad (630)$$

$$
\begin{aligned}
P_{69}=&\,331N^{10}+1179N^9-848N^8-4754N^7-2157N^6+4247N^5+3474N^4\\
&-2528N^3-4976N^2-2704N-480\,, \qquad (631)
\end{aligned}
$$

$$P_{70}=2N^6-2N^5-3N^4+26N^3-45N^2-34N-48\,, \qquad (632)$$

$$P_{71}=219N^6+657N^5+1193N^4+763N^3-40N^2-48N+72\,, \qquad (633)$$

$$P_{72}=1371N^6+2517N^5+1397N^4+31N^3+140N^2+648N+360\,, \qquad (634)$$

$$P_{73}=3155N^5+11607N^4+12279N^3+3329N^2+510N+792\,, \qquad (635)$$

$$P_{74}=16395N^8+47520N^7-51416N^6-162042N^5-99843N^4+7930N^3$$

$$+ 21432N^2 - 25848N - 23760\,, \tag{636}$$
$$\tag{637}$$

$$\begin{aligned}
H_{2,q}^{W^+-W^-,\mathrm{NS},(2)} = H_{2,q}^{W^++W^-,\mathrm{NS},(2)} + C_F(C_F - C_A/2)\Bigg\{ & 64(-1)^N S_{-3,1} - \frac{64(-1)^N(2N-1)}{N(N+1)} S_{-2,1} \\
& - 64(-1)^N S_1 S_{-2,1} + 32(-1)^N S_{-2,2} + \frac{16(2N^2+2N+1)}{N^3(N+1)^3} S_1 \\
& - \frac{16P_{75}}{(N-2)N^2(N+1)^2(N+2)(N+3)} \zeta_2 \\
& + \frac{16(-1)^N P_{76}}{(N-2)N^2(N+1)^2(N+2)(N+3)} S_{-2} \\
& + \frac{8(-1)^N P_{76}}{(N-2)N^2(N+1)^2(N+2)(N+3)} \zeta_2 \\
& - \frac{4P_{77}}{(N-2)N^4(N+1)^4(N+2)(N+3)} + 32(-1)^N \zeta_2 {S_1}^2 \\
& + 48(-1)^N \zeta_2 S_{-2} + \frac{16(-1)^N(4N-3)}{N(N+1)} S_1 \zeta_2 - 16(-1)^N \zeta_2 S_2 \\
& - 64(-1)^N \zeta_3 S_1 + 64(-1)^N S_{-2} {S_1}^2 - 80(-1)^N S_{-4} + \frac{64(-1)^N}{N+1} S_{-3} \\
& - 32(-1)^N S_{-3} S_1 + \frac{32(-1)^N(4N-3)}{N(N+1)} S_1 S_{-2} - 32(-1)^N S_{-2} S_2 \\
& + \frac{128}{5}(-1)^N \zeta_2^2 - \frac{8(-1)^N(4N-5)}{N(N+1)} \zeta_3 \Bigg\}\,,
\end{aligned} \tag{638}$$

$$P_{75} = 2N^5 + 6N^4 - 3N^3 - 33N^2 - 26N - 24\,, \tag{639}$$
$$P_{76} = 2N^7 + 2N^6 - 11N^5 + 8N^4 + 13N^3 - 58N^2 - 64N - 48\,, \tag{640}$$
$$P_{77} = N^9 + 6N^8 - 3N^7 + 75N^6 + 278N^5 + 239N^4 - 186N^3 - 386N^2 - 264N - 72\,, \tag{641}$$

$$\begin{aligned}
H_{2,q}^{W,\mathrm{PS},(2)} = & - C_F T_F \ln^2\left(\frac{m^2}{Q^2}\right) \frac{2(N^2+N+2)^2}{(N-1)N^2(N+1)^2(N+2)} \\
& - C_F T_F \ln\left(\frac{m^2}{Q^2}\right) \frac{4P_{78}}{(N-1)N^3(N+1)^3(N+2)^2} \\
& + C_F T_F \left\{ \frac{2P_{79}}{(N-1)N^4(N+1)^4(N+2)^3} - \frac{4(N^2+N+2)^2 S_2}{(N-1)N^2(N+1)^2(N+2)} \right\} \\
& + C_F \left\{ \frac{2(N^2+N+2)^2}{(N-1)N^2(N+1)^2(N+2)} {S_1}^2 - \frac{2(N^2+N+2)^2}{(N-1)N^2(N+1)^2(N+2)} S_2 \right. \\
& \left. + \frac{4P_{80}}{(N-1)N^3(N+1)^3(N+2)^2} S_1 + \frac{2P_{81}}{(N-1)N^4(N+1)^4(N+2)^3} \right.
\end{aligned}$$

$$+\frac{32(-1)^N}{(N-1)N(N+1)(N+2)}S_{-2}+\frac{16(-1)^N}{(N-1)N(N+1)(N+2)}\zeta_2$$
$$-\frac{16}{(N-1)N(N+1)(N+2)}\zeta_2\Bigg\}, \tag{642}$$

$$P_{78}=5N^5+32N^4+49N^3+38N^2+28N+8\,, \tag{643}$$
$$P_{79}=N^{10}+8N^9+29N^8+49N^7-11N^6-131N^5-161N^4-160N^3-168N^2$$
$$-80N-16\,, \tag{644}$$
$$P_{80}=N^7-15N^5-58N^4-92N^3-76N^2-48N-16\,, \tag{645}$$
$$P_{81}=3N^{10}+14N^9+33N^8+79N^7+297N^6+849N^5+1373N^4+1312N^3$$
$$+840N^2+368N+80\,, \tag{646}$$

$$L_{2,g}^{W,(2)}=T_F\ln\left(\frac{m^2}{Q^2}\right)\left\{-\frac{8(N^2+N+2)}{3N(N+1)(N+2)}S_1-\frac{8(N^3-4N^2-N-2)}{3N^2(N+1)(N+2)}\right\}, \tag{647}$$

$$\begin{aligned}H_{2,g}^{W,(2)}=\;&\ln^2\left(\frac{m^2}{Q^2}\right)\Bigg\{-T_F^2\frac{8(N^2+N+2)}{3N(N+1)(N+2)}+C_FT_F\Bigg(\frac{3N^4+6N^3+11N^2+8N+4}{N^2(N+1)^2(N+2)}\\
&-\frac{4(N^2+N+2)}{N(N+1)(N+2)}S_1\Bigg)+C_AT_F\Bigg(\frac{4(N^2+N+2)}{N(N+1)(N+2)}S_1\\
&-\frac{8(N^4+2N^3+4N^2+3N+2)}{(N-1)N^2(N+1)^2(N+2)^2}\Bigg)\Bigg\}+\ln\left(\frac{m^2}{Q^2}\right)\Bigg\{T_F\Bigg(-\frac{8(N^3-4N^2-N-2)}{3N^2(N+1)(N+2)}\\
&-\frac{8(N^2+N+2)}{3N(N+1)(N+2)}S_1\Bigg)+C_AT_F\Bigg(\frac{4(N^2+N+2)}{N(N+1)(N+2)}{S_1}^2-\frac{16(2N+3)}{(N+1)^2(N+2)^2}S_1\\
&-\frac{4P_{82}}{(N-1)N^3(N+1)^3(N+2)^3}+\frac{4(-1)^N(N^2+N+2)}{N(N+1)(N+2)}\zeta_2-\frac{4(N^2+N+2)}{N(N+1)(N+2)}\zeta_2\\
&+\frac{8(-1)^N(N^2+N+2)S_{-2}}{N(N+1)(N+2)}+\frac{4(N^2+N+2)}{N(N+1)(N+2)}S_2\Bigg)\\
&+C_FT_F\Bigg(-\frac{8(N^2+N+2)}{N(N+1)(N+2)}{S_1}^2-\frac{2(3N^4+2N^3-9N^2-16N-12)}{N^2(N+1)^2(N+2)}S_1\\
&+\frac{2(4N^6+5N^5-10N^4-39N^3-40N^2-24N-8)}{N^3(N+1)^3(N+2)}+\frac{8(N^2+N+2)}{N(N+1)(N+2)}S_2\Bigg)\Bigg\}\\
&+C_FT_F\Bigg\{-\frac{2(N^2+N+2)}{3N(N+1)(N+2)}{S_1}^3+\frac{2(3N+2)}{N^2(N+2)}{S_1}^2\\
&+\frac{2(N^4-N^3-20N^2-10N-4)}{N^2(N+1)^2(N+2)}S_1-\frac{2(N^2+N+2)}{N(N+1)(N+2)}S_1S_2+\frac{P_{83}}{N^4(N+1)^4(N+2)}\\
&+\frac{2(N^4+17N^3+17N^2-5N-2)}{N^2(N+1)^2(N+2)}S_2+\frac{8(N^2+N+2)}{3N(N+1)(N+2)}S_3\Bigg\}\end{aligned}$$

$$
+ C_A T_F \left\{ \frac{2(N^2+N+2)}{3N(N+1)(N+2)} {S_1}^3 - \frac{2(N^3+8N^2+11N+2)}{N(N+1)^2(N+2)^2} {S_1}^2 \right.
$$
$$
- \frac{2P_{84}}{N(N+1)^3(N+2)^3} S_1 + \frac{4(-1)^N(N^2+N+2)}{N(N+1)(N+2)} S_1\zeta_2 - \frac{4(N^2+N+2)}{N(N+1)(N+2)} S_1\zeta_2
$$
$$
+ \frac{8(-1)^N(N^2+N+2)}{N(N+1)(N+2)} S_1 S_{-2} + \frac{6(N^2+N+2)}{N(N+1)(N+2)} S_1 S_2
$$
$$
+ \frac{2P_{85}}{(N-1)N^4(N+1)^4(N+2)^4} + \frac{4(-1)^N(N^2-N-4)}{(N+1)^2(N+2)^2}\zeta_2 - \frac{4(N^2-N-4)}{(N+1)^2(N+2)^2}\zeta_2
$$
$$
- \frac{2(-1)^N(N^2+N+2)}{N(N+1)(N+2)}\zeta_3 + \frac{2(N^2+N+2)}{N(N+1)(N+2)}\zeta_3 + \frac{4(-1)^N(N^2+N+2)}{N(N+1)(N+2)} S_{-3}
$$
$$
+ \frac{8(-1)^N(N^2-N-4)}{(N+1)^2(N+2)^2} S_{-2} - \frac{2P_{86}}{(N-1)N^2(N+1)^2(N+2)^2} S_2
$$
$$
\left. + \frac{16(N^2+N+2)}{3N(N+1)(N+2)} S_3 - \frac{8(-1)^N(N^2+N+2)}{N(N+1)(N+2)} S_{-2,1} \right\}
$$
$$
+ C_A \left\{ -\frac{2(N^2+N+2)}{3N(N+1)(N+2)} {S_1}^3 - \frac{4P_{87}}{(N-1)N(N+1)^2(N+2)^2} {S_1}^2 \right.
$$
$$
- \frac{2P_{88}}{(N-1)N^3(N+1)^3(N+2)^3} S_1 + \frac{4(-1)^N(N-1)}{N(N+1)} S_1\zeta_2 - \frac{4(N-1)}{N(N+1)} S_1\zeta_2
$$
$$
+ \frac{8(-1)^N(N-1)}{N(N+1)} S_1 S_{-2} + \frac{10(N^2+N+2)}{N(N+1)(N+2)} S_1 S_2 - \frac{2P_{89}}{(N-1)N^4(N+1)^4(N+2)^4}
$$
$$
+ \frac{4(-1)^N P_{90}}{(N-1)N(N+1)^2(N+2)^2}\zeta_2 - \frac{4P_{90}}{(N-1)N(N+1)^2(N+2)^2}\zeta_2
$$
$$
- \frac{2(3N^2+3N-14)}{N(N+1)(N+2)}\zeta_3 - \frac{2(-1)^N(3N^2+3N+2)}{N(N+1)(N+2)}\zeta_3 - \frac{8(-1)^N(N^2+N+4)}{N(N+1)(N+2)} S_{-3}
$$
$$
+ \frac{8(-1)^N P_{90}}{(N-1)N(N+1)^2(N+2)^2} S_{-2} + \frac{4P_{91}}{(N-1)N(N+1)^2(N+2)^2} S_2
$$
$$
\left. + \frac{4(5N^2+5N-2)}{3N(N+1)(N+2)} S_3 + \frac{32(-1)^N}{N(N+1)(N+2)} S_{-2,1} - \frac{8(N^2+N+2)}{N(N+1)(N+2)} S_{2,1} \right\}
$$
$$
+ C_F \left\{ -\frac{10(N^2+N+2)}{3N(N+1)(N+2)} {S_1}^3 - \frac{(9N^4+12N^3+N^2-14N-16)}{N^2(N+1)^2(N+2)} {S_1}^2 \right.
$$
$$
+ \frac{2P_{92}}{N^3(N+1)^3(N+2)} S_1 + \frac{32(-1)^N}{N(N+1)(N+2)} S_1\zeta_2 - \frac{32}{N(N+1)(N+2)} S_1\zeta_2
$$
$$
+ \frac{64(-1)^N}{N(N+1)(N+2)} S_1 S_{-2} + \frac{6(N^2+N+2)}{N(N+1)(N+2)} S_1 S_2
$$
$$
- \frac{P_{93}}{(N-2)N^4(N+1)^4(N+2)(N+3)} + \frac{4(-1)^N P_{94}}{(N-2)N^2(N+1)^2(N+2)(N+3)}\zeta_2
$$
$$
- \frac{4P_{94}}{(N-2)N^2(N+1)^2(N+2)(N+3)}\zeta_2 + \frac{8(3N^2+3N-4)}{N(N+1)(N+2)}\zeta_3
$$
$$
- \frac{16(-1)^N}{N(N+1)(N+2)}\zeta_3 + \frac{32(-1)^N}{N(N+1)(N+2)} S_{-3}
$$

$$+\frac{8(-1)^N P_{94}}{(N-2)N^2(N+1)^2(N+2)(N+3)}S_{-2}+\frac{9N^4+8N^3+9N^2+6N-8}{N^2(N+1)^2(N+2)}S_2$$
$$-\frac{32(N^2+N-1)}{3N(N+1)(N+2)}S_3-\frac{64(-1)^N}{N(N+1)(N+2)}S_{-2,1}+\frac{8(N^2+N+2)}{N(N+1)(N+2)}S_{2,1}\Bigg\}, \quad (648)$$

$$P_{82}=N^9+6N^8+15N^7+25N^6+36N^5+85N^4+128N^3+104N^2+64N+16\,, \quad (649)$$
$$P_{83}=12N^8+52N^7+132N^6+216N^5+191N^4+54N^3-25N^2-20N-4\,, \quad (650)$$
$$P_{84}=N^6+8N^5+23N^4+54N^3+94N^2+72N+8\,, \quad (651)$$
$$P_{85}=2N^{12}+20N^{11}+86N^{10}+192N^9+199N^8-N^7-297N^6-495N^5-514N^4$$
$$-488N^3-416N^2-176N-32\,, \quad (652)$$
$$P_{86}=7N^5+21N^4+13N^3+21N^2+18N+16\,, \quad (653)$$
$$P_{87}=N^5-2N^4-6N^3-3N^2-12N-2\,, \quad (654)$$
$$P_{88}=7N^9+5N^8-43N^7+25N^6+296N^5+498N^4+524N^3+336N^2+144N+32\,, \quad (655)$$
$$P_{89}=4N^{12}+34N^{11}+100N^{10}+116N^9-81N^8-637N^7-1677N^6-3093N^5$$
$$-3998N^4-3472N^3-2064N^2-816N-160\,, \quad (656)$$
$$P_{90}=N^5-N^4-5N^3+3N^2+14N+12\,, \quad (657)$$
$$P_{91}=N^5-10N^3-9N^2-4N-2\,, \quad (658)$$
$$P_{92}=N^6-7N^5-3N^4-5N^3-30N^2-40N-16\,, \quad (659)$$
$$P_{93}=2N^{10}+18N^9+98N^8+98N^7-425N^6-1071N^5-477N^4+651N^3+886N^2$$
$$+484N+120\,, \quad (660)$$
$$P_{94}=N^6+7N^5-7N^4-39N^3+14N^2+40N+48\,, \quad (661)$$

$$L_{3,q}^{W^+ + W^-,\mathrm{NS},(2)}=L_{2,q}^{W^+ + W^-,\mathrm{NS},(2)}+C_F\left\{\frac{2(38N^3+27N^2-17N-12)}{9N^2(N+1)^2}+\frac{4(2N+1)}{3N(N+1)}S_1\right\}, \quad (662)$$

$$H_{3,q}^{W^+ + W^-,\mathrm{NS},(2)}=H_{2,q}^{W^+ + W^-,\mathrm{NS},(2)}+C_F^2\Bigg\{\frac{128}{5}(-1)^N\zeta_2^2+32(-1)^N{S_1}^2\zeta_2$$
$$+\frac{32P_{95}}{(N-2)(N-1)N^2(N+1)^2(N+2)(N+3)}\zeta_2$$
$$+\frac{8(-1)^N P_{96}}{(N-2)(N-1)N^2(N+1)^2(N+2)(N+3)}\zeta_2+48(-1)^N S_{-2}\zeta_2$$
$$-\frac{16(2N-1)}{N(N+1)}\zeta_2 S_1+\frac{32(-1)^N(N-1)}{N(N+1)}\zeta_2 S_1-16(-1)^N S_2\zeta_2$$
$$-\frac{4(2N+1)}{N(N+1)}{S_1}^2+64(-1)^N S_{-2}{S_1}^2$$
$$+\frac{P_{97}}{(N-2)(N-1)N^4(N+1)^4(N+2)(N+3)}-\frac{40(2N-1)}{N(N+1)}\zeta_3$$
$$-\frac{16(-1)^N(N-2)}{N(N+1)}\zeta_3-80(-1)^N S_{-4}+\frac{16(-1)^N(2N+1)}{N(N+1)}S_{-3}$$

$$
\begin{aligned}
&+\frac{16(-1)^N P_{96}}{(N-2)(N-1)N^2(N+1)^2(N+2)(N+3)}S_{-2}+\frac{2P_{98}}{N^3(N+1)^3}S_1\\
&-64(-1)^N\zeta_3 S_1-32(-1)^N S_{-3}S_1+\frac{64(-1)^N(N-1)}{N(N+1)}S_1S_{-2}+\frac{4(2N+1)}{N(N+1)}S_2\\
&-32(-1)^N S_{-2}S_2+\frac{16(2N-1)}{N(N+1)}S_3+64(-1)^N S_{-3,1}-\frac{32(-1)^N(2N-1)}{N(N+1)}S_{-2,1}\\
&-64(-1)^N S_1S_{-2,1}+32(-1)^N S_{-2,2}\Bigg\}+n_fC_F\Bigg\{\frac{2(38N^3+27N^2-17N-12)}{9N^2(N+1)^2}\\
&+\frac{4(2N+1)S_1}{3N(N+1)}\Bigg\}+C_F\Bigg\{\frac{2(38N^3+27N^2-17N-12)}{9N^2(N+1)^2}+\frac{4(2N+1)S_1}{3N(N+1)}\Bigg\}\\
&+C_AC_F\Bigg\{-\frac{64}{5}(-1)^N\zeta_2^2-16(-1)^N{S_1}^2\zeta_2\\
&-\frac{16P_{95}}{(N-2)(N-1)N^2(N+1)^2(N+2)(N+3)}\zeta_2\\
&-\frac{4(-1)^N P_{96}}{(N-2)(N-1)N^2(N+1)^2(N+2)(N+3)}\zeta_2-24(-1)^N S_{-2}\zeta_2\\
&+\frac{8(2N-1)}{N(N+1)}\zeta_2S_1-\frac{16(-1)^N(N-1)}{N(N+1)}\zeta_2S_1+8(-1)^N S_2\zeta_2-32(-1)^N S_{-2}{S_1}^2\\
&+\frac{P_{99}}{9(N-2)(N-1)N^4(N+1)^4(N+2)(N+3)}+\frac{20(2N-1)}{N(N+1)}\zeta_3\\
&+\frac{8(-1)^N(N-2)}{N(N+1)}\zeta_3+40(-1)^N S_{-4}-\frac{8(-1)^N(2N+1)}{N(N+1)}S_{-3}\\
&-\frac{8(-1)^N P_{96}}{(N-2)(N-1)N^2(N+1)^2(N+2)(N+3)}S_{-2}\\
&-\frac{2(46N^5+67N^4-4N^3-N^2+24N+12)}{3N^3(N+1)^3}S_1+32(-1)^N\zeta_3S_1\\
&+16(-1)^N S_{-3}S_1-\frac{32(-1)^N(N-1)}{N(N+1)}S_1S_{-2}+16(-1)^N S_{-2}S_2-\frac{8(2N-1)}{N(N+1)}S_3\\
&-32(-1)^N S_{-3,1}+\frac{16(-1)^N(2N-1)}{N(N+1)}S_{-2,1}+32(-1)^N S_1S_{-2,1}\\
&-16(-1)^N S_{-2,2}\Bigg\}, \qquad (663)
\end{aligned}
$$

$$
\begin{aligned}
P_{95} &= N^7+N^6-7N^5-N^4+16N^3-6N^2-4N-12\,, &(664)\\
P_{96} &= 2N^8+4N^7-5N^6-N^5-17N^4-67N^3-16N^2+4N+48\,, &(665)\\
P_{97} &= 34N^{11}+161N^{10}-135N^9-1238N^8-832N^7+1573N^6+2113N^5\\
&\quad +1352N^4+884N^3+120N^2-672N-288\,, &(666)\\
P_{98} &= 18N^5+23N^4-4N^3+13N^2+22N+8\,, &(667)\\
P_{99} &= -430N^{11}-2089N^{10}+159N^9+11688N^8+11736N^7-9189N^6-16613N^5-8006N^4\\
&\quad -3708N^3-1260N^2+2592N+1296\,, &(668)
\end{aligned}
$$

$$
\begin{aligned}
H_{3,q}^{W^+-W^-,\mathrm{NS},(2)} = H_{3,q}^{W^++W^-,\mathrm{NS},(2)} &+ C_F(C_F - C_A/2)\Bigg\{-64(-1)^N S_{-3,1} + 64(-1)^N S_1 S_{-2,1} \\
&- 32(-1)^N S_{-2,2} - \frac{16(2N^2+2N+1)}{N^3(N+1)^3} S_1 \\
&- \frac{16(-1)^N(2N^4+2N^3+N^2+2N-4)}{(N-1)N^2(N+2)} S_{-2} \\
&+ \frac{16(N^4+2N^3-3N^2-4N-2)}{(N-1)N^2(N+1)^2(N+2)} \zeta_2 \\
&- \frac{8(-1)^N(2N^4+2N^3+N^2+2N-4)}{(N-1)N^2(N+2)} \zeta_2 + \frac{4P_{100}}{(N-1)N^4(N+1)^4(N+2)} \\
&- 32(-1)^N \zeta_2 {S_1}^2 - 48(-1)^N \zeta_2 S_{-2} + \frac{16(-1)^N}{N(N+1)} S_1 \zeta_2 + 16(-1)^N \zeta_2 S_2 \\
&+ 64(-1)^N \zeta_3 S_1 - 64(-1)^N S_{-2} {S_1}^2 + 80(-1)^N S_{-4} - \frac{32(-1)^N}{N(N+1)} S_{-3} \\
&+ 32(-1)^N S_{-3} S_1 + \frac{32(-1)^N}{N(N+1)} S_1 S_{-2} + 32(-1)^N S_{-2} S_2 \\
&- \frac{128}{5}(-1)^N \zeta_2^2 - \frac{24(-1)^N}{N(N+1)} \zeta_3 \Bigg\}, \qquad (669)
\end{aligned}
$$

$$
P_{100} = 9N^8 + 36N^7 + 41N^6 + 13N^5 + 44N^4 + 67N^3 + 20N^2 - 26N - 12\,, \qquad (670)
$$

$$
\begin{aligned}
H_{3,q}^{W,\mathrm{PS},(2)} &= C_F T_F \ln^2\left(\frac{m^2}{Q^2}\right) \frac{2(N^2+N+2)^2}{(N-1)N^2(N+1)^2(N+2)} \\
&+ C_F T_F \ln\left(\frac{m^2}{Q^2}\right) \frac{4P_{101}}{(N-1)N^3(N+1)^3(N+2)^2} \\
&+ C_F T_F \left\{\frac{4(N^2+N+2)^2}{(N-1)N^2(N+1)^2(N+2)} S_2 - \frac{2P_{102}}{(N-1)N^4(N+1)^4(N+2)^3}\right\}, \qquad (671)
\end{aligned}
$$

$$
P_{101} = 5N^5 + 32N^4 + 49N^3 + 38N^2 + 28N + 8\,, \qquad (672)
$$

$$
\begin{aligned}
P_{102} = {} & N^{10} + 8N^9 + 29N^8 + 49N^7 - 11N^6 - 131N^5 - 161N^4 - 160N^3 \\
& - 168N^2 - 80N - 16\,, \qquad (673)
\end{aligned}
$$

$$
\begin{aligned}
H_{3,g}^{W,(2)} = {} & \ln^2\left(\frac{m^2}{Q^2}\right)\Bigg\{T_F^2 \frac{8(N^2+N+2)}{3N(N+1)(N+2)} + C_A T_F \left(\frac{8(N^4+2N^3+4N^2+3N+2)}{(N-1)N^2(N+1)^2(N+2)^2}\right. \\
& \left. - \frac{4(N^2+N+2)}{N(N+1)(N+2)} S_1\right) + C_F T_F \left(\frac{4(N^2+N+2)}{N(N+1)(N+2)} S_1\right.
\end{aligned}
$$

$$
- \frac{3N^4+6N^3+11N^2+8N+4}{N^2(N+1)^2(N+2)}\Bigg)\Bigg\} + \ln\left(\frac{m^2}{Q^2}\right)\Bigg\{C_F T_F\left(\frac{8(N^2+N+2){S_1}^2}{N(N+1)(N+2)}\right.
$$
$$
+ \frac{2(3N^4+2N^3-9N^2-16N-12)S_1}{N^2(N+1)^2(N+2)} - \frac{2P_{103}}{N^3(N+1)^3(N+2)}
$$
$$
\left. - \frac{8(N^2+N+2)}{N(N+1)(N+2)}S_2\right) + C_A T_F\left(-\frac{4(N^2+N+2)}{N(N+1)(N+2)}{S_1}^2 + \frac{16(2N+3)}{(N+1)^2(N+2)^2}S_1\right.
$$
$$
+ \frac{4P_{104}}{(N-1)N^3(N+1)^3(N+2)^3} - \frac{4(-1)^N(N^2+N+2)}{N(N+1)(N+2)}\zeta_2 + \frac{4(N^2+N+2)}{N(N+1)(N+2)}\zeta_2
$$
$$
\left. - \frac{8(-1)^N(N^2+N+2)}{N(N+1)(N+2)}S_{-2} - \frac{4(N^2+N+2)}{N(N+1)(N+2)}S_2\right)\Bigg\}
$$
$$
+ C_F T_F\Bigg\{\frac{2(N^2+N+2)}{3N(N+1)(N+2)}{S_1}^3 - \frac{2(3N+2)}{N^2(N+2)}{S_1}^2
$$
$$
- \frac{2(N^4-N^3-20N^2-10N-4)}{N^2(N+1)^2(N+2)}S_1 + \frac{2(N^2+N+2)}{N(N+1)(N+2)}S_1S_2 - \frac{P_{105}}{N^4(N+1)^4(N+2)}
$$
$$
\left. - \frac{2(N^4+17N^3+17N^2-5N-2)}{N^2(N+1)^2(N+2)}S_2 - \frac{8(N^2+N+2)}{3N(N+1)(N+2)}S_3\right\}
$$
$$
+ C_A T_F\Bigg\{-\frac{2(N^2+N+2)}{3N(N+1)(N+2)}{S_1}^3 + \frac{2(N^3+8N^2+11N+2)}{N(N+1)^2(N+2)^2}{S_1}^2
$$
$$
+ \frac{2P_{106}}{N(N+1)^3(N+2)^3}S_1 - \frac{4(-1)^N(N^2+N+2)}{N(N+1)(N+2)}S_1\zeta_2 + \frac{4(N^2+N+2)}{N(N+1)(N+2)}S_1\zeta_2
$$
$$
- \frac{8(-1)^N(N^2+N+2)}{N(N+1)(N+2)}S_1S_{-2} - \frac{6(N^2+N+2)}{N(N+1)(N+2)}S_1S_2
$$
$$
- \frac{2P_{107}}{(N-1)N^4(N+1)^4(N+2)^4} - \frac{4(-1)^N(N^2-N-4)}{(N+1)^2(N+2)^2}\zeta_2 + \frac{4(N^2-N-4)}{(N+1)^2(N+2)^2}\zeta_2
$$
$$
+ \frac{2(-1)^N(N^2+N+2)}{N(N+1)(N+2)}\zeta_3 - \frac{2(N^2+N+2)}{N(N+1)(N+2)}\zeta_3 - \frac{4(-1)^N(N^2+N+2)}{N(N+1)(N+2)}S_{-3}
$$
$$
- \frac{8(-1)^N(N^2-N-4)}{(N+1)^2(N+2)^2}S_{-2} + \frac{2(7N^5+21N^4+13N^3+21N^2+18N+16)}{(N-1)N^2(N+1)^2(N+2)^2}S_2
$$
$$
\left. - \frac{16(N^2+N+2)}{3N(N+1)(N+2)}S_3 + \frac{8(-1)^N(N^2+N+2)}{N(N+1)(N+2)}S_{-2,1}\right\}, \tag{674}
$$

$$
P_{103} = 4N^6+7N^5-5N^4-31N^3-33N^2-22N-8\,, \tag{675}
$$
$$
P_{104} = N^9+6N^8+15N^7+25N^6+36N^5+85N^4+128N^3+104N^2+64N+16\,, \tag{676}
$$
$$
P_{105} = 12N^8+52N^7+132N^6+216N^5+191N^4+54N^3-25N^2-20N-4\,, \tag{677}
$$
$$
P_{106} = N^6+8N^5+23N^4+54N^3+94N^2+72N+8\,, \tag{678}
$$
$$
P_{107} = 2N^{12}+20N^{11}+86N^{10}+192N^9+199N^8-N^7-297N^6-495N^5
$$
$$
- 514N^4-488N^3-416N^2-176N-32\,. \tag{679}
$$

Since QCD analyses of deep-inelastic scattering data are commonly performed in x-space, the heavy flavor Wilson coefficients are also given after a Mellin inversion. Here the harmonic

polylogarithms occur, which are reduced to the following basis set :

$$\{H_0(x), H_1(x), H_{-1}(x), H_{0,1}(x), H_{0,-1}(x), H_{0,0,1}(x), H_{0,0,-1}(x), H_{0,1,1}(x), H_{0,1,-1}(x), H_{0,-1,1}(x), H_{0,-1,-1}(x)\} . \tag{680}$$

Also here, arguments x will not be written explicitly. The coefficients then take the form :

$$\begin{aligned}
L_{2,q}^{W^+ + W^-,\mathrm{NS},(2)} &= C_F \Bigg\{ \frac{457}{36}\delta(1-x) + \Bigg[\frac{8H_{0,1}}{3(1-x)} + \frac{10{H_0}^2}{3(1-x)} + \frac{8H_1H_0}{3(1-x)} + \frac{38H_0}{3(1-x)} \\
&+ \frac{4{H_1}^2}{3(1-x)} + \frac{58H_1}{9(1-x)} - \frac{16\zeta_2}{3(1-x)} + \frac{247}{27(1-x)} \Bigg]_+ - \frac{4}{3}(x+1)H_{0,1} \\
&- \frac{5}{3}(x+1){H_0}^2 - \frac{2}{3}(19x+13)H_0 - \frac{4}{3}(x+1)H_1H_0 - \frac{2}{3}(x+1){H_1}^2 \\
&- \frac{4}{9}(17x+8)H_1 + \frac{8}{3}(x+1)\zeta_2 - \frac{488x}{27} - \frac{158}{27} \Bigg\} \\
&+ C_F T_F \ln\left(\frac{m^2}{Q^2}\right) \Bigg\{ \frac{2}{3}\delta(1-x) + \Bigg[\frac{16H_0}{3(1-x)} + \frac{80}{9(1-x)} \Bigg]_+ - \frac{8}{3}(x+1)H_0 \\
&- \frac{88x}{9} + \frac{8}{9} \Bigg\} + C_F T_F \Bigg\{ \frac{73}{18}\delta(1-x) + \Bigg[\frac{4{H_0}^2}{3(1-x)} + \frac{40H_0}{9(1-x)} + \frac{224}{27(1-x)} \Bigg]_+ \\
&- \frac{2}{3}(x+1){H_0}^2 - \frac{4}{9}(11x-1)H_0 - \frac{268x}{27} + \frac{44}{27} \Bigg\} \\
&+ C_F T_F \ln^2\left(\frac{m^2}{Q^2}\right) \Bigg\{ 2\delta(1-x) - \Bigg[\frac{8}{3(x-1)} \Bigg]_+ - \frac{4x}{3} - \frac{4}{3} \Bigg\} ,
\end{aligned} \tag{681}$$

$$\begin{aligned}
H_{2,q}^{W^+ + W^-,\mathrm{NS},(2)} &= C_F^2 \Bigg\{ \left(\frac{64\zeta_2^2}{5} + 8\zeta_2 - 72\zeta_3 + \frac{331}{8} \right)\delta(1-x) + \Bigg[-\frac{8{H_0}^3}{3(1-x)} - \frac{12H_1{H_0}^2}{1-x} \\
&- \frac{3{H_0}^2}{1-x} - \frac{32{H_1}^2H_0}{1-x} + \frac{48\zeta_2H_0}{1-x} - \frac{36H_1H_0}{1-x} + \frac{48H_{0,-1}H_0}{1-x} - \frac{24H_{0,1}H_0}{1-x} \\
&+ \frac{61H_0}{1-x} - \frac{8{H_1}^3}{1-x} - \frac{18{H_1}^2}{1-x} + \frac{24\zeta_2}{1-x} + \frac{64\zeta_3}{1-x} + \frac{16\zeta_2H_1}{1-x} + \frac{27H_1}{1-x} + \frac{16H_1H_{0,1}}{1-x} \\
&+ \frac{12H_{0,1}}{1-x} - \frac{96H_{0,0,-1}}{1-x} + \frac{24H_{0,0,1}}{1-x} - \frac{24H_{0,1,1}}{1-x} + \frac{51}{2(1-x)} \Bigg]_+ \\
&+ \left(x + 5 - \frac{4}{x+1} \right){H_0}^3 + \left(40x - 16 + \frac{40}{x+1} \right)H_{-1}{H_0}^2 + (10-14x)H_1{H_0}^2 \\
&+ \left(-56x + 8 - \frac{32}{x+1} \right){H_{-1}}^2H_0 + 16(x+1){H_1}^2H_0 + \left(\frac{72x^3}{5} - 2x + 12 \right){H_0}^2 \\
&+ \left(\frac{144x^2}{5} - \frac{502x}{5} - \frac{132}{5} - \frac{16}{x+1} - \frac{16}{5x} \right)H_0 + \left(-24x - 40 + \frac{16}{x+1} \right)\zeta_2H_0
\end{aligned}$$

$$+\left(-\frac{144x^3}{5}+40x+72+\frac{16}{5x^2}\right)H_{-1}H_0+32(x+1)H_1H_0$$
$$+\left(-80x-\frac{32}{x+1}\right)H_{0,-1}H_0+(56x+8)H_{0,1}H_0+4(x+1){H_1}^3+\frac{144x^2}{5}$$
$$+(18x+14){H_1}^2-\frac{461x}{5}+\left(-\frac{144x^3}{5}-8x-32\right)\zeta_2$$
$$+\left(72x-64+\frac{56}{x+1}\right)\zeta_3+\left(-72x-\frac{64}{x+1}+24\right)\zeta_2H_{-1}$$
$$+(16-68x)H_1+(32x-16)\zeta_2H_1+\left(\frac{144x^3}{5}-40x-72-\frac{16}{5x^2}\right)H_{0,-1}$$
$$+\left(112x-16+\frac{64}{x+1}\right)H_{-1}H_{0,-1}+16xH_{0,1}+\left(16x-16+\frac{32}{x+1}\right)H_{-1}H_{0,1}$$
$$-8(x+1)H_1H_{0,1}+\left(-112x+16-\frac{64}{x+1}\right)H_{0,-1,-1}$$
$$+\left(-16x+16-\frac{32}{x+1}\right)H_{0,-1,1}+\left(80x+32-\frac{16}{x+1}\right)H_{0,0,-1}$$
$$+\left(-60x+4-\frac{16}{x+1}\right)H_{0,0,1}+\left(-16x+16-\frac{32}{x+1}\right)H_{0,1,-1}$$
$$+16(x+1)H_{0,1,1}+\frac{16}{5x}-\frac{124}{5}\Bigg\}+\ln^2\left(\frac{m^2}{Q^2}\right)C_FT_F\Bigg\{2\delta(1-x)$$
$$+\left[\frac{8}{3(1-x)}\right]_+-\frac{4x}{3}-\frac{4}{3}\Bigg\}+\ln\left(\frac{m^2}{Q^2}\right)C_FT_F\Bigg\{\frac{2}{3}\delta(1-x)$$
$$+\left[\frac{16H_0}{3(1-x)}+\frac{80}{9(1-x)}\right]_+-\frac{88x}{9}-\frac{8}{3}(x+1)H_0+\frac{8}{9}\Bigg\}$$
$$+C_FT_F\Bigg\{\frac{73}{18}\delta(1-x)+\left[\frac{4{H_0}^2}{3(1-x)}+\frac{40H_0}{9(1-x)}+\frac{224}{27(1-x)}\right]_+-\frac{2}{3}(x+1){H_0}^2$$
$$-\frac{4}{9}(11x-1)H_0-\frac{268x}{27}+\frac{44}{27}\Bigg\}+n_fC_F\Bigg\{\frac{457}{36}\delta(1-x)+\Bigg[+\frac{10{H_0}^2}{3(1-x)}$$
$$+\frac{8H_1H_0}{3(1-x)}+\frac{38H_0}{3(1-x)}+\frac{4{H_1}^2}{3(1-x)}-\frac{16\zeta_2}{3(1-x)}+\frac{58H_1}{9(1-x)}+\frac{8H_{0,1}}{3(1-x)}$$
$$+\frac{247}{27(1-x)}\Bigg]_+-\frac{5}{3}(x+1){H_0}^2-\frac{2}{3}(19x+13)H_0-\frac{4}{3}(x+1)H_1H_0$$
$$-\frac{2}{3}(x+1){H_1}^2-\frac{488x}{27}+\frac{8}{3}(x+1)\zeta_2-\frac{4}{9}(17x+8)H_1-\frac{4}{3}(x+1)H_{0,1}-\frac{158}{27}\Bigg\}$$

$$+ C_F\Bigg\{\frac{457}{36}\delta(1-x) + \Bigg[\frac{10{H_0}^2}{3(1-x)} + \frac{8H_1H_0}{3(1-x)} + \frac{38H_0}{3(1-x)} + \frac{4{H_1}^2}{3(1-x)}$$
$$- \frac{16\zeta_2}{3(1-x)} + \frac{58H_1}{9(1-x)} + \frac{8H_{0,1}}{3(1-x)} + \frac{247}{27(1-x)}\Bigg]_+ - \frac{5}{3}(x+1){H_0}^2$$
$$- \frac{2}{3}(19x+13)H_0 - \frac{4}{3}(x+1)H_1H_0 - \frac{2}{3}(x+1){H_1}^2 - \frac{488x}{27} + \frac{8}{3}(x+1)\zeta_2$$
$$- \frac{4}{9}(17x+8)H_1 - \frac{4}{3}(x+1)H_{0,1} - \frac{158}{27}\Bigg\} + C_AC_F\Bigg\{\Bigg(-\frac{32\zeta_2^2}{5} - 4\zeta_2$$
$$+ 54\zeta_3 - \frac{5465}{72}\Bigg)\delta(1-x) + \Bigg[-\frac{2{H_0}^3}{1-x} - \frac{8H_1{H_0}^2}{1-x} - \frac{55{H_0}^2}{3(1-x)} + \frac{4{H_1}^2H_0}{1-x}$$
$$+ \frac{8\zeta_2H_0}{1-x} - \frac{44H_1H_0}{3(1-x)} - \frac{24H_{0,-1}H_0}{1-x} + \frac{16H_{0,1}H_0}{1-x} - \frac{239H_0}{3(1-x)} - \frac{22{H_1}^2}{3(1-x)}$$
$$+ \frac{88\zeta_2}{3(1-x)} + \frac{4\zeta_3}{1-x} + \frac{24\zeta_2H_1}{1-x} - \frac{367H_1}{9(1-x)} - \frac{16H_1H_{0,1}}{1-x} - \frac{44H_{0,1}}{3(1-x)}$$
$$+ \frac{48H_{0,0,-1}}{1-x} - \frac{24H_{0,0,1}}{1-x} + \frac{24H_{0,1,1}}{1-x} - \frac{3155}{54(1-x)}\Bigg]_+ + \Bigg(2x + \frac{2}{x+1}\Bigg){H_0}^3$$
$$+ \Bigg(-\frac{36x^3}{5} + \frac{115x}{6} + \frac{55}{6}\Bigg){H_0}^2 + \Bigg(-20x + 8 - \frac{20}{x+1}\Bigg)H_{-1}{H_0}^2$$
$$+ (14x+2)H_1{H_0}^2 + \Bigg(28x - 4 + \frac{16}{x+1}\Bigg){H_{-1}}^2H_0 - 2(x+1){H_1}^2H_0$$
$$+ \Bigg(-\frac{72x^2}{5} + \frac{1693x}{15} + \frac{8}{x+1} + \frac{583}{15} + \frac{8}{5x}\Bigg)H_0 + \Bigg(-8x - \frac{8}{x+1}\Bigg)\zeta_2H_0$$
$$+ \Bigg(\frac{72x^3}{5} - 20x - 36 - \frac{8}{5x^2}\Bigg)H_{-1}H_0 + \frac{22}{3}(x+1)H_1H_0$$
$$+ \Bigg(40x + \frac{16}{x+1}\Bigg)H_{0,-1}H_0 - (28x+4)H_{0,1}H_0 - \frac{72x^2}{5} + \frac{11}{3}(x+1){H_1}^2$$
$$+ \frac{17626x}{135} + \Bigg(\frac{72x^3}{5} - \frac{104x}{3} - \frac{44}{3}\Bigg)\zeta_2 + \Bigg(-56x + 12 - \frac{28}{x+1}\Bigg)\zeta_3$$
$$+ \Bigg(36x - 12 + \frac{32}{x+1}\Bigg)\zeta_2H_{-1} + \frac{4}{9}(167x+14)H_1 - (32x+8)\zeta_2H_1$$
$$+ \Bigg(-\frac{72x^3}{5} + 20x + 36 + \frac{8}{5x^2}\Bigg)H_{0,-1} + \Bigg(-56x + 8 - \frac{32}{x+1}\Bigg)H_{-1}H_{0,-1}$$
$$+ \frac{22}{3}(x+1)H_{0,1} + \Bigg(-8x + 8 - \frac{16}{x+1}\Bigg)H_{-1}H_{0,1} + 8(x+1)H_1H_{0,1}$$
$$+ \Bigg(56x - 8 + \frac{32}{x+1}\Bigg)H_{0,-1,-1} + \Bigg(8x - 8 + \frac{16}{x+1}\Bigg)H_{0,-1,1}$$

$$+\left(-40x-16+\frac{8}{x+1}\right)H_{0,0,-1}+\left(36x+4+\frac{8}{x+1}\right)H_{0,0,1}$$
$$+\left(8x-8+\frac{16}{x+1}\right)H_{0,1,-1}-12(x+1)H_{0,1,1}-\frac{8}{5x}+\frac{3709}{135}\Bigg\}, \tag{682}$$

$$H_{2,q}^{W^+-W^-,\mathrm{NS},(2)} = H_{2,q}^{W^++W^-,\mathrm{NS},(2)}+C_F(C_F-C_A/2)\Bigg\{\left(-\frac{144x^3}{5}+96x^2+\frac{16}{5x^2}\right.$$
$$\left.+64x+64\right)H_{0,-1}+\left(32x-32+\frac{64}{x+1}\right)H_0H_{0,-1}$$
$$+\left(-224x+32-\frac{128}{x+1}\right)H_{-1}H_{0,-1}+\left(-32x+32-\frac{64}{x+1}\right)H_{-1}H_{0,1}$$
$$+16(x+1)H_{0,1}+\left(224x-32+\frac{128}{x+1}\right)H_{0,-1,-1}$$
$$+\left(32x-32+\frac{64}{x+1}\right)H_{0,-1,1}+\left(96x+\frac{32}{x+1}\right)H_{0,0,-1}$$
$$+\left(16x-16+\frac{32}{x+1}\right)H_{0,0,1}+\left(32x-32+\frac{64}{x+1}\right)H_{0,1,-1}$$
$$+\left(-\frac{144x^2}{5}+\frac{292x}{5}+\frac{32}{x+1}-\frac{28}{5}+\frac{16}{5x}\right)H_0+\left(-\frac{72x^3}{5}+48x^2\right.$$
$$\left.+32x+8\right){H_0}^2+\left(\frac{144x^3}{5}-96x^2-\frac{16}{5x^2}-64x-64\right)H_{-1}H_0$$
$$+\left(-16x+16-\frac{32}{x+1}\right)\zeta_2H_0+\left(144x-48+\frac{128}{x+1}\right)\zeta_2H_{-1}$$
$$+\left(4x-4+\frac{8}{x+1}\right){H_0}^3+\left(-80x+32-\frac{80}{x+1}\right)H_{-1}{H_0}^2$$
$$+\left(112x-16+\frac{64}{x+1}\right){H_{-1}}^2H_0-32(x-1)H_1+\left(\frac{144x^3}{5}-96x^2\right.$$
$$\left.-56x-8\right)\zeta_2+\left(-136x+40-\frac{112}{x+1}\right)\zeta_3-\frac{144x^2}{5}-\frac{164x}{5}-\frac{16}{5x}+\frac{324}{5}\Bigg\}, \tag{683}$$

$$H_{2,q}^{W,\mathrm{PS},(2)} = C_FT_F\Bigg\{\left(\frac{16x^2}{3}+4x-4-\frac{16}{3x}\right)H_{0,1}+8(x+1)H_0H_{0,1}-16(x+1)H_{0,0,1}$$
$$+\left(\frac{8x^2}{3}+5x+1\right){H_0}^2+\left(-\frac{224x^2}{9}-\frac{44x}{3}-\frac{28}{3}\right)H_0+\left(-\frac{16x^2}{3}-4x\right.$$

$$
\begin{aligned}
&+ 4 + \frac{16}{3x}\Bigg) H_1 H_0 - \frac{2}{3}(x+1){H_0}^3 + \frac{800x^2}{27} + 16(x+1)\zeta_3 - \frac{62x}{3} - \frac{224}{27x} - \frac{2}{3}\Bigg\} \\
&+ C_F\Bigg\{\left(\frac{16x^2}{3} + 16x + 16 + \frac{16}{3x}\right) H_{0,-1} + \left(-\frac{32x^2}{3} + 4x - 4 - \frac{16}{3x}\right) H_{0,1} \\
&+ 8(x+1) H_0 H_{0,1} + 8(x+1) H_{0,1,1} + \left(-\frac{32x^2}{3} + 15x - 1\right) {H_0}^2 \\
&+ \left(-\frac{128x^2}{9} - \frac{88x}{3} + 56\right) H_0 + \left(-\frac{16x^2}{3} - 16x - 16 - \frac{16}{3x}\right) H_{-1} H_0 \\
&+ \left(-\frac{16x^2}{3} - 4x + 4 + \frac{16}{3x}\right) H_1 H_0 + \left(-\frac{8x^2}{3} - 2x + 2 + \frac{8}{3x}\right) {H_1}^2 \\
&+ \left(\frac{32x^2}{9} - \frac{80x}{3} + \frac{104}{3} - \frac{104}{9x}\right) H_1 - 16(x+1)\zeta_2 H_0 + \frac{10}{3}(x+1){H_0}^3 \\
&+ \left(16x^2 - 16x - \frac{16}{3x}\right)\zeta_2 + \frac{448x^2}{27} - 8(x+1)\zeta_3 - \frac{422x}{9} + \frac{344}{27x} + \frac{158}{9}\Bigg\} \\
&+ C_F T_F \ln^2\left(\frac{m^2}{Q^2}\right)\left\{-4(x+1)H_0 + \frac{8x^2}{3} + 2x - 2 - \frac{8}{3x}\right\} \\
&+ C_F T_F \ln\left(\frac{m^2}{Q^2}\right)\Bigg\{\left(-\frac{32x^2}{3} - 20x - 4\right) H_0 + 4(x+1){H_0}^2 + \frac{224x^2}{9} \\
&- 24x + 8 - \frac{80}{9x}\Bigg\}, \qquad (684)
\end{aligned}
$$

$$
\begin{aligned}
L_{2,g}^{W,(2)} = \ & \ln\left(\frac{m^2}{Q^2}\right) T_F \Bigg\{\left(-\frac{16x^2}{3} - \frac{8}{3} + \frac{16x}{3}\right) H_0 + \left(-\frac{16x^2}{3} - \frac{8}{3} + \frac{16x}{3}\right) H_1 \\
&- \frac{64x^2}{3} + \frac{64x}{3} - \frac{8}{3}\Bigg\}, \qquad (685)
\end{aligned}
$$

$$
\begin{aligned}
H_{2,g}^{W,(2)} = \ & \ln^2\left(\frac{m^2}{Q^2}\right)\Bigg\{T_F^2\left(-\frac{16x^2}{3} + \frac{16x}{3} - \frac{8}{3}\right) + C_F T_F\Big(\Big(-8x^2 + 4x - 2\Big) H_0 \\
&+ \Big(-8x^2 + 8x - 4\Big) H_1 + 4x - 1\Big) + C_A T_F\Bigg((-16x - 4)H_0 + \Big(8x^2 - 8x + 4\Big) H_1 \\
&+ \frac{62x^2}{3} - 16x - 2 - \frac{8}{3x}\Bigg)\Bigg\} + \ln\left(\frac{m^2}{Q^2}\right)\Bigg\{T_F\Bigg(\left(-\frac{16x^2}{3} + \frac{16x}{3} - \frac{8}{3}\right) H_0 \\
&+ \left(-\frac{16x^2}{3} + \frac{16x}{3} - \frac{8}{3}\right) H_1 - \frac{64x^2}{3} + \frac{64x}{3} - \frac{8}{3}\Bigg\} + C_A T_F\Bigg\{16\zeta_2 x + (8x+4){H_0}^2 \\
&+ \Big(8x^2 - 8x + 4\Big) {H_1}^2 + \left(-\frac{176x^2}{3} - 32x - 4\right) H_0 + \Big(16x^2 + 16x + 8\Big) H_{-1} H_0
\end{aligned}
$$

$$+\left(16x^2-16x\right)H_1+\left(-16x^2-16x-8\right)H_{0,-1}+\frac{872x^2}{9}-100x+8-\frac{80}{9x}\Bigg)$$
$$+C_FT_F(+\left(-16x^2+8x-4\right){H_0}^2+\left(-16x^2+16x-8\right){H_1}^2+\left(32x^2-24x+12\right)\zeta_2$$
$$+\left(-40x^2+24x-4\right)H_0+\left(-40x^2+48x-14\right)H_1+\left(-32x^2+32x-16\right)H_0H_1$$
$$+(4-8x)H_{0,1}-8x^2+34x-18)\Bigg\}+C_A\Bigg\{\frac{2}{3}(14x+5){H_0}^3$$
$$+\left(-\frac{194x^2}{3}+88x-1\right){H_0}^2+\left(12x^2+8x+4\right)H_{-1}{H_0}^2+\left(-8x^2+12x-6\right)H_1{H_0}^2$$
$$+(8x+4){H_{-1}}^2H_0+\left(-12x^2+12x-6\right){H_1}^2H_0+\left(-\frac{2090x^2}{9}+\frac{584x}{3}+58\right)H_0$$
$$+\left(16x^2-64x-8\right)\zeta_2H_0+\left(\frac{80x^2}{3}-24-\frac{16}{3x}\right)H_{-1}H_0+\left(-\frac{268x^2}{3}+80x\right.$$
$$\left.-4+\frac{16}{3x}\right)H_1H_0+\left(-8x^2-16x-8\right)H_{0,-1}H_0+(24x+12)H_{0,1}H_0$$
$$+\left(-\frac{4x^2}{3}+\frac{4x}{3}-\frac{2}{3}\right){H_1}^3-\frac{4493x^2}{27}+\left(-\frac{122x^2}{3}+36x-2+\frac{8}{3x}\right){H_1}^2+\frac{1072x}{9}$$
$$+\left(148x^2-144x+8-\frac{16}{3x}\right)\zeta_2+\left(24x^2-48x+4\right)\zeta_3+\left(-16x^2-8x-4\right)\zeta_2H_{-1}$$
$$+\left(-\frac{1570x^2}{9}+\frac{454x}{3}+\frac{62}{3}-\frac{104}{9x}\right)H_1+\left(8x^2-16x+8\right)\zeta_2H_1$$
$$+\left(-\frac{80x^2}{3}+24+\frac{16}{3x}\right)H_{0,-1}+(-16x-8)H_{-1}H_{0,-1}+\left(-\frac{176x^2}{3}+64x\right.$$
$$\left.-4-\frac{16}{3x}\right)H_{0,1}+\left(16x^2+16x+8\right)H_{-1}H_{0,1}+\left(16x^2-16x+8\right)H_1H_{0,1}$$
$$+(16x+8)H_{0,-1,-1}+\left(-16x^2-16x-8\right)H_{0,-1,1}+\left(-8x^2+16x+8\right)H_{0,0,-1}$$
$$+(-8x-4)H_{0,0,1}+\left(-16x^2-16x-8\right)H_{0,1,-1}+\left(-24x^2+56x-4\right)H_{0,1,1}$$
$$+\frac{344}{27x}+\frac{239}{9}\Bigg\}+C_FT_F\Bigg\{\left(\frac{4x^2}{3}-\frac{2x}{3}+\frac{1}{3}\right){H_0}^3+\left(10x^2-6x-\frac{1}{2}\right){H_0}^2$$
$$+\left(4x^2-4x+2\right)H_1{H_0}^2+\left(-24x^2-9x-8\right)H_0+\left(20x^2-24x+2\right)H_1H_0$$
$$+\left(-8x^2+16x-8\right)H_{0,1}H_0+\left(-\frac{4x^2}{3}+\frac{4x}{3}-\frac{2}{3}\right){H_1}^3+\left(-6x^2+4x+2\right){H_1}^2$$
$$+\left(12x^2-24x-4\right)\zeta_2+\left(8x^2+8x-4\right)\zeta_3+\left(26x-24x^2\right)H_1$$
$$+\left(-32x^2+48x+2\right)H_{0,1}+\left(8x^2-24x+12\right)H_{0,0,1}+\left(-8x^2+8x-4\right)H_{0,1,1}$$

$$+ 40x^2 - 41x + 13\Bigg\} + C_A T_F \Bigg\{ -\frac{2}{3}(2x+1){H_0}^3 + \left(\frac{23x^2}{3} + 4x + 1\right){H_0}^2$$
$$+ \left(4x^2 + 4x + 2\right) H_{-1}{H_0}^2 + \left(-8x^2 - 8x - 4\right) {H_{-1}}^2 H_0 + \left(-4x^2 + 4x - 2\right) {H_1}^2 H_0$$
$$+ \left(-\frac{800x^2}{9} - \frac{86x}{3} - \frac{28}{3}\right) H_0 + \left(8x^2 + 8x\right) H_{-1} H_0 + \Bigg(-\frac{130x^2}{3} + 32x$$
$$+ 6 + \frac{16}{3x}\Bigg) H_1 H_0 + \left(-8x^2 - 8x - 4\right) H_{0,-1} H_0 + (32x + 8) H_{0,1} H_0$$
$$+ \left(\frac{4x^2}{3} - \frac{4x}{3} + \frac{2}{3}\right) {H_1}^3 + \frac{3176x^2}{27} + \left(5x^2 - 4x - 1\right) {H_1}^2 - \frac{314x}{3} + \left(8x - 2x^2\right) \zeta_2$$
$$+ (56x + 16)\zeta_3 + \left(-8x^2 - 8x - 4\right) \zeta_2 H_{-1} + \left(8x^2 - 8x - 2\right) H_1 + \left(-8x^2 - 8x\right) H_{0,-1}$$
$$+ \left(16x^2 + 16x + 8\right) H_{-1} H_{0,-1} + \left(\frac{136x^2}{3} - 32x - 6 - \frac{16}{3x}\right) H_{0,1}$$
$$+ \left(-16x^2 - 16x - 8\right) H_{0,-1,-1} + \left(8x^2 + 8x + 4\right) H_{0,0,-1} + (-64x - 16) H_{0,0,1}$$
$$+ \left(8x^2 - 8x + 4\right) H_{0,1,1} - \frac{224}{27x} - \frac{2}{3}\Bigg\} + C_F \Bigg\{ \left(-\frac{20x^2}{3} + \frac{10x}{3} - \frac{5}{3}\right) {H_0}^3$$
$$+ \left(-\frac{48x^3}{5} - 36x^2 + \frac{22x}{3} - \frac{3}{2}\right) {H_0}^2 + \left(8x^2 + 16x + 8\right) H_{-1} {H_0}^2$$
$$+ \left(-12x^2 + 4x - 2\right) H_1 {H_0}^2 + \left(-16x^2 - 32x - 16\right) {H_{-1}}^2 H_0$$
$$+ \left(-16x^2 + 16x - 8\right) {H_1}^2 H_0 + \left(-\frac{216x^2}{5} + \frac{113x}{5} - \frac{236}{15} - \frac{8}{15x}\right) H_0$$
$$+ \left(48x^2 - 32x + 16\right) \zeta_2 H_0 + \left(\frac{96x^3}{5} + \frac{64x}{3} + 48 + \frac{8}{15x^2}\right) H_{-1} H_0$$
$$+ \left(-72x^2 + 80x - 26\right) H_1 H_0 + \left(16x^2 - 32x + 16\right) H_{0,-1} H_0$$
$$+ \left(-8x^2 + 16x - 8\right) H_{0,1} H_0 + \left(-\frac{20x^2}{3} + \frac{20x}{3} - \frac{10}{3}\right) {H_1}^3 - \frac{36x^2}{5}$$
$$+ \left(-36x^2 + 40x - 13\right) {H_1}^2 + \frac{239x}{5} + \left(\frac{96x^3}{5} + 72x^2 - \frac{104x}{3} + 16\right) \zeta_2$$
$$+ \left(72x^2 + 32\right) \zeta_3 + \left(-16x^2 - 32x - 16\right) \zeta_2 H_{-1} + \left(-24x^2 + 40x - 14\right) H_1$$
$$+ \left(32x^2 - 16x + 8\right) \zeta_2 H_1 + \left(-\frac{96x^3}{5} - \frac{64x}{3} - 48 - \frac{8}{15x^2}\right) H_{0,-1}$$
$$+ \left(32x^2 + 64x + 32\right) H_{-1} H_{0,-1} + (10 - 24x) H_{0,1} + \left(-16x^2 + 16x - 8\right) H_1 H_{0,1}$$
$$+ \left(-32x^2 - 64x - 32\right) H_{0,-1,-1} + \left(-48x^2 + 32x - 48\right) H_{0,0,-1}$$
$$+ \left(-8x^2 - 8x + 4\right) H_{0,0,1} + \left(24x^2 - 32x + 16\right) H_{0,1,1} + \frac{8}{15x} - \frac{647}{15}\Bigg\}, \tag{686}$$

$$
\begin{aligned}
L_{3,q}^{W^+ + W^-,\mathrm{NS},(2)} = C_F \Bigg(& \frac{457}{36}\delta(1-x) + \left[\frac{8H_{0,1}}{3(1-x)} + \frac{10{H_0}^2}{3(1-x)} + \frac{8H_1 H_0}{3(1-x)} + \frac{38H_0}{3(1-x)} + \frac{4{H_1}^2}{3(1-x)} \right. \\
& \left. + \frac{58H_1}{9(1-x)} - \frac{16\zeta_2}{3(1-x)} + \frac{247}{27(1-x)} \right]_+ - \frac{4}{3}(x+1)H_{0,1} - \frac{5}{3}(x+1){H_0}^2 \\
& + (-10x-6)H_0 - \frac{4}{3}(x+1)H_1 H_0 - \frac{2}{3}(x+1){H_1}^2 - \frac{4}{9}(14x+5)H_1 \\
& + \frac{8}{3}(x+1)\zeta_2 - \frac{302x}{27} - \frac{116}{27} \Bigg) + C_F T_F \ln\left(\frac{m^2}{Q^2}\right) \Bigg(\frac{2}{3}\delta(1-x) \\
& + \left[\frac{16H_0}{3(1-x)} + \frac{80}{9(1-x)} \right]_+ - \frac{8}{3}(x+1)H_0 - \frac{88x}{9} + \frac{8}{9} \Bigg) + C_F T_F \Bigg(\frac{73}{18}\delta(1-x) \\
& + \left[\frac{4{H_0}^2}{3(1-x)} + \frac{40H_0}{9(1-x)} + \frac{224}{27(1-x)} \right]_+ - \frac{2}{3}(x+1){H_0}^2 - \frac{4}{9}(11x-1)H_0 \\
& - \frac{268x}{27} + \frac{44}{27} \Bigg) + C_F T_F \ln^2\left(\frac{m^2}{Q^2}\right) \left(2\delta(1-x) + \left[\frac{8}{3(1-x)} \right]_+ - \frac{4x}{3} - \frac{4}{3} \right),
\end{aligned}
\tag{687}
$$

$$
\begin{aligned}
H_{3,q}^{W^+ + W^-,\mathrm{NS},(2)} = & H_{2,q}^{W^+ + W^-,\mathrm{NS},(2)} + C_F^2 \Bigg\{ \left(4x - 4 + \frac{8}{x+1} \right) {H_0}^3 + \left(-\frac{72x^3}{5} + 8x^2 \right. \\
& \left. + 28x + 12 \right) {H_0}^2 + \left(-56x + 40 - \frac{80}{x+1} \right) H_{-1}{H_0}^2 + (24x-8)H_1{H_0}^2 \\
& + \left(64x - 32 + \frac{64}{x+1} \right) {H_{-1}}^2 H_0 + \left(-\frac{144x^2}{5} + \frac{192x}{5} - \frac{68}{5} \right. \\
& \left. + \frac{32}{x+1} + \frac{16}{5x} \right) H_0 + \left(-16x + 16 - \frac{32}{x+1} \right) \zeta_2 H_0 + \left(\frac{144x^3}{5} - 16x^2 - 48x \right. \\
& \left. - 80 - \frac{16}{x} - \frac{16}{5x^2} \right) H_{-1} H_0 - 8(x+1)H_1 H_0 + \left(80x - 48 + \frac{64}{x+1} \right) H_{0,-1} H_0 \\
& + (16-48x)H_{0,1}H_0 - 4(x+1){H_1}^2 + \left(\frac{144x^3}{5} - 16x^2 - 44x - 12 \right) \zeta_2 \\
& + \left(-136x + 72 - \frac{112}{x+1} \right) \zeta_3 + \left(96x - 64 + \frac{128}{x+1} \right) \zeta_2 H_{-1} + (46x-10)H_1 \\
& + (16-48x)\zeta_2 H_1 + \left(-\frac{144x^3}{5} + 16x^2 + 48x + 80 + \frac{16}{x} + \frac{16}{5x^2} \right) H_{0,-1} \\
& + \left(-128x + 64 - \frac{128}{x+1} \right) H_{-1} H_{0,-1} + 12(x+1)H_{0,1}
\end{aligned}
$$

$$
+\left(-32x+32-\frac{64}{x+1}\right)H_{-1}H_{0,1}+\left(128x-64+\frac{128}{x+1}\right)H_{0,-1,-1}
+\left(32x-32+\frac{64}{x+1}\right)H_{0,-1,1}+\left(-48x+16+\frac{32}{x+1}\right)H_{0,0,-1}
+\left(64x-32+\frac{32}{x+1}\right)H_{0,0,1}+\left(32x-32+\frac{64}{x+1}\right)H_{0,1,-1}-\frac{144x^2}{5}
+\frac{561x}{5}-\frac{231}{5}-\frac{16}{5x}\right\}+n_fC_F\left\{\frac{62x}{9}+\frac{8}{3}(x+1)H_0+\frac{4}{3}(x+1)H_1+\frac{14}{9}\right\}
+C_F\left\{\frac{62x}{9}+\frac{8}{3}(x+1)H_0+\frac{4}{3}(x+1)H_1+\frac{14}{9}\right\}
+C_AC_F\left\{\left(-2x+2-\frac{4}{x+1}\right){H_0}^3+\left(\frac{36x^3}{5}-4x^2-16x-8\right){H_0}^2
+\left(28x-20+\frac{40}{x+1}\right)H_{-1}{H_0}^2+(4-12x)H_1{H_0}^2
+\left(-32x+16-\frac{32}{x+1}\right){H_{-1}}^2H_0+\left(\frac{72x^2}{5}-\frac{478x}{15}+\frac{2}{15}-\frac{16}{x+1}-\frac{8}{5x}\right)H_0
+\left(8x-8+\frac{16}{x+1}\right)\zeta_2H_0+\left(-\frac{72x^3}{5}+8x^2+24x+40+\frac{8}{x}+\frac{8}{5x^2}\right)H_{-1}H_0
+\left(-40x+24-\frac{32}{x+1}\right)H_{0,-1}H_0+(24x-8)H_{0,1}H_0+\left(-\frac{72x^3}{5}+8x^2
+28x+12\right)\zeta_2+\left(68x-36+\frac{56}{x+1}\right)\zeta_3+\left(-48x+32-\frac{64}{x+1}\right)\zeta_2H_{-1}
-\frac{2}{3}(47x-1)H_1+(24x-8)\zeta_2H_1+\left(\frac{72x^3}{5}-8x^2-24x-40
-\frac{8}{x}-\frac{8}{5x^2}\right)H_{0,-1}+\left(64x-32+\frac{64}{x+1}\right)H_{-1}H_{0,-1}-8(x+1)H_{0,1}
+\left(16x-16+\frac{32}{x+1}\right)H_{-1}H_{0,1}+\left(-64x+32-\frac{64}{x+1}\right)H_{0,-1,-1}
+\left(-16x+16-\frac{32}{x+1}\right)H_{0,-1,1}+\left(24x-8-\frac{16}{x+1}\right)H_{0,0,-1}
+\left(-32x+16-\frac{16}{x+1}\right)H_{0,0,1}+\left(-16x+16-\frac{32}{x+1}\right)H_{0,1,-1}+\frac{72x^2}{5}
-\frac{3517x}{45}+\frac{8}{5x}+\frac{647}{45}\right\},
\tag{688}
$$

$$
\begin{aligned}
H_{3,q}^{W^+-W^-,\mathrm{NS},(2)} &= H_{3,q}^{W^++W^-,\mathrm{NS},(2)} + C_F(C_F - C_A/2)\Bigg\{\left(-16x^2 - \frac{16}{x}\right)H_{0,-1} \\
&+ \left(-32x + 32 - \frac{64}{x+1}\right)H_0H_{0,-1} + \left(32x - 96 + \frac{128}{x+1}\right)H_{-1}H_{0,-1} \\
&- 16(x+1)H_{0,1} + \left(32x - 32 + \frac{64}{x+1}\right)H_{-1}H_{0,1} \\
&+ \left(-32x + 96 - \frac{128}{x+1}\right)H_{0,-1,-1} + \left(-32x + 32 - \frac{64}{x+1}\right)H_{0,-1,1} \\
&+ \left(32 - \frac{32}{x+1}\right)H_{0,0,-1} + \left(-16x + 16 - \frac{32}{x+1}\right)H_{0,0,1} \\
&+ \left(-32x + 32 - \frac{64}{x+1}\right)H_{0,1,-1} + \left(-8x^2 - 8x - 16\right){H_0}^2 \\
&+ \left(16x^2 + \frac{16}{x}\right)H_{-1}H_0 + \left(16x - 16 + \frac{32}{x+1}\right)\zeta_2 H_0 \\
&+ \left(-48x + 80 - \frac{128}{x+1}\right)\zeta_2 H_{-1} + \left(-4x + 4 - \frac{8}{x+1}\right){H_0}^3 \\
&+ \left(32x - 48 + \frac{80}{x+1}\right)H_{-1}{H_0}^2 + \left(-16x + 48 - \frac{64}{x+1}\right){H_{-1}}^2H_0 \\
&+ \left(60x + 28 - \frac{32}{x+1}\right)H_0 + 32(x-1)H_1 + \left(16x^2 + 8x + 24\right)\zeta_2 \\
&+ \left(40x - 72 + \frac{112}{x+1}\right)\zeta_3 - 60x + 60\Bigg\}, \qquad (689)
\end{aligned}
$$

$$
\begin{aligned}
H_{3,q}^{W,\mathrm{PS},(2)} &= C_FT_F\Bigg\{\left(-\frac{16x^2}{3} - 4x + \frac{16}{3x} + 4\right)H_{0,1} - 8(x+1)H_0H_{0,1} + 16(x+1)H_{0,0,1} \\
&+ \left(-\frac{8x^2}{3} - 5x - 1\right){H_0}^2 + \left(\frac{224x^2}{9} + \frac{44x}{3} + \frac{28}{3}\right)H_0 + \Bigg(\frac{16x^2}{3} + 4x \\
&- 4 - \frac{16}{3x}\Bigg)H_1H_0 + \frac{2}{3}(x+1){H_0}^3 - 16(x+1)\zeta_3 - \frac{800x^2}{27} + \frac{62x}{3} + \frac{224}{27x} + \frac{2}{3}\Bigg\} \\
&+ C_FT_F\ln^2\left(\frac{m^2}{Q^2}\right)\left\{4(x+1)H_0 - \frac{8x^2}{3} - 2x + 2 + \frac{8}{3x}\right\} \\
&+ C_FT_F\ln\left(\frac{m^2}{Q^2}\right)\Bigg\{\left(\frac{32x^2}{3} + 20x + 4\right)H_0 - 4(x+1){H_0}^2 - \frac{224x^2}{9} \\
&+ 24x - 8 + \frac{80}{9x}\Bigg\}, \qquad (690)
\end{aligned}
$$

$$
\begin{aligned}
H_{3,g}^{W,(2)} = \ & \ln^2\left(\frac{m^2}{Q^2}\right)\Bigg\{T_F^2\left(\frac{16x^2}{3}-\frac{16x}{3}+\frac{8}{3}\right)+C_AT_F\Bigg(-\frac{62x^2}{3}+16x+(16x+4)H_0 \\
& +\left(-8x^2+8x-4\right)H_1+2+\frac{8}{3x}\Bigg)+C_FT_F\Big(-4x+\left(8x^2-4x+2\right)H_0 \\
& +\left(8x^2-8x+4\right)H_1+1\Big)\Bigg\}+\ln\left(\frac{m^2}{Q^2}\right)\Bigg\{C_AT_F\Bigg(-16\zeta_2x+(-8x-4){H_0}^2 \\
& +\left(-8x^2+8x-4\right){H_1}^2+\left(\frac{176x^2}{3}+32x+4\right)H_0+\left(-16x^2-16x-8\right)H_{-1}H_0 \\
& +\left(16x-16x^2\right)H_1+\left(16x^2+16x+8\right)H_{0,-1}-\frac{872x^2}{9}+100x-8+\frac{80}{9x}\Bigg) \\
& +C_FT_F(14x^2-40x+\left(16x^2-8x+4\right){H_0}^2+\left(16x^2-16x+8\right){H_1}^2 \\
& +\left(-32x^2+24x-12\right)\zeta_2+\left(40x^2-28x+6\right)H_0+\left(40x^2-48x+14\right)H_1 \\
& +\left(32x^2-32x+16\right)H_0H_1+(8x-4)H_{0,1}+18)\Bigg\}+C_AT_F\Bigg\{\left(\frac{4x}{3}+\frac{2}{3}\right){H_0}^3 \\
& +\left(-\frac{23x^2}{3}-4x-1\right){H_0}^2+\left(-4x^2-4x-2\right)H_{-1}{H_0}^2+\left(8x^2+8x+4\right){H_{-1}}^2H_0 \\
& +\left(4x^2-4x+2\right){H_1}^2H_0+\left(\frac{800x^2}{9}+\frac{86x}{3}+\frac{28}{3}\right)H_0+\left(-8x^2-8x\right)H_{-1}H_0 \\
& +\left(\frac{130x^2}{3}-32x-6-\frac{16}{3x}\right)H_1H_0+\left(8x^2+8x+4\right)H_{0,-1}H_0+(-32x-8)H_{0,1}H_0 \\
& +\left(-\frac{4x^2}{3}+\frac{4x}{3}-\frac{2}{3}\right){H_1}^3-\frac{3176x^2}{27}+\left(-5x^2+4x+1\right){H_1}^2+\frac{314x}{3}+\left(2x^2-8x\right)\zeta_2 \\
& +(-56x-16)\zeta_3+\left(8x^2+8x+4\right)\zeta_2H_{-1}+\left(-8x^2+8x+2\right)H_1+\left(8x^2+8x\right)H_{0,-1} \\
& +\left(-16x^2-16x-8\right)H_{-1}H_{0,-1}+\left(-\frac{136x^2}{3}+32x+6+\frac{16}{3x}\right)H_{0,1} \\
& +\left(16x^2+16x+8\right)H_{0,-1,-1}+\left(-8x^2-8x-4\right)H_{0,0,-1}+(64x+16)H_{0,0,1} \\
& +\left(-8x^2+8x-4\right)H_{0,1,1}+\frac{224}{27x}+\frac{2}{3}\Bigg\}+C_FT_F\Bigg\{\left(-\frac{4x^2}{3}+\frac{2x}{3}-\frac{1}{3}\right){H_0}^3 \\
& +\left(-10x^2+6x+\frac{1}{2}\right){H_0}^2+\left(-4x^2+4x-2\right)H_1{H_0}^2+\left(24x^2+9x+8\right)H_0 \\
& +\left(-20x^2+24x-2\right)H_1H_0+\left(8x^2-16x+8\right)H_{0,1}H_0+\left(\frac{4x^2}{3}-\frac{4x}{3}+\frac{2}{3}\right){H_1}^3 \\
& -40x^2+\left(6x^2-4x-2\right){H_1}^2+41x+\left(-12x^2+24x+4\right)\zeta_2+\left(-8x^2-8x+4\right)\zeta_3 \\
& +\left(24x^2-26x\right)H_1+\left(32x^2-48x-2\right)H_{0,1}+\left(-8x^2+24x-12\right)H_{0,0,1}
\end{aligned}
$$

$$+\left(8x^2-8x+4\right)H_{0,1,1}-13\Bigg\}. \tag{691}$$

With these expressions at hand, the asymptotic 2-loop corrections of charm production in charged current DIS can be implemented numerically both in N- and in x-space, for phenomenological applications. This work is underway and the results will be given elsewhere. The respective relations will allow especially to access the charged current data at HERA, improving the accuracy of the heavy flavor corrections used in global PDF analyses and the determination of α_s.

11 Conclusions

The $O(\alpha_s^3)$ heavy flavor corrections to deep-inelastic scattering constitute a yet missing part in the precision analysis of the HERA data to measure α_s and the mass of the charm quark at the 1% level. At the same time, the parton distribution functions are extracted, which are an important input for measurements at the LHC, such as the measurement of properties of the Higgs boson or new physics searches. The $O(\alpha_s^3)$ corrections are currently on the way to be accomplished. In the present thesis several new contributions are made to achieve this goal. While on the side of the Mellin moments up to $N = 10(12..14)$ the $O(\alpha_s^3)$ corrections are fully understood, the major task now consists in deriving general-N results. Therefore, different gauge-invariant subsets of graphs, i.e. whole color factors, are calculated, in order to break the ground for the systematic evaluation of new topologies and to develop corresponding computer-algebra codes and computational algorithms to render a part of these problems. Furthermore, also some new results are obtained on the 2-loop level.

The work focuses on the heavy quark corrections in the asymptotic region $Q^2 \gg m^2$, where the heavy flavor Wilson coefficients factorize into the light flavor Wilson coefficients and massive operator matrix elements [76, 87]. This is not an essential restriction, since this representation holds for $Q^2/m^2 \geq 10$ [76] in case of the precisely measured structure function $F_2(x, Q^2)$, which forms the major data set to be analyzed. Since the light flavor Wilson coefficients are known at next-to-next-to-leading order (NNLO), the massive operator matrix elements are needed to the same precision, in order to obtain a complete NNLO description.

New contributions are obtained for the complete $O(\alpha_s^3 n_f T_F^2)$ corrections to the operator matrix elements $A_{gq,Q}$ and $A_{gg,Q}$ [131]. These operator matrix elements are needed for the construction of a variable flavor number scheme, and thus for the definition of heavy quark parton distribution functions at sufficiently high scales. The computation of the Feynman integrals is performed using representations in generalized hypergeometric functions and finite sums. These sums are performed using modern symbolic summation methods implemented in the packages Sigma [93–101], EvaluateMultiSums [101–103], and SumProduction [101]. The results are renormalized as described in [87] and checked against the Mellin moments derived there. Furthermore, also the 2-loop corrections to the polarized massive OMEs $\Delta A_{gq,Q}$ and $\Delta A_{gg,Q}$ are calculated. Since the calculations are performed in dimensional regularization and Levi-Civita tensors are present in the diagrams, the OMEs are subject to a finite renormalization. For the above OMEs, together with the quarkonic corrections calculated elsewhere, the finite renormalization has to be fully accomplished at general N. The solution of this problem is more complex than in case of single (lowest) moments only.

At the technology side new methods are developed to calculate genuine 3-loop topologies of ladder- and V-type, taking into account the number of heavy quark lines involved. The methods can now be applied for larger diagram classes. The calculation methods involves mapping the Feynman parameterized representations onto multi-sums and using properties of Appell functions and other generalizations of hypergeometric functions. In most cases, suitable sum representations are sufficient for being solved by the afore mentioned summation packages. The results involve generalized harmonic sums [111, 254], which in earlier calculations only occurred at intermediate stages. The methods using symbolic summation are of interest, since they can be applied to graphs with numerator structure in the same way as to the scalar graphs. Two integrals are presented, for which the solution with summation methods remains yet an open problem. Although these scalar prototypes have already been solved by the method of hyperlogarithms [315], making use of the finiteness in four dimensions, the corresponding QCD diagrams contain ε-poles, and thus need a different treatment. The summation methods, on the other

hand, are fully capable of treating diagrams with ε-poles, as shown e.g. in [88] and this thesis.

At three loops, for the first time also graphs with two distinct massive lines occur. A new method is presented for the calculation of such diagrams with equal masses, contributing to the OMEs $A_{gg,Q}$ and $A_{gq,Q}$. The method uses a Mellin-Barnes representation instead of a generalized hypergeometric function and keeps, for convergence reasons, one of the Feynman parameter integrals unintegrated. The above symbolic summation methods are used to solve the sum of residues in terms of cyclotomic harmonic polylogarithms. Many properties of these functions are implemented in the package HarmonicSums [108–111]. The remaining integral can then be performed in the space of iterated integrals using suitable limit procedures. Since the result is first derived as a generating function, the symbolic summation machinery is applied a second time, solving difference equations and simplifying sums needed to derive the Nth Taylor coefficient for symbolic N. With this method at hand, the corresponding QCD graphs can be calculated, and the results will be published subsequently.

Besides neutral current deep-inelastic scattering, also charged current processes are of importance. They predominantly describe strange-charm quark transitions and are therefore well suited to extract the strange quark distribution of nucleons at larger values of the virtuality Q^2. First the $O(\alpha_s)$ contributions are revisited, due to partly different results in the foregoing literature, which can be clarified. At 1-loop order, an efficient representation in Mellin space allowing for fast numerical evaluations is designed, including power corrections. Also here errors in the literature are corrected [134]. Additionally, the higher order heavy quark corrections in the asymptotic region naturally emerge in Mellin space, so it is useful to have the 1-loop corrections in a compatible representation. Here the 1-loop expressions are also expanded for $1 \gg m^2/Q^2$ up to the constant term. Comparing these asymptotic heavy flavor Wilson coefficients with expressions derived in terms of massive OMEs and light flavor Wilson coefficients in [86], a sign difference is observed for the gluonic contribution to F_3. A careful recalculation of the gluonic contribution is performed as well as a calculation in leading logarithmic approximation. Both calculations provide evidence for a sign error in [86]. The leading logarithmic calculation shows that the same sign error occurs for the pure-singlet contribution at two loops.

The heavy quark corrections of charged current deep-inelastic scattering are extended to 2-loop order. The factorization of the heavy flavor Wilson coefficients at large values of Q^2 [76, 87] is derived for the charged current case, completing and correcting the expressions given in [86]. The above considerations concerning factors (-1) are confirmed. Using the light flavor Wilson coefficients and operator matrix elements up to 2-loop order from the literature, x- and N-space expressions for all heavy flavor Wilson coefficients at two loops are given. Hence the results are ready for phenomenological applications to e.g. deep-inelastic neutrino-nucleon scattering data. For this purpose a numerical implementation of the results is available.

The results of the present investigations extend the formerly known results for fixed moments in various cases to results at general values of the Mellin variable N. These are first contributions of more to come in case of massive Wilson coefficients in the asymptotic region. Structurally it is interesting that for the moments rational numbers appear, supplemented by the constants ζ_2 and ζ_3. The general-N results describe the rational numbers in terms of rather complicated mathematical structures comprising rational functions in N, the usual harmonic sums, cyclotomic harmonic sums, generalized harmonic sums, generalized cyclotomic sums, and most recently also binomially and inverse binomially weighted generalized harmonic sums, cf. [340]. In this way more and more structures are unraveled in different domains, when evaluating 1-dimensional quantities, like massive Wilson coefficients in QCD at and beyond 2-loop order. At the same time, further insight is gained in the beautiful hierarchy of mathematical structures governing the micro cosmos.

Acknowledgements

The work for the thesis took place at DESY in Zeuthen, Germany and at RISC in Linz, Austria. It was financially supported by DESY and the Initial Training Network LHCPhenoNet PITN-GA-2010-264564, and received additional support from DFG Sonderforschungsbereich Transregio 9, Computergestützte Theoretische Teilchenphysik.

Several people had influence on me during the work on the thesis.
First and foremost, I thank Prof. J. Blümlein for his constant support and effort towards a comprehensive result during the whole time, as well as for offering regular contact to the scientific community through many conferences, workshops and schools that I could attend.

I would also like to thank Prof. E. Reya for providing the contact to DESY in the first place, and for several helpful remarks on the thesis. Additionally I would like to thank Prof. G. Hiller and Prof. M. Steinhauser for accepting the responsibility of examining the work.

I am particularly grateful to C. Schneider and J. Ablinger for several helpful discussions and their instant replies to many requests.

I am indebted to F. Wißbrock for many interesting and stimulating discussions, to V. Yundin for answering lots of questions about (T)FORM, and to T. Pfoh for numerous helpful questions and remarks on parts of the thesis.

It is a pleasure to thank all my colleagues at DESY and RISC for a pleasant and motivating working atmosphere, particularly I am grateful to M. Round, A. De Freitas, G. Hotzel, P. Kovacikova, and C. Raab for helpful discussions.

Finally I would like to thank my family and friends, especially my parents for their support and motivation during my time as Diploma and Ph.D. student.

And Ina, Thank you!

A The Γ-Function and Residues

For products and ratios of Euler's Γ-function we sometimes use the notation

$$\Gamma\left[\begin{array}{c} a_1,\ldots,a_n \\ b_1,\ldots,b_m \end{array}\right] = \prod_{k=1}^{n}\Gamma(a_k)\prod_{l=1}^{m}\Gamma^{-1}(b_l)\,. \tag{692}$$

The Legendre duplication formula

$$\Gamma(2z) \;=\; \frac{2^{2z-1}}{\sqrt{\pi}}\Gamma(z)\Gamma\left(z+\frac{1}{2}\right) \tag{693}$$

is sometimes useful, as well as the reflection formula of the Γ-function

$$\Gamma(\varepsilon-m) \;=\; \frac{\Gamma(\varepsilon)\Gamma(1-\varepsilon)}{\Gamma(m+1-\varepsilon)}(-1)^m\,. \tag{694}$$

Mellin-Barnes integrals (204) lead to complex contour integrals, which can be calculated using Cauchy's residue theorem

$$\frac{1}{2\pi i}\oint_{\partial G} d\xi f(\xi) = \pm\sum_{y\in G}\operatorname*{Res}_{x\to y} f(x)\,. \tag{695}$$

The sign is positive if the contour encircles the area G counter clockwise, and negative otherwise. The residue for an n-fold pole may be calculated via

$$\operatorname*{Res}_{x\to y} f(x) = \frac{1}{(n-1)!}\lim_{x\to y}\left(\frac{d^{n-1}}{dx^{n-1}}[(x-y)^n f(x)]\right)\,. \tag{696}$$

Especially for the Γ-functions we have

$$\operatorname*{Res}_{x\to -k}\Gamma(x) \;=\; \frac{(-1)^k}{k!}, \qquad \forall a,k\in\mathbb{N}_0\,. \tag{697}$$

B Coordinate Transformations of Feynman Parameter Integrals

Two integrals may be shuffled and mapped back onto the hypercube:

$$\int_0^1 dx\int_0^1 dy f(x,y) = \int_0^1 dx\int_0^1 dy\; x\; f(x,xy) + \int_0^1 dx\int_0^1 dy\; y\; f(xy,y)\,. \tag{698}$$

Furthermore, in the calculation of 2-loop massive OMEs [77–79, 341], the following transformations of double parameter integrals [342] were useful. We write them here in a self inverse form:

$$\begin{aligned} x' \;:=\;& 1-xy, \quad y' := \frac{1-x}{1-xy}, \qquad x := 1-x'y', \quad y := \frac{1-x'}{1-x'y'} \\ & x'(1-y') = x(1-y), \qquad \left|\frac{\partial(x,y)}{\partial(x',y')}\right| = \frac{x'}{1-x'y'}\,. \end{aligned} \tag{699}$$

The latter transformation is a representative of a whole class of coordinate transformations, which can be constructed via the steps in Eq. (404) and which occur naturally when comparing different ways of eliminating δ-distributions and θ-functions. For example:

$$\begin{aligned}
& f\left[x_1, \frac{x_2}{1-x_1}, x_3\right] \frac{1}{1-x_1} \delta(1-x_1-x_2-x_3) dx_1\, dx_2\, dx_3 \\
= \;& f\left[x_1, \frac{x_2}{1-x_1}, 1-x_1-x_2\right] \frac{1}{1-x_1} \theta(1-x_1-x_2) dx_1\, dx_2 \\
= \;& f[x_1, x_2, (1-x_1)(1-x_2)] dx_1\, dx_2 \qquad (700) \\
= \;& f\left[x_1(1-x_2), \frac{x_2}{1-x_1(1-x_2)}, (1-x_1)(1-x_2)\right] \frac{(1-x_2)}{1-x_1(1-x_2)} dx_1\, dx_2\,. \qquad (701)
\end{aligned}$$

So using (700)=(701) one rediscovers the transformation (699).

C Transformations of Sums

In the Feynman rules for the operator insertions the following sums occur:

$$\sum_{j=0}^{N} A^j B^{N-j} = \frac{A^{N+1}}{A-B} + \frac{B^{N+1}}{B-A}\,, \qquad (702)$$

$$\sum_{j=0}^{N} \sum_{l=0}^{N-j} A^j B^l C^{N-j-l} = \frac{A^{N+2}}{(A-B)(A-C)} + \frac{B^{N+2}}{(B-A)(B-C)} + \frac{C^{N+2}}{(C-A)(C-B)}\,. \qquad (703)$$

They can be reordered as follows:

$$\sum_{j=0}^{N} A^j B^{N-j} = \sum_{j=0}^{N} \binom{N+1}{j+1} (A-B)^j B^{N-j}\,, \qquad (704)$$

$$\sum_{j=0}^{N} \sum_{l=0}^{N-j} A^j B^{N-j-l} C^l = \sum_{j=0}^{N} \sum_{k=0}^{j} \binom{N+2}{j+2} \binom{j+1}{k+1} (B-C)^k (C-A)^{j-k} A^{N-j}\,. \qquad (705)$$

It is sometimes useful to consider their generating functions:

$$\sum_{N=0}^{\infty} \kappa^N \sum_{j=0}^{N} A^j B^{N-j} = \frac{1}{(1-\kappa A)(1-\kappa B)}\,, \qquad (706)$$

$$\sum_{N=0}^{\infty} \kappa^N \sum_{j=0}^{N} \sum_{l=0}^{N-j} A^j B^l C^{N-j-l} = \frac{1}{(1-\kappa A)(1-\kappa B)(1-\kappa C)}\,. \qquad (707)$$

D An Argument Relation for Cyclotomic Polynomials

For the transformation of squared arguments of cyclotomic HPLs one needs the corresponding transformation formula of cyclotomic polynomials. One finds

$$\Phi_n(x^2) = \Phi_{2n}(x), \quad \text{if } n \text{ even}$$

$$\Phi_n(x^2) = \Phi_n(x)\Phi_{2n}(x), \quad \text{if } n \text{ odd}\,. \tag{708}$$

For even n this can be seen from the definition

$$\begin{aligned}
\Phi_n(x^2) &= \prod_{\substack{1\le k\le n-1\\ \gcd(k,n)=1}} \left(x^2 - e^{2i\pi\frac{k}{n}}\right) \\
&= \prod_{\substack{1\le k\le n-1\\ \gcd(k,n)=1}} \left(x - e^{2i\pi\frac{k}{2n}}\right)\left(x + e^{2i\pi\frac{k}{2n}}\right) \\
&= \prod_{\substack{1\le k\le n-1\\ \gcd(k,n)=1}} \left(x - e^{2i\pi\frac{k}{2n}}\right)\left(x - e^{2i\pi\frac{n+k}{2n}}\right) \\
&= \prod_{\substack{1\le k\le 2n-1\\ \gcd(k,2n)=1}} \left(x - e^{2i\pi\frac{k}{2n}}\right) \\
&= \Phi_{2n}(x)\,.
\end{aligned} \tag{709}$$

Since for odd d obviously $d \nmid n \Leftrightarrow d \nmid 2n$, and for all even n and odd k one finds $\gcd(n,k) = \gcd(2n, n+k)$. For odd n one finds by induction starting from prime numbers p

$$\Phi_n(x^2) = \frac{x^{2p}-1}{x^2-1} = \frac{x^p-1}{x-1}\frac{x^p+1}{x+1} = \Phi_p(x)\Phi_p(-x)\,, \tag{710}$$

with the inductive step

$$\Phi_n(x^2) = \frac{x^{2n}-1}{\prod\limits_{\substack{d|n\\ d<n}} \Phi_d(x^2)} = \frac{x^n-1}{\prod\limits_{\substack{d|n\\ d<n}} \Phi_d(x)} \frac{x^n+1}{\prod\limits_{\substack{d|n\\ d<n}} \Phi_d(-x)} = \Phi_n(x)\Phi_n(-x)\,. \tag{711}$$

And by the property $\Phi_n(-x) = \Phi_{2n}(x)$ for odd n, the result follows.

E QCD Feynman Rules

For convenience, the QCD Feynman rules [343, 344] given in [87, 229] are summarized, which follow the conventions of [141]. D–dimensional momenta are denoted by p_i and Lorentz-indices by Greek letters. Color indices are $a, b, ...$ and i, j are indices of the color matrices. Solid lines represent fermions, wavy lines gluons and dashed lines ghosts. Arrows denote the direction of the momenta. A factor (-1) has to be included for each closed fermion– or ghost loop.

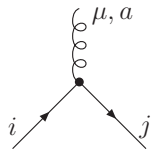

$$ig_s\gamma_\mu t^a_{ji}$$

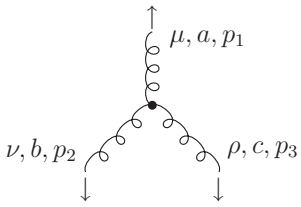

$$-g_s f^{abc}[(p_1-p_2)_\rho g_{\mu\nu}+(p_2-p_3)_\mu g_{\nu\rho}+(p_3-p_1)_\nu g_{\mu\rho}]$$

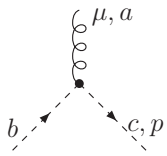

$$-g_s f^{abc} p_\mu$$

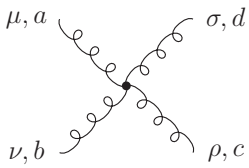

$$\begin{aligned}-ig_s^2 \textstyle\sum_e \Big\{ & f^{abe}f^{cde}[g_{\mu\rho}g_{\nu\sigma}-g_{\mu\sigma}g_{\nu\rho}] \\ & + f^{ace}f^{bde}[g_{\mu\nu}g_{\rho\sigma}-g_{\mu\sigma}g_{\nu\rho}] \\ & + f^{ade}f^{cbe}[g_{\mu\rho}g_{\nu\sigma}-g_{\mu\nu}g_{\rho\sigma}]\Big\}\end{aligned}$$

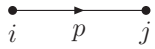

$$\tfrac{i}{\not{p}-m+i0}\delta_{ij}$$

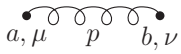

$$\tfrac{i}{p^2+i0}(-g_{\mu\nu}+\xi p_\mu p_\nu/(p^2+i0))\delta_{ab}$$

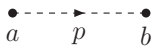

$$\tfrac{i}{p^2+i0}\delta_{ab}$$

The following Feynman rules for the quarkonic composite operators are again taken over from [87, 229], see also [184, 307]. The terms $\gamma_\pm$ refer to the unpolarized (+) and polarized (−) case, respectively. Gluon momenta are taken to be incoming. Δ denotes a light-like 4-vector, i.e. $\Delta^2 = 0$.

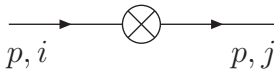

$$\delta^{ij}\not{\Delta}\gamma_\pm(\Delta\cdot p)^{N-1}\ , \quad N\geq 1$$

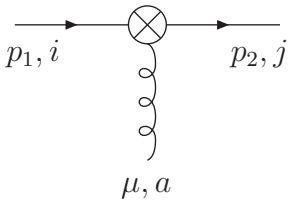

$$gt^a_{ji}\Delta^\mu\not{\Delta}\gamma_\pm\sum_{j=0}^{N-2}(\Delta\cdot p_1)^j(\Delta\cdot p_2)^{N-j-2}\ , \quad N\geq 2$$

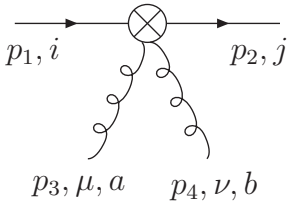

$$g^2\Delta^\mu\Delta^\nu\not{\Delta}\gamma_\pm\sum_{j=0}^{N-3}\sum_{l=j+1}^{N-2}(\Delta p_2)^j(\Delta p_1)^{N-l-2}$$
$$\Big[(t^at^b)_{ji}(\Delta p_1+\Delta p_4)^{l-j-1}+(t^bt^a)_{ji}(\Delta p_1+\Delta p_3)^{l-j-1}\Big]\ ,$$
$$N\geq 3$$

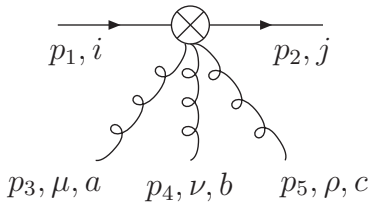

$$g^3\Delta^\mu\Delta^\nu\Delta^\rho\not{\Delta}\gamma_\pm\sum_{j=0}^{N-4}\sum_{l=j+1}^{N-3}\sum_{m=l+1}^{N-2}(\Delta.p_2)^j(\Delta.p_1)^{N-m-2}$$
$$\Big[\ (t^at^bt^c)_{ji}(\Delta.p_4+\Delta.p_5+\Delta.p_1)^{l-j-1}(\Delta.p_5+\Delta.p_1)^{m-l-1}$$
$$+(t^at^ct^b)_{ji}(\Delta.p_4+\Delta.p_5+\Delta.p_1)^{l-j-1}(\Delta.p_4+\Delta.p_1)^{m-l-1}$$
$$+(t^bt^at^c)_{ji}(\Delta.p_3+\Delta.p_5+\Delta.p_1)^{l-j-1}(\Delta.p_5+\Delta.p_1)^{m-l-1}$$
$$+(t^bt^ct^a)_{ji}(\Delta.p_3+\Delta.p_5+\Delta.p_1)^{l-j-1}(\Delta.p_3+\Delta.p_1)^{m-l-1}$$
$$+(t^ct^at^b)_{ji}(\Delta.p_3+\Delta.p_4+\Delta.p_1)^{l-j-1}(\Delta.p_4+\Delta.p_1)^{m-l-1}$$
$$+(t^ct^bt^a)_{ji}(\Delta.p_3+\Delta.p_4+\Delta.p_1)^{l-j-1}(\Delta.p_3+\Delta.p_1)^{m-l-1}\Big]\ ,$$
$$N\geq 4$$

$\gamma_+ = 1\ , \quad \gamma_- = \gamma_5\ .$ For transversity, one has to replace: $\not{\Delta}\gamma_\pm \rightarrow\ \sigma^{\mu\nu}\Delta_\nu$.

The Feynman rules for the unpolarized gluonic composite operators were derived in [87, 229] and compared to earlier results [185, 191]. Here Δ is defined as above.

$$\frac{1+(-1)^N}{2}\delta^{ab}(\Delta\cdot p)^{N-2}$$
$$\Big[g_{\mu\nu}(\Delta\cdot p)^2-(\Delta_\mu p_\nu+\Delta_\nu p_\mu)\Delta\cdot p+p^2\Delta_\mu\Delta_\nu\Big]\ ,\quad N\geq 2$$

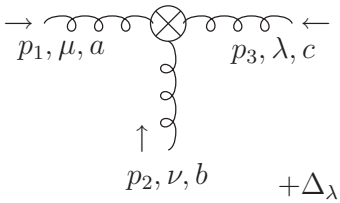

$$-ig\frac{1+(-1)^N}{2}f^{abc}\Bigg($$
$$\Big[(\Delta_\nu g_{\lambda\mu}-\Delta_\lambda g_{\mu\nu})\Delta\cdot p_1+\Delta_\mu(p_{1,\nu}\Delta_\lambda-p_{1,\lambda}\Delta_\nu)\Big](\Delta\cdot p_1)^{N-2}$$
$$+\Delta_\lambda\Big[\Delta\cdot p_1 p_{2,\mu}\Delta_\nu+\Delta\cdot p_2 p_{1,\nu}\Delta_\mu-\Delta\cdot p_1\Delta\cdot p_2 g_{\mu\nu}-p_1\cdot p_2\Delta_\mu\Delta_\nu\Big]$$
$$\times\textstyle\sum_{j=0}^{N-3}(-\Delta\cdot p_1)^j(\Delta\cdot p_2)^{N-3-j}$$
$$+\left\{\begin{smallmatrix}p_1\to p_2\to p_3\to p_1\\ \mu\to\nu\to\lambda\to\mu\end{smallmatrix}\right\}+\left\{\begin{smallmatrix}p_1\to p_3\to p_2\to p_1\\ \mu\to\lambda\to\nu\to\mu\end{smallmatrix}\right\}\Bigg)\ ,\quad N\geq 2$$

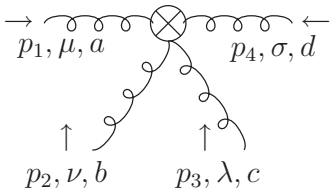

$$g^2\frac{1+(-1)^N}{2}\Bigg(f^{abe}f^{cde}O_{\mu\nu\lambda\sigma}(p_1,p_2,p_3,p_4)$$
$$+f^{ace}f^{bde}O_{\mu\lambda\nu\sigma}(p_1,p_3,p_2,p_4)+f^{ade}f^{bce}O_{\mu\sigma\nu\lambda}(p_1,p_4,p_2,p_3)\Bigg)\ ,$$
$$O_{\mu\nu\lambda\sigma}(p_1,p_2,p_3,p_4)=\Delta_\nu\Delta_\lambda\Bigg\{-g_{\mu\sigma}(\Delta\cdot p_3+\Delta\cdot p_4)^{N-2}$$
$$+[p_{4,\mu}\Delta_\sigma-\Delta\cdot p_4 g_{\mu\sigma}]\textstyle\sum_{i=0}^{N-3}(\Delta\cdot p_3+\Delta\cdot p_4)^i(\Delta\cdot p_4)^{N-3-i}$$
$$-[p_{1,\sigma}\Delta_\mu-\Delta\cdot p_1 g_{\mu\sigma}]\textstyle\sum_{i=0}^{N-3}(-\Delta\cdot p_1)^i(\Delta\cdot p_3+\Delta\cdot p_4)^{N-3-i}$$
$$+[\Delta\cdot p_1\Delta\cdot p_4 g_{\mu\sigma}+p_1\cdot p_4\Delta_\mu\Delta_\sigma-\Delta\cdot p_4 p_{1,\sigma}\Delta_\mu-\Delta\cdot p_1 p_{4,\mu}\Delta_\sigma]$$
$$\times\textstyle\sum_{i=0}^{N-4}\sum_{j=0}^{i}(-\Delta\cdot p_1)^{N-4-i}(\Delta\cdot p_3+\Delta\cdot p_4)^{i-j}(\Delta\cdot p_4)^j\Bigg\}$$
$$-\left\{\begin{smallmatrix}p_1\leftrightarrow p_2\\ \mu\leftrightarrow\nu\end{smallmatrix}\right\}-\left\{\begin{smallmatrix}p_3\leftrightarrow p_4\\ \lambda\leftrightarrow\sigma\end{smallmatrix}\right\}+\left\{\begin{smallmatrix}p_1\leftrightarrow p_2,\ p_3\leftrightarrow p_4\\ \mu\leftrightarrow\nu,\ \lambda\leftrightarrow\sigma\end{smallmatrix}\right\}\ ,\quad N\geq 2$$

F Scalar Feynman Rules

For the calculation of scalar prototype diagrams we used the following Feynman rules :

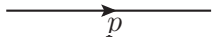

$$\frac{1}{(p^2-m^2)}$$

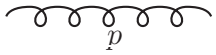

$$\frac{1}{p^2}$$

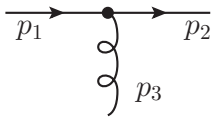

$$g$$

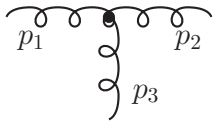

$$g$$

$$(\Delta.p)^N$$

$$\frac{1+(-1)^N}{2}(\Delta.p)^N$$

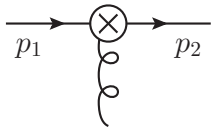

$$g\sum_{j=0}^{N}(\Delta.p_1)^j(\Delta.p_2)^{N-j}$$

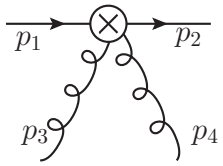

a) $$g^2\sum_{j=0}^{N}\sum_{l=0}^{N-j}(\Delta.p_2)^j(\Delta.p_1)^{N-l-j}(\Delta.p_1+\Delta.p_4)^l$$

b) $$g^2\sum_{j=0}^{N}\sum_{l=0}^{N-j}(\Delta.p_2)^j(\Delta.p_1)^{N-l-j}(\Delta.p_1+\Delta.p_3)^l$$

References

[1] M. Gell-Mann. A Schematic Model of Baryons and Mesons. *Phys. Lett.*, **8** (1964) 214–215.

[2] G. Zweig. An SU(3) Model for Strong Interaction Symmetry and its Breaking, 1964. CERN-TH-401.

[3] G. Zweig. An SU(3) Model for Strong Interaction Symmetry and its Breaking 2, 1964. CERN-TH-412, NP-14146.

[4] O. W. Greenberg. Spin and Unitary Spin Independence in a Paraquark Model of Baryons and Mesons. *Phys. Rev. Lett.*, **13** (1964) 598–602.

[5] DASP Collaboration, R. Brandelik et al. Total Cross-Section for Hadron Production by e^+ e^- Annihilation at Center-of-Mass Energies Between 3.6 GeV and 5.2 GeV. *Phys. Lett. B*, **76** (1978) 361–365.

[6] C. Quigg. *Gauge Theories of the Strong, Weak, and Electromagnetic Interactions.* (Benjamin, New York, 1983).

[7] Particle Data Group, J. Beringer et al. Review of Particle Physics (RPP). *Phys. Rev. D*, **86** (2012) 010001.

[8] W. K. H. Panofsky. Low q electrodynamics, elastic and inelastic electron (and muon) scattering. In: J. Prentki and J. Steinberger, Eds., *Proc. 14th International Conference on High-energy Physics, CERN, Geneva*, (1968) 23–42.

[9] R. E. Taylor. Inelastic electron-proton scattering in the deep continuum region. In: D. W. Braben and R. E. Rand, Eds., *Proc. of the 4th Int. Symp. on Electron and Photon Interactions at High Energies, Liverpool*, (1969) 251–260.

[10] E. D. Bloom et al. High-Energy Inelastic e p Scattering at 6-Degrees and 10-Degrees. *Phys. Rev. Lett.*, **23** (1969) 930–934.

[11] M. Breidenbach et al. Observed Behavior of Highly Inelastic electron-Proton Scattering. *Phys. Rev. Lett.*, **23** (1969) 935–939.

[12] R. E. Taylor. Deep inelastic scattering: The Early Years. *Rev. Mod. Phys.*, **63** (1991) 573–595.

[13] H. W. Kendall. Deep inelastic scattering: Experiments on the proton and the observation. *Rev. Mod. Phys.*, **63** (1991) 597–614.

[14] J. I. Friedman. Deep inelastic scattering: Comparisons with the quark model. *Rev. Mod. Phys.*, **63** (1991) 615–629.

[15] J. D. Bjorken. Asymptotic Sum Rules at Infinite Momentum. *Phys. Rev.*, **179** (1969) 1547–1553.

[16] C. G. Callan and D. J. Gross. High-energy electroproduction and the constitution of the electric current. *Phys. Rev. Lett.*, **22** (1969) 156–159.

[17] R. P. Feynman. The behavior of hadron collisions at extreme energies. In: C. N. Yang, Ed., *Proc. of the 3rd International Conference on High Energy Collisions, Stony Brook, New York*. Gordon & Breach, (1969) 237–258.

[18] R. P. Feynman. Very high-energy collisions of hadrons. *Phys. Rev. Lett.*, **23** (1969) 1415–1417.

[19] R. P. Feynman. *Photon-hadron interactions*. (Benjamin, Reading, MA, 1972).

[20] C.-N. Yang and R. L. Mills. Conservation of Isotopic Spin and Isotopic Gauge Invariance. *Phys. Rev.*, **96** (1954) 191–195.

[21] G. 't Hooft. Renormalization of Massless Yang-Mills Fields. *Nucl. Phys. B*, **33** (1971) 173–199.

[22] H. Fritzsch and M. Gell-Mann. Current algebra: Quarks and what else? In: J. D. Jackson and A. Roberts, Eds., *Proceedings of the 16th International Conference on High-Energy Physics, 6–13 Sep 1972. Batavia, Illinois*, (1972) 135–165. (arXiv:hep-ph/0208010).

[23] W. A. Bardeen, H. Fritzsch, and M. Gell-Mann. Light cone current algebra, π_0-decay, and e^+ e^- annihilation. In: R. Gatto, Ed., *Scale and Conformal Symmetry in Hadron Physics, Proc. of the Topical Meeting on the Outlook for Broken Conformal Symmetry in Elementary Particle Physics, 1972, Frascati, Italy*, (1973). (arXiv:hep-ph/0211388).

[24] H. Fritzsch, M. Gell-Mann, and H. Leutwyler. Advantages of the Color Octet Gluon Picture. *Phys. Lett. B*, **47** (1973) 365–368.

[25] L. Hoddeson, L. Braun, M. Riordan, and M. Dresden, Eds. *The Rise of the Standard Model — Particle Physics in the 1960s and 1970s*. (Cambridge University Press, Cambridge, 1997).

[26] D. Gross and F. Wilczek. A watershed: the emergence of QCD. *CERN Courier*, **53**(1) (Jan./Feb. 2013) 24–27.

[27] D. J. Gross and F. Wilczek. Ultraviolet Behavior of Nonabelian Gauge Theories. *Phys. Rev. Lett.*, **30** (1973) 1343–1346.

[28] H. D. Politzer. Reliable Perturbative Results for Strong Interactions? *Phys. Rev. Lett.*, **30** (1973) 1346–1349.

[29] K. G. Wilson. Non-Lagrangian Models of Current Algebra. *Phys. Rev.*, **179 (5)** (1969) 1499–1512.

[30] R. A. Brandt and G. Preparata. Operator Product Expansions Near the Light Cone. *Nucl. Phys. B*, **27** (1971) 541–567.

[31] N. H. Christ, B. Hasslacher, and A. H. Mueller. Light cone behavior of perturbation theory. *Phys. Rev. D*, **6** (1972) 3543–3562.

[32] D. J. Gross and F. Wilczek. Asymptotically Free Gauge Theories. 2. *Phys. Rev. D*, **9** (1974) 980–993.

[33] H. D. Politzer. Asymptotic Freedom: An Approach to Strong Interactions. *Phys. Rept.*, **14** (1974) 129–180.

[34] G. Altarelli and G. Parisi. Asymptotic Freedom in Parton Language. *Nucl. Phys. B*, **126** (1977) 298–318.

[35] J. B. Kogut and L. Susskind. Scale invariant parton model. *Phys. Rev. D*, **9** (1974) 697–705.

[36] A. Casher, J. B. Kogut, and L. Susskind. Consequences of the scale-invariant parton model for deep-inelastic neutrino scattering. *Phys. Rev. D*, **9** (1974) 706–714.

[37] J. B. Kogut and L. Susskind. Parton models and asymptotic freedom. *Phys. Rev. D*, **9** (1974) 3391–3399.

[38] H. D. Politzer. Gluon Corrections to Drell-Yan Processes. *Nucl. Phys. B*, **129** (1977) 301–318.

[39] D. Amati, R. Petronzio, and G. Veneziano. Relating Hard QCD Processes Through Universality of Mass Singularities. *Nucl. Phys. B*, **140** (1978) 54–72.

[40] D. Amati, R. Petronzio, and G. Veneziano. Relating Hard QCD Processes Through Universality of Mass Singularities. 2. *Nucl. Phys. B*, **146** (1978) 29–49.

[41] S. B. Libby and G. F. Sterman. Mass Divergences in Two Particle Inelastic Scattering. *Phys. Rev. D*, **18** (1978) 4737–4745.

[42] S. B. Libby and G. F. Sterman. Jet and Lepton Pair Production in High-Energy Lepton-Hadron and Hadron-Hadron Scattering. *Phys. Rev. D*, **18** (1978) 3252–3268.

[43] A. H. Mueller. Cut Vertices and their Renormalization: A Generalization of the Wilson Expansion. *Phys. Rev. D*, **18** (1978) 3705–3727.

[44] J. C. Collins and G. F. Sterman. Soft Partons in QCD. *Nucl. Phys. B*, **185** (1981) 172–188.

[45] J. C. Collins, D. E. Soper, and G. F. Sterman. Factorization for Short Distance Hadron-Hadron Scattering. *Nucl. Phys. B*, **261** (1985) 104–142.

[46] J. C. Collins, D. E. Soper, and G. F. Sterman. Factorization of Hard Processes in QCD. *Adv. Ser. Direct. High Energy Phys.*, **5** (1988) 1–91. (arXiv:hep-ph/0409313).

[47] D. J. Gross and S. B. Treiman. Light cone structure of current commutators in the gluon quark model. *Phys. Rev. D*, **4** (1971) 1059–1072.

[48] E. C. G. Stueckelberg and A. Petermann. The normalization group in quantum theory. *Helv. Phys. Acta*, **24** (1951) 317–319.

[49] M. Gell-Mann and F. E. Low. Quantum electrodynamics at small distances. *Phys. Rev.*, **95** (1954) 1300–1312.

[50] N. N Bogoliubov and D. V. Shirkov. *Introduction to the Theory of Quantized Fields.* (Interscience Publ., New York, 1959).

[51] C. G. Callan. Broken scale invariance in scalar field theory. *Phys. Rev. D*, **2** (1970) 1541–1547.

[52] K. Symanzik. Small distance behavior in field theory and power counting. *Commun. Math. Phys.*, **18** (1970) 227–246.

[53] C. Chang et al. Observed Deviations from Scale Invariance in High-Energy Muon Scattering. *Phys. Rev. Lett.*, **35** (1975) 901–904.

[54] Y. Watanabe et al. Test of Scale Invariance in Ratios of Muon Scattering Cross-Sections at 150 GeV and 56 GeV. *Phys. Rev. Lett.*, **35** (1975) 898–901.

[55] H1 and ZEUS Collaboration, F. D. Aaron et al. Combined Measurement and QCD Analysis of the Inclusive $e^{\pm}p$ Scattering Cross Sections at HERA. *JHEP*, **1001** (2010) 109. (arXiv:0911.0884 [hep-ex]).

[56] S. Alekhin, J. Blümlein, and S. Moch. Parton Distribution Functions and Benchmark Cross Sections at NNLO. *Phys. Rev. D*, **86** (2012) 054009–1–49. (arXiv:1202.2281 [hep-ph]).

[57] J. Gao, M. Guzzi, J. Huston, H.-L. Lai, Z. Li, P. Nadolski, J. Pumplin, D. Stump, and C.-P. Yuan. The CT10 NNLO Global Analysis of QCD, 2013. (arXiv:1302.6246 [hep-ph]).

[58] HERAPDF collab. `https://www.desy.de/h1zeus/combined_results/herapdftable/`.

[59] P. Jimenez-Delgado and E. Reya. Dynamical NNLO parton distributions. *Phys. Rev. D*, **79** (2009) 074023–1–15. (arXiv:0810.4274 [hep-ph]).

[60] A. D. Martin, W. J. Stirling, R. S. Thorne, and G. Watt. Parton distributions for the LHC. *Eur. Phys. J. C*, **63** (2009) 189–285. (arXiv:0901.0002 [hep-ph]).

[61] R. D. Ball, V. Bertone, F. Cerutti, L. Del Debbio, S. Forte, A. Guffanti, J. I. Latorre, J. Rojo, and M. Ubiali. Impact of Heavy Quark Masses on Parton Distributions and LHC Phenomenology. *Nucl. Phys. B*, **849** (2011) 296–363. (arXiv:1101.1300 [hep-ph]).

[62] J. Blümlein. The Theory of Deeply Inelastic Scattering. *Prog. Part. Nucl. Phys.*, **69** (2013) 28–84. (arXiv:1208.6087 [hep-ph]).

[63] S. Bethke, A. H. Hoang, S. Kluth, J. Schieck, I. W. Stewart, et al. Workshop on Precision Measurements of α_s, 2011. (arXiv:1110.0016 [hep-ph]).

[64] J. A. M. Vermaseren, A. Vogt, and S. Moch. The Third-order QCD corrections to deep-inelastic scattering by photon exchange. *Nucl. Phys. B*, **724** (2005) 3–182. (arXiv:hep-ph/0504242).

[65] E. Witten. Heavy Quark Contributions to Deep Inelastic Scattering. *Nucl. Phys. B*, **104** (1976) 445–476.

[66] J. Babcock, D. W. Sivers, and S. Wolfram. QCD Estimates for Heavy Particle Production. *Phys. Rev. D*, **18** (1978) 162–181.

[67] M. A. Shifman, A. I. Vainshtein, and V. I. Zakharov. Remarks on Charm Electroproduction in QCD. *Nucl. Phys. B*, **136** (1978) 157–176.

[68] J. P. Leveille and T. J. Weiler. Characteristics of Heavy Quark Leptoproduction in QCD. *Nucl. Phys. B*, **147** (1979) 147–173.

[69] A. D. Watson. Spin-Spin Asymmetries in Inclusive Muon Proton Charm Production. *Z. Phys. C*, **12** (1982) 123–125.

[70] E. Laenen, S. Riemersma, J. Smith, and W. L. van Neerven. Complete $O(\alpha_s)$ corrections to heavy flavor structure functions in electroproduction. *Nucl. Phys. B*, **392** (1993) 162–228.

[71] E. Laenen, S. Riemersma, J. Smith, and W. L. van Neerven. $O(\alpha_s)$ corrections to heavy flavor inclusive distributions in electroproduction. *Nucl. Phys. B*, **392** (1993) 229–250.

[72] S. Riemersma, J. Smith, and W. L. van Neerven. Rates for inclusive deep-inelastic electroproduction of charm quarks at HERA. *Phys. Lett. B*, **347** (1995) 143–151. (arXiv:hep-ph/9411431).

[73] T. Gottschalk. Chromodynamic Corrections To Neutrino Production Of Heavy Quarks. *Phys. Rev. D*, **23** (1981) 56–74.

[74] M. Glück, S. Kretzer, and E. Reya. The Strange sea density and charm production in deep inelastic charged current processes. *Phys. Lett. B*, **380** (1996) 171–176. [Erratum-ibid. 405 (1997) 391], (arXiv:hep-ph/9603304).

[75] M. Buza, Y. Matiounine, J. Smith, and W. L. van Neerven. Charm electroproduction viewed in the variable-flavour number scheme versus fixed-order perturbation theory. *Eur. Phys. J. C*, **1** (1998) 301–320.

[76] M. Buza, Y. Matiounine, J. Smith, R. Migneron, and W. L. van Neerven. Heavy quark coefficient functions at asymptotic values $Q^2 \gg m^2$. *Nucl. Phys. B*, **472** (1996) 611–658. (arXiv:hep-ph/9601302).

[77] I. Bierenbaum, J. Blümlein, and S. Klein. Calculation of massive 2-loop operator matrix elements with outer gluon lines. *Phys. Lett. B*, **648** (2007) 195–200. (arXiv:hep-ph/0702265).

[78] I. Bierenbaum, J. Blümlein, and S. Klein. Two-Loop Massive Operator Matrix Elements and Unpolarized Heavy Flavor Production at Asymptotic Values $Q^2 \gg m^2$. *Nucl. Phys. B*, **780** (2007) 40–75. (arXiv:hep-ph/0703285).

[79] I. Bierenbaum, J. Blümlein, S. Klein, and C. Schneider. Two-Loop Massive Operator Matrix Elements for Unpolarized Heavy Flavor Production to $O(\varepsilon)$. *Nucl. Phys. B*, **803** (2008) 1–41. (arXiv:0803.0273 [hep-ph]).

[80] I. Bierenbaum, J. Blümlein, and S. Klein. The Gluonic Operator Matrix Elements at $O(\alpha_s^2)$ for DIS Heavy Flavor Production. *Phys. Lett. B*, **672** (2009) 401–406. (arXiv:0901.0669 [hep-ph]).

[81] W. L. van Neerven and E. B. Zijlstra. Order α_s^2 contributions to the deep inelastic Wilson coefficient. *Phys. Lett. B*, **272** (1991) 127–133.

[82] E. B. Zijlstra and W. L. van Neerven. Contribution of the second order gluonic Wilson coefficient to the deep inelastic structure function. *Phys. Lett. B*, **273** (1991) 476–482.

[83] E. B. Zijlstra and W. L. van Neerven. Order α_s^2 QCD corrections to the deep inelastic proton structure functions F_2 and F_L. *Nucl. Phys. B*, **383** (1992) 525–574.

[84] E. B. Zijlstra and W. L. van Neerven. Order α_s^2 correction to the structure function $F_3(x, Q^2)$ in deep inelastic neutrino-hadron scattering. *Phys. Lett. B*, **297** (1992) 377–384.

[85] S. Moch and J. A. M. Vermaseren. Deep inelastic structure functions at two loops. *Nucl. Phys. B*, **573** (2000) 853–907. (arXiv:hep-ph/9912355).

[86] M. Buza and W. L. van Neerven. $O(\alpha_s^2)$ contributions to charm production in charged current deep inelastic lepton-hadron scattering. *Nucl. Phys. B*, **500** (1997) 301–324. (arXiv:hep-ph/9702242).

[87] I. Bierenbaum, J. Blümlein, and S. Klein. Mellin Moments of the $O(\alpha_s^3)$ Heavy Flavor Contributions to unpolarized Deep-Inelastic Scattering at $Q^2 \gg m^2$ and Anomalous Dimensions. *Nucl. Phys. B*, **820** (2009) 417–482. (arXiv:0904.3563 [hep-ph]).

[88] J. Ablinger, J. Blümlein, S. Klein, C. Schneider, and F. Wißbrock. The $O(\alpha_s^3)$ Massive Operator Matrix Elements of $O(n_f)$ for the Structure Function $F_2(x, Q^2)$ and Transversity. *Nucl. Phys. B*, **844** (2011) 26–54. (arXiv:1008.3347 [hep-ph]).

[89] G. 't Hooft and M. J. G. Veltman. Regularization and Renormalization of Gauge Fields. *Nucl. Phys. B*, **44** (1972) 189–213.

[90] J. F. Ashmore. A Method of Gauge Invariant Regularization. *Lett. Nuovo Cim.*, **4** (1972) 289–290.

[91] G. M. Cicuta and E. Montaldi. Analytic renormalization via continuous space dimension. *Lett. Nuovo Cim.*, **4** (1972) 329–332.

[92] C. G. Bollini and J. J. Giambiagi. Dimensional Renormalization: The Number of Dimensions as a Regularizing Parameter. *Nuovo Cim. B*, **12** (1972) 20–25.

[93] C. Schneider. A refined difference field theory for symbolic summation. *J. Symbolic Comput.*, **43**(9) (2008) 611–644. (arXiv:0808.2543).

[94] C. Schneider. Product Representations in $\Pi\Sigma$-Fields. *Ann. Comb.*, **9**(1) (2005) 75–99.

[95] C. Schneider. Solving parameterized linear difference equations in terms of indefinite nested sums and products. *J. Differ. Equations Appl.*, **11**(9) (2005) 799–821.

[96] C. Schneider. Parameterized Telescoping Proves Algebraic Independence of Sums. *Ann. Comb.*, **14**(4) (2010) 533–552. (arXiv:0808.2596).

[97] C. Schneider. A Symbolic Summation Approach to Find Optimal Nested Sum Representations. In: A. Carey, D. Ellwood, S. Paycha, and S. Rosenberg, Eds., *Proceedings of the Workshop Motives, Quantum Field Theory, and Pseudodifferential Operators, Boston, 2008*. Clay Mathematics Proceedings, (2010).

[98] C. Schneider. Symbolic Summation Assists Combinatorics. *Sém. Lothar. Combin.*, **56** (2006) Article B56b.

[99] C. Schneider. Multi-Summation in Difference Fields, Habilitationsschrift, Johannes Kepler Universität Linz, Austria, 2007. and references therein.

[100] J. Ablinger, J. Blümlein, S. Klein, and C. Schneider. Modern Summation Methods and the Computation of 2- and 3-loop Feynman Diagrams. *Nucl. Phys. Proc. Suppl.*, **205–206** (2010) 110–115. (arXiv:1006.4797 [math-ph]).

[101] J. Blümlein, A. Hasselhuhn, and C. Schneider. Evaluation of Multi-Sums for Large Scale Problems. *PoS*, **RADCOR2011** (2011) 032. (arXiv:1202.4303 [math-ph]).

[102] J. Ablinger, I. Bierenbaum, J. Blümlein, A. Hasselhuhn, S. Klein, C. Schneider, and F. Wißbrock. Heavy Flavor DIS Wilson coefficients in the asymptotic regime. *Nucl. Phys. Proc. Suppl.*, **205–206** (2010) 242–249. (arXiv:1007.0375 [hep-ph]).

[103] C. Schneider. Simplifying Multiple Sums in Difference Fields. In: J. Blümlein and C. Schneider, Eds., *Computer Algebra in Quantum Field Theory: Integration, Summation and Special Functions*. Springer, Berlin, 2013. To appear.

[104] J. A. M. Vermaseren. Harmonic sums, Mellin transforms and integrals. *Int. J. Mod. Phys. A*, **14** (1999) 2037–2076. (arXiv:hep-ph/9806280).

[105] J. Blümlein and S. Kurth. Harmonic sums and Mellin transforms up to two loop order. *Phys. Rev. D*, **60** (1999) 014018–1–31. (arXiv:hep-ph/9810241).

[106] J. Blümlein. Structural Relations of Harmonic Sums and Mellin Transforms up to Weight $w = 5$. *Comput. Phys. Commun.*, **180** (2009) 2218–2249. (arXiv:0901.3106 [hep-ph]).

[107] J. Blümlein. Structural Relations of Harmonic Sums and Mellin Transforms at Weight $w = 6$. In: A. Carey, D. Ellwood, S. Paycha, and S. Rosenberg, Eds., *Proceedings of the Workshop Motives, Quantum Field Theory, and Pseudodifferential Operators, Boston, 2008*. Clay Mathematics Proceedings, (2010) 167–186. (arXiv:0901.0837 [math-ph]).

[108] J. Ablinger. A Computer Algebra Toolbox for Harmonic Sums Related to Particle Physics. Diploma thesis, Johannes Kepler Universität, Linz, Austria, 2010. (arXiv:1011.1176 [math-ph]).

[109] J. Ablinger. *Computer Algebra Algorithms for Special Functions in Particle Physics*. PhD thesis, Johannes Kepler Universität, Linz, Austria, 2012. (arXiv:1305.0687 [math-ph]).

[110] J. Ablinger, J. Blümlein, and C. Schneider. Harmonic Sums and Polylogarithms Generated by Cyclotomic Polynomials. *J. Math. Phys.*, **52** (2011) 102301–1–52. (arXiv:1105.6063 [math-ph]).

[111] J. Ablinger, J. Blümlein, and C. Schneider. Analytic and Algorithmic Aspects of Generalized Harmonic Sums and Polylogarithms. J. Math. Phys. (2013), in print, (arXiv:1302.0378 [math-ph]).

[112] K. G. Chetyrkin, A. L. Kataev, and F. V. Tkachov. New Approach to Evaluation of Multiloop Feynman Integrals: The Gegenbauer Polynomial x Space Technique. *Nucl. Phys. B*, **174** (1980) 345–377.

[113] K. G. Chetyrkin and F. V. Tkachov. Integration by Parts: The Algorithm to Calculate beta Functions in 4 Loops. *Nucl. Phys. B*, **192** (1981) 159–204.

[114] H. Mellin. Om definita integraler, hvilka för obegränsadt, växande värden af vissa heltaliga parametrar hafva till graenser hypergeometriska funktioner af särskilda ordningar. *Acta Societatis Scientiarum Fennicae*, **XX.**(7) (1895) 1–39.

[115] E. W. Barnes. A New Development of the Theory of the Hypergeometric Functions. *Proc. London Math. Soc.*, **s2-6** (1908) 141–177.

[116] V. A. Smirnov. Analytical result for dimensionally regularized massless on shell double box. *Phys. Lett. B*, **460** (1999) 397–404. (arXiv:hep-ph/9905323).

[117] J. B. Tausk. Non-planar massless two loop Feynman diagrams with four on-shell legs. *Phys. Lett. B*, **469** (1999) 225–234. (arXiv:hep-ph/9909506).

[118] G. Racah. Sopra l'irradiazione nell'urto di particelle veloci. *Nuovo Cim.*, **11** (1934) 461–476.

[119] K. S. Kölbig, J. A. Mignaco, and E. Remiddi. On Nielsen's Generalized Polylogarithms and their Numerical Calculation. *BIT Num. Math.*, **10** (1970) 38–73.

[120] R. Barbieri, J. A. Mignaco, and E. Remiddi. Electron form-factors up to fourth order. 1. *Nuovo Cim. A*, **11** (1972) 824–864.

[121] M. J. Levine, E. Remiddi, and R. Roskies. Analytic contributions to the g factor of the electron in sixth order. *Phys. Rev. D*, **20** (1979) 2068–2076.

[122] E. Remiddi and J. A. M. Vermaseren. Harmonic polylogarithms. *Int. J. Mod. Phys. A*, **15** (2000) 725–754. (arXiv:hep-ph/9905237).

[123] J. Blümlein, D. J. Broadhurst, and J. A. M. Vermaseren. The Multiple Zeta Value Data Mine. *Comput. Phys. Commun.*, **181** (2010) 582–625. (arXiv:0907.2557 [math-ph]).

[124] T. Gehrmann and E. Remiddi. Numerical evaluation of harmonic polylogarithms. *Comput. Phys. Commun.*, **141** (2001) 296–312. (arXiv:hep-ph/0107173).

[125] T. Gehrmann and E. Remiddi. Numerical evaluation of two-dimensional harmonic polylogarithms. *Comput. Phys. Commun.*, **144** (2002) 200–223. (arXiv:hep-ph/0111255).

[126] S. Moch, J. A. M. Vermaseren, and A. Vogt. The three-loop splitting functions in QCD: The nonsinglet case. *Nucl. Phys. B*, **688** (2004) 101–134. (arXiv:hep-ph/0403192).

[127] A. Vogt, S. O. Moch, and J. A. M. Vermaseren. The three-loop splitting functions in QCD: The singlet case. *Nucl. Phys. B*, **691** (2004) 129–181. (arXiv:hep-ph/0404111).

[128] J. Blümlein. Algebraic relations between harmonic sums and associated quantities. *Comput. Phys. Commun.*, **159** (2004) 19–54. (arXiv:hep-ph/0311046).

[129] J. Ablinger, J. Blumlein, A. Hasselhuhn, S. Klein, C. Schneider, and F. Wißbrock. New Heavy Flavor Contributions to the DIS Structure Function $F_2(x, Q^2)$ at $O(\alpha_s^3)$. *PoS*, **RADCOR2011** (2011) 031. (arXiv:1202.2700 [hep-ph]).

[130] J. Ablinger, J. Blümlein, A. De Freitas, A. Hasselhuhn, S. Klein, C. Raab, M. Round, C. Schneider, and F. Wißbrock. Three-Loop Contributions to the Gluonic Massive Operator Matrix Elements at General Values of N. *PoS*, **LL2012** (2012) 033. (arXiv:1212.6823 [hep-ph]).

[131] J. Blümlein, A. Hasselhuhn, S. Klein, and C. Schneider. The $O(\alpha_s^3 n_f T_F^2 C_{A,F})$ Contributions to the Gluonic Massive Operator Matrix Elements. *Nucl. Phys. B*, **866** (2013) 196–211. (arXiv:1205.4184 [hep-ph]).

[132] J. Ablinger, J. Blümlein, A. De Freitas, A. Hasselhuhn, S. Klein, C. Schneider, and F. Wißbrock. New Results on the 3-Loop Heavy Flavor Wilson Coefficients in Deep-Inelastic Scattering, 2012. (arXiv:1212.5950 [hep-ph]).

[133] J. Ablinger, J. Blümlein, A. Hasselhuhn, S. Klein, C. Schneider, and F. Wißbrock. Massive 3-loop Ladder Diagrams for Quarkonic Local Operator Matrix Elements. *Nucl. Phys. B*, **864** (2012) 52–84. (arXiv:1206.2252 [hep-ph]).

[134] J. Blümlein, A. Hasselhuhn, P. Kovacikova, and S. Moch. $O(\alpha_s)$ Heavy Flavor Corrections to Charged Current Deep-Inelastic Scattering in Mellin Space. *Phys. Lett. B*, **700** (2011) 294–304. (arXiv:1104.3449 [hep-ph]).

[135] A. Arbuzov, D. Yu. Bardin, J. Blümlein, L. Kalinovskaya, and T. Riemann. Hector 1.00: A Program for the calculation of QED, QCD and electroweak corrections to *ep* and $l^{\pm}N$ deep inelastic neutral and charged current scattering. *Comput. Phys. Commun.*, **94** (1996) 128–184. (arXiv:hep-ph/9511434).

[136] O. Nachtmann. Positivity constraints for anomalous dimensions. *Nucl. Phys. B*, **63** (1973) 237–247.

[137] H. Georgi and H. D. Politzer. Freedom at Moderate Energies: Masses in Color Dynamics. *Phys. Rev. D*, **14** (1976) 1829–1848.

[138] J. Blümlein, M. Klein, T. Naumann, and T. Riemann. Structure Functions, Quark Distributions and $\Lambda_{\rm QCD}$ at HERA. In: R. D. Peccei, Ed., *Proc. of the DESY Theory Workshop on Physics at HERA, Hamburg, F.R. Germany*, volume 1, (1987) 67–106.

[139] A. Kwiatkowski, H. Spiesberger, and H. J. Möhring. HERACLES: An Event Generator for *e p* Interactions at HERA Energies Including Radiative Processes: Version 1.0. *Comput. Phys. Commun.*, **69** (1992) 155–172.

[140] J. Blümlein. $O(\alpha^2 L^2)$ radiative corrections to deep inelastic *ep* scattering for different kinematical variables. *Z. Phys. C*, **65** (1995) 293–298. (arXiv:hep-ph/9403342).

[141] F. J. Yndurain. *The theory of quark and gluon interactions.* (Springer, Berlin, 2006), 4th edition.

[142] E. Reya. Perturbative Quantum Chromodynamics. *Phys. Rept.*, **69** (1981) 195–333.

[143] A. J. Buras. Asymptotic Freedom in Deep Inelastic Processes in the Leading Order and Beyond. *Rev. Mod. Phys.*, **52** (1980) 199–276.

[144] J. Blümlein and A. Tkabladze. Target mass corrections for polarized structure functions and new sum rules. *Nucl. Phys. B*, **553** (1999) 427–464. (arXiv:hep-ph/9812478).

[145] J. Blümlein and N. Kochelev. On the twist-2 contributions to polarized structure functions and new sum rules. *Phys. Lett. B*, **381** (1996) 296–304. (arXiv:hep-ph/9603397).

[146] J. Blümlein and N. Kochelev. On the twist 2 and twist 3 contributions to the spin dependent electroweak structure functions. *Nucl. Phys. B*, **498** (1997) 285–309. (arXiv:hep-ph/9612318).

[147] S. D. Drell and T.-M. Yan. Partons and their Applications at High-Energies. *Annals Phys.*, **66** (1971) 578.

[148] E. Derman. Persistent Threshold Effects Characterizing Dimuon and Hadron Distributions Due to Charmed Particle Production by Neutrinos. *Nucl. Phys. B*, **110** (1976) 40–66.

[149] R. M. Barnett. Evidence for New Quarks and New Currents. *Phys. Rev. Lett.*, **36** (1976) 1163–1166.

[150] R. Barbieri, J. R. Ellis, M. K. Gaillard, and G. G. Ross. A Quest for a Wholly Scaling Variable. *Phys. Lett. B*, **64** (1976) 171–176.

[151] R. Barbieri, J. R. Ellis, M. K. Gaillard, and G. G. Ross. Mass Corrections to Scaling in Deep Inelastic Processes. *Nucl. Phys. B*, **117** (1976) 50–76.

[152] T. Muta. *Foundations Of Quantum Chromodynamics: An Introduction to Perturbative Methods in Gauge Theories*. (World Scientific, Singapore, 2010).

[153] J. Collins. *Foundations of perturbative QCD*. (Cambridge Univ. Press, Cambridge, England, 2011).

[154] L. D. Faddeev and V. N. Popov. Feynman Diagrams for the Yang-Mills Field. *Phys. Lett. B*, **25** (1967) 29–30.

[155] R. L. Arnowitt and S. I. Fickler. Quantization of the Yang-Mills field. *Phys. Rev.*, **127** (1962) 1821–1829.

[156] G. 't Hooft, 1972. unpublished.

[157] K. G. Wilson. Confinement of Quarks. *Phys. Rev. D*, **10** (1974) 2445–2459.

[158] W. Zimmermann. Local Operator Products and Renormalization in Quantum Field Theory. In: S. Deser, M. Gisaru, and H. Pendleton, Eds., *Lectures on Elementary Particle Physics and Quantum Field Theory, Proceedings of the 1970 Brandeis Summer Institute in Theoretical Physics*, 399–589. MIT Press, Cambridge, MA, 1970.

[159] K. G. Wilson and W. Zimmermann. Operator product expansions and composite field operators in the general framework of quantum field theory. *Commun. Math. Phys.*, **24** (1972) 87–106.

[160] Y. Frishman. Operator products at almost light like distances. *Annals Phys.*, **66** (1971) 373–389.

[161] B. Geyer, M. Lazar, and D. Robaschik. Decomposition of nonlocal light cone operators into harmonic operators of definite twist. *Nucl. Phys. B*, **559** (1999) 339–377. (arXiv:hep-th/9901090).

[162] B. Geyer and M. Lazar. Twist decomposition of nonlocal light cone operators. 2. General tensors of 2nd rank. *Nucl. Phys. B*, **581** (2000) 341–390. (arXiv:hep-th/0003080).

[163] H. D. Politzer. Power Corrections at Short Distances. *Nucl. Phys. B*, **172** (1980) 349–382.

[164] R. K. Ellis, W. Furmanski, and R. Petronzio. Power Corrections to the Parton Model in QCD. *Nucl. Phys. B*, **207** (1982) 1–14.

[165] R. K. Ellis, W. Furmanski, and R. Petronzio. Unraveling Higher Twists. *Nucl. Phys. B*, **212** (1983) 29–98.

[166] E. V. Shuryak and A. I. Vainshtein. QCD Power Corrections to Deep Inelastic Scattering. *Phys. Lett. B*, **105** (1981) 65–67.

[167] E. V. Shuryak and A. I. Vainshtein. Theory of Power Corrections to Deep Inelastic Scattering in Quantum Chromodynamics. 1. Q^2 Effects. *Nucl. Phys. B*, **199** (1982) 451–481.

[168] E. V. Shuryak and A. I. Vainshtein. Theory of Power Corrections to Deep Inelastic Scattering in Quantum Chromodynamics. 2. Q^4 Effects: Polarized Target. *Nucl. Phys. B*, **201** (1982) 141–158.

[169] R. L. Jaffe. Parton Distribution Functions for Twist Four. *Nucl. Phys. B*, **229** (1983) 205–230.

[170] A. P. Bukhvostov, G. V. Frolov, L. N. Lipatov, and E. A. Kuraev. Evolution Equations for Quasi-Partonic Operators. *Nucl. Phys. B*, **258** (1985) 601–646.

[171] A. P. Bukhvostov and G. V. Frolov. Anomalous Dimensionalities of Quasiparton Twist = Four Operators. *Yad. Fiz.*, **45** (1987) 1136–1144.

[172] J. Blümlein, H. Böttcher, and A. Guffanti. Non-singlet QCD analysis of deep inelastic world data at $O(\alpha_s^3)$. *Nucl. Phys. B*, **774** (2007) 182–207. (arXiv:hep-ph/0607200).

[173] J. Blümlein and H. Böttcher. Higher twist contributions to the structure functions $F_2^p(x, Q^2)$ and $F_2^d(x, Q^2)$ at large x at high orders. *Phys. Lett. B*, **662** (2008) 336–340. (arXiv:0802.0408 [hep-ph]).

[174] S. Alekhin, J. Blümlein, and S. Moch. Higher order constraints on the Higgs production rate from fixed-target DIS data. *Eur. Phys. J. C*, **71** (2011) 1723–1–6. (arXiv:1101.5261 [hep-ph]).

[175] N. Cabibbo. Unitary Symmetry and Leptonic Decays. *Phys. Rev. Lett.*, **10** (1963) 531–533.

[176] M. Kobayashi and T. Maskawa. CP Violation in the Renormalizable Theory of Weak Interaction. *Prog. Theor. Phys.*, **49** (1973) 652–657.

[177] K. Nowak. QCD NLO analysis of inclusive, charm and jet data (HERAPDF 1.7). In *Proc. 20th International Workshop on Deep-Inelastic Scattering and Related Subjects (DIS 2012)*, (2012) 403–406.

[178] H.-L. Lai, M. Guzzi, J. Huston, Z. Li, P. M. Nadolsky, J. Pumplin, and C.-P. Yuan. New parton distributions for collider physics. *Phys. Rev. D*, **82** (2010) 074024–1–24. (arXiv:1007.2241 [hep-ph]).

[179] J. F. Owens, A. Accardi, and W. Melnitchouk. Global parton distributions with nuclear and finite-Q^2 corrections, 2012. (arXiv:1212.1702 [hep-ph]).

[180] NNPDF Collaboration, R. D. Ball et al. Unbiased global determination of parton distributions and their uncertainties at NNLO and at LO. *Nucl. Phys. B*, **855** (2012) 153–221. (arXiv:1107.2652 [hep-ph]).

[181] J. Blümlein, V. Ravindran, and W. L. van Neerven. On the Drell-Levy-Yan relation to $O(\alpha_s^2)$. *Nucl. Phys. B*, **586** (2000) 349–381. (arXiv:hep-ph/0004172).

[182] D. J. Gross and F. Wilczek. Asymptotically Free Gauge Theories. 1. *Phys. Rev. D*, **8** (1973) 3633–3652.

[183] H. Georgi and H. D. Politzer. Electroproduction scaling in an asymptotically free theory of strong interactions. *Phys. Rev. D*, **9** (1974) 416–420.

[184] E. G. Floratos, D. A. Ross, and C. T. Sachrajda. Higher Order Effects in Asymptotically Free Gauge Theories: The Anomalous Dimensions of Wilson Operators. *Nucl. Phys. B*, **129** (1977) 66–88. Erratum-ibid. **139** (1978) 545–546.

[185] E. G. Floratos, D. A. Ross, and C. T. Sachrajda. Higher Order Effects in Asymptotically Free Gauge Theories. 2. Flavor Singlet Wilson Operators and Coefficient Functions. *Nucl. Phys. B*, **152** (1979) 493–520.

[186] A. Gonzalez-Arroyo, C. Lopez, and F. J. Yndurain. Second Order Contributions to the Structure Functions in Deep Inelastic Scattering. 1. Theoretical Calculations. *Nucl. Phys. B*, **153** (1979) 161–186.

[187] A. Gonzalez-Arroyo and C. Lopez. Second Order Contributions to the Structure Functions in Deep Inelastic Scattering. 3. The Singlet Case. *Nucl. Phys. B*, **166** (1980) 429–459.

[188] G. Curci, W. Furmanski, and R. Petronzio. Evolution of Parton Densities Beyond Leading Order: The Nonsinglet Case. *Nucl. Phys. B*, **175** (1980) 27–92.

[189] W. Furmanski and R. Petronzio. Singlet Parton Densities Beyond Leading Order. *Phys. Lett. B*, **97** (1980) 437–442.

[190] E. G. Floratos, C. Kounnas, and R. Lacaze. Higher Order QCD Effects in Inclusive Annihilation and Deep Inelastic Scattering. *Nucl. Phys. B*, **192** (1981) 417–462.

[191] R. Hamberg and W. L. van Neerven. The Correct renormalization of the gluon operator in a covariant gauge. *Nucl. Phys. B*, **379** (1992) 143–171.

[192] S. A. Larin, T. van Ritbergen, and J. A. M. Vermaseren. The Next next-to-leading QCD approximation for nonsinglet moments of deep inelastic structure functions. *Nucl. Phys. B*, **427** (1994) 41–52.

[193] S. A. Larin, P. Nogueira, T. van Ritbergen, and J. A. M. Vermaseren. The Three loop QCD calculation of the moments of deep inelastic structure functions. *Nucl. Phys. B*, **492** (1997) 338–378. (arXiv:hep-ph/9605317).

[194] A. Retey and J. A. M. Vermaseren. Some higher moments of deep inelastic structure functions at next-to-next-to-leading order of perturbative QCD. *Nucl. Phys. B*, **604** (2001) 281–311. (arXiv:hep-ph/0007294).

[195] J. Blümlein and J. A. M. Vermaseren. The 16th moment of the non-singlet structure functions $F_2(x, Q^2)$ and $F_L(x, Q^2)$ to $O(\alpha_s^3)$. *Phys. Lett. B*, **606** (2005) 130–138. (arXiv:hep-ph/0411111).

[196] W. A. Bardeen, A. J. Buras, D. W. Duke, and T. Muta. Deep Inelastic Scattering Beyond the Leading Order in Asymptotically Free Gauge Theories. *Phys. Rev. D*, **18** (1978) 3998–4017.

[197] G. Altarelli, R. K. Ellis, and G. Martinelli. Leptoproduction and Drell-Yan Processes Beyond the Leading Approximation in Chromodynamics. *Nucl. Phys. B*, **143** (1978) 521–545. Erratum-ibid. **146** (1978) 544.

[198] B. Humpert and W. L. van Neerven. Infrared and Mass Regularization in AF Field Theories 2. QCD. *Nucl. Phys. B*, **184** (1981) 225–268.

[199] W. Furmanski and R. Petronzio. Lepton-Hadron Processes Beyond Leading Order in Quantum Chromodynamics. *Z. Phys. C*, **11** (1982) 293–314.

[200] D. I. Kazakov and A. V. Kotikov. Total α_s Correction to Deep Inelastic Scattering Cross-Section Ratio, $R = \sigma_L/\sigma_t$ in QCD. Calculation of Longitudinal Structure Function. *Nucl. Phys. B*, **307** (1988) 721–762. Erratum-ibid. **345** (1990) 299.

[201] D. I. Kazakov, A. V. Kotikov, G. Parente, O. A. Sampayo, and J. Sánchez Guillén. Complete quartic (α_s^2) correction to the deep inelastic longitudinal structure function F_L in QCD. *Phys. Rev. Lett.*, **65** (1990) 1535–1538. Erratum-ibid. **65** (1990) 2921.

[202] J. Sánchez Guillén, J. Miramontes, M. Miramontes, G. Parente, and O. A. Sampayo. Next-to-leading order analysis of the deep inelastic $R = \sigma_L/\sigma_{\text{total}}$. *Nucl. Phys. B*, **353** (1991) 337–345.

[203] S. D. Drell and T.-M. Yan. Massive Lepton Pair Production in Hadron-Hadron Collisions at High-Energies. *Phys. Rev. Lett.*, **25** (1970) 316–320. Erratum-ibid. **25** (1970) 902–902.

[204] M. Glück, E. Hoffmann, and E. Reya. Scaling Violations and the Gluon Distribution of the Nucleon. *Z. Phys. C*, **13** (1982) 119–130.

[205] M. A. G. Aivazis, John C. Collins, F. I. Olness, and W. Tung. Leptoproduction of heavy quarks. 2. A Unified QCD formulation of charged and neutral current processes from fixed target to collider energies. *Phys. Rev. D*, **50** (1994) 3102–3118. (arXiv:hep-ph/9312319).

[206] T. Appelquist and J. Carazzone. Infrared Singularities and Massive Fields. *Phys. Rev. D*, **11** (1975) 2856–2861.

[207] F. Bloch and A. Nordsieck. Note on the Radiation Field of the electron. *Phys. Rev.*, **52** (1937) 54–59.

[208] T. Kinoshita. Mass singularities of Feynman amplitudes. *J. Math. Phys.*, **3** (1962) 650–677.

[209] T. D. Lee and M. Nauenberg. Degenerate Systems and Mass Singularities. *Phys. Rev.*, **133** (1964) B1549–B1562.

[210] M. Glück and E. Reya. Deep Inelastic Quantum Chromodynamic Charm Leptoproduction. *Phys. Lett. B*, **83** (1979) 98–102.

[211] E. Laenen and S.-O. Moch. Soft gluon resummation for heavy quark electroproduction. *Phys. Rev. D*, **59** (1999) 034027–1–18. (arXiv:hep-ph/9809550).

[212] S. Alekhin and S. Moch. Higher order QCD corrections to charged-lepton deep-inelastic scattering and global fits of parton distributions. *Phys. Lett. B*, **672** (2009) 166–171. (arXiv:0811.1412 [hep-ph]).

[213] J. Blümlein, A. De Freitas, W. L. van Neerven, and S. Klein. The Longitudinal Heavy Quark Structure Function $F_L^{Q\bar{Q}}$ in the Region $Q^2 \gg m^2$ at $O(\alpha_s^3)$. *Nucl. Phys. B*, **755** (2006) 272–285. (arXiv:hep-ph/0608024).

[214] G. A. Schuler. Heavy Flavor Production at Hera. *Nucl. Phys. B*, **299** (1988) 21–51.

[215] M. Glück, R. M. Godbole, and E. Reya. Heavy Flavor Production at High-Energy *ep* Colliders. *Z. Phys. C*, **38** (1988) 441–447.

[216] U. Baur and J. J. van der Bij. Top Quark Production at Hera. *Nucl. Phys. B*, **304** (1988) 451–462.

[217] J. J. van der Bij and G. J. van Oldenborgh. QCD radiative corrections to charged current heavy quark production. *Z. Phys. C*, **51** (1991) 477–484.

[218] H1 Collaboration, ZEUS Collaboration, K. Lipka et al. Heavy flavour production at HERA. *Nucl. Phys. Proc. Suppl.*, **152** (2006) 128–135.

[219] P. D. Thompson. Comparison of inclusive charm and beauty cross-sections in deep-inelastic scattering at HERA with theoretical predictions. *J. Phys. G*, **34** (2007) N177–N192. (arXiv:hep-ph/0703103).

[220] ZEUS Collaboration, S. Chekanov et al. Measurement of $D^{*\pm}$ production in deep inelastic $e^{\pm}p$ scattering at HERA. *Phys. Rev. D*, **69** (2004) 012004–1–17. (arXiv:hep-ex/0308068).

[221] H1 Collaboration, A. Aktas et al. Measurement of $F_2^{c\bar{c}}$ and $F_2^{b\bar{b}}$ at high Q^2 using the H1 vertex detector at HERA. *Eur. Phys. J. C*, **40** (2005) 349–359. (arXiv:hep-ex/0411046).

[222] E. Eichten, I. Hinchliffe, K. D. Lane, and C. Quigg. Super Collider Physics. *Rev. Mod. Phys.*, **56** (1984) 579–707.

[223] M. Glück, E. Reya, and M. Stratmann. Heavy quarks at high-energy colliders. *Nucl. Phys. B*, **422** (1994) 37–56.

[224] J. Blümlein and S. Riemersma. QCD corrections to $F_L(x, Q^2)$. In: G. Ingelman, A. De Roeck, and R. Klanner, Eds., *Proc. of the Workshop Future Physics at HERA*. DESY, (1996) 82–85. (arXiv:hep-ph/9609394).

[225] S. A. Rabinowitz et al. Measurement of the strange sea distribution using neutrino charm production. *Phys. Rev. Lett.*, **70** (1993) 134–137.

[226] CCFR Collaboration, A. O. Bazarko et al. Determination of the strange quark content of the nucleon from a next-to-leading order QCD analysis of neutrino charm production. *Z. Phys. C*, **65** (1995) 189–198. (arXiv:hep-ex/9406007).

[227] B. A. Kniehl, G. Kramer, I. Schienbein, and H. Spiesberger. Open charm hadroproduction and the charm content of the proton. *Phys. Rev. D*, **79** (2009) 094009–1–10. and references therein, (arXiv:0901.4130 [hep-ph]).

[228] Y. Matiounine, J. Smith, and W. L. van Neerven. Two loop operator matrix elements calculated up to finite terms. *Phys. Rev. D*, **57** (1998) 6701–6722. (arXiv:hep-ph/9801224).

[229] S. Klein. *Mellin Moments of Heavy Flavor Contributions to $F_2(x, Q^2)$ at NNLO*. PhD thesis, TU Dortmund University, 2009. (arXiv:0910.3101 [hep-ph]).

[230] D. A. Akyeampong and R. Delbourgo. Dimensional regularization, abnormal amplitudes and anomalies. *Nuovo Cim. A*, **17** (1973) 578–586.

[231] P. Breitenlohner and D. Maison. Dimensional Renormalization and the Action Principle. *Commun. Math. Phys.*, **52** (1977) 11–38, 39–54, 55–75.

[232] S. A. Larin. The renormalization of the axial anomaly in dimensional regularization. *Phys. Lett. B*, **303** (1993) 113–118.

[233] G. 't Hooft. Dimensional regularization and the renormalization group. *Nucl. Phys. B*, **61** (1973) 455–468.

[234] R. Tarrach. The Pole Mass in Perturbative QCD. *Nucl. Phys. B*, **183** (1981) 384–396.

[235] O. Nachtmann and W. Wetzel. The Beta Function for Effective Quark Masses to Two Loops in QCD. *Nucl. Phys. B*, **187** (1981) 333–342.

[236] N. Gray, D. J. Broadhurst, W. Grafe, and K. Schilcher. Three Loop Relation of Quark (modified) MS and Pole Masses. *Z. Phys. C*, **48** (1990) 673–680.

[237] D. J. Broadhurst, N. Gray, and K. Schilcher. Gauge invariant on-shell Z_2 in QED, QCD and the effective field theory of a static quark. *Z. Phys. C*, **52** (1991) 111–122.

[238] J. Fleischer, F. Jegerlehner, O. V. Tarasov, and O. L. Veretin. Two loop QCD corrections of the massive fermion propagator. *Nucl. Phys. B*, **539** (1999) 671–690. Erratum-ibid. 571 (2000) 511–512, (arXiv:hep-ph/9803493).

[239] I. B. Khriplovich. Green's functions in theories with non-abelian gauge group. *Sov. J. Nucl. Phys.*, **10** (1969) 235–242.

[240] W. E. Caswell. Asymptotic Behavior of Nonabelian Gauge Theories to Two Loop Order. *Phys. Rev. Lett.*, **33** (1974) 244–246.

[241] D. R. T. Jones. Two Loop Diagrams in Yang-Mills Theory. *Nucl. Phys. B*, **75** (1974) 531–538.

[242] L. F. Abbott. The Background Field Method Beyond One Loop. *Nucl. Phys. B*, **185** (1981) 189–203.

[243] A. Rebhan. Momentum Subtraction Scheme and the Background Field Method in QCD. *Z. Phys. C*, **30** (1986) 309–315.

[244] F. Jegerlehner and O. V. Tarasov. Exact mass dependent two loop $\bar{\alpha}_s(Q^2)$ in the background MOM renormalization scheme. *Nucl. Phys. B*, **549** (1999) 481–498. (arXiv:hep-ph/9809485).

[245] A. Devoto and D. W. Duke. Table of Integrals And Formulae for Feynman Diagram Calculations. *Riv. Nuovo Cim.*, **7N6** (1984) 1–39.

[246] H. Poincaré. Sur les groupes des équations linéaires. *Acta Math.*, **4** (1884) 201–312.

[247] J. A. Lappo-Danilevsky. *Mémoires sur la théorie des systèmes des équations différentielles linéaires*. (Chelsea Pub. Co., New York, 1953).

[248] K.-T. Chen. Formal Differential Equations. *The Annals Math.*, **73** (1961) 110–133.

[249] F. D. Carlson. *Sur une classe de séries de Taylor*. PhD thesis, Uppsala University, 1914. see also `http://en.wikipedia.org/wiki/Carlson's_theorem`.

[250] E. C. Titchmarsh. *The Theory of Functions*. (Oxford University Press, 1939), 2nd ed. edition.

[251] M. E. Hoffman. Quasi-Shuffle Products. *Journal of Algebraic Combinatorics*, **11**(1) (2000) 49–68.

[252] J. Blümlein. Analytic continuation of Mellin transforms up to two loop order. *Comput. Phys. Commun.*, **133** (2000) 76–104. (arXiv:hep-ph/0003100).

[253] J. Blümlein and S.-O. Moch. Analytic continuation of the harmonic sums for the 3-loop anomalous dimensions. *Phys. Lett. B*, **614** (2005) 53–61. (arXiv:hep-ph/0503188).

[254] S. Moch, P. Uwer, and S. Weinzierl. Nested sums, expansion of transcendental functions and multiscale multiloop integrals. *J. Math. Phys.*, **43** (2002) 3363–3386. (arXiv:hep-ph/0110083).

[255] S. Lang. *Algebra*. (Springer, New York, 2002), 3rd edition.

[256] A. Kratzer and W. Franz. *Transzendente Funktionen*. (Akademische Verlagsgesellschaft, Leipzig, 1960).

[257] P. Appell and J. Kampé de Fériet. *Fonctions hypergéométriques et hypersphériques: polynômes d'Hermite*. (Gauthier-Villars, Paris, 1926).

[258] J. Kampé de Fériet. *La fonction hypergéométrique*. (Gauthier-Villars, Paris, 1937).

[259] J. Horn. Hypergeometrische Funktionen zweier Veränderlichen. *Math. Ann.*, **105** (1931) 381–407.

[260] A. Erdélyi, Ed. *Higher Transcendental Functions*. (McGraw-Hill Book Company, New York, 1953).

[261] L. J. Slater. *Generalized Hypergeometric Functions*. (Cambridge University Press, Cambridge, UK, 1966).

[262] H. Exton. *Multiple Hypergeometric Functions and Applications*. (Ellis Horwood, Chichester, 1976).

[263] H. Exton. *Handbook of Hypergeometric Integrals.* (Ellis Horwood, Chichester, 1978).

[264] H. M. Srivastava and P. W. Karlsson. *Multiple Gaussian hypergeometric series.* (Ellis Horwood, Chichester, 1985).

[265] C. F. Gauß. Disquisitiones generales circa seriem infinitam $1 + \frac{\alpha\beta}{1.\gamma}x + \frac{\alpha(\alpha+1)\beta(\beta+1)}{1.2.\gamma(\gamma+1)}x\ x + \frac{\alpha(\alpha+1)(\alpha+2)\beta(\beta+1)(\beta+2)}{1.2.3.\gamma(\gamma+1)(\gamma+2)}x^3 + \text{etc.}$ *Commentationes Societatis Regiae Scientiarum Gottingensis recentiores, classis mathematicae*, (1812) 3–48.

[266] E. E. Kummer. Über die hypergeometrische Reihe $1 + \frac{\alpha\beta}{1.\gamma}x + \frac{\alpha(\alpha+1)\beta(\beta+1)}{1.2.\gamma(\gamma+1)}x^2 + \frac{\alpha(\alpha+1)(\alpha+2)\beta(\beta+1)(\beta+2)}{1.2.3.\gamma(\gamma+1)(\gamma+2)}x^3 + \ldots.$ *J. reine angew. Math.*, **15** (1836) 39–83 and 127–172.

[267] A. Jeffrey and D. Zwillinger, Eds. *Gradshteyn and Ryzhik's Table of Integrals, Series, and Products.* (Academic Press, London, 2007).

[268] G. E. Andrews, R. Askey, and R. Roy. *Special Functions.* (Cambridge University Press, Cambridge, UK, 2001).

[269] G. B. Arfken and H.-J. Weber. *Mathematical methods for physicists, sixth edition.* (Elsevier, Acad. Press, Amsterdam, 2008).

[270] D. T. Whiteside. Newton's Discovery of the General Binomial Theorem. *The Mathematical Gazette*, **45**(353) (1961) 175–180.

[271] V. A. Smirnov. *Feynman Integral Calculus.* (Springer, Berlin, 2006).

[272] M. Czakon. Automatized analytic continuation of Mellin-Barnes integrals. *Comput. Phys. Commun.*, **175** (2006) 559–571. (arXiv:hep-ph/0511200).

[273] J. Gluza, K. Kajda, and T. Riemann. AMBRE: A Mathematica package for the construction of Mellin-Barnes representations for Feynman integrals. *Comput. Phys. Commun.*, **177** (2007) 879–893. (arXiv:0704.2423 [hep-ph]).

[274] E. W. Barnes. A Transformation of Generalised Hypergeometric Series. *Quart. J.*, **41** (1910) 136–140.

[275] W. Tung, S. Kretzer, and C. Schmidt. Open heavy flavor production in QCD: Conceptual framework and implementation issues. *J. Phys. G*, **28** (2002) 983–996. (arXiv:hep-ph/0110247).

[276] R. S. Thorne and R. G. Roberts. A practical procedure for evolving heavy flavor structure functions. *Phys. Lett. B*, **421** (1998) 303–311. (arXiv:hep-ph/9711223).

[277] S. Alekhin, J. Blümlein, S. Klein, and S. Moch. The 3, 4, and 5-flavor NNLO Parton from Deep-Inelastic-Scattering Data and at Hadron Colliders. *Phys. Rev. D*, **81** (2010) 014032. (arXiv:0908.2766 [hep-ph]).

[278] J. Blümlein and W. L. van Neerven. Heavy flavor contributions to the deep inelastic scattering sum rules. *Phys. Lett. B*, **450** (1999) 417–426. (arXiv:hep-ph/9811351).

[279] S. Forte, E. Laenen, P. Nason, and J. Rojo. Heavy quarks in deep-inelastic scattering. *Nucl. Phys. B*, **834** (2010) 116–162. (arXiv:1001.2312 [hep-ph]).

[280] J. Blümlein and F. Wißbrock. in preparation.

[281] I. Bierenbaum, J. Blümlein, and S. Klein. Logarithmic $O(\alpha_s^3)$ contributions to the DIS Heavy Flavor Wilson Coefficients at $Q^2 \gg m^2$. *PoS*, **DIS2010** (2010) 148. (arXiv:1008.0792 [hep-ph]).

[282] P. Nogueira. Automatic Feynman graph generation. *J. Comput. Phys.*, **105** (1993) 279–289.

[283] T. van Ritbergen, A. N. Schellekens, and J. A. M. Vermaseren. Group theory factors for Feynman diagrams. *Int. J. Mod. Phys. A*, **14** (1999) 41–96. (arXiv:hep-ph/9802376).

[284] J. A. M. Vermaseren. New features of FORM, 2000. (arXiv:math-ph/0010025).

[285] M. Steinhauser. MATAD: A program package for the computation of MAssive TADpoles. *Comput. Phys. Commun.*, **134** (2001) 335–364. (arXiv:hep-ph/0009029).

[286] J. F. Bennett and J. A. Gracey. Determination of the anomalous dimension of gluonic operators in deep inelastic scattering at $O(1/N_f)$. *Nucl. Phys. B*, **517** (1998) 241–268. (arXiv:hep-ph/9710364).

[287] J. Blümlein and A. Vogt. The Evolution of unpolarized singlet structure functions at small x. *Phys. Rev. D*, **58** (1998) 014020–1–26. (arXiv:hep-ph/9712546).

[288] J. Ablinger, J. Blümlein, and C. Schneider. DESY-13-064.

[289] N. Nielsen. Der Eulersche Dilogarithmus und seine Verallgemeinerungen. *Nova Acta Leopoldina*, **90** (1909) 121–212.

[290] K. S. Kölbig. Nielsen's Generalized Polylogarithms. *SIAM J. Math. Anal.*, **17** (1986) 1232–1258.

[291] W. Spence. *An essay of the theory of the various orders of logarithmic transcendents.* (J. Murray, London, 1809).

[292] E. E. Kummer. Ueber die Transcendenten, welche aus wiederholten Integrationen rationaler Formeln entstehen. *J. reine angew. Math. (Crelle)*, **21** (1840) 74–90.

[293] L. Lewin. *Polylogarithms and Associated Functions.* (North Holland, Amsterdam, 1981).

[294] I. Bierenbaum, J. Blümlein, and S. Klein. Two-loop massive operator matrix elements for polarized and unpolarized deep-inelastic scattering. *PoS*, **ACAT** (2007) 070. (arXiv:0706.2738 [hep-ph]).

[295] J. Blümlein, M. Kauers, S. Klein, and C. Schneider. Determining the closed forms of the $O(\alpha_s^3)$ anomalous dimensions and Wilson coefficients from Mellin moments by means of computer algebra. *Comput. Phys. Commun.*, **180** (2009) 2143–2165. (arXiv:0902.4091 [hep-ph]).

[296] B. Lampe and E. Reya. Spin physics and polarized structure functions. *Phys. Rept.*, **332** (2000) 1–163. (arXiv:hep-ph/9810270).

[297] S. Wandzura and Frank Wilczek. Sum Rules for Spin Dependent Electroproduction: Test of Relativistic Constituent Quarks. *Phys. Lett. B*, **72** (1977) 195–198.

[298] J. Blümlein, V. Ravindran, and W. L. van Neerven. Twist-2 heavy flavor contributions to the structure function $g_2(x, Q^2)$. *Phys. Rev. D*, **68** (2003) 114004–1–9. (arXiv:hep-ph/0304292).

[299] J. Blümlein and D. Robaschik. On the structure of the virtual Compton amplitude in the generalized Bjorken region: Integral relations. *Nucl. Phys. B*, **581** (2000) 449–473. (arXiv:hep-ph/0002071).

[300] J. Blümlein and D. Robaschik. Polarized deep inelastic diffractive $e\,p$ scattering: Operator approach. *Phys. Rev. D*, **65** (2002) 096002–1–7. (arXiv:hep-ph/0202077).

[301] J. Blümlein, B. Geyer, and D. Robaschik. Target mass and finite momentum transfer corrections to unpolarized and polarized diffractive scattering. *Nucl. Phys. B*, **755** (2006) 112–136. (arXiv:hep-ph/0605310).

[302] J. Blümlein, D. Robaschik, and B. Geyer. Target mass and finite t corrections to diffractive deeply inelastic scattering. *Eur. Phys. J. C*, **61** (2009) 279–298. (arXiv:0812.1899 [hep-ph]).

[303] M. Glück, E. Reya, and W. Vogelsang. Determination of spin dependent parton distributions in polarized leptoproduction of jets and heavy quarks. *Nucl. Phys. B*, **351** (1991) 579–592.

[304] W. Vogelsang. The Gluonic contribution to $g_1^p(x, Q^2)$ in the parton model. *Z. Phys. C*, **50** (1991) 275–284.

[305] M. Buza, Y. Matiounine, J. Smith, and W. L. van Neerven. $O(\alpha_s^2)$ Corrections to Polarized Heavy Flavor Production at Q^2 is $\gg m^2$. *Nucl. Phys. B*, **485** (1997) 420–456. (arXiv:hep-ph/9608342).

[306] I. Bierenbaum, J. Blümlein, A. De Freitas, A. Hasselhuhn, and S. Klein. in preparation.

[307] R. Mertig and W. L. van Neerven. The Calculation of the two loop spin splitting functions $P_{ij}^{(1)}(x)$. *Z. Phys. C*, **70** (1996) 637–654. (arXiv:hep-ph/9506451).

[308] I. Bierenbaum, J. Blümlein, and S. Klein. Two-loop massive operator matrix elements for polarized and unpolarized deep-inelastic scattering. *PoS*, **ACAT** (2007) 070. (arXiv:0706.2738 [hep-ph]).

[309] W. Vogelsang. A Rederivation of the spin dependent next-to-leading order splitting functions. *Phys. Rev. D*, **54** (1996) 2023–2029. (arXiv:hep-ph/9512218).

[310] W. Vogelsang. The Spin dependent two loop splitting functions. *Nucl. Phys. B*, **475** (1996) 47–72. (arXiv:hep-ph/9603366).

[311] I. Bierenbaum, J. Blümlein, and S. Klein. Evaluating Two-Loop Massive Operator Matrix Elements with Mellin-Barnes Integrals. *Nucl. Phys. Proc. Suppl.*, **160** (2006) 85–90. (arXiv:hep-ph/0607300).

[312] F. Brown. The massless higher-loop two-point function. *Commun. Math. Phys.*, **287** (2009) 925–958. (arXiv:0804.1660 [math.AG]).

[313] G. Almkvist and D. Zeilberger. The method of differentiating under the integral sign. *J. Symb. Comp.*, **10** (1990) 571–591.

[314] M. Apagodu and D. Zeilberger. Multi-variable Zeilberger and Almkvist-Zeilberger algorithms and the sharpening of Wilf-Zeilberger theory. *Adv. Appl. Math.*, **37**(2) (2006) 139–152.

[315] J. Ablinger, J. Blümlein, C. Raab, C. Schneider, and F. Wißbrock. in preparation.

[316] J. Blümlein and V. Ravindran. Mellin moments of the next-to-next-to leading order coefficient functions for the Drell-Yan process and hadronic Higgs-boson production. *Nucl. Phys. B*, **716** (2005) 128–172. (arXiv:hep-ph/0501178).

[317] J. Blümlein and V. Ravindran. $O(\alpha_s^2)$ Timelike Wilson Coefficients for Parton-Fragmentation Functions in Mellin Space. *Nucl. Phys. B*, **749** (2006) 1–24. (arXiv:hep-ph/0604019).

[318] C. Mallinger. Algorithmic Manipulations and Transformations of Univariate Holonomic Functions and Sequences, 1996. Diploma Thesis, RISC, J. Kepler University, Linz.

[319] F. Bergeron and S. Plouffe. Computing the generating function of a series given its first terms. *Journal of Experimental Mathematics*, **1** (1992) 307–312.

[320] M. Kauers. Guessing Handbook, 2009. Technical Report RISC 09-07, Johannes Kepler Universität Linz.

[321] J. Fleischer, A. V. Kotikov, and O. L. Veretin. Analytic two loop results for selfenergy type and vertex type diagrams with one nonzero mass. *Nucl. Phys. B*, **547** (1999) 343–374. (arXiv:hep-ph/9808242).

[322] M. Yu. Kalmykov and O. Veretin. Single scale diagrams and multiple binomial sums. *Phys. Lett. B*, **483** (2000) 315–323. (arXiv:hep-th/0004010).

[323] A. I. Davydychev and M. Yu. Kalmykov. Massive Feynman diagrams and inverse binomial sums. *Nucl. Phys. B*, **699** (2004) 3–64. (arXiv:hep-th/0303162).

[324] J. Ablinger, J. Blümlein, C. Raab, and C. Schneider. in preparation.

[325] S. I. Alekhin and J. Blümlein. Mellin representation for the heavy flavor contributions to deep inelastic structure functions. *Phys. Lett. B*, **594** (2004) 299–307. (arXiv:hep-ph/0404034).

[326] M. J. D. Powell. *Approximation Theory and Methods.* (Cambridge University Press, Cambridge, UK, 1981).

[327] C. Hastings Jr. *Approximations for Digital Computers.* (Princeton Univ. Press, Princeton, NJ, 1953).

[328] M. Abramowitz and I. A. Stegun. *Handbook of Mathematical Functions.* (NBS, Washington, D.C., 1964).

[329] Maple 10. Maplesoft, a division of Waterloo Maple Inc., Waterloo, Ontario.

[330] M. Glück, E. Reya, and A. Vogt. Radiatively generated parton distributions for high-energy collisions. *Z. Phys. C*, **48** (1990) 471–482.

[331] J. Blümlein, S. Klein, and B. Tödtli. $O(\alpha_s^2)$ and $O(\alpha_s^3)$ Heavy Flavor Contributions to Transversity at $Q^2 \gg m^2$. *Phys. Rev. D*, **80** (2009) 094010–1–12. (arXiv:0909.1547 [hep-ph]).

[332] G. Kramer and B. Lampe. QCD corrections to charm quark production in deep inelastic neutrino scattering. *Z. Phys. C*, **54** (1992) 139–146.

[333] S. Kretzer. *Heavy Quark Production and Fragmentation Processes in Next-to-Leading Order QCD*. PhD thesis, Universität Dortmund, Germany, 1999.

[334] Yu. L. Dokshitzer, V. A. Khoze, A. H. Mueller, and S. I. Troian. *Basics of perturbative QCD*. (Editions Frontières, 1991).

[335] V. V. Sudakov. Vertex parts at very high-energies in quantum electrodynamics. *Sov. Phys. JETP*, **3** (1956) 65–71.

[336] E. Byckling and K. Kajantie. *Particle Kinematics*. (John Wiley & Sons, New York, 1973).

[337] T.-P. Cheng and L.-F. Li. *Gauge theory of elementary particle physics*. (Oxford University Press, Oxford, 1984).

[338] N. Schmitz. *Neutrinophysik*. (Teubner, Stuttgart, 1997).

[339] S. Moch, M. Rogal, and A. Vogt. Differences between charged-current coefficient functions. *Nucl. Phys. B*, **790** (2008) 317–335. (arXiv:0708.3731 [hep-ph]).

[340] J. Ablinger and J. Blümlein. Harmonic Sums, Polylogarithms, Special Numbers, and their Generalizations, 2013. (arXiv:1304.7071 [math-ph]).

[341] S. Klein. Heavy Flavor Coefficient Functions in Deep-Inelastic Scattering at $O(a_s^2)$ and Large Virtualities, 2006. Diploma thesis at Universität Potsdam, Institut für Physik.

[342] R. Hamberg. *Second order gluonic contributions to physical quantities*. PhD thesis, Leiden University, 1991.

[343] M. J. G. Veltman. *Diagrammatica: The Path to Feynman rules*. (Cambridge University Press, Cambridge, UK, 1994).

[344] G. 't Hooft and M. J. G. Veltman. *Diagrammar*. Yellow Reports. (CERN, Geneva, 1973).